Bio-morphodynamics of coastal wetlands with mangrove vegetation

Danghan Xie (谢当汉)

258 UTRECHT STUDIES IN EARTH SCIENCES

Bio-morphodynamics of coastal wetlands with mangrove vegetation

Biomorfodynamiek van kustgebieden met mangrove vegetatie

(met een samenvatting in het Nederlands)

P R O E F S C H R I F T

ter verkrijging van de graad van doctor aan de Universiteit Utrecht
op gezag van de rector magnificus, prof. dr. H.R.B.M. Kummeling,
ingevolge het besluit van het college voor promoties in het openbaar te verdedigen
op woensdag 13 juli 2022 des morgens te 10.15 uur

door

Danghan Xie (谢当汉)
geboren op 18 juli 1991 te Fujian, China

Promotor:
Prof. dr. M.G. Kleinhans

Copromotor:
Dr. B. van Maanen

Cosupervisor:
Dr. C. Schwarz

This work was financially supported by the China Scholarship Council grant 201706710005.

Bio-morphodynamics of coastal wetlands with mangrove vegetation

Promotor:
Prof. dr. M.G. Kleinhans

Copromotor:
Dr. B. van Maanen

Cosupervisor:
Dr. C. Schwarz

Examination committee:
Prof. dr. Z.B. Wang
Technische Universiteit Delft, The Netherlands

Prof. dr. T.J. Bouma
Universiteit Utrecht, The Netherlands

Prof. dr. K.R. Bryan
University of Waikato, New Zealand

Prof. dr. L. Chen
Xiamen University, China

Prof. dr. K. Rogers
University of Wollongong, Australia

ISBN 978-90-6266-626-3

DOI https://doi.org/10.33540/927

Published by Faculty of Geosciences, Universiteit Utrecht, The Netherlands, in:
Utrecht Studies in Earth Sciences (USES 258), ISSN 2211-4335

Typeset using XeLaTeX

Cover: Creeks in the Gulf of Carpentaria, Australia. Board painting, Danghan Xie and WONE. Inspired by Scott Portelli.

Photography chapter covers: Job de vries [1, 3 and 5] | Barend van Maanen [2] | Steven Michael De Jong [4]

Printed by Ipskamp Printing, Enschede, The Netherlands

Correspondence to: Danghan Xie, xiedanghan@gmail.com

Utrecht Studies in Earth Sciences 258

Bio-morphodynamics of coastal wetlands with mangrove vegetation

Danghan Xie

Utrecht 2022

Faculty of Geosciences, Utrecht University

Contents

Summary

Mangroves, occupying the transition between land and sea, provide valuable ecosystem services for hundreds of millions of people across the tropics and subtropics. What would happen in a world without mangroves? Large amounts of carbon dioxide would be released into the atmosphere, contributing to global warming and accelerating global climate change, affecting humans, animals, plants and almost all other organisms on the planet. Dismal scenarios would be seen in almost every (sub)tropical coastal city, for example, a barren coast with unprotected shorelines periodically inundated by polluted water, driving away coastal inhabitants from the shore. Although this extreme situation is predicted not to occur within this century, global loss of mangrove coverage is currently occurring under the pressure from sea-level rise and human interventions. While the appeal to the conservation of mangrove forests has become globally recognized, limited knowledge on the complex interactions between ecosystems and coastal morphology hampers coastal zone management and the safeguarding of mangroves. External forcings, such as sea-level rise, tidal currents, wind waves, river flows, sediment supply, and human activity vary with mangrove systems influencing profile changes and vegetation dynamics. It is often thought that mangroves can keep up with sea-level rise and withstand natural and human-induced pressures, but to what extent is this true and which non-linear relations with the external forcings and internal dynamics are most important? Sustainable coastal management needs to be based on a better understanding of the underlying mechanisms controlling the development of mangrove ecosystems, especially in the face of predicted sea-level rise and intensifying human interventions.

Mangroves are often characterized by numerous pneumatophores, which are their special aerial root systems growing upward out of the mud and water so that mangroves can stand in seawater without asphyxiation. These root systems add flow resistance when water flushes through mangrove-covered areas. As a result, currents slow down, which promotes sedimentation and increasing bed surface elevation. Locally, flow between vegetated flats, such as in tidal channels, becomes more concentrated due to convergence of water flow, leading to a larger flow velocity and sediment erosion and thus lowering channel bed elevation. These hydro-morphodynamic interactions in turn affect vegetation biological processes, such as seedling establishment, mangrove growth and mortality, which then further change the impacts of vegetation on the above physical processes. Such non-linear interactions between vegetation dynamics, water movement, sediment transport and morphological changes are called bio-morphodynamic feedbacks. Sea-level rise and increasing human interventions have increasingly affected mangrove ecosystems and caused more uncertainty about future system evolution. Rising sea levels disturb hydro-morphodynamic processes through modulating water levels, which directly and indirectly influence vegetation distribution. Coastal populations deprive mangroves of habitat area by building coastal defence constructions, reshaping estuary morphology through regulating upstream water and sediment influx, and reducing mangrove coverage by removal of trees. The complexity of bio-morphodynamic and societal feedbacks increase the difficulty of predicting mangrove evolution and our ability for sustainable mangrove management. To address the underlying knowledge gaps, this thesis investigates the non-linear interactions between mangrove forests and their surrounding environment, particularly under sea-level rise effects and human interventions.

To quantify and forecast mangrove dynamics in response to changes in the coastal environment, in particular the long-term evolution of mangrove ecosystems, a process-based wetland model was developed that accounts for the non-linear bio-morphodynamic interactions between mangrove vegetation and the coastal profile. Given the required sensitivity of the trees to changing conditions,

the vegetation model considers species-specific characteristics at different vegetation life stages, including seedling establishment, vegetation growth and mortality, which are determined by coastal environmental conditions and vegetation competition. Vegetation in turn interacts with hydro-morphodynamic processes, utilizing a state-of-the-art and well-verified hydro-morphodynamic model (i.e. Delft3D), through increased flow resistance as a function of vegetation density. The treatment of this two-way feedback between the trees and the morphology is advanced beyond previous modelling approaches and the newly developed mangrove model is able to simulate the long-term evolution of the mangrove ecosystem by integrating detailed vegetation dynamics and comprehensive hydro-morphodynamic processes. The model is used to predict mangrove diversity over sea-level rise, identify the governing environmental factors for mangrove survival and evaluate the role of human interventions shaping mangrove systems directly and indirectly through centuries. More specifically, sea-level rise is simulated by incrementally raising the water level at the seaward boundary, and human activity increasing soil erosion in upstream catchments is represented by adjusting sediment supply at the riverine boundary. I first investigate the dynamics of multi-species mangrove assemblages under sea-level rise and human barriers (Chapter 2), then I widen the environmental conditions to identify which combinations are most determinantal for mangrove forests (Chapter 3), and finally, I investigate the interactions between mangroves and estuarine morphology driven by human interventions with the conditions in New Zealand (Chapter 4).

The model applied to the multi-species mangrove assemblage systems is the first study, to my knowledge, to resolve distinct behaviours of mangrove assemblages and zonation patterns in response to sea-level rise. Under high environmental pressure (i.e. low sediment supply and high sea-level rise), loss of mangrove coverage and mangrove diversity loss go hand in hand, especially when human-made barriers impede landward migration. However, under low environmental pressure (i.e. high sediment supply and low sea-level rise), an unexpected behaviour emerges as mangrove coverage can increase but a loss in diversity still occurs. This is due to the variations in accretion across the forest arising from the interactions between vegetation characteristics and sediment transport. Pioneer forests with dense structures limit sediment landward delivery and thus cause seaward bed level gain while upper-forest sediment starvation. Sea-level rise will then prolong the upper inundation regime, which limits vegetation growth and may eventually lead to vegetation replacement and diversity loss. The study therefore shows that such changes in mangrove diversity are dependent on the bio-morphodynamic feedback strength (determined by root density) of mangrove vegetation (Chapter 2).

A systematic exploration of mangrove vulnerability to sea-level rise under various coastal environmental conditions, including tides, small wind waves, sediment supply and coastal slopes, shows that nonlinear interactions between vegetation, profile evolution and these conditions cause distinct mangrove behaviours. Mangroves in micro-tidal systems are found to be extremely vulnerable as even slow sea-level rise can cause substantial landward retreat. The presence of wind waves in addition to strong tidal currents limits mangrove colonization to higher bed elevations with more favorable inundation regimes, such that sea-level rise impacts are mitigated. It is thought that full sediment infilling is needed before the creation of new landward accommodation space under sea-level rise, however, this research indicates complete infilling of the available accommodation space is not the essential factor for mangrove colonization when sea level increases. This is because the model considers a more natural vegetation process where vegetation can colonize at a range of hydroperiods. The newly created upper-intertidal area due to sea-level rise allows mangrove seedlings to settle, even though less sedimentation occurs. Overall, this study shines new light on an emerging discussion of whether wetlands can expand under sea-level rise. Moreover, the model results show that sediment accretion may accelerate with sea-level rise, but the timing and magnitude of acceleration depend on cross-shore location within the forest (Chapter 3).

Finally, the model is applied to idealized back-barrier estuarine systems to explore the effects of historic human interventions in the hinterland through centuries and current coastal mangrove management (i.e. mangrove removal projects). Human interventions in the hinterland lead to increasing fine sediment deposited on the coasts, which were sandy flats before European settlement, transforming the coasts to muddy flats with widespread mangrove forests. The model results show that when fluvial mud supply is increased, mangroves dominate the flats close to the channels and expand seaward as soon as the surface elevation raises to the suitable level. A large mud input not only creates habitat for mangroves, but also transforms the estuarine system into a more muddy environment. Removal of mangroves has been proposed to reduce mud capture and loss of unvegetated tidal flats, which are considered valuable in New Zealand, but the model shows that under continued high mud supply, removing mangrove trees lead to more mud deposition in the channels or on the flats further away from the channels, leading to a shallower channel and more muddy regions. In contrast, reducing mud supply from the hinterland reduces mud thickness from the muddy channels and tidal flats, and deepens channels while reducing or stopping mangrove expansion. As historic land-use changes caused the increase of mud supply, this model study shows how human interventions interact with the bio-morphodynamic feedbacks within the system. Coastal zone management will need to consider these complex feedbacks such that the most effective sustainable management strategies can be selected (Chapter 4).

The new insights and complex model reported from this thesis provide an advanced approach to assess and understand mangrove vulnerability and test coastal management strategies. Furthermore, it may serve as a basis to study other processes within coastal systems, including, but not limited to, the interactions between mangroves and waves, variations in boundary conditions (e.g. seasonal variations), the contribution of organic matter to morphological change, the impacts of mangrove and salt marsh ecotones on coastal resilience and more comprehensive theories controlling mangrove life stages (e.g. impacts from salt, nutrient and temperature) (Chapter 5).

Samenvatting

Mangroves groeien op de overgang tussen land en zee en leveren waardevolle ecosysteemdiensten aan honderden miljoenen mensen in de tropen en subtropen. Wat zou er gebeuren in een wereld zonder mangroves? Er zouden grote hoeveelheden kooldioxide in de atmosfeer vrijkomen, wat zou bijdragen aan de opwarming van de aarde en de wereldwijde klimaatverandering zou versnellen, met alle gevolgen van dien voor mensen, dieren, planten en bijna alle andere organismen op de planeet. In bijna elke (sub)tropische kuststad zouden zich rampzalige scenario's voordoen, waarbij onbegroeide en onbeschermde kustlijnen periodiek worden overspoeld door zout water, waardoor de kustbewoners van de kust worden verdreven. Hoewel wordt voorspeld dat deze extreme situatie zich deze eeuw nog niet zal voordoen, is er wel al sprake van een wereldwijd verlies aan mangrovebedekking onder druk van menselijke ingrepen en de stijging van de zeespiegel.

Ofschoon de roep om instandhouding van mangrovebossen wereldwijd wordt gehoord, belemmert de beperkte kennis over de complexe interacties tussen ecosystemen en kustmorfologie het beheer van kustgebieden en de bescherming van mangroves. Externe invloeden, zoals zeespiegelstijging, getijdenstromingen, windgolven, rivierstromingen, sedimentaanvoer en menselijke activiteit, hebben een wisselwerking met mangrove-systemen die van invloed is op veranderingen van het kustprofiel en vegetatiedynamiek. Vaak wordt gedacht dat mangroves de zeespiegelstijging kunnen bijhouden en bestand zijn tegen natuurlijke en door de mens veroorzaakte druk, maar in hoeverre dit het geval is, en welke niet-lineaire relaties met de externe forceringen en de interne dynamiek het belangrijkst zijn, is niet goed begrepen. Duurzaam kustbeheer moet gebaseerd zijn op een beter inzicht in de onderliggende mechanismen die de ontwikkeling van mangrove-ecosystemen sturen, met name in het licht van de voorspelde stijging van de zeespiegel en de intensivering van menselijke ingrepen.

Mangroves worden vaak gekenmerkt door talrijke luchtwortels, of pneumatoforen, die uit de modder en het water omhoog groeien zodat mangroves in zeewater kunnen groeien zonder te stikken. Deze wortelsystemen zorgen voor extra stromingsweerstand wanneer het water door met mangrove begroeide gebieden stroomt. Als gevolg daarvan vertraagt de waterbeweging, wat de sedimentatie en de verhoging van het bodemoppervlak bevordert. Tussen begroeide banken wordt de stroming juist geconcentreerd in getijgeulen, wat leidt tot een grotere stroomsnelheid, erosie en verdieping van de geulen. Deze interacties tussen waterbeweging en bodemligging zijn op hun beurt weer van invloed op de biologische processen van de vegetatie, zoals de vestiging van zaailingen, de groei en sterfte van de mangrove. Dit heeft vervolgens weer effecten op de bovengenoemde fysische processen. Dergelijke niet-lineaire interacties tussen vegetatiedynamica, waterbeweging, sedimenttransport en morfologische veranderingen worden bio-morfodynamische terugkoppelingen genoemd. De stijging van de zeespiegel en de toenemende menselijke ingrepen hebben de mangrove-ecosystemen in toenemende mate beïnvloed en hebben geleid tot meer onzekerheid over de toekomstige ontwikkeling van het systeem. De stijging van de zeespiegel verstoort de verspreiding van de vegetatie. Kustbewoners reduceren het habitat van de mangroves door kustverdedigingswerken aan te leggen, de morfologie van estuaria te wijzigen door baggeren en door de toevoer van rivierwater en sediment stroomopwaarts te reguleren, en de mangrovebedekking te verminderen door bomen te verwijderen. De complexiteit van de biomorfodynamische en maatschappelijke terugkoppelingen leggen de lat hoger voor voorspelling van de ontwikkeling van mangroves en van onze mogelijkheden voor duurzaam mangrovebeheer. Om de hiaten in onze kennis op te vullen, onderzoekt dit proefschrift de complexe interacties tussen mangrovebossen en hun omgeving, met name onder invloed van zeespiegelstijging en van menselijke interventies.

Hiertoe werd een procesgebaseerd wetlandmodel ontwikkeld dat rekening houdt met de niet-lineaire biomorfodynamische interacties tussen de mangrove-vegetatie en het kustprofiel. Gezien de werkelijke gevoeligheid van de bomen voor veranderende omstandigheden, houdt het vegetatiemodel rekening met soortspecifieke kenmerken in verschillende levensfasen van de vegetatie, met inbegrip van vestiging van zaailingen, vegetatiegroei en -sterfte, die worden bepaald door de omstandigheden aan de kust en door de onderlinge concurrentie tussen vegetatiesoorten. Voor de wisselwerking van vegetatie met waterbeweging en bodemligging wordt gebruik gemaakt van een geavanceerd en goed geverifieerd hydromorfodynamisch model, Delft3D. Een nieuwe code voor vegetatie zorgt dat deze hierin is gerepresenteerd als een verhoogde stromingsweerstand als functie van de vegetatiedichtheid. De afhandeling van de terugkoppelingen tussen de bomen en de morfologie is geavanceerder dan eerdere modelbenaderingen en het nieuw ontwikkelde mangrove-model is in staat de langetermijnevolutie van het mangrove-ecosysteem te simuleren.

Het model wordt gebruikt om de mangrovendiversiteit bij zeespiegelstijging te voorspellen, de bepalende omgevingsfactoren voor het voortbestaan van de mangrove te identificeren en de rol van menselijke ingrepen te evalueren die mangrove-systemen direct en indirect door de eeuwen heen vormgaven en zullen vormgeven. Zeespiegelstijging wordt opgelegd door het waterpeil aan de zeewaartse grens te verhogen, en menselijke activiteit die bodemerosie in stroomopwaarts gelegen stroomgebieden bevordert, wordt gerepresenteerd door de sedimenttoevoer via de rivier aan te passen. Eerst onderzoek ik de dynamiek van meersoortige mangroves onder zeespiegelstijging en in aanwezigheid van menselijke barrières (hoofdstuk 2). Vervolgens breid ik het bereik van omstandigheden uit om te bepalen welke combinaties het meest bepalend zijn voor het voortbestaan van mangrovebossen (hoofdstuk 3), en tenslotte onderzoek ik de interacties tussen mangroven en morfologie van riviermondingen onder invloed van historisch en modern menselijk ingrijpen zoals deze plaatsvonden in Nieuw-Zeeland (hoofdstuk 4).

Het model met meerrdere mangrovesoorten is, voor zover ik weet, de eerste studie die de verschillende gedragingen en zoneringspatronen in reactie op zeespiegelstijging onderzoekt. Onder een hoge gecombineerde stress van lage sedimentaanvoer en hoge zeespiegelstijging gaan verlies van mangrovebedekking en verlies van diversiteit van soorten hand in hand, vooral wanneer door de mens opgeworpen barrières de landwaartse migratie met stijgende zeespiegel belemmeren. Bij minder stress met een hoge sedimentaanvoer en een geringe zeespiegelstijging doet zich onverwacht gedrag voor: de mangrovebedekking kan toenemen, maar er kan nog steeds een verlies van biodiversiteit optreden. Dit is te wijten aan de interacties tussen dichte vegetatie en aanslibbing. Dichte pionierbossen beperken de aanvoer van water met sediment in landwaartse richting. Dit leidt tot ophoging van het zeewaartse deel van het bos, terwijl het landwaartse deel niet ophoogt. Zeespiegelstijging zal dan in het landwaartse deel de inundatieduur verlengen, wat de vegetatiegroei beperkt en soorten kan doen verdwijnen, met diversiteitsverlies als gevolg. Uit de modellering blijkt dat een dergelijke afname van mangrove-diversiteit afhangt van de intensiteit van biomorfodynamische terugkoppelingen (hoofdstuk 2).

Een systematisch onderzoek naar de kwetsbaarheid van mangrovebossen voor zeespiegelstijging onder diverse omstandigheden aan de kust, waaronder getijden, kleine windgolven, sedimentaanvoer en helling van de vooroever, laat zien dat de complexe interacties tot verschillende gedragingen van mangrovebossen leiden. Mangroves in microgetijde-systemen blijken uiterst kwetsbaar te zijn, aangezien zelfs een langzame stijging van de zeespiegel een aanzienlijke landwaartse terugtrekking kan veroorzaken. De aanwezigheid van windgolven beperkt bovendien de kolonisatie van mangroven tot hoger gelegen delen die minder langdurig worden overstroomd. Er wordt vaak aangenomen dat mangrovegebied net zo snel als de zeespiegelstijging moet sedimenteren voordat het landwaarts uitbreidt, maar dit onderzoek wijst uit dat dit niet de essentiële factor is voor mangrovebehoud bij een stijgende zeespiegel. De reden hiervoor is dat het gemodelleerde natuurlijke vegetatieproces staat

direct vestiging van vegetatie toe in het nieuw ontstane hogere intergetijdegebied als gevolg van de zeespiegelstijging, ook al treedt er minder sedimentatie op. Dit werpt nieuw licht op het lopende debat over de vraag of kustmoerassen zich wel kunnen uitbreiden onder invloed van de zeespiegelstijging. Daarbij laten de modelresultaten zien dat de aanslibbing kan versnellen met de stijging van de zeespiegel, maar dat het tijdstip en de omvang van de versnelling afhangen van de breedte van het bos en de kustwaartse positie waar de sedimentatie zich voordoet (hoofdstuk 3).

Tenslotte wordt het model toegepast op geïdealiseerde estuariene systemen met vastliggende mondingen bij de zee om de effecten te onderzoeken van historische menselijke ingrepen in het achterland door de eeuwen heen. Ook wordt onderzocht wat de effecten zijn van het huidige mangrovebeheer, namelijk verwijdering van recent uitgebreide mangroves om de onbegroeide platen te herstellen, zoals dit in Nieuw Zeeland gebeurt. Menselijke ingrepen in het achterland leidden tot een toename van de afzetting van fijn sediment op de kusten, die vóór de Europese nederzettingen zandplaten waren, waardoor de kusten veranderen in slibrijke platen met een sterke uitbreiding van mangrovebossen. Uit de modelresultaten blijkt dat wanneer de aanvoer van slib door de rivieren toeneemt, de mangroven de randen van de platen naast de geulen bezetten en zich zeewaarts uitbreiden zodra de bodemhoogte het geschikte niveau bereikt. Een grote slibtoevoer creëert niet alleen habitat voor mangroves, maar verandert het estuariene systeem ook in een slibrijker milieu. Dit heeft negatieve effecten op het ecosystem. Verwijdering van de mangroven wordt nu al toegepast op kleine schaal om de slibaanvoer en het verlies van onbegroeide wadplaten, die in Nieuw-Zeeland als waardevol worden beschouwd, te verminderen. De modelresultaten tonen echter aan dat bij een blijvend hoge slibaanvoer het verwijderen van de mangroven leidt tot meer slibafzetting in de geulen en op de platen verder weg van de geulen, wat leidt tot een ondiepere geul en nog meer slibbige gebieden. Een vermindering van de slibaanvoer vanuit het achterland daarentegen vermindert de sedimentatie van slib in de geulen en op de platen, waardoor de uitbreiding van de mangroven afneemt of tot stand wordt gebracht. Gezien dat de historische veranderingen in landgebruik de toename van de slibaanvoer hebben veroorzaakt, toont deze modelstudie aan hoezeer menselijk handelen, niet lokaal maar in het achterland, de biomorfodynamische terugkoppelingen binnen de natuurlijk systemen hebben veranderd. Bij het beheer van kustgebieden zal rekening moeten worden gehouden met deze complexe terugkoppelingen, zodat de meest effectieve duurzame beheersstrategieën kunnen worden geselecteerd (hoofdstuk 4).

De nieuwe inzichten en het complexe model in dit proefschrift zijn een geavanceerd gereedschap voor het beoordelen en begrijpen van de kwetsbaarheid van mangroven en het testen van kustbeheerstrategieën. Bovendien kan het model dienen als basis voor het bestuderen van andere processen binnen kustsystemen, zoals interacties tussen mangroven en golven, variaties in randvoorwaarden (bijv. seizoensgebonden variaties), de bijdrage van organisch materiaal aan morfologische veranderingen, de effecten van mangroven en andere ecosystemen (bijv. bodemdieren op de onbegroeide platen) op de veerkracht van de kust, en andere effecten die de levensstadia van mangroven beheersen (bijv. de invloed van zout, nutriënten en temperatuur) (Hoofdstuk 5).

摘要

红树林，作为一种生长于陆地和海洋过渡地带的植被系统，为数以亿计生活在热带和亚热带地区的人类提供了宝贵的生态系统服务。想象一下，如果没有红树林，世界将会是怎么样的呢？大量的二氧化碳被释放到大气中，导致全球变暖、气候加速变化，进而影响人类、动物、植物和地球上几乎所有其他生物的生存。随之而来的环境退化将席卷几乎每一个（亚）热带沿海城市。例如，荒芜的海岸带被污染的海水不断地淹没，海岸不再适宜人类的居住。尽管这种极端情况大概率不会在本世纪内发生，但随着海平面的不断上升以及人类对自然的不断干扰，全球红树林的覆盖率正逐渐减少。虽然全球都在呼吁保护红树林，但受限于生态系统和海岸地貌之间复杂的相互作用机制，海岸带的管理和红树林的保护仍然受到一定的阻碍。除此之外，外部因素，如海平面上升、潮汐流、风浪、河流、泥沙补给和人类活动，都会影响红树林系统的地貌和植被变化。人们通常认为，红树林能够自我调整其所处的地理位置以适应海平面上升的步伐，同时它还能承受来自自然和人类的压力。但这样的假设有多大程度是真实的，哪些外部作用力和内部动态的非线性关系主导着红树林对海平面上升的响应目前尚不清楚。只有更好地理解控制红树林生态系统发展的潜在机制才能制定可持续的海岸管理，这一点在面对未来可预测的海平面上升和不断加强的人类干预环境下显得尤为重要。

红树林有一个很显著的特点，就是它们的躯干会附带很多气根。这些特殊的气根系统从泥里向上生长，穿过土层和水层，使得红树林可以生长在海水中而不会因为缺氧失去生命。当水流流经红树林时，这些根系会增加水流阻力削弱水流速度，进而促进泥沙沉降并抬升红树林床面高程。然而在局部地区，水流流经红树林间的非植被覆盖区域，比如潮沟，由于水流受两侧红树林的影响不断在非植被区域汇聚，会形成较大的流速并不断侵蚀床面，降低潮沟床面的高度。而且这些水动力-地貌的相互作用还会影响红树林的生物过程，如红树林幼苗的着陆、红树林的生长和死亡，最终又进一步调整红树林对上述物理过程的作用。这种红树林生长状态、水流运动、泥沙迁移和地貌变化的非线性相互作用被称为生物-动力地貌反馈。海平面上升和日益增强的人类干预对红树林生态系统的影响越来越大，并给红树林生态系统的未来演变带来更多的不确定性。例如，海平面上升将改变水位进而干扰水流-地貌过程，从而直接或间接地影响植被的分布。沿海居民建造的沿岸堤防侵占红树林的栖息地，上游来水和来沙量的改变将可能重塑河口地貌形态，而砍伐红树林会直接减少植被覆盖率。生物地貌动力过程和社会反馈的复杂性增加了红树林演变预测的难度，给人类对红树林的可持续管理带来了挑战。为了解决潜在的科学问题，本博士论文研究了红树林及其周围环境之间的非线性相互作用，尤其关注在海平面上升和人类干预大背景下红树林对环境的反应机制。

为了量化和预测红树林对沿海环境变化的反应，特别是红树林生态系统的长期演变，本博士论文开发了一个基于物理过程的生态模型。该模型考虑了红树林植被和沿海床面之间的生物-动力地貌非线性作用过程。鉴于植被对周围环境变化的敏感性，该植被模型考虑了不同植被生命阶段的特定物种特征，包括幼苗着陆、植被生长和死亡，这些过程由海岸环境条件和植被间的竞争共同决定。此外，该模型还考虑了植被与水动力的相互作用过程。该过程的模拟是基于当前一个先进的、经过充分验证的水动力模型（Delft3D）进行的。这个水流动力模型将植被密度作为额外水流阻力进行考虑，其对树木和地貌之间的这种双向反馈的处理优于先前的建模手段，而且本博士论文新开发的红树林模型能够通过整合详细的植被动态变化和全面的水文-地貌动力过程来模拟红树林生态系统的长期演变。本博士论文中，该模型被用来预测以世纪为时间尺度的海平面上升过程中的红树林多样性，确定了影响红树林生存的环境因素，并评估人类直接和间接干预下红树林系统的变化。模型参数设置具体如下：通过逐步提高向海边界的水位来模拟海平面上升，通过调整河流边界的泥沙补给来表示河流上游受人类活动而引起的水土流失。本论文首先研究了多物种红树林组合在海平面上升和人类障碍物设置情况下的动态变化（第二章），然后扩大了模型所考虑的环境条件，来确定哪些组合对红

树林的变化影响最大（第三章），最后，以新西兰的红树林为背景研究了红树林与受人类干预影响下的河口地貌间的相互作用（第四章）。

据我所知，本研究应该是迄今为止首次实现了将模型应用于多物种红树林组合系统以探讨海平面上升影响下红树林组合和分区模式的反应机制。研究发现在高环境压力下（即少量泥沙补给和快速海平面上升），红树林覆盖率的损失和红树林多样性的损失是一致的，特别是当人工障碍物阻碍了红树林向内陆迁移时。然而，意外的是，在低环境压力下（即大量泥沙补给和缓慢海平面上升），红树林的覆盖率会增加，但植被多样性的损失依然存在。这是因为植被和泥沙运输之间的相互作用导致泥沙沉积率在整个森林尺度上存在差异。如果前部的植被密度大，就限制了泥沙向内陆输送，从而导致了海侧的床面在抬升，而内陆床面由于缺少泥沙补给则无法获得相应的高程增加。此外，海平面上升延长了红树林在内陆区域的淹没时间，限制植被生长，并可能最终导致不同植被物种间的演替以及生物多样性减少。总之，本研究表明，红树林多样性的变化取决于红树林植被的生物-动力地貌的反馈强度（由植被的根系密度来决定）（第二章）。

本研究在考虑在各种沿海环境条件下，包括潮汐、小风浪、泥沙补给和海岸坡度，对红树林响应海平面上升的脆弱性进行了系统的探索。研究表明植被、地貌演变及其与环境条件的非线性相互作用会导致红树林的不同反应。在小潮汐系统中的红树林是非常脆弱的，因为即使是缓慢的海平面上升也会导致大尺度的陆向迁徙演变。除了强潮流外，风浪的存在限制了红树林只能在更高的床面上生长，然而这却让红树林具有更有利的淹没空间，以抵抗海平面上升对它们生长的威胁。在海平面上升的情况下，为创造新的陆侧容纳空间，充分的泥沙补给是必不可少的。然而，本研究表明，当海平面上升时，完全填充可用的容纳空间并不是红树林生长的先决条件。这是因为该模型考虑了一个更自然的植被生长过程，即植被可以在一定淹没周期的水中生长，即便是有较少的泥沙补给，由于海平面上升而新产生的潮间带上部区域也可以让红树林幼苗生长。此外，模型结果显示，床面泥沙的累积可能会随着海平面上升而加速，但加速的时间和幅度与该研究点所处于红树林的内部位置有关。总的来说，本研究为当前关于湿地是否能在海平面上升的背景下进行扩展的讨论带来了新的线索和参考（第三章）。

最后，本研究将该模型应用于理想化的带有前端阻碍的新西兰河口系统，以探讨几个世纪以来人类对内陆的历史干预和当前海岸红树林管理（即红树林清除项目）的影响。在欧洲人殖民之前，新西兰海滩的主导泥沙成分为沙质泥沙。然而在欧洲人殖民之后，人类对内陆的干预导致越来越多的细颗粒泥沙沉积在海岸上，逐渐将海岸转变为具有广泛红树林分布的泥质海滩。模型结果显示，当河道泥沙补给增加时，红树林首先在靠近河道的滩地上生长，一旦海侧的河床高度上升到合适的水平，红树林就会向外海扩展。大量的泥沙输入不仅为红树林创造了可能的栖息地，也使得河口环境变得更加泥泞。在新西兰，人们提议移除红树林以减少泥沙的淤积并且增加无植被覆盖的滩涂面积。但模型显示，在持续的高浓度细颗粒泥沙补给下，移除红树林会导致更多的泥沙淤积在河道中或离河道更远的滩涂上，导致河道变浅，并且使整个河口环境变得更泥泞。相反，如果能减少来自上游的泥沙补给，则可以减少河道和滩涂的淤泥厚度，加深河道水深，同时减缓红树林的持续扩张。由于历史上上游土地使用的变化导致了细颗粒泥沙补给的增加，该模型展示了人类干预如何与系统内的生物-动力地貌的相互作用过程，而沿海地区的管理将需要考虑这些复杂的反馈，以便选择最有效的可持续管理策略（第四章）。

本论文研究结果展示的新观点和开发的复杂模型为评估和理解红树林的脆弱性以及测试海岸管理策略提供了一种新的思维方法。它可以作为研究沿海系统内其他过程的基础，包括但不限于红树林和海浪之间的相互作用、边界条件的变化（如季节性变化）、有机物对地貌变化的贡献、红树林和盐沼交错带对海岸恢复力的影响以及控制红树林生命阶段的更全面理论（如来自盐度、营养物和温度的影响）（第五章）。

Chapter 1 | Introduction

1.1 Context

1.1.1 Locations, functions and current conditions of mangroves

Mangrove forests are comprised of unique plant species that colonize the intertidal zone along tropical and subtropical shorelines in over 123 countries and territories (Figure 1.1) (Spalding et al., 2010). Due to their distinctive morphological and physiological adaptations, such as aerial-roots and pneumatophores, salt-excreting leaves and viviparous propagules, these halophytes can survive in saline and anoxic environments (Kathiresan and Bingham, 2001). These features endow mangrove forests to function as critical interfaces between terrestrial, estuarine, and near-shore marine ecosystems that are periodically flooded by tidal currents and waves (Woodroffe et al., 2016). As one of the pioneer coastal ecosystems connecting the ocean to the land, mangroves provide valuable ecosystem functions to society. For example, mangroves help prevent the coastlines and inland human communities from damage caused by coastal erosion and storms (van Hespen et al., 2021). Besides, mangroves also serve as important ecosystem services providers, through nurturing grounds for a variety of flora and fauna (Odum et al., 1982; Kathiresan and Bingham, 2001; Aburto-Oropeza et al., 2008), sequestering carbon to mitigate climate change (Alongi, 2012; Sippo et al., 2020), and providing resources for human living and activities (Duke et al., 2017; Chakraborty et al., 2020). However, the frequent or occasional scouring by tidal currents and wave activity inevitably cause a risk of mangrove dieback (Sippo et al., 2018), potentially threatening coastal ecosystems and inland human livelihood. Mangrove forests covered an area of more than 2×10^5 km^2 in 1990 globally, their loss rates vary greatly among countries, ranging from 1 to 20% preceding 2000, which were faster than the neighboring coral reefs or tropical forests (Spalding et al., 1997; Alongi, 2002; Duke et al., 2007). Efforts to restore and protect mangroves appear to be effective over decadal timescales, leading to a declining loss rate globally, with a net average loss rate of 0.11% per year (Friess et al., 2019; Spalding and Leal, 2021). Mangroves have now been considered as high-priority ecosystems with widespread restoration and rehabilitation projects worldwide, however, substantial challenges for mangrove ecosystems still exist to remain ecologically functional and adaptable to the sea-level rise and human interventions, which are ascribed to the main causes of mangrove losses (Woodroffe et al., 2016; Friess and Sidik, 2020; Goldberg et al., 2020). In view of accelerating climate change and human interference, it is more important than ever to predict the future development of mangrove forests.

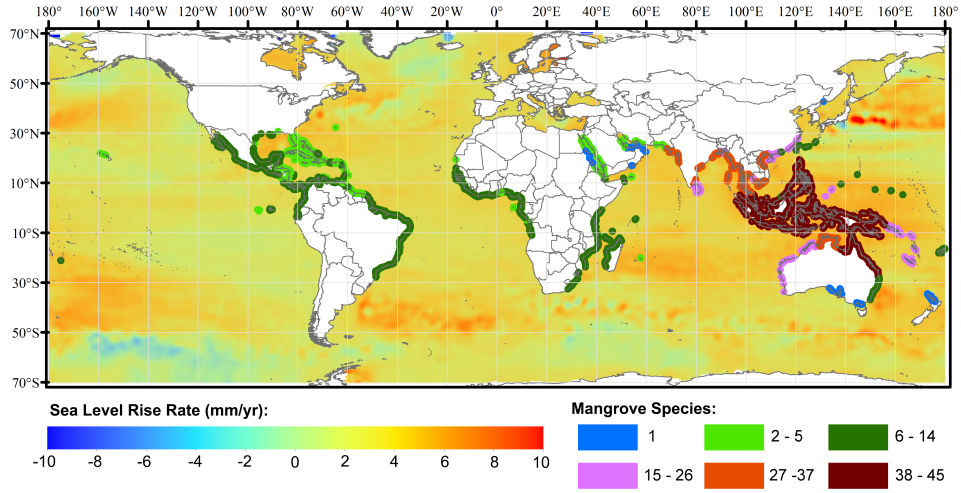

Figure 1.1 Spatial distribution of mangrove habitat with numbers of species (data obtained from Spalding et al. (2010)) and global sea-level rise rate (since 1992) from TOPEX/Poseidon and Jason satellite altimetry data.

1.1.2 Mangroves in the Holocene

The distribution of mangroves during the Holocene was mainly controlled by the rate of sea-level rise (Friess et al., 2019). Mangroves settle approximately between mean water level and mean high water level, and are sensitive to tidal inundation, making this ecosystem particularly vulnerable to habitat changes with fast sea-level rise (Chapman, 1976; Ellison, 2014; Kumbier et al., 2021). Sea-level rise drives changes in local water level and tidal inundation, to which mangroves are sensitive. This natural response of mangroves to water level variation has linked the mangrove distribution with sea-level rise, enabling the sedimentation record beneath mangrove forests to be used as a geological proxy for sea-level rise and mangrove response (Cohen et al., 2005; Woodroffe, 2018). Mangrove forests have settled and drowned since the onset of deglaciation and sea-level rise 26000 to 20000 years ago (Lambeck et al., 2014; Saintilan et al., 2020), causing shorelines and mangrove forests to migrate landward (Hanebuth et al., 2000). Before the Holocene, sea-level rise rates (> 7 mm/yr) were higher than the capacity of mangroves to maintain their position through vertical accumulation and thus a wide area of mangroves drowned on regressive shorelines (Saintilan et al., 2020; Woodroffe, 2018). The rates of sea-level rise varied but generally decelerated during the early and mid-Holocene, providing opportunities for the extension of mangrove forests on floodplains developing through fluvial sediment infilling (Woodroffe et al., 1985). Lower rates of sea-level rise continued from the mid-Holocene to 1450-1550 cal. yrs BP and henceforth mangroves expanded seaward (Punwong et al., 2013). This century, sea-level rise rate is expected to accelerate again, increasing the risk of mangroves being drowned and coastal shoreline regression (Oppenheimer et al., 2019). Human activity was initially minor during the mid-to-late Holocene, with a limited amount of wood resources and land spaces exploited for basic living. However, in the last two centuries, increased human activity has threatened mangrove habitats either directly or indirectly. With the high demand for mangrove wood and land resources for human activity, such as ship construction, agriculture and social trades as well as urban expansion, substantial deforestation and degradation reduced the mangrove area, leading to a direct loss of mangrove forests (Friess et al., 2019; Goldberg et al., 2020). In addition, human activity in areas adjacent to the mangrove ecosystems influenced mangrove distribution indirectly. Fluvial sediment loads are reduced as a result of upstream dam constructions,

limiting the vertical accretion of the mangrove habitats and thus causing mangrove loss and shoreline retreat under sea-level rise (Malini and Rao, 2004). In contrast, there are also locations, such as North Island of New Zealand, where mangroves have expanded due to land-use changes upstream following European settlement, such as expanding agriculture, pasture and deforestation, which increased sediment supply to the rivers and contribute to the mangrove habitats creation (Jones, 2008; Lundquist et al., 2014; Horstman et al., 2018b; Glover et al., 2022). Former mangrove shorelines have been derived from paleorecord data, which also contribute to informing how mangroves may respond in the future (Woodroffe, 2018). However, the coastal environment has become more complex with increasing human interventions (Duke et al., 2007; Schuerch et al., 2018) and increasing rates of current and future sea-level rise (Oppenheimer et al., 2019). Therefore, it is necessary to use a comprehensive evaluation approach that accounts for the potential changes in sea-level rise and sediment delivery rates and their impact on mangrove conditions to evaluate the future behaviours of mangrove forests (Kirwan and Megonigal, 2013; Friess et al., 2019).

1.1.3 Current mangrove behaviour and challenges of forecasting future mangrove behaviour

Mangroves typically display zonation patterns, with distinct species colonizing different elevations or distances from shores in response to inundation frequency (Snedaker, 1982; Duke et al., 1998; Tomlinson, 2016; Fagherazzi et al., 2017). The shifts in mangrove zones represent the changes in the range of possible local hydroperiods in which each mangrove species can thrive. Mangroves are adapted to ever-changing landscapes, where they may expand seaward or retreat landward driven by hydroperiod. Remote sensing and instrument-based field measurements allow tracking the changes of global mangrove distribution as well as the surrounding coastal environment. Regional differences and temporal variations in natural mangrove behaviours (e.g. seaward expansion or landward migration) have been monitored to inform future mangrove vulnerability (Lovelock et al., 2015; Duncan et al., 2018; de Jong et al., 2021). The balance between vertical sediment accretion rates and sea-level rise rates has been identified as one of the key factors determining mangrove vulnerability (Woodroffe et al., 2016; Rodriguez et al., 2017; Schuerch et al., 2018). Sea-level rise increases the water level and may drown the mangroves when there are no gains in mangrove surface elevation. However, vertical accretion as a result of mineral sediment deposition can offset the prolonged inundation from sea-level rise and help mangroves to keep pace with rising water levels. Sediment accretion rates within one area mainly depend on the inundation period and the local sediment availability. Inundation period depends on elevation and tides, which change under sea-level rise. Sediment supply varies with locations, leading to contrasting mangrove behaviours globally. For example, on the Amazon-Orinoco coast (South America), the Firth of Thames (New Zealand) and around Hong Kong (China), where sea-level rise rates are low but sediment supplies are high, mangroves are found to colonize at elevated mudflats and propagate seaward (Anthony et al., 2010; Lovelock et al., 2010; Asbridge et al., 2016; Nardin et al., 2016b; Liu et al., 2018). In contrast, in American Samoa or Southwest Papua New Guinea, where sea-level rise rates are high but sediment supplies are low, sea-level rise rates may exceed sediment accretion rates, leading to landward retreat of mangrove forests (Gilman et al., 2007; Ellison, 2014).

In addition, sediment accretion rates are predicted to increase due to the prolonged flooding from sea-level rise, potentially protecting the coastal wetland from drowning if this feedback is sufficiently strong without limitations of the sediment supply (Kirwan and Guntenspergen, 2010; Fagherazzi et al., 2012; Mogensen and Rogers, 2018). However, sediment supply varies with coastal systems, and sediment delivery rates along the tidal flats are influenced by both physical processes (i.e. the strength of hydrodynamic forces) and biological objects (i.e. vegetation stems and root structures) (Furukawa et al., 1997; Mazda et al., 1997b). Thus, sediment availability will vary spatially and temporally. In this case, sediment accretion rates may even decline at areas with prolonged flooding due to the limit of

sediment supply, while those areas with limited flooding regime may accrete more sediment when there is sufficient sediment supply. Such changes in the inundation regime due to sedimentation variations will further influence mangrove species distribution. These counterintuitive behaviors are dependent on the underlying bio-geomorphological interactions including biological and physical processes, which require additional attention in wetland vulnerability assessments (Cahoon et al., 2020). Previous wetland models have simplified the sediment transport dynamics by assuming a constant or a distance-based sediment availability (from channels), and this may inhibit us from accurately capturing mangrove behaviours in the future (Furukawa and Wolanski, 1996; D'Alpaos et al., 2007; Kirwan and Guntenspergen, 2010; Fu et al., 2019). As such, we need to understand how the biotic and abiotic processes, and their interactions, control mangrove system evolution.

1.1.4 Aim of this thesis

This thesis aims to shed light on the bio-morphodynamic feedbacks between mangroves and coastal environmental conditions to understand possible future mangrove behaviours under sea-level rise and human interventions. In order to gain sufficient control on boundary conditions and bio-morphodynamic feedbacks, and to gain long-term forecasting capability, a novel bio-morphodynamic model incorporating hydro-sedimentary processes, morphological changes and vegetation dynamics is developed to investigate the complex changes in mangrove forests in response to changing boundary conditions.

1.2 The importance of mangroves and their life-stages

1.2.1 Current features of mangrove forests and their associative economic and ecological values

The economic and ecological values of mangrove forests have been widely documented, including carbon sequestration (Rogers et al., 2019; Suyadi et al., 2020), coastal protection against erosion (Mazda et al., 1997a; Horstman et al., 2014), ground nursery for a plethora of organisms in some, or all life stages (Kathiresan and Rajendran, 2005; Aburto-Oropeza et al., 2008) and water quality purification (Schaffelke et al., 2005). Estimated by the products and services they provide the annual economic values of mangroves can reach 2-9×10^5 USD ha^{-1} with a current occupation of coastline ∼1.3×10^5 km^2. However, only 6.9% of mangrove area is protected under the existing protected area network (Wells, 2006; Giri et al., 2011). The loss of mangroves not only means the loss of functions that mangroves provided, but the costs to restore or enhance mangrove areas is outweighing the costs for their protection. For example, in Thailand only 189 USD ha^{-1} is needed to protect the existing mangrove area, while it takes 4 times more (∼946 USD ha^{-1}) to restore mangrove forests that have been eliminated or degraded (Secretariat, 2001; Gilman et al., 2008). To minimize future mangrove losses, land management and site planning with adequate preparation time are suggested, which require accurate predictions of mangrove changes in the future.

Although mangroves mainly occur across tropical and subtropical latitudes, the coverage area and the number of mangrove species vary between regions (Figure 1.1). For example, the largest area of mangroves is in the Indian Ocean region, accounting for 47% of the total area of mangroves globally (94984.56 km^2). A total number of 55 mangrove species, which is nearly 85% of the total number of global mangrove species worldwide (around 65 species) can be found in the Indian Ocean (Kathiresan and Rajendran, 2005). Preserving this biodiversity is vital as the the provision of ecosystem services is highly dependent on mangrove species assemblages, and the loss of individual species can have dramatic economic and environmental consequences for coastal communities (Duke et al., 2007; Polidoro et al., 2010). An example related directly to the economic consequences for human livelihoods is found in the Gulf of California. Although the area is mainly dominated by four

mangrove species (*Avicennia germinans*, *Rhizophora samoensis*, *Laguncularia racemosa* and *Conocarpus erectus*), the direct economic values provided from each species are estimated to reach $\sim 4 \times 10^4$ USD ha^{-1} including fish and blue crab fisheries (Aburto-Oropeza et al., 2008). Recently, due to the severe climate changes, nearly 7650 ha of mangroves across the Gulf of Carpentaria have been reported to be damaged or died, leading to a great loss in ecological and economic services (Duke et al., 2021). Clearly, the loss of mangrove species not only reduces the ecosystem functioning, but also affects human livelihoods.

1.2.2 Mangrove properties and life-stages

Inundation frequency often varies with intertidal elevation (Kumbier et al., 2021). To survive at different elevations or in different coastal environments across tidal flats, mangrove species have different types of aerial roots and these roots play a vital role in supporting mangrove survival in aerobic conditions through gas exchanges (Kitaya et al., 2002), sediment trapping (Furukawa and Wolanski, 1996) and hydrodynamic damping (Mazda et al., 1997b). Typically, in mangrove forests, aerial roots specialized for gaseous exchange are also known as pneumatophores. Due to species-specific characteristics, different mangrove species may have different capacities to sustain water submergence, resulting in typical mangrove assemblages with the presence of distinct mangrove species at different elevations from the shore and relative to mean sea level, further referred to as mangrove zonation (Snedaker, 1982; Duke et al., 1998; Fagherazzi et al., 2007; Bullock et al., 2017). Besides, varying shapes and numbers of pneumatophores with different species (Chapman, 1976), they also lead to different resistance (drag) to the tidal currents along the flats, which potentially result in spatial variations of sediment accretion (Krauss et al., 2003). Moreover, the number of pneumatophores also increases with stem diameter through different life-stages (Young and Harvey, 1996), resulting in a gradually increasing extent of resistance exerted by different ages of mangroves. Therefore, the role of mangrove objects and their associated pneumatophores on driving the changes of hydrodynamic systems and sediment transport processes vary with the sizes and ages of individual mangrove trees (Furukawa et al., 1997; Mazda et al., 2005; van Maanen et al., 2015).

Transitions of mangrove distributions in response to environmental conditions are highly related to the mode of their reproduction. The production and release of hydrochorous propagules from parental mangrove stands are the first stage for the successful establishment of mangrove seedlings (Van der Stocken et al., 2019). Although generally a large number of propagules are produced by each plant (e.g. *Avicennia marina*, produces 422 to 5210 propagules/year) (Clarke, 1992), successful colonization and growth are largely dependent on external hydraulic conditions. According to a flume experiment conducted by Balke et al. (2011), successful establishment of mangrove seedling requires 1) an inundation-free period for propagules to quickly anchor after stranding; 2) a long enough root length to withstand the following hydrodynamic forces from waves and currents, and 3) a sufficient root length to resist disturbance from sediment erosion. As long as the root length exceeded 4 cm, which is roughly after 8 days of propagule arrival, all seedlings could resist the highest level of bed shear stress applied in the flume. This seedling establishment was linked to the so-called window of opportunity concept that controls mangrove distribution. Given the sensitivity of mangrove propagules to the hydrodynamic forces, the vegetation traits also imply that gradual change of the environmental conditions (hydrodynamics or sediment dynamics) may cause an abrupt shift in the success of mangrove seedling establishment, and thus influence the eventual mangrove distribution and their recovery efficiency (Balke et al., 2014).

After seedlings successfully establish, mangroves can grow with an increase in stem diameter, height and the number of aerial roots over time. However, due to the peculiar growing environment which is periodically flooded by tidal currents, many external factors will influence mangrove growth, including the hydroperiod and available resources (Chapman, 1976; van Maanen et al., 2015). Each mangrove species has specific preferential inundation regimes influencing their growth rate. On a

community level, inundation dependent optimal growth rates determine the dominance of mangrove species across the intertidal area, leading to characteristic spatial variations in mangrove distribution across the tidal flats (Lovelock et al., 2016; Zhu et al., 2019). Similar to typical terrestrial plants, locations either too dry or nearly permanently inundated will reduce the photosynthetic performance and gas exchanges and thus are unfavourable for mangrove growth (Watson, 1928; Hoppe-Speer et al., 2011). In addition, the intra-species and inter-species competition for available resources, such as light and nutrients, also affect vegetation growth (Berger and Hildenbrandt, 2000; Chen et al., 2013). The intra-species competition within mangrove forests help to reduce vegetation density, which is known as self-thinning processes, leading to a reduction in the competition for resources amongst mangrove trees (Analuddin et al., 2009). Mangrove mortality induced by extreme changes in climate, such as tropical cyclones or other climate extreme events, has been well established (Duke et al., 2017; Sippo et al., 2018). However, this short-term behaviour due to the energetic events is beyond the scope of this study.

I mainly focus on the causal factors linked to sea-level rise and human interventions, such as changing inundation regimes and human disturbances, as these are the general factors influencing the long-term, large-scale landscape development of mangroves worldwide, but may change significantly within the life span of individual trees. As an example, in the Kosi Estuary in KwaZulu Natal, South Africa, mangroves experience prolonged inundation leading to gradual die off (Branch et al., 1981). Since mangroves growth rates are influenced by their surrounding inundation regime and competition stress, a persistently unfavourable growth environment will threaten the growth quality and reduce the growth rate (Hoppe-Speer et al., 2011). Thus, the continuously reduced growth rate has become a signal to identify mangrove mortality (van Maanen et al., 2015).

1.3 Threats caused by mangrove deforestation

Mangroves are essential for the well-being of coastal communities, as a large population of humans relies on coastal resources for water, food, shelter and activity (Kathiresan and Bingham, 2001). The increase in settlements and use of coastal space enhance the interactions between humans and the coastal environment, including the mangrove-based resources exploitation and the availability of space for mangroves to grow in. Thus, risks to mangroves not only stem from sea-level rise, but also human interventions, such as coastal constructions, upstream land-use change, aquaculture, dams, and other human-induced changes in the coastal environment. Mangrove coverage has recently decreased and even halved in some regions (Giri et al., 2011; Kozhikkodan Veettil and Quang, 2019). Mangrove deforestation for agriculture or aquaculture is one of the direct ways to degrade mangrove forests (Goldberg et al., 2020). Mangroves are expected to be lost before the end of the century if deforestation continues at a rate of 1-2% per year (Alongi, 2008), although the global deforestation rate (0.16% to 0.39%) was an order of magnitude lower since the year 2000 (Hamilton and Casey, 2016). While the global loss rate of mangrove forests is now declining, there are still substantial challenges in reducing mangrove loss (Friess et al., 2020). Mangroves suffering from the lack of available space and habitat are particularly located in Southeast Asian countries like Indonesia, Myanmar, Malaysia, the Philippines, Thailand and Vietnam (Spalding et al., 2010; Goldberg et al., 2020). The population in these countries has doubled in the recent 40 years and is projected to continually increase in this century (Jones, 2014). This raises concerns about the future coverage of mangrove forests given the projected increasing human activities in the future. The outcome of mangrove loss will eventually affect humans living in the coastal zone and their safety due to the increased risk of coastal hazards and reduced biodiversity (Gilman et al., 2008). In addition, carbon stored within mangrove ecosystems will be released, exacerbating global warming and other climate change trends (Lovelock et al., 2022). So far, sea-level rise and human interventions have been

identified as two main factors influencing mangrove coverage, which are predicted to exert increased impacts in the future (Duke et al., 2007; Oppenheimer et al., 2019).

Although mangroves have the capability to adjust their elevation to avoid prolonged inundation from sea-level rise by capturing suspended sediment and/or organic matter accretion (Krauss et al., 2014; Woodroffe et al., 2016), there are still risks for mangroves being drowned when the rate of change in surface elevation of mangrove forests is exceeded by sea-level rise rate over an extended period of time (Gilman et al., 2007; Gilman et al., 2008). Given a landscape-level scale and time scales of multiple decades, mangrove responses to sea-level rise in the absence of human barriers can be categorized into three general scenarios. (Figure 1.2) (Gilman et al., 2007). These scenarios are based on relative difference between mangrove accretion and sea-level rise: 1) When sea level and mangrove surface remains on the same elevation, mangrove communities remain constant and their margins will persist on the same location (Figure 1.2a); 2) When mangrove accretion rates outpace sea-level rise rates, mangrove community may expand seaward, displacing other coastal habitats at a lower elevation than mangroves (Figure 1.2b); 3) When sea-level is rising faster than mangrove accretion, both mangrove seaward and landward margins will retreat inland to keep their preferential inundation regimes (Figure 1.2c). These behaviours are based on the premise that relative sea-level rise and sediment supply are the predominant forces shaping mangrove behaviours, while organic matter accretion, sediment auto-compaction, and other climate factors, such as temperature, precipitation and storminess, may generate other forms of mangrove distributions (Sippo et al., 2018; Rogers, 2021). For example, a drop in sea level together with increased drought as well as decreased precipitation in the Gulf of Carpentaria (Australia) has caused large-scale dieback of mangrove forests instead of seaward mangrove propagation (Duke et al., 2017).

To sustain bed elevation and avoid excess flooding, mangroves require preserving enough marine sediment, which is ultimately sourced from the continents by rivers (Törnqvist et al., 2019), although in some carbonate dominated settings peat accumulation raises mangrove elevation (McKee et al., 2007). However, human activity has a large impact on the amount of sediment transported to the coastal system and mangrove movement. Two contrasting trends in sediment supply change due to human interventions have been observed. Sufficient sediment supply may allow mangrove habitats to persist within the intertidal area whereas mangroves lacking sediment will suffer from prolonged inundation leading to die-off of mangrove fringes. For example, upstream dam constructions will restrict the sediment to reach the coasts (Syvitski et al., 2005), causing sediment deficit in the coastal area and limiting the surface sediment accretion. Thus, mangroves might be submerged and need to migrate to the landward area with higher bed elevation for a preference inundation regime. On the other hand, mangroves in some areas are identified as problematic due to their overwhelming seedling recruitment and vegetation reproduction, occupying a large area of estuaries and preventing the restoration of sandy flats. For instance, in the estuaries of North Island, New Zealand, deforestation and agricultural activity in upstream catchments enhance soil erosion rates and thus cause oversupply of sediment to the coasts, changing the original sandy flats to muddy environments, associated with the rapid expansion of mangrove forests, which dampens hydrodynamic forces and may contribute to mud deposition (Morrisey et al., 2007). Thus, local residents remove mangroves in order to restore sandy flats (Jones, 2008). In addition, coastal constructions, such as sea walls, dikes and other shoreline protection structures, will obstruct mangrove landward migration, when sea-level rise exceeds the change of bed elevation, resulting in a narrow mangrove fringe or even loss of mangrove community (Figure 1.2d) (Gilman et al., 2007; Phan et al., 2015). Taken together, to understand the fate of mangroves in the future, more research on mangroves response to climate change and human interventions is imperative.

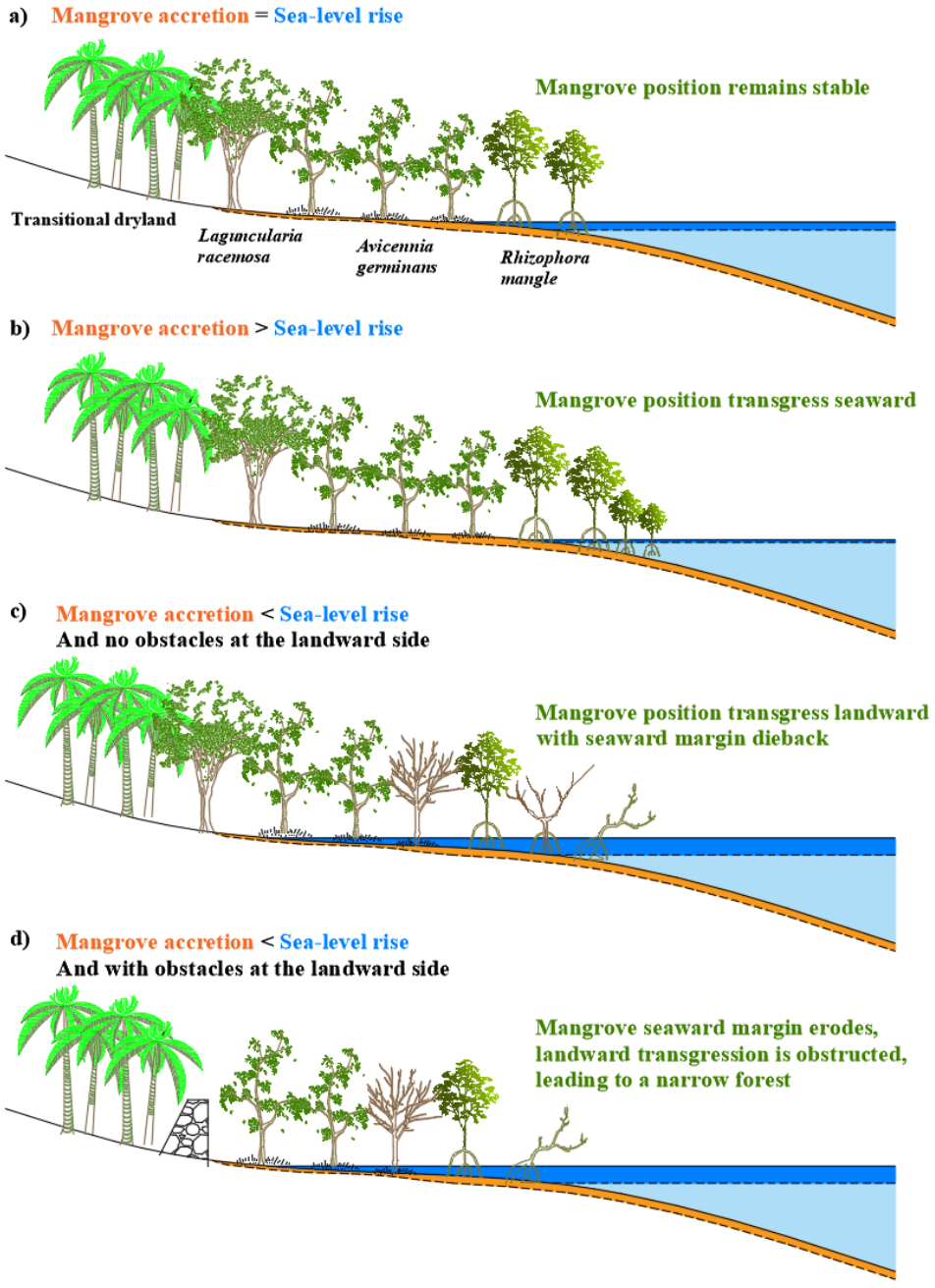

Figure 1.2 Four scenarios for generalized mangrove response to relative sea-level rise, taking into account the balance between mangrove accretion and sea-level rise, modified after Gilman et al. (2007)). Distinct mangrove species distribute across the coastal lines create a typical mangrove zonation system.

1.4 Bio-morphodynamic feedback processes

1.4.1 Mechanisms within mangrove systems

Coasts are generally subject to hydrodynamic drivers, such as tidal currents, waves and sometimes fluvial flows. The interplay between coastal morphology and hydrodynamic drivers affects the shapes and evolution of the geomorphic systems (Coco et al., 2013). Sediment transport processes, which determine topographic features, create a connection between hydrodynamic and morphodynamic processes. Traditional hydro-morphodynamic process models consist of three major components (i.e. hydrodynamics, sediment motion and morphological changes), in which hydrodynamic drivers modulate sediment motion, generating sediment erosion/deposition and resulting in morphological changes. In turn, the changes in morphology adjust the hydrodynamic forces and influence their capability to modulate sediment motion (Figure 1.3).

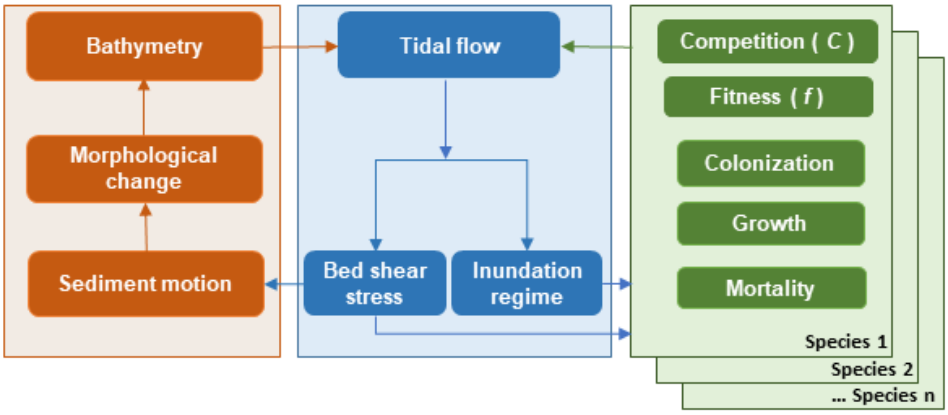

Figure 1.3 The connections of bio-morphodynamic processes, taking into account the traditional hydro-morphodynamic process and biological process, modified after Coco et al. (2013)

As soon as the coastal environment is suitable for the colonization of halophytic vegetation, which is determined by bed elevation, inundation regime and the strength of hydrodynamic drivers, there are chances for vegetation (e.g. salt marsh, mangroves and coral reefs) to settle and develop their own habitats (Balke et al., 2011; D'Alpaos, 2011). The presence of halophytic vegetation, has two-way biophysical interactions with hydro-morphodynamic processes, further referred to as bio-morphodynamic feedbacks (Zhou et al., 2016). A number of studies have shown that vegetation changes hydrodynamics and sediment transport. Locally, the presence of vegetation increases the bed roughness and flow resistance, resulting in a reduction of flow velocity and wave energy (Baptist et al., 2007; Nardin et al., 2016a). This will reduce the sediment transport capability in the water column and contribute the sediment to settle down on the profile. Besides, vegetation can directly interact with sediment transport processes by trapping sediment through their stems/leaves and enhance the soil stability against erosion. Profile elevation can also be modulated by the increase of their below-ground root volume, in particular in mangrove forests, which have numerous roots grown below the soil (Krauss et al., 2014). On the landscape scale, the presence of mangroves and local sedimentation influence the transport of currents across the plants, and sediment may vary along the coastal wetland depending on the spatial connections of flow and sediment. For example, pioneer mangroves with dense root structures dampen tidal currents and enhance sediment trapping, leading to a limited sediment availability in the upper land (Furukawa et al., 1997; Mazda et al., 1997b;

Kumara et al., 2010; Swales et al., 2019). In the meanwhile, the presence of vegetation also affects the flow in the channelized areas where vegetation is absent. Vegetation colonizing along the banks of channels provides extra hydraulic resistance on the flats, which focuses flow into channels (Kleinhans et al., 2018). However, channels would become shallower with more sedimentation when the adjacent plants are removed (Temmerman et al., 2012). Furthermore, the growth of vegetation may also increase sedimentation and create new habitats for associated species. In the Mekong Delta, Vietnam, the development of *Sonneratia spp.* mangroves, which are the natural pioneer species, facilitates initial sedimentation, creating suitable establishment conditions for secondary species, such as *Aegiceras corniculatum* and *Avicennia spp.* (Bullock et al., 2017). These feedbacks are applicable for a variety of organisms in the coastal wetland, such as microphytobenthos, seagrass, salt marsh, meiofauna and macrobenthos, which can all be 'ecosystem engineers' as introduced by Jones et al. (1994). They 'modify, maintain and create habitat' through changing the physical state of the ecosystem based on the availability of resources. Previously, mangroves were identified as ecosystem engineers to create intertidal habitats by dampening waves/flows and retain sediment (Carlton, 1974; Lugo, 1980; Woodroffe, 1993; Mazda et al., 1997b), however, recent work also indicated mangroves act as opportunistic colonizers, occupying intertidal areas after the bed level increased to a suitable situation for mangrove to settle (Swales et al., 2015; Glover et al., 2022).

On the other hand, changes in hydro-morphodynamic factors (such as tides, waves and sediment) will also affect vegetation distribution. Mangroves typically occur in the intertidal area between mean water level and mean high water level (Chapman, 1976). A recent field observation based on the southern coast of New South Wales, Australia indicates different inundation characteristics between mangroves and salt marshes, where mangroves are inundated approximately 15-70% of the time while salt marshes are submerged only <15% of the time (Kumbier et al., 2021). In addition to the coastal conditions created by hydro-morphodynamic processes which control vegetation distribution, the hydrodynamic information also affects the growth of vegetation. For example, mangrove forests have a preference on a particular inundation regime, either too dry or too wet conditions will limit their growth and even cause vegetation mortality (Chapman, 1976; Hoppe-Speer et al., 2011). The ending of tidal flooding along the mangrove forests due to sea level drops has been linked to one of the main factors leading to the great mangrove mortality in the Gulf of Carpentaria, Australia (Asbridge et al., 2019; Duke et al., 2021). In a multiple species mangrove zonation, the pioneer mangrove species can either enhance sedimentation trapping, causing upper flats sediment starvation, or dampen currents transport, causing upper flats to be less inundated. Such changes in hydrodynamic factors adjusted by pioneer species would indirectly affect the growth or mortality of upper land mangrove species (Horstman et al., 2018b). Therefore, two-way interactions between vegetation dynamics and hydro-morphodynamic processes control the evolution of coastal ecosystems, which should be taken into account when making predictions (Friess et al., 2019; Cahoon et al., 2020).

1.4.2 Bio-morphodynamic model approaches

In the past decades, a variety of wetland models have been developed to predict the future changes of coastal wetlands, in particular under sea-level rise and human interventions. One of the first attempts in the previous studies is to assume a uniform water level under sea-level rise without considering the friction and flow attenuation, known as 'bathtub model' (Traill et al., 2010; Boon et al., 2011) which fills the wetland like a bathtub where water level increases/decreases up/down. This approach used to be commonly undertaken as a first step in estimating the estuarine flooding under sea-level rise. Although bathtub models provide poor estimates of the likely impact of water level changes on wetland extent, its fast simulation causes this approach to be still used in current research, in particular for large-scale assessments (Menendez et al., 2018). However, the assumption of the bathtub model that friction and flow resistance are neglected during sea-level rise and vegetation presence is problematic. Sediment deposition is simply dependent on the duration of tidal

inundation. Coastal systems are found to be dynamic and wetland elevation changes due to external sediment deposition or internal sediment erosion (Rogers et al., 2012). To consider the changes of wetland surface elevation driven by sea-level rise, historical accretion rates have been used to infer the wetland vulnerability in the face of future sea-level rise (Orson et al., 1998; French, 2006). This is because most coastal wetland build vertically at the same speed or even exceed the rate of historical sea-level rise, but it still remains imperfect as human disturbances continue to change water environment and sediment availability, more importantly, the sea-level rise rate is predicted to become faster (Kirwan and Megonigal, 2013; Lambeck et al., 2014). Thus, wetland vulnerability assessment based on these empirical relations or constant historical accretion rates miss important feedbacks and therefore remain unreliable.

More recent modelling work has related the vertical accretion to wetland elevation (Akumu et al., 2011) and may further conjunct with measured sedimentation cores including sedimentation and organic accumulation (Rogers et al., 2012). Other models incorporate the sediment availability and combine the vertical accretion rate with inundation regime (Kirwan and Guntenspergen, 2010; D'Alpaos, 2011; Kirwan and Megonigal, 2013; Thorne et al., 2018). In each of these models, the wetland surface accretes at a rate determined by the duration of tidal inundation, which increases with sea-level rise. Therefore, sediment accretion rates are predicted to be a function of sea-level rise rates and thus wetlands are predicted to keep pace with sea-level rise before vegetation is over-flooded. However, these projections being a good first indication, still simplify the role of bio-morphological interactions (e.g. increased surface roughness) on sediment accretion and survival (Mazda et al., 1997b; Mazda et al., 2005; Baptist et al., 2007). Although some subsequent attempts adopt the approach that tidal currents along the flats are attenuated by wetland plants (Fagherazzi et al., 2012; Fagherazzi et al., 2017), they typically simplify sediment availability as a distance-related parameter (from channels) without considering the complex processes between erosion and sedimentation. The failure to incorporate biological feedbacks between wetland vegetation, tidal current movement, sediment transport and coastal morphological changes may lead to discrepancies among estimates of coastal vulnerability. For example, some regional or global-scale assessments conclude that coastal wetlands such as salt marshes and mangroves will be overwhelmed by rising sea levels in the foreseeable decades (Lovelock et al., 2015; Crosby et al., 2016; Spencer et al., 2016), while others project low loss of global wetlands (Kirwan et al., 2016a) or even gains when the same model is applied but landward habitats are available (DIVA model in Schuerch et al. (2018), compared with Spencer et al. (2016)). Thus, to better predict the impacts of sea-level rise on coastal systems, recent studies begin to highlight the necessity to further incorporate the complex linkages and feedbacks between physical and biological processes driving sediment changes and morphological evolution (Passeri et al., 2015; Friess et al., 2019; Cahoon et al., 2020).

Over recent years, a very noticeable trend for wetland model development exists characterized by including more complex processes, namely the bio-morphodynamic feedbacks between biologic, hydrodynamic and morphology changes (Nardin et al., 2016a; Best et al., 2018). Vegetation dynamics included in these bio-morphodynamic models have become more comprehensive to include colonization, growth and mortality, which strongly affect sedimentation and system evolution (van Oorschot et al., 2016; Schwarz et al., 2018; Brückner et al., 2019). This now opens possibilities to explore mangrove dynamics (van Maanen et al., 2015), study effects of multiple vegetation species (Bij de Vaate et al., 2020), evaluate effects of coastal conditions (Horstman et al., 2015; Belonje, 2019) and evaluate a broad range of human impacts (Zhang et al., 2019). While these models emphasize the non-linear feedbacks among wetland system evolution, we still lack sophisticated bio-morphodynamic model that capture complex mangrove behaviours at the large spatial and temporal scales of sea-level rise and human interventions.

1.4.3 Model approaches developed in this thesis

To gain a further insight in understanding how mangrove forests respond to sea-level rise and interact with the evolution of coastal morphology, I developed a novel bio-morphodynamic model based on the framework of Brückner et al. (2019) by improving mangrove models from van Maanen et al. (2015). Therefore, our mangrove models can simulate the response of mangrove behaviors involving profile changes under sea-level rise and human interventions. Throughout my thesis chapters, the mangrove models are improved to solve different research questions.

First, in Chapter 2, I developed a multi-species mangrove assemblage model that accounts for species-specific vegetation types and life-stages, such as colonization, growth and mortality (Figure 1.4). We couple our mangrove model with a widely-used hydro-morphodynamic model (i.e. Delft3D) so that 1) we can capture spatio-temporal variations in sediment availability across the tidal flats; 2) the survival of mangroves is highly dependent on environmental settings (i.e. tidal duration), and 3) mangrove coverage can in fact increase despite, or even because of, sea-level rise under sufficient sediment inputs and accommodation space. To my knowledge, this is the first study to resolve distinct behaviours of mangrove assemblages and related zonation patterns in response to sea-level rise. This approach is crucial and timely because it shows how important the mitigation actions are to reduce the loss in mangrove extent and mangrove diversity.

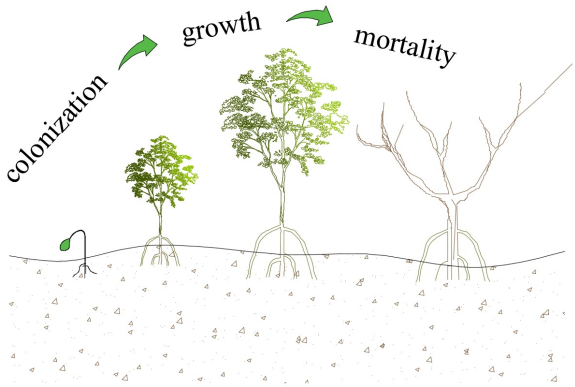

Figure 1.4 Life stages incorporated in the bio-morphodynamic model, including colonization, growth and mortality

Second, in Chapter 3, I included processes restricting colonization, which determines the settlement of mangrove seedlings under the control of inundation period and hydrodynamic forces, and extends the model to a broader range of coastal environmental conditions, including tides, small wind waves, sediment supply and coastal slopes, to study the future mangrove vulnerability under sea-level rise. In contrast to previous mangrove models, the approach in this study takes into account 1) multiple colonization restrictions that not only control initial mangrove colonization, but also the subsequent response to sea-level rise; 2) the possibility of coastal progradation and seaward mangrove expansion despite sea-level rise under high sediment supply; 3) modulation of tidal currents based on coastal profile evolution which in turn affects mangrove growth, and (4) profile reconfiguration under sea-level rise which may contribute to infilling of new accommodation space. It is vital to understand distinct mangrove behaviours controlled by non-linear relations between vegetation dynamics and profile evolution.

The two research steps in Chapters 2 and 3 are based on a one-dimensional setting with only one sediment type, mud. In Chapter 4, this bio-morphodynamic model is extended to a two-dimensional

domain to represent the effects of mud on mangrove expansion and human interventions on sediment sorting and landscape development. This model allows the formation of channels and mangrove distribution in different directions. Two different sediment classes, i.e. sand and mud, are applied in this model study. The impacts of human interventions, including the changes in fluvial sediment supply and estuary mangrove clearance, are investigated using this two-dimensional model. We show how coastal systems are modified by an excess mud supply and how the mangrove system can be modified by human interventions, such as a reduction of mud input and mangrove removal.

Overall, this novel mangrove model takes into account 1) the dynamics of multi-species mangrove assemblages, 2) colonization restrictions that control seedling settlement, 3) profile changes, 4) sediment transport processes and 5) interactions between vegetation dynamics and hydro-morphodynamic processes. As a result, we are able to study the interactions between mangrove forests and coastal environmental conditions under human interventions and climate changes, predicting potential changes of mangrove systems in the future.

1.5 Research questions and thesis outline

In this thesis, the aims are 1) to understand non-linear relations between mangrove dynamics and profile changes and 2) to predict the potential changes of mangrove systems under changing boundary conditions. The detailed research questions and thesis outlines are listed as follows:

Chapter 2 explores changes in mangrove forest extent and diversity under a broad range of sea-level rise rates and sediment supply conditions, both in the presence and absence of a tidal barrier (e.g. dike or seawall) that obstructs mangrove inland migration. The chapter quantifies how well multi-species mangrove assemblages are predicted by the model with the following specific research questions:

1) how do spatial-temporal variations in sediment dynamics control coastal profile evolution and species distribution?
2) how does the role of bio-morphodynamic feedbacks in determining system dynamics vary under different levels of environmental pressure, such as sea level, sediment availability and coastal accommodation space?
3) how does the presence of human constructions (such as dikes and seawalls) dictate hydro-sedimentary processes and mangrove survival (i.e. coastal squeeze) under sea-level rise?

Chapter 3 investigates how non-linear biophysical interactions control coastal profile evolution and mangrove coverage in the face of sea-level rise in various coastal environmental conditions. The chapter is a successor by covering a broad range of coastal conditions compared to the previous chapter, addressing the following specific research questions:

1) how do multiple colonization restrictions control initial mangrove colonization and potentially the subsequent mangrove response to sea-level rise?
2) how do coastal profile evolution and seaward mangroves respond under different combinations of sea-level rise and sediment availability among different coastal conditions?
3) how does profile reconfiguration affect coastal accommodation space and mangrove vulnerability?

Chapter 4 extends the one-dimensional model to a two-dimensional model and further elucidates the impacts of upstream land-use changes and human interventions on mangrove behaviours and coastal sediment composition. Since mangrove clearance has been launched as one of main approaches to restore sand flats, while the likelihood of successful restoration still remains unknown. The specific research questions addressed here are:

1) how do changes in the hinterland due to land use change of humans influence mangrove expansion, morphology evolution and sediment composition?
2) how does mangrove clearance affect morphological evolution and sediment distribution?
3) how will a back-barrier estuary system evolve in the future under human interference, such as continued high mud supply, vegetation clearance and reduced mud supply?

Finally, Chapter 5 summarizes the main findings of this thesis in the context of the literature, and discusses specific needs for future research.


2

Chapter 2 | Mangrove diversity loss under sea-level rise triggered by bio-morphodynamic feedbacks and anthropogenic pressures

Abstract

Mangrove forests are valuable ecosystems, but their extent and diversity are increasingly threatened by sea-level rise and anthropogenic pressures. Here we develop a bio-morphodynamic model that captures the interaction between multiple mangrove species and hydro-sedimentary processes across a dynamic coastal profile. Numerical experiments are conducted to elucidate the response of mangrove assemblages under a range of sea-level rise and sediment supply conditions, both in the absence and presence of anthropogenic barriers impeding inland migration. We find that mangrove coverage can increase despite sea-level rise if sediment supply is sufficient and landward accommodation space is available. Tidal barriers are mainly detrimental to mangrove coverage and result in species loss. Importantly, we show that bio-morphodynamic feedbacks can cause spatio-temporal variations in sediment delivery across the forest, leading to upper-forest sediment starvation and reduced deposition despite extended inundation. As such, bio-morphodynamic feedbacks can decouple accretion rates from inundation time, altering mangrove habitat conditions and causing mangrove diversity loss even when total forest coverage remains constant or is increasing. A further examination of bio-morphodynamic feedback strength reveals that vegetation-induced flow resistance linked to mangrove root density is a major factor steering the inundation-accretion decoupling and as such species distribution. Our findings have important implications for ecosystem vulnerability assessments, which should account for the interactions between bio-morphodynamics and mangrove diversity when evaluating the impacts of sea-level rise on species assemblages.

Published as: Xie, D., Schwarz, C., Brückner, M. Z. M., Kleinhans, M. G., Urrego, D. H., Zhou, Z., & van Maanen, B. (2020). Mangrove diversity loss under sea-level rise triggered by bio-morphodynamic feedbacks and anthropogenic pressures. *Environmental Research Letters, 15(11), 114033.* DOI: https://doi.org/10.1088/1748-9326/abc122.

2.1 Introduction

Mangrove forests are found along tropical and subtropical shorelines and typically show distinct zonation patterns, with each zone being characterized by a dominant mangrove species (Duke et al., 1998; Tomlinson, 2016). However, mangrove zonation not only implies changes in species but also in biophysical tree characteristics. Mangrove species along the intertidal gradient show great differences in both aerial root structure and density, which allows them to survive under specific inundation regimes (Chapman, 1976; Duke et al., 1998). Sea-level rise may modify the inundation time along mangrove habitats thereby potentially altering forest width, zonation and thus species diversity (Duke et al., 2007). Shrinking mangrove forests have raised concern on the loss of individual mangrove species, especially as even pristine mangrove forests are species-poor compared with other tropical ecosystems and because these systems are subject to 'coastal squeeze' (Alongi, 2002; Gilman et al., 2008). Mangroves provide valuable ecosystem services, including carbon sequestration, coastal protection and habitat provision for a plethora of organisms in some, or all life stages (Kathiresan and Rajendran, 2005; Aburto-Oropeza et al., 2008; Alongi, 2014). As the provision of ecosystem services is highly dependent on the composition of mangrove species assemblages, the loss of species diversity can have dramatic economic and environmental consequences for coastal communities (Duke et al., 2007; Polidoro et al., 2010). Improving our ability to predict the response of mangrove assemblages and zonation to external pressures is thus urgently needed (Jennerjahn et al., 2017).

Predicting the fate of mangrove forests is hampered by a limited representation of bio-morphodynamic feedbacks in numerical models, especially in the case of multiple co-existing mangrove species (Tomlinson, 2016; Fagherazzi et al., 2007). Here, bio-morphodynamic feedbacks are considered as the physical effects of mangrove trees on tidal currents, sedimentation/erosion patterns and hydroperiods, which in turn affect tree growth and species distribution. So far, models evaluating wetland resilience to sea-level rise have primarily focused on parameterized processes controlling vertical accretion and the ability of wetlands to counteract rising water levels through enhanced sediment deposition (Kirwan and Guntenspergen, 2010; Fagherazzi et al., 2012; Mogensen and Rogers, 2018; Schuerch et al., 2018). Other recent approaches include a more comprehensive treatment of sediment transport and morphological processes but focus on single-species dominated saltmarsh systems (Zhou et al., 2016; Mariotti and Canestrelli, 2017). Developing reliable projections for mangrove assemblages requires capturing the interaction between hydro-sedimentary processes across the mangrove forest, multi-species vegetation growth and coastal profile change. Such bio-morphodynamic feedbacks depend on vegetation properties and the coastal setting but may also be greatly affected by sea-level rise and anthropogenic interventions including changes in sediment supply and lateral accommodation space, the latter describing the upland space available for vegetation colonization (Schuerch et al., 2018).

Here we present a novel modelling approach by coupling a detailed hydro-morphodynamic model that computes the deposition, erosion and transport of sediment across the coastal profile with a newly developed vegetation model that captures the dynamics of mangrove species occupying the lower, middle and upper intertidal area (Figure 2.1). As such, we account for sediment transport between different vegetation zones and potential spatio-temporal variations in sediment availability. We conduct numerical experiments to systematically explore changes in mangrove forest extent and diversity under a broad range of sea-level rise rates and sediment supply conditions, both in the absence and presence of a tidal barrier (e.g. dike or seawall) that obstructs inland migration. This enables us to investigate for the first time shifts in mangrove species zonation linked to a dynamic coastal profile, differences in lateral accommodation space (i.e. possibility of coastal progradation and landward migration) and mangrove properties (i.e. root density).

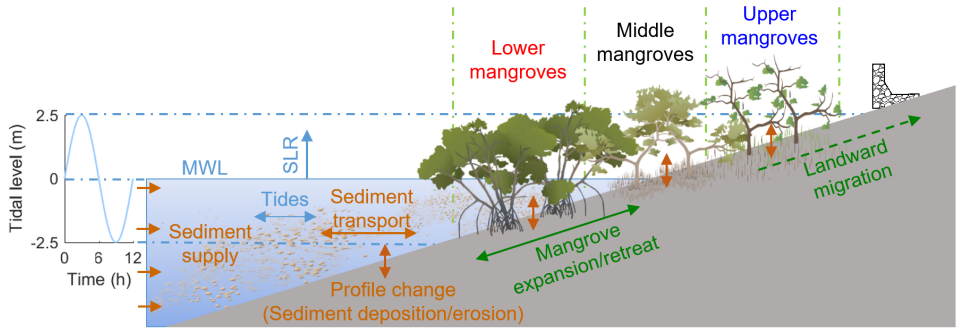

Figure 2.1 Schematic overview of the bio-morphodynamic modelling approach. The model captures interactions between multi-species mangrove assemblages colonizing the lower, middle and upper intertidal area (hereafter referred to as lower mangroves, middle mangroves and upper mangroves, respectively), hydro-sedimentary processes and coastal profile evolution. MWL and SLR represent mean water level and sea-level rise, respectively.

2.2 Methods

Mangrove and coastal profile dynamics are simulated by coupling an open-source hydro-morphodynamic model (Delft3D) (Lesser et al., 2004; Brückner et al., 2019) to a new dynamic vegetation model that considers multiple mangrove species thriving at specific inundation regimes. Information on local hydroperiod generated by the hydro-morphodynamic model is provided to the vegetation model controlling colonization, growth and mortality of mangrove trees. In turn, the vegetation model provides information on the dimensions and densities of vegetation objects to the hydro-morphodynamic model so that the effect of mangroves on tidal flow and consequently sediment transport is accounted for (Figure 2.6). Although organic matter accretion within mangrove forests is known to increase resilience to sea-level rise (Krauss et al., 2014; Woodroffe et al., 2016), this process is not included here as we focus on the role of above-ground bio-morphodynamic feedbacks, thus providing conservative estimates on mangrove survival. Also, rather than simulating particular mangrove sites, we use simplified forcing conditions and parameterizations to describe forest characteristics, in order to explore distinct mangrove behaviours and identify the driving processes behind changes in mangrove extent, zonation and thus diversity under a broad range of environmental conditions.

2.2.1 Model description

To effectively capture mangrove lateral movement and changes in mangrove zonation, a one-dimensional cross-shore profile modelling strategy is used, assuming alongshore uniformity and absence of tidal channels (Roberts et al., 2000; Zhou et al., 2016). A detailed overview of the governing equations is provided in the supporting information (Sections 2.5.2 and 2.5.3). Tidal flow, sediment transport and bathymetric changes are calculated by the Delft3D model suite (Lesser et al., 2004). Delft3D has been successfully applied in the past to investigate the evolution of vegetated muddy coasts (Zhou et al., 2016).The presence of mangrove vegetation is incorporated by increasing flow resistance (Baptist et al., 2007). We consider pure cohesive sediment as mangroves commonly thrive in muddy environments (Woodroffe et al., 2016).

Based on earlier work on single-species mangrove modelling (van Maanen et al., 2015), we developed a dynamic vegetation model considering mangrove assemblages growing along intertidal gradients and interacting with morphological change. We selected three species, namely *Rhizophora mangle*, *Avicennia germinans* and *Laguncularia racemosa*, to represent lower, middle and upper

intertidal mangroves, respectively (Figure 2.6). These species were chosen as they are known to thrive at different elevations (Lugo and Snedaker, 1974; Chapman, 1976; Duke et al., 1998) and detailed information on their growth parameters is available (Chen and Twilley, 1998; Berger and Hildenbrandt, 2000; Komiyama et al., 2008). Even though these specific species are adopted, our study also investigates the sensitivity to species characteristics (i.e. species distribution criteria and root densities) and therefore provides general insights on bio-morphodynamic interactions within mangrove assemblages.

Mangrove tree growth is represented by increasing stem diameter (D_i; cm) (Chen and Twilley, 1998; Berger and Hildenbrandt, 2000; van Maanen et al., 2015):

$$\frac{dD_i}{dt} = \frac{G_i D_i \left(1 - \dfrac{D_i H_i}{D_{max,i} H_{max,i}}\right)}{(274 + 3b_{2i} D_i - 4b_{3i} D_i^2)} \cdot f_i \cdot C \tag{2.1}$$

where *t* is time (years), $D_{max,i}$ and $H_{max,i}$ are the species-specific maximum stem diameter and tree height, respectively. G_i, b_{2i} and b_{3i} are growth parameters. As such, the first term on the right-hand side of Equation 2.1 describes optimal tree growth rates based on the actual stem diameter and tree height. Tree growth rates may be reduced under sub-optimal inundation conditions or because of limited resources through vegetation competition effects. This is incorporated through species-specific fitness functions (f_i) and a competition stress factor (C) which are included as additional terms in Equation (2.1) (van Maanen et al., 2015; D'Alpaos and Marani, 2016). f_i is dependent on inundation conditions (computed by Delft3D) and specifies that each species has an optimal hydroperiod for growth, while C is dependent on mangrove biomass (Figure 2.7). Thus, if f_i=1 and C=1 then tree growth is optimal; while lower values mean that tree growth is limited by inundation stress and competition. These two parameters also control mangrove colonization and mortality such that the habitat of mangroves is restricted to intertidal areas and sea-level rise can cause mangrove dieback through extensive inundation. Finally, the model includes a description of mangrove root densities by relating the number of root elements to stem diameter and define a species-specific maximum number of elements per tree (Figure 2.8 and Section 2.5.3). The diameter, height and density of stems and aerial roots, both of which are simplified as cylindrical objects, are then used by Delft3D to compute additional flow resistance (Equations 2.5 and 2.6). Since species-dominance and their accompanied root structures vary greatly across mangrove ecosystems, we also investigate the impact of root density on mangrove forest evolution and thus provide deeper insights into the role of bio-morphodynamic feedbacks in response to environmental factors.

To quantify mangrove diversity across the intertidal gradient, we developed a customized index, named the assemblage diversity index (ADI):

$$ADI = \sum_{i=1}^{n} p_i \cdot \ln p_i \tag{2.2}$$

The ADI is based on the Shannon's index (Hill, 1973; Spellerberg and Fedor, 2003), but here p_i represents the cross-shore extent of species *i* relative to the total forest extent. The above index uses the proportional extent of each species to provide a measure of diversity, accounting for both species richness and evenness along the cross-shore profile (Peet, 1974). Thus, the value of ADI increases, and so does diversity, if the number of species present within the forest increases (increased species richness) and/or if their relative abundance becomes more similar (increased evenness). Accordingly, the maximum value of the ADI in our research is expected to reach 1.1 (when $p1 = p2 = p3 = 1/3$) while the minimum value is 0 when only one mangrove species is present. In our study we use the ADI as a post-processing step to effectively capture diversity changes in a single number that can be easily evaluated over time.

2.2.2 Design of model simulations

Mangrove environments are highly variable and although we do not simulate specific sites, we design our model simulations based on existing literature describing mangrove growth conditions. As such, an initial bed slope of 1/1000 is adopted based on field observations (Lovelock et al., 2010; Phan et al., 2015; Bryan et al., 2017). This slope is also close to the equilibrium profile under current model settings, according to preliminary tests. The model is forced by semidiurnal tides of 2.5 m amplitude. Such settings provide a greater mangrove extent, thus helping to study the changes in mangrove zonation as well as in the coastal profile (Ellison, 2015). We adopted a 50 m by 50 m grid size as such a resolution is commonly used in morphodynamic modelling and captures coastal profile and vegetation dynamics (Zhou et al., 2016), while at the same time guaranteeing a reasonable simulation efficiency so that a large number of scenarios can be evaluated. An overview of the model settings is presented in the Table 2.1 and Table 2.2 on Supplementary Section 2.5.

We investigate the response of mangrove assemblages to environmental change through a series of simulations with different combinations of sea-level rise rate and sediment supply, both in the absence and presence of a tidal barrier. For practical reasons we use two different domain sizes for scenarios with and without a barrier (Figure 2.9). To focus on non-linear bio-morphodynamic feedbacks, sea-level rise rates are assumed constant through time varying from 0 to 10 mm/year covering the range of IPCC RCP2.6 to RCP8.5 sea-level rise estimates towards the end of this century (Oppenheimer et al., 2019). Rising sea levels are incorporated by incrementally raising the water level (η in Equation 2.3) at the seaward boundary. Variations in sediment supply are imposed by varying suspended sediment concentrations at the offshore boundary from 0 to 50 mg/L (Lovelock et al., 2015). Simulations are conducted for a period of 330 years. The first 30 years are used as an adaptation period during which mangroves can settle, allowing the analysis of mangrove assemblage dynamics over the remaining 300 years. The model tracks key forest characteristics, including tree density, type of species, stem diameter, tree height and associated biomass. We here focus on changes in total forest coverage and species distribution (i.e. ADI).

2.3 Results

2.3.1 Mangrove coverage and diversity under environmental change

To explore distinct mangrove responses, we first considered extreme combinations in sea-level rise rate and sediment supply. A high sea-level rise rate (10 mm/yr) and low sediment supply (10 mg/L) led to retreat of the mangrove forest over time (Figure 2.2(a) and (b)). In the absence of a tidal barrier all mangrove species could shift upland (ADI$\sim$1.1) (Figure 2.2(a)), whereas the presence of a tidal barrier led to a reduction in forest extent and loss of the middle and upper mangroves (ADI$\sim$0.6) (Figure 2.2(b)). Under intermediate to high sea-level rise rates (4 mm/yr for no barrier; 10mm/yr for barrier) and intermediate sediment supply (25 mg/L), sea-level rise was balanced by vertical accretion, keeping the forest seaward edge relatively stable (Figure 2.2(c) and (d)). This led to an increased forest extent due to landward migration and stable ADI in the absence of a tidal barrier (Figure 2.2(c)). When inland migration was restricted, forest extent remained constant through larger vertical accretion compared to the scenario without a barrier, but a redistribution in mangrove species resulted in a lower ADI (Figure 2.2(d)). Under low sea-level rise (2 mm/yr) and high sediment supply (50 mg/L), coastal progradation was possible and this caused seaward mangrove expansion. Even though both scenarios with and without barrier showed an increasing forest extent, a reduction in ADI occurred because of the increased dominance of lower mangroves and a reduced extent of upper mangroves (Figure 2.2(e) and (f)).

We then considered the full range of simulated sea-level rise (0-10 mm/yr) and sediment supply (0-50 mg/L) combinations to provide a clear overview of conditions that led to the above described

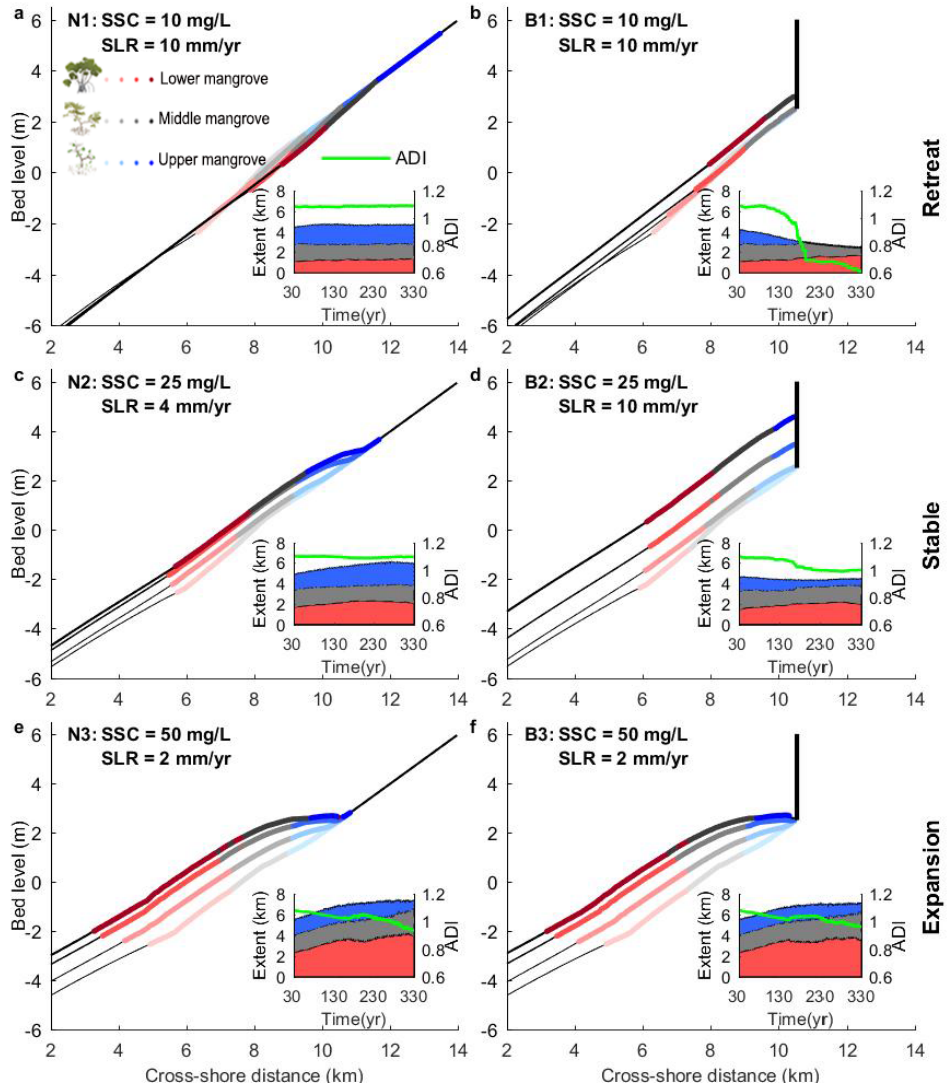

Figure 2.2 Distinct forest behaviours in response to different combinations of sea-level rise and sediment supply (left panels: without barrier; right panels: with barrier). (a,b) Landward retreat of mangrove species. (c,d) Temporal stability of the seaward forest edge. (e,f) Seaward expansion of the mangrove forest. Evolution of the coastal profile and mangrove forest are shown after 30, 100, 200 and 300 years (shaded lines). Red, black and blue colours indicate where lower, middle and upper mangroves are dominant, respectively, with increasingly darker shades representing temporal evolution. Multiple species may co-exist within a grid cell and dominance is then defined as the species with the largest biomass. The inserts show changes in the extent of each species and the green lines represent changes in ADI. SSC represents external suspended sediment concentration. The labels refer to 'No Barrier' (N1-3) and 'Barrier' (B1-3) and are further used in figure 3 to identify the corresponding scenarios.

mangrove behaviours (retreat, stable and expansion), and to identify when losses in diversity and mangrove extent were most significant (Figure 2.3). In the presence of a tidal barrier (Figure 2.3(b),

(d), (f) and (h)), changes in the mangrove seaward edge, forest extent, and mangrove diversity (ADI) followed a similar pattern. High sea-level rise rates combined with reduced sediment supplies led to increased landward retreat and forest shrinkage (both up to 8 m/yr), and a strong decrease in ADI (up to 0.4 reduction) (Figure 2.3(b), (f) and (h) B1). In contrast, low sea-level rise rates and high sediment supplies allowed for seaward expansion and an increase in mangrove forest extent (both up to 6 m/yr), with only minor changes in ADI (up to 0.08 reduction) (Figure 2.3(b), (f) and (h) B3). In the absence of a tidal barrier, changes in the mangrove seaward edge did not show the same trend in response to sea-level rise and sediment supply as the mangrove forest extent and mangrove diversity (Figure 2.3(a), (c), (e) and (g)). Although an increasing/decreasing sea-level rise rate and decreasing/increasing sediment supply resulted in increasing mangrove landward retreat/seaward expansion (Figure 2.3(a) N1 and N3), forest extent was mainly increasing especially with higher sediment supplies (> 6 m/yr) (Figure 2.3(e)). Mangrove diversity remained mainly stable when there was no tidal barrier present and only exhibited a slight decrease for combinations of low sea-level rise rates and high sediment supplies (Figure 2.3(g) N3). This particular ADI reduction, however, was independent from the presence of a tidal barrier (Figure 2.3(g) N3 and (h) B3) and was caused by the aforementioned coastal progradation with lower mangroves rapidly expanding while upper mangroves were overtaken by middle mangroves (Figure 2.2(e) and (f)).

Our simulations further showed that with comparable sediment supply, the presence of a barrier enabled mean seaward expansion under higher rates of sea-level rise in comparison to the scenarios without a barrier (Figure 2.3(a) and (b)). Investigation of temporal changes in the lateral movement of the forests over the 300-year simulation period revealed that the forest sea edge could shift from seaward expansion to landward retreat, or vice versa (green area in Figure 2.3(c) and (d)). The presence of a barrier in this context reduced the parameter space that led to directional shifts and, as a consequence, the likelihood for continuous seaward expansion increased (red area in Figure 2.3(c) and (d)). Nevertheless, loss in mangrove diversity and forest extent was more pronounced in the scenarios with a barrier.

2.3.2 Mangrove dynamics driven by bio-morphodynamic feedbacks

To unravel the bio-morphodynamic feedbacks that govern species-specific responses, we also assessed how key physical variables changed in the scenario with low sea-level rise (2 mm/yr) and high sediment supply (50 mg/L) as this resulted in diversity loss while overall mangrove extent was increasing (Figure 2.4). First, we focused on mangrove behaviours and related bio-morphodynamic processes in the simulation with original root settings (first column of Figure 2.4; Figure 2.8). In all regions of the mangrove forest, sediment accretion was initially well above the sea-level rise rate (around 10-15 mm/yr) (Figure 2.4(e)). Accretion then slowed down but it continued to outpace sea-level rise in the lower forest. In the upper forest, reduced accretion caused a gradually flattening profile and a progressively increasing inundation regime (blue line in Figure 2.4(i)). Such prolonged inundation was expected to trigger accelerated surface elevation gain through enhanced sediment deposition, thus promoting wetland stability. However, our results showed a contrasting response that emerged from temporal changes in sediment delivery towards the upper part of the mangrove forest. Over time, advection of suspended material diminished because tidal currents were being dissipated more strongly as the mangroves expanded seaward (Figure 2.4(q); Figure 2.12). Thus, while inundation periods increased in the upper forest (from 0.3 to 0.6) (Figure 2.4(i)), bed level accretion was hindered as sediment availability became limited (from 5 to 0 mg/L) (Figure 2.4(m)). This caused a shift in species occurrence where middle mangroves replaced upper mangroves. The transition to supply-limited conditions occurred under constant sea-level rise and external sediment supply and was thus purely controlled by internal system dynamics. Essentially, the lower mangroves expanded, and by mediating the physical processes they reduced the extent of upper mangroves, implying that indirect species interactions played a critical role in driving forest diversity changes.

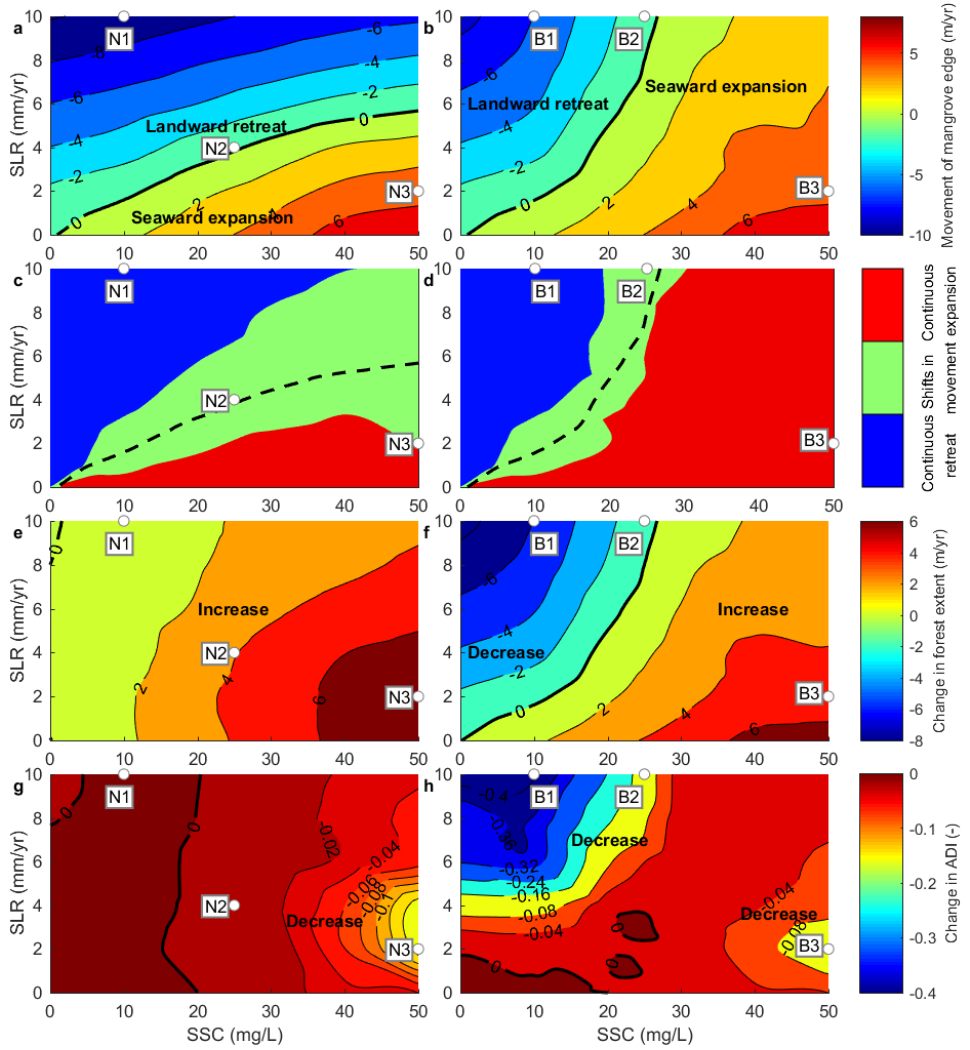

Figure 2.3 Changes in mangrove forest characteristics as a function of sediment supply, sea-level rise rates and lateral accommodation space (left panels: without barrier; right panels: with barrier). (a,b) Mean movement of the seaward forest edge averaged over 300 years. (c,d) Temporal evolution of the seaward forest edge, where green represents shifts from expansion to retreat, or vice versa. Red and blue indicate continuous expansion and retreat, respectively. For analysis, see Figures 2.10 and 2.11. The dashed lines represent a stable seaward edge when evaluated over 300 years and correspond to the 0 m/yr contour lines in a and b. (e,f) Change in total forest extent averaged over 300 years. (g,h) Change in ADI over 300 years. The labels indicate combinations of sediment supply and sea-level rise for which simulations are shown in detail in Figure 2.2.

Model simulations indicated that forest behaviours regarding mangrove seaward and landward movement (Figure 2.2) remained consistent under the additional sensitivity runs with different species distribution criteria and root densities (Figures 2.13 and 2.14). However, interestingly, root density exerted a major influence on the ADI in the case of coastal progradation and seaward mangrove expansion, where higher root densities caused a greater loss of diversity (Figure 2.14(m)-(p)). Although general accretion trends along the profile and through time were

comparable among different root settings, the maximum accretion rate increased with increasing root density (Figure 2.4(f)-(h)) and overall deposition in the lower and middle intertidal area was approximately half a meter more under higher root densities (Figure 2.4(b)-(d) and Figure 2.15). Increased root density accelerated mangrove seaward expansion, but it thus also reduced the extent of upper mangroves at a faster rate (Figure 2.4(b)-(d)). Although accretion was typically slower under low root densities, it was also more uniform across the forest and profile flattening was therefore less profound (Figure 2.4(b) and Figure 2.15). In contrast to the scenarios with higher root densities where hydroperiods increased in the upper forest causing changes in dominant species, hydroperiods decreased throughout the entire forest when root density was low (Figure 2.4(j)) and species distributions remained relatively constant.

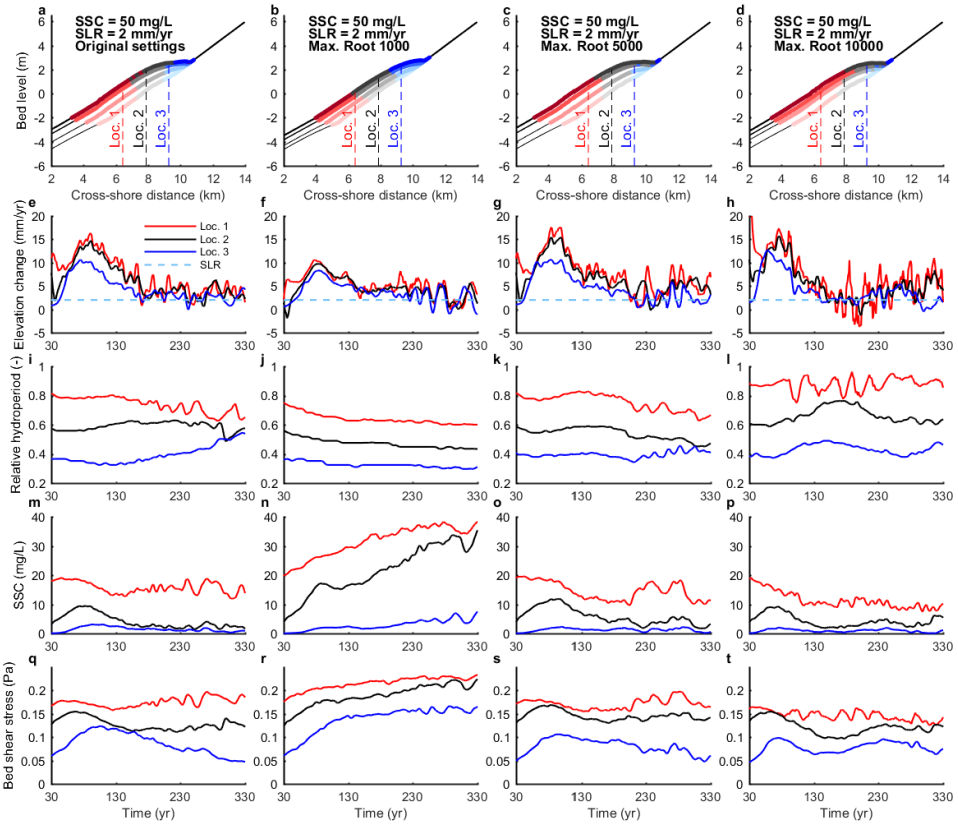

Figure 2.4 Spatio-temporal changes in key physical variables controlling mangrove forest zonation under different root densities. First column shows the simulation with original root settings, whereby the maximum number of root elements per tree varies for each species and is set to 5000, 10000 and 1000 for the lower, middle and upper mangroves, respectively. Second, third and fourth columns show simulations when the maximum number of root elements per tree is species-independent and set to 1000, 5000 and 10000, respectively. (a-d) Mangrove assemblage after 30, 100, 200, 300 years. Dashed lines indicate locations which are representative for different regions within the forest and from which physical variables have been extracted. (e-h) Bed elevation change, where positive values indicate accretion and negative values indicate erosion. Dashed line represents the sea-level rise rate. (i-l) Relative hydroperiod (whereby 0 implies never inundated and 1 implies permanently inundated). (m-p) Suspended sediment concentration. (q-t) Bed shear stress.

2.4 Discussion and conclusions

To summarize the findings of our numerical experiments, we propose a conceptual model to illustrate the response of mangrove assemblages and related bio-morphodynamic feedbacks under low and high environmental pressures, represented by different combinations of sea-level rise and sediment supply (Figure 2.5). We demonstrate that under low sea-level rise rates and high sediment supplies, system dynamics are dominated by coastal progradation and seaward mangrove expansion, while anthropogenic barriers exert little stress. As our approach uses idealized numerical simulations to unravel the controlling processes driving changes in mangrove forests, model testing should involve an evaluation of model behaviours and trends (Murray, 2013). In this context, our simulations of seaward mangrove expansion are in agreement with observations at locations that experience large sediment inputs (Anthony et al., 2010; Lovelock et al., 2010; Nardin et al., 2016b; Liu et al., 2018). In such settings, mangroves are able to colonize elevated mudflats, stressing the importance of hydro-sedimentary processes in the unvegetated intertidal area fringing the mangrove forest combined with dynamic vegetation growth. In northern Australia, mangrove coverage along particular coastal sections has recently increased not only through seaward but also landward expansion, the latter being driven by the combined effects of sea-level rise and prolonged inundation of coastal lowlands (Asbridge et al., 2016). Our modelled scenarios qualitatively capture such behaviours and, in addition, they highlight the conditions that can lead to sea-level rise driven expansion of mangrove forests.

What is more, at low environmental pressures, the bio-morphodynamic feedback, whereby vegetation influences hydro-sedimentary processes and morphological evolution in turn affects vegetation growth, plays a key role in driving mangrove species distributions. Our model results indicate that the density of root elements, and thus the strength of biotic interactions, will influence this feedback and steer changes in diversity. For the same environmental conditions, sparse roots allow more sediment to be transported towards the upper region of the forest as tidal currents are stronger, causing a uniform accretion across the forest such that coastal profile shape and species zonation remain relatively stable. Dense root structures, as also supported by field studies (Furukawa et al., 1997; Mazda et al., 1997b; Kumara et al., 2010; Swales et al., 2019), cause dampening of tidal currents and enhance sediment trapping, and this may then lead to upper-forest sediment starvation. Here we show that such interactions can cause variations in accretion across the forest resulting in profile change and, more importantly, trigger diversity loss (Figure 2.5). Bio-morphodynamic feedbacks thus generally promote vertical accretion and seaward expansion, which enhance overall forest resilience, but at the same time these feedbacks reduce sediment delivery to the more landward region of the forest, thus preventing upper species to capture sediment with sea level rise and making them more vulnerable to be replaced by species adapted to higher inundation time.

Under high environmental pressures, when sea-level rise is fast and sediment input is low, mangrove behaviours are mainly controlled by the abiotic drivers (i.e. enhanced inundation caused by sea-level rise) instead of bio-morphodynamic feedbacks. Hereby the presence of anthropogenic barriers exerts a major impact on the fate of mangrove assemblages. Barriers prove to be mainly detrimental for both mangrove coverage and diversity while species distributions can remain stable if landward habitat is available (Figure 2.5). Globally, anthropogenic activities, including urbanization and the construction of flood protection works, heavily impact coastal ecosystem resilience with an estimated loss of up to 30% of wetland area within this century if no further lateral accommodation space is created (Schuerch et al., 2018). Clearly, for coastal systems where sediment supplies are in decline and losses are irrevocable, removing barriers that obstruct inland migration is of critical importance to safeguard mangrove survival.

The degree to which such bio-morphodynamic feedbacks and anthropogenic pressures control wetland behaviour may rely on wetland characteristics (e.g. vegetation type and density, surface area

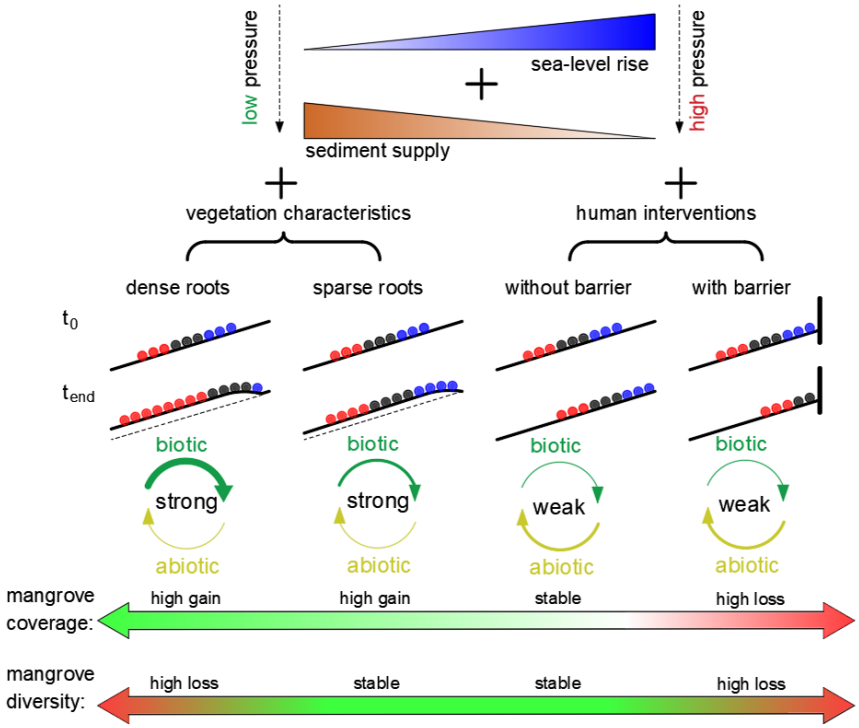

Figure 2.5 Conceptual model showing the response of mangrove assemblages under different sea-level rise and sediment supply conditions. Under low environmental pressures, profile and vegetation distribution changes are determined by vegetation characteristics while assemblage behaviours under high environmental pressures are mainly impacted by the presence or absence of anthropogenic barriers. The role of bio-morpodynamic feedbacks on system dynamics is indicated (i.e. 'strong' versus 'weak') and arrow thickness represents the relative strengths of biotic and abiotic interactions.

and slope) and hydrodynamic forcing (e.g. tidal range, waves) and thus depends on the overall bio-geomorpholocial setting (Balke and Friess, 2016; Woodroffe et al., 2016; Bryan et al., 2017). As such, parameterizing our model for a range of real world mangrove settings to predict mangrove responses at specific field sites should be further explored in the future. In addition, sub-surface processes can play an important role in controlling substrate elevation change and wetland resilience (Krauss et al., 2014). Mangrove root accumulation helps raising bed elevations (McKee et al., 2007; McKee, 2011), which is not included here. Our modelling approach may therefore underestimate the ability of mangrove forests to cope with sea-level rise. However, subsidence due to decomposition and sediment autocompaction limits mangrove elevation gain (Rogers et al., 2005). The mechanisms governing subsurface processes are still not fully understood and the net effect is highly dependent on site conditions (Krauss et al., 2014; Sasmito et al., 2016). As such, our model focusses on above-ground interactions between vegetation and hydro-sedimentary processes and provides new insights into the dynamics that govern bio-morphological response to changing environmental drivers.

Our results indicate that above-ground bio-morphodynamic feedbacks cause spatio-temporal variations in sediment accretion. As mangrove vegetation modulates tidal currents, transport of sediment inland is reduced resulting in varying accretion rates across the mangrove forest. Our

simulations show this can cause counterintuitive behaviours with respect to sea-level rise as accretion rates and inundation time are being decoupled. As such, wetland accretion may fail to accelerate despite extended inundation and, in the longer term, this can cause a loss in mangrove diversity. Changes in mangrove coverage and composition are of course also affected by other major drivers, including mangrove poleward migration with the potential of mangroves encroaching into salt marsh areas (Saintilan et al., 2014). A bio-morphodynamic modelling approach, as presented here, will be useful to study the loss or gain in coastal ecosystem diversity in the face of such global change impacts.

Overall, our study implies that projections of mangrove assemblages in the face of sea-level rise need to capture the complex interactions between multi-species mangrove dynamics and hydro-sedimentary processes across the coastal profile, as well as the impacts of surrounding anthropogenic conditions. As the loss of mangrove species will have dramatic ecological and economic implications, comprehensive evaluations of species-specific responses are crucial in order to evaluate the future extent and diversity of mangrove forests, and to develop nature-based, integrated coastal zone management approaches to protect these vulnerable ecosystems.

2.5 Supplementary material

This Supplementary material includes ten supplementary figures (Figure 2.6 to Figure 2.15), detailed information on the hydro-morphodynamic model (Section 2.5.2) and dynamic vegetation model (Section 2.5.3), and an overview of model parameter settings (Table 2.1 and Table 2.2).

2.5.1 Supplementary figures

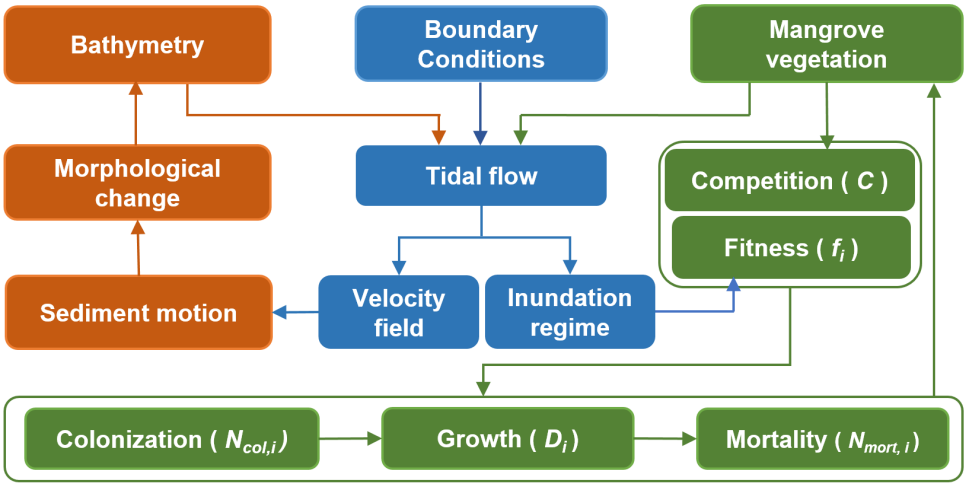

Figure 2.6 Overview of bio-morphodynamic interactions incorporated into the model. The modelling approach couples a hydro-morphodynamic model and a new dynamic vegetation model so that the interaction between tidal flow, sediment motion, morphological change and mangrove vegetation can be investigated. The vegetation model receives information on the inundation regime from the hydro-morphodynamic model and then regulates the colonization, growth and mortality of species-specific mangrove trees. Information on mangrove vegetation characteristics is in turn exchanged with the hydro-morphodynamic model which then accounts for vegetation effects on tidal flow resistance.

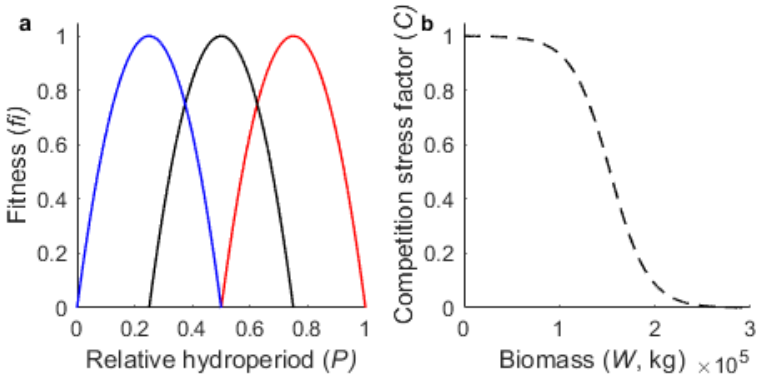

Figure 2.7 Growth control factors used in the vegetation model. (a) Multi-species fitness functions, characterised by different optimal relative hydroperiods (P = 0 implies never inundated; P = 1 implies permanently inundated). Red, black and blue lines represent the fitness of lower (i.e. *Rhizophora mangle*), middle (i.e. *Avicennia germinans*) and upper mangroves (i.e. *Laguncularia racemosa*), respectively. (b) Competition stress factor representing the influence of vegetation population on growth conditions as neighbouring trees have to share resources.

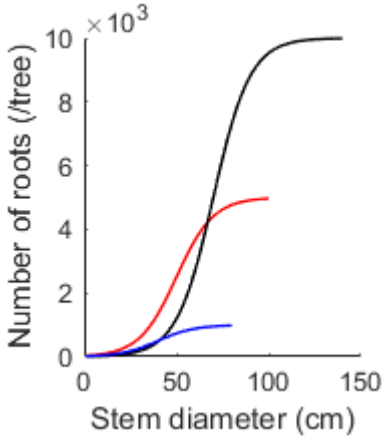

Figure 2.8 Species-specific number of root elements per tree as a function of mangrove stem diameter. Red, black and blue lines represent lower, middle and upper mangroves. The maximum number of elements per tree varies in order to represent species-specific differences in root structures. Additional simulations are conducted to study the effects of root densities (Figure 2.14).

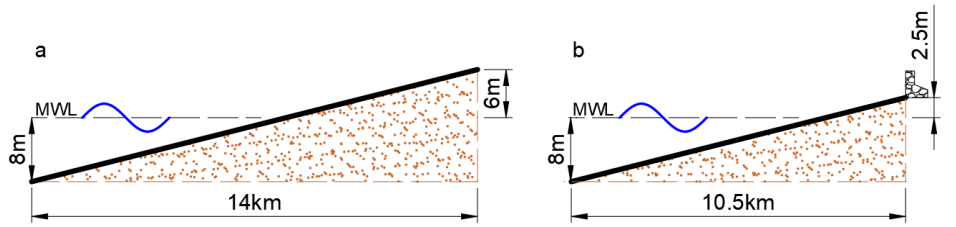

Figure 2.9 Initial bathymetry and domain settings. a) Domain without tidal barrier, characterised by a 14-km cross-shore distance and a bed elevation of 6 m at the landward boundary, such that sea-level rise causes flooding of previously dry areas and a dynamic wetting/drying boundary exists. b) Domain with tidal barrier, characterised by a 10.5-km cross-shore distance and a bed elevation of 2.5 m at the landward boundary, which is equal to the high water level at the beginning of the simulation. This means that the entire domain gets submerged and the landward side acts as a closed boundary similar to a non-permeable dike or seawall (Zhou et al., 2016).

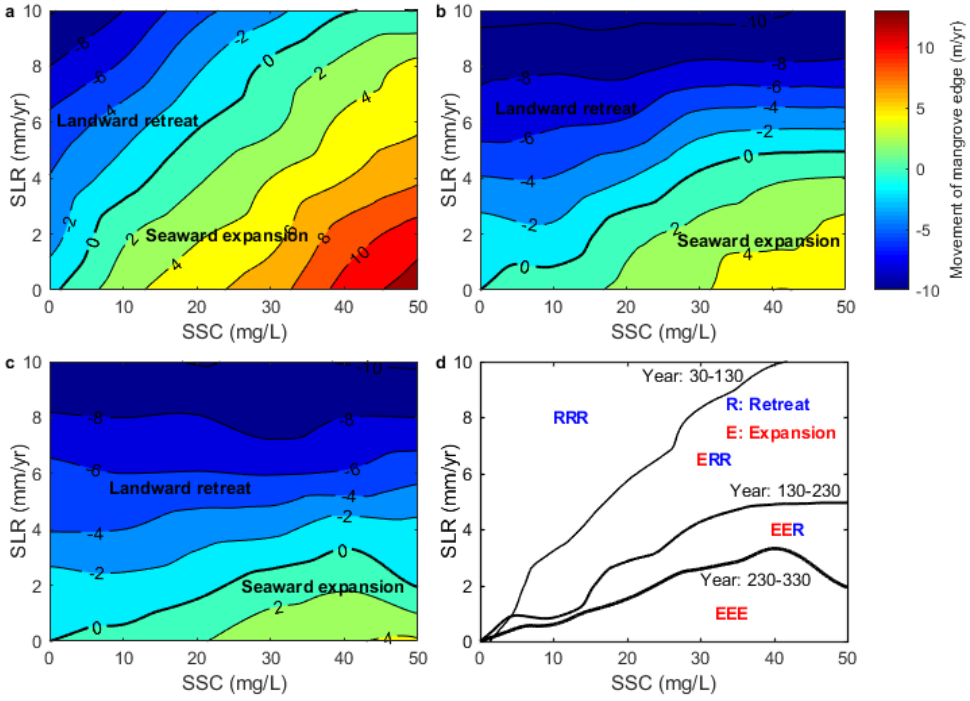

Figure 2.10 Temporal variation in the movement of the seaward forest edge under different combinations of external suspended sediment concentration (SSC) and sea-level rise rate (SLR) without barrier. (a) Movement of the seaward forest edge in the first 100 years (i.e., from year 30 to year 130) shows that more than half of the simulated SSC-SLR combinations result in initial mangrove expansion. (b) Mangrove movement in the second 100 years (i.e., from year 130 to year 230) reveals that a shift from expansion to retreat can emerge, highlighting dynamic forest behaviour and the effects of prolonged sea-level rise. (c) Mangrove movement in the third 100 years (i.e., from year 230 to year 330) indicates that persistent mangrove expansion is only possible under low sea-level rise. (d) Overview of mangrove movement over the different 100-year periods, suggesting that shifts from expansion to retreat are possible for a broad range of SSC-SLR combinations. The black lines in d represent a stable seaward forest edge when evaluated over each distinct period and correspond to the 0 m/yr contour lines in a, b and c.

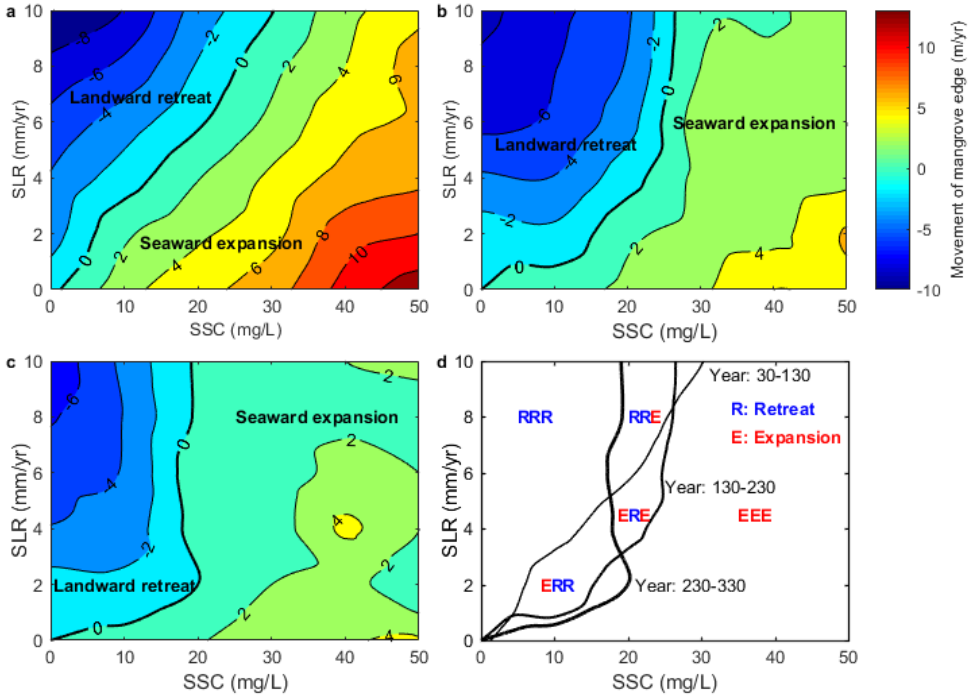

Figure 2.11 Temporal variation in the movement of the seaward forest edge under different combinations of external suspended sediment concentration (SSC) and sea-level rise rate (SLR) with barrier. (a) Movement of the seaward forest edge in the first 100 years (i.e., from year 30 to year 130) shows that the majority of simulated SSC-SLR combinations drives initial mangrove expansion. (b) Mangrove movement in the second 100 years (i.e., from year 130 to year 230) indicates that mangrove expansion is generally maintained, although the rate of expansion reduces. (c) Mangrove movement in the third 100 years (i.e., from year 230 to year 330) highlights that shifts from mangrove retreat to expansion are also possible. (d) Overview of mangrove movement over the different 100-year periods, highlighting that the presence of a barrier reduces the parameter space that results in shifts from expansion to retreat, or vice versa. The black lines in d represent a stable seaward forest edge when evaluated over each distinct period and correspond to the 0 m/yr contour lines in a, b and c.

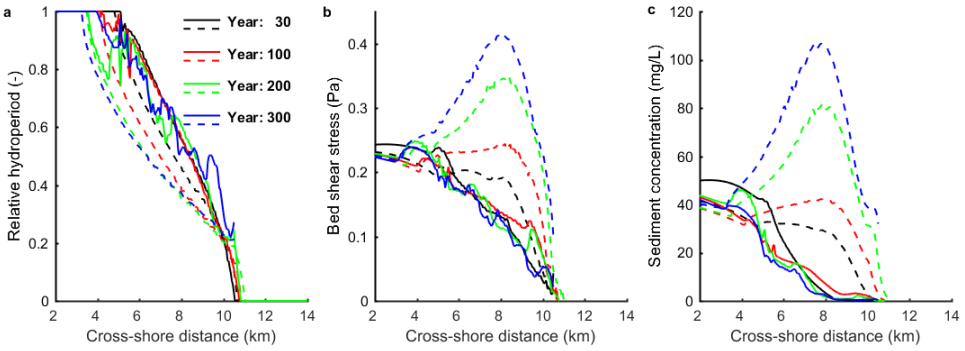

Figure 2.12 Cross-shore trends in relative hydroperiod, bed shear stress and sediment concentration obtained after 30, 100, 200 and 300 years of profile and forest development with original root settings. Results are extracted from a simulation driven with an external sediment supply of 50 mg/L and sea-level rise rate of 2 mm/yr (see first column of Figure 2.4 in the main paper). Solid lines represent the corresponding trends when the effects of vegetation on flow resistance are included, while the dashed lines represent the trends without vegetation impacts (using the same bathymetry). a-c indicate that vegetation is responsible for increasing inundation periods, weakening tidal currents and reducing suspended sediment concentration levels. The delivery of sediment to the upper part of the forest becomes increasingly limited as mangroves are expanding under these high external sediment supply conditions.

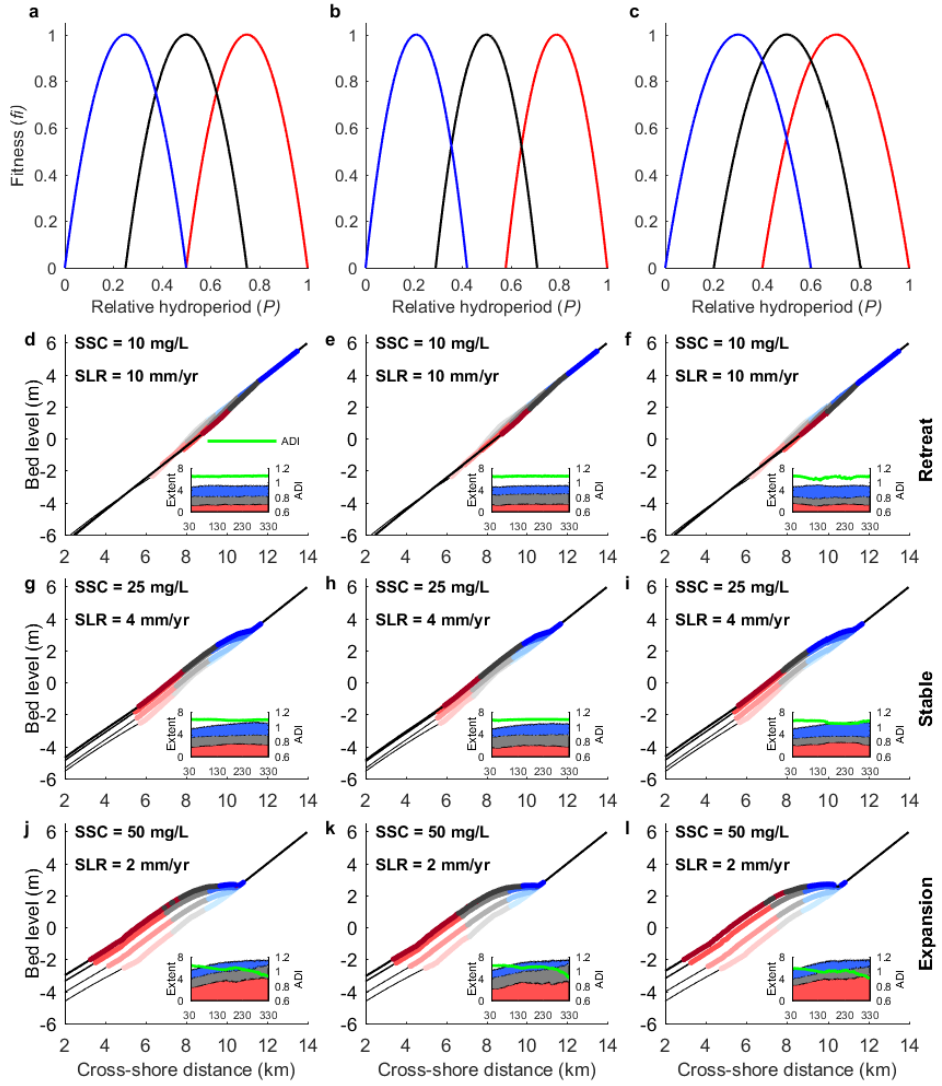

Figure 2.13 Distinct forest behaviours in response to different combinations of sea-level rise and sediment supply under different species distribution criteria (first column: original settings; second column: narrower species distributions; third column: wider species distributions). (a-c) Fitness functions for the different species distribution criteria. Red, black and blue lines indicate the fitness of lower, middle and upper mangroves, respectively. (d-f) Landward retreat of mangrove species. (g-i) Temporal stability of the seaward forest edge. (j-l) Seaward expansion of the mangrove forest. Evolution of the coastal profile and mangrove forest are shown after 30, 100, 200 and 300 years.

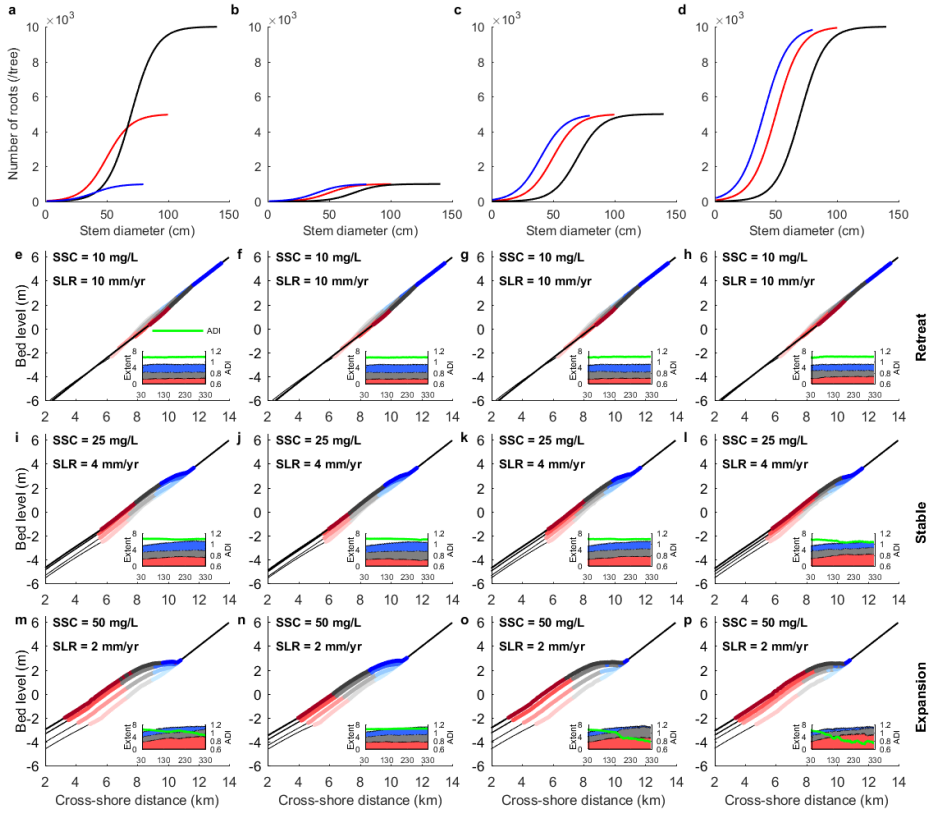

Figure 2.14 Distinct forest behaviours in response to different combinations of sea-level rise and sediment supply under different root densities (first column: original settings; second to fourth columns: maximum number of root elements per tree is species-independent and set to 1000, 5000 and 10000, respectively). (a-d) Species-specific number of root elements per tree as a function of mangrove stem diameter for the different root density settings. Red, black and blue lines indicate the number of root elements of lower, middle and upper mangroves, respectively. (e-h) Landward retreat of mangrove species. (i-l) Temporal stability of the seaward forest edge. (m-p) Seaward expansion of the mangrove forest. Evolution of the coastal profile and mangrove forest are shown after 30, 100, 200 and 300 years.

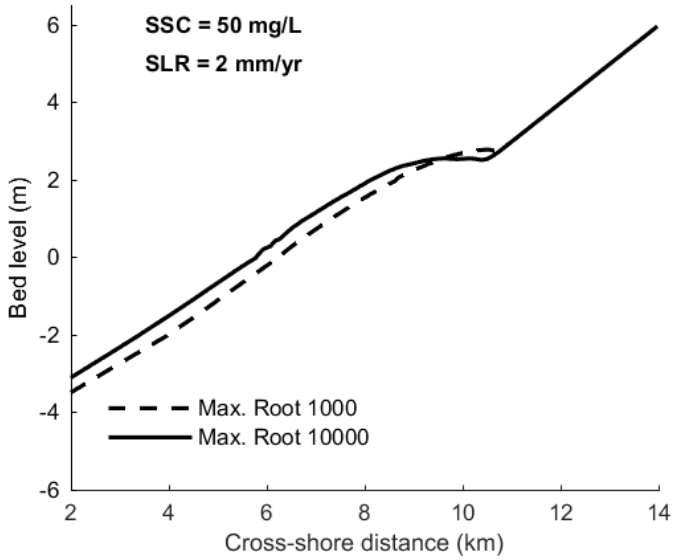

Figure 2.15 Comparison of coastal profiles after 300 years between low and high root densities. Maximum number of root elements per tree is species-independent and set to 1000 and 10000. Dense roots contribute to profile progradation while less roots allow for enhanced sediment delivery to the more landward region and a slightly larger accretion in the upper part of the mangrove forest.

2.5.2 Hydro-morphodynamic model description

The Delft3D hydro-morphodynamic model computes tidal flow, sediment transport and related bathymetric changes. A detailed description of the model can be found elsewhere (Lesser et al., 2004; Zhou et al., 2016); here we provide a short overview of the governing equations. Water level and flow velocity are obtained by solving the basic conservation of mass and momentum equations as follows:

$$\frac{\partial \eta}{\partial t} + \frac{\partial (hu)}{\partial x} = 0 \tag{2.3}$$

$$\frac{\partial u}{\partial t} + u\frac{\partial u}{\partial x} = -g\frac{\partial \eta}{\partial x} + \nu\frac{\partial^2 u}{\partial x^2} - g\frac{u|u|}{C^2 h} + M_x \tag{2.4}$$

where η is the water level (m) with respect to datum (e.g. mean sea level); h is the water depth (m); u is the depth-averaged flow velocity (m/s); g=9.81 m/s^2 is the gravitational acceleration; ν=10 m^2/s is the horizontal eddy viscosity coefficient; C is the Chézy friction coefficient (m$^{1/2}$/s) and M_x is an extra momentum term linked to vegetation effects. The presence of vegetation is incorporated by including additional hydraulic resistance, which is considered through calculation of the Chézy friction coefficient and the additional resistance term ($M_x = -\frac{\lambda}{2} \cdot u^2$). Both λ and C are derived from vegetation characteristics (diameter, height, density) and water depth (Brückner et al., 2019):

$$\lambda = \begin{cases} C_D n \frac{h_v}{h}\frac{C_b^2}{C^2}, & \text{if } h \geq h_v \\ C_D n, & \text{if } h < h_v \end{cases} \tag{2.5}$$

$$C = \begin{cases} C_b + \frac{\sqrt{g}}{\kappa}\ln\left(\frac{h}{h_v}\right)\sqrt{1 + \frac{C_D n h_v C_b^2}{2g}}, & \text{if } h \geq h_v \\ C_b, & \text{if } h < h_v \end{cases} \tag{2.6}$$

where C_b is the non-vegetated Chézy coefficient, set to 65 (m$^{1/2}$/s); κ=0.41 is the Von Kármán constant; h_v is the height of vegetation objects (stems or roots) (m); C_D is the drag coefficient and $n = mD$ where m is the number of vegetation objects per square metre and D is the diameter of this object. If vegetation biomass, such as roots and trunks with different sizes co-exist in one grid cell, C and λ are calculated separately for each vegetation object and averaged with the specific fraction coverage of each vegetation object (Brückner et al., 2019).

Regarding sediment transport, we consider pure cohesive sediment as mangroves commonly thrive in muddy environments. Deposition ($Q_{mud,d}, kg \cdot m^{-2}s^{-1}$) and erosion fluxes ($Q_{mud,e}, kg \cdot m^{-2}s^{-1}$) are estimated through the widely-adopted Partheniades-Krone formulations as follows:

$$Q_{mud,d} = \begin{cases} \omega_s c\left(1 - \frac{\tau_c}{\tau_{cr,d}}\right), & \text{if } \tau_c < \tau_{cr,d} \\ 0, & \text{if } \tau_c \geq \tau_{cr,d} \end{cases} \tag{2.7}$$

$$Q_{mud,e} = \begin{cases} M_e\left(\frac{\tau_c}{\tau_{cr,e}} - 1\right), & \text{if } \tau_c > \tau_{cr,e} \\ 0, & \text{if } \tau_c \leq \tau_{cr,e} \end{cases} \tag{2.8}$$

where $\omega_s = 5 \times 10^{-4}$ m/s is the settling velocity, c is the depth-averaged sediment concentration (kg/m^3), $\tau_c = \rho g u^2/C^2$ is the tide-induced bottom bed shear stress (Pa), $\tau_{cr,d}$ = 1000 Pa and $\tau_{cr,e}$ = 0.2 Pa are the critical shear stresses for deposition and erosion, respectively. $M_e = 5 \times 10^{-5}$ kg/m^2/s is the erosion parameter. These parameter settings are representative for mud dominated environments

(Zhou et al., 2016). The transport of suspended sediment is calculated according to the advection-diffusion equation and this allows us to model the transport of sediment between different regions of the mangrove forest:

$$\frac{\partial (ch)}{\partial t} + \frac{\partial (uch)}{\partial x} = Q_{mud,e} - Q_{mud,d} \tag{2.9}$$

Bed level changes are then calculated following the mass conservation equation of cohesive sediment:

$$(1 - \varepsilon_p) \frac{\partial z_b}{\partial t} = \frac{1}{\rho_s} (Q_{mud,d} - Q_{mud,e}) \tag{2.10}$$

where ε_p is the bed porosity, set to 0.4; z_b is the bed profile elevation (m) and ρ_s is the density of sediment (kg/m^3), set to 2650 kg/m^3. A morphological acceleration factor (Brückner et al., 2019; Lesser et al., 2004) was used, meaning that the erosion and deposition fluxes computed during a hydrodynamic time step are enlarged by this factor (set to 30 in this study based on earlier tests). This approach is commonly used in morphodynamic modelling and allow us to accomplish long-term simulations.

2.5.3 Dynamic vegetation model description

To simulate the colonization, growth and mortality of mangroves, a dynamic vegetation model was developed based on earlier work on mangrove modelling (van Maanen et al., 2015). The major advancement is the ability to simulate the dynamics of mangrove assemblages with multiple species occupying the lower, middle and upper intertidal area. In this study, we represent the physical characteristics of mangroves in each zone by a characteristic species. We therefore selected three species, namely *Rhizophora mangle*, *Avicennia germinans* and *Laguncularia racemosa*, to represent lower, middle and upper intertidal mangroves, respectively. These species commonly co-exist in intertidal habitats and are known to thrive at different elevations (Chapman, 1976; Duke et al., 1998; Lugo and Snedaker, 1974). Furthermore, detailed information on the growth parameters for these species is available (Berger and Hildenbrandt, 2000; Chen and Twilley, 1998).

Colonization by mangroves occurs each year and is dependent on suitable inundation regimes. We therefore used inundation based fitness functions to define species-specific growth conditions (D'Alpaos and Marani, 2016; van Maanen et al., 2015):

$$f_i = a_i \cdot P^2 + b_i \cdot P + c_i \tag{2.11}$$

where P is the relative hydroperiod calculated as the proportion of time that the bed is inundated per tidal cycle and a_i, b_i and c_i are species-specific constants. The fitness functions suggest that each species has a specific hydroperiod for which growth is optimal while growth conditions diminish when mangroves are inundated for either longer or shorter periods (van Maanen et al., 2015). For the sake of comparability, all species were given an equal maximum fitness (i.e., $f_{max,1} = f_{max,2} = f_{max,3} = 1$) and the shape of each fitness function is symmetric and equal as well (Figure 2.7a). These functions then control colonization processes: mangrove trees of a specific species can only colonize when its fitness exceeds zero ($f_i > 0$). If that is the case, mangroves establish with an initial mangrove density of 30 individuals per 100 m^2 which is assumed to be the maximum density and an initial stem diameter of 1.37 cm (Berger and Hildenbrandt, 2000; van Maanen et al., 2015). If inundation conditions allow co-existence of multiple species, then the number of individuals per species able to colonize is weighted by its fitness level (f_i):

$$N_{col,i} = N_{col,max} \cdot \frac{f_i}{\sum_{i=1}^{n} f_i} \tag{2.12}$$

where $N_{col,i}$ is the number of colonizing trees of species i and $N_{col,max}$ is the maximum number of trees that can be added to one grid cell, which is equal to the initial mangrove density multiplied by grid size.

Mangrove growth is implemented by increasing both stem diameter and tree height over time, and is described as (Berger and Hildenbrandt, 2000; Chen and Twilley, 1998; van Maanen et al., 2015):

$$\frac{dD_i}{dt} = \frac{G_i D_i \left(1 - \left(D_i H_i\right) / \left(D_{max,i} H_{max,i}\right)\right)}{\left(274 + 3b_{2i} D_i - 4b_{3i} D_i^2\right)} \cdot f_i \cdot C \tag{2.13}$$

$$H_i = 137 + b_{2i} D_i - b_{3i} D_i^2 \tag{2.14}$$

where D_i is the stem diameter (cm) and H_i is the height (cm) for the ith tree species, and t is time (years). $D_{(max,i}$ and $H_{max,i}$ are the species-specific maximum stem diameter and tree height, respectively. G_i, b_{2i} and b_{3i} are growth parameters. The growth function considers species-specific fitness which is added as an additional factor and modifies mangrove growth. A reduction in growth rate takes place when inundation conditions are sub-optimal reflected by a fitness smaller than 1 ($f_i < 1$). Tree growth is further affected by limitations in available resources, which is incorporated by adding a competition stress factor (van Maanen et al., 2015):

$$C = \frac{1}{1 + exp\left[d\left(W_{0.5} - W\right)\right]} \tag{2.15}$$

where d is a constant controlling the overall shape of the function, and is set to -0.00005. W is the actual above-ground biomass (kg) that is present in a grid cell and $W_{0.5}$ is a characteristic biomass (kg) defined as the value of W for which $C = 0.5$ (Figure 2.7b). In order to compute W, we consider the total number of trees per grid cell and the weight of each single tree, derived through species-specific allometric equation (Komiyama et al., 2008):

$$W = \sum_{i}^{n} \sum_{j}^{m} \alpha_i \cdot D_{i,j}^{\beta_i} \tag{2.16}$$

where n is the total number of mangrove species and m is the total number of trees per species i. α_i and β_i are species-specific constants. To derive $W_{0.5}$, the 'zone of influence' concept (Berger and Hildenbrandt, 2000) is applied which considers a circular zone around each mangrove tree, with radius R, in which the tree exploits resources (Berger and Hildenbrandt, 2000):

$$R = 10\sqrt{rbh} \tag{2.17}$$

where rbh is the stem radius (m). As there may be more than one species in a grid cell, we adopted an average biomass to calculate $W_{0.5}$:

$$W_{0.5} = \frac{1}{n} \sum_{i=1}^{n} \left(\frac{A_{cell}}{\left(2 \cdot R_i\right)^2} \cdot W_{max,i} \right) \tag{2.18}$$

where A_{cell} is the grid cell surface area (m^2) and $W_{max,i}$ is the maximum tree weight (kg) of species i. The above equation provides a characteristic biomass per grid cell under the condition that the zones of influence around each tree are not overlapping (i.e. limited competition for resources) (van Maanen et al., 2015). As A_{cell} equals to 2500 m^2 in our study, application of Equation 2.18 leads to $W_{0.5}$ being set to 1.53×10^5kg for each grid cell (Figure 2.7b); $C = 0.5$, if $W = W_{0.5}$).

Mangrove mortality occurs due to prolonged periods of suppressed growth (Berger and Hildenbrandt, 2000). At the end of every year, the growth condition of each tree is therefore

evaluated by calculating the yearly averaged value of $f_i \cdot C$ which controls the growth rate as defined by Equation 2.13. Trees die when the growth is less than 50% of the growth under optimal conditions (i.e., $f_i \cdot C < 0.5$) for 5 consecutive years (van Maanen et al., 2015). This drives a self-thinning process as the density of trees decreases, leading to an overall biomass reduction, until the growth condition of remaining trees is no longer suppressed, and the values of $f_i \cdot C$ thus equal or exceed 0.5. Small trees are assumed to be more fragile and die first. If tree mortality occurs among multiple species co-existing in a grid cell, then the removal of trees is weighted by the relative fitness factors, such that a lower fitness results in a higher mortality:

$$N_{mort,i} = \frac{N_{mort,tot}}{f_i \sum_i^n \frac{1}{f_i}} \tag{2.19}$$

where $N_{mort,i}$ is the number of trees of species i and $N_{mort,tot}$ is the total number of trees that need to be removed. On the other hand, if growth conditions are favourable (i.e., $f_i \cdot C > 0.5$) and the maximum density is not reached, young mangrove trees are added such that a single grid cell can contain trees of different sizes (van Maanen et al., 2015).

Apart from tree trunks, mangrove aerial roots are known to provide significant flow resistance (Asbridge et al., 2016; Krauss et al., 2014; Mazda et al., 1997b; van Maanen et al., 2015), hence a description of mangrove root systems is required. Aerial root structures vary greatly among species (Tomlinson, 2016). For example, *Rhizophora mangle* trees have prop roots arching from their trunks to the ground, while *Avicennia germinans* trees have pencil-like pneumatophores extending upward from underground cable roots. The root system of Laguncularia racemosa trees is less extensive and may include limited pneumatophores. As the hydro-morphodynamic model only allows for inclusion of cylindrical objects, we simplified the shape of roots to cylinders characterized by a fixed diameter and height. The number of root elements is related to stem diameter according to a sigmoid function and increases with tree size (Figure 2.8) (van Maanen et al., 2015):

$$N_{roots,i} = m_i \cdot \frac{1}{1 + exp\left[f\left(\frac{D_{max,i}}{2} - D\right)\right]} \tag{2.20}$$

where m_i is the maximum number of root elements for one single tree of species i and $f = 0.1$ is a constant describing the rate of increase. The maximum number of root elements per tree is species-specific in order to represent differences in root structures. The sensitivity of mangrove forest behaviour to different root densities has been investigated (Figure 2.14).

2.5.4 Supplementary tables

Table 2.1 Hydro-morphodynamic model parameter settings

Category	Parameter	Value/Description	Unit
Time reference	Hydrodynamic time step	0.5	min
	Morphological acceleration factor	30	-
	Simulated period	330	years
Domain	Initial slope	1/1000	m/m
	Domain size ($x \times y$) without barrier	14000 × 14 (-8 to 6)	m
	Domain size ($x \times y$) with barrier	10500 × 10.5 (-8 to 2.5)	m
	Grid size ($N \times M$)	50 × 50	m
Bottom roughness	Chézy value at bare substrate	65	$m^{1/2}/s$
Boundary condition	Tidal amplitude	2.5	m
Sediment	Critical bed shear stress for erosion	0.2	N/m^2
	Critical bed shear stress for deposition	1000	N/m^2
	Erosion parameter	5×10^{-5}	$kg/m^2/s$

Table 2.2 Dynamic vegetation model parameter settings. Values for maximum root number and fitness function constants reported here are the original settings. Sensitivity to these parameter settings has been investigated to explore the influence of species distribution criteria (Figure 2.13) and root densities (Figure 2.14) on mangrove assemblage behaviour.

Category	Parameter	Lower-mangroves	Middle-mangroves	Upper-mangroves	Unit	Source
		R. mangle	*A. germinans*	*L. racemosa*		
Vegetation parameters	Initial stem diameter	1.37	1.37	1.37	cm	*1,2*
	Maximum root number	5000	10000	1000	-	*2,3*
	Root diameter	1	1	1	cm	*3*
	Root height	15	15	15	cm	
	Drag coefficient of vegetation	1	1	1	-	*4*
Growth parameters	Maximum stem diameter	100	140	80	cm	
	Maximum tree height	4000	3500	3000	cm	
	Growth constant G	267	162	243	cm/yr	*1,5*
	Growth constant b_2	77.26	48.04	71.58	-	
	Growth constant b_3	0.396	0.172	0.447	-	
	Fitness function constant a	-16	-16	-16	-	
	Fitness function constant b	24	16	8	-	
	Fitness function constant c	-8	-3	0	-	
	Biomass constant α	0.178	0.14	0.102	-	*6*
	Biomass constant η	2.47	2.4	2.5	-	

Source: *1*=Berger and Hildenbrandt (2000); *2*=van Maanen et al. (2015); *3*=Tomlinson (2016); *4*=Brückner et al. (2019); *5*=Chen and Twilley (1998); *6*=Komiyama et al. (2008).

Acknowledgments

We thank the reviewers for providing detailed and constructive feedback. This study is supported by the China Scholarship Council. MZMB and MGK acknowledge funding by ERC Consolidator agreement 647570 to MGK. DU is funded by NERC AHRC (NE/R017980/1). ZZ is funded by the National Natural Science Foundation of China (Grant Nos.51620105005, 41976156). BVM is funded by the NWO WOTRO Joint Sustainable Development Goal Research Program (W07.303.106).

Data availability statement

The data that support the findings of this study are openly available at the following URL/DOI: https://doi.org/10.5281/zenodo.3749866. Data will be available from 01 January 2021.


3

Chapter 3 | Implications of coastal conditions and sea-level rise on mangrove vulnerability: A bio-morphodynamic modelling study

Abstract

Mangrove forests are valuable coastal ecosystems that have been shown to persist on muddy intertidal flats through bio-morphodynamic feedbacks. However, the role of coastal conditions on mangrove behavior remains uncertain. This study conducts numerical experiments to systematically explore the effects of tidal range, small wind waves, sediment supply and coastal slope on mangrove development under sea-level rise (SLR). Our results show that mangroves in micro-tidal conditions are more vulnerable because of the gentler coastal equilibrium slope and the limited ability to capture sediment, which leads to substantial mangrove landward displacement even under slow SLR. Macro-tidal conditions with large sediment supply promote accretion along the profile and platform formation, reducing mangrove vulnerability for slow and medium SLR, but still cause rapid mangrove retreat under fast SLR. Small wind waves promote sediment accretion, and exert an extra bed shear stress that confines the mangrove forest to higher elevations with more favorable inundation regimes, offsetting SLR impacts. These processes also have important implications for the development of new landward habitats under SLR. In particular, our experiments show that landward habitat can be created even with limited sediment supply and thus without complete infilling of the available accommodation space. Nevertheless, new accommodation space may be filled over time with sediment originating from erosion of the lower coastal profile. Consistent with field data, model simulations indicate that sediment accretion within the forest can accelerate under SLR, but the timing and magnitude of accretion depend non-linearly on coastal conditions and distance from the mangrove seaward edge.

Published as: Xie, D., Schwarz, C., Kleinhans, M. G., Zhou, Z., & van Maanen, B. (2022). Implications of coastal conditions and sea-level rise on mangrove vulnerability: A bio-morphodynamic modeling study. *Journal of Geophysical Research: Earth Surface, 127, e2021JF006301.* DOI: https://doi.org/10.1029/2021JF006301.

3.1 Introduction

Mangrove forests inhabiting the margin between land and sea at low latitudes provide crucial ecosystem services to coastal communities including resource provisioning (e.g., timber and fuelwood), coastal protection, organism habitat (e.g., shrimp and fish) and cultural services (Barbier et al., 2011; Brander et al., 2012; Alongi and Mukhopadhyay, 2015). When submerged by tides, mangrove trees dissipate wave energy and reduce tidal currents, protecting the coast from erosion and hydraulic scouring (Temmerman et al., 2013). Reduced hydrodynamic forces within the forest moreover facilitate settling of suspended sediment, which increases bed elevation and thus promotes wetland survival with rising sea levels (Krauss et al., 2014). Sea-level rise (SLR) is a major stressor for mangrove forests which are only able to tolerate limited durations of tidal inundation (Woodroffe et al., 2016). Changes in inundation time and depth are not only a function of the rate of SLR, but also dependent on coastal slope and morphological adaptation, which in turn are linked to hydro-sedimentary boundary conditions such as tidal range, wave action and sediment supply (Blasco et al., 1996; FitzGerald et al., 2008; Passeri et al., 2015). Although field data have revealed that ecosystem services provided by mangroves are non-linearly related to mangrove coverage (Barbier et al., 2008), the fate of mangrove forests in response to SLR remains debated (Krauss et al., 2014; Woodroffe et al., 2016). Considering the complex interplay between physical processes and vegetation dynamics in such environments (Xie et al., 2020), it is still unclear how non-linear bio-physical feedbacks determine mangrove survival under varying boundary conditions. As such, in order to develop accurate vulnerability assessments of mangrove forests, we need to systematically evaluate mangrove behavior and their potential future responses to SLR under a broad range of coastal conditions (Friess et al., 2019).

The balance between SLR and sediment accretion is often suggested to be the controlling factor in determining mangrove vulnerability under SLR (Lovelock et al., 2015). Regions with fast SLR and low sediment availability are shown to experience increased flooding leading to tree mortality at seaward mangrove margins and landward migration in the absence of any obstructions (Gilman et al., 2008). In contrast, mangrove forests located in regions with high sediment availability are shown to expand seaward despite rising sea levels (Nardin et al., 2016b; de Jong et al., 2021). Although mangroves can elevate the bed through organic accumulation in addition to trapping suspended sediment (Krauss et al., 2014), the net surface elevation change is additionally governed by other sub-surface processes (shallow subsidence, remineralization and compaction of organic sediment) which may offset this elevation gain (McKee, 2011; McKee et al., 2021). In wetland models, the availability of suspended sediment is typically assumed to be constant across the wetland surface or dependent on distance from the wetland edge (Kirwan and Murray, 2007; Kirwan et al., 2010; Swanson et al., 2014; Mogensen and Rogers, 2018; Schuerch et al., 2018; Thorne et al., 2018), implying that wetland accretion will accelerate under SLR-driven increases in inundation. However, recent mangrove modelling has shown that such an assumption can lead to an underestimation of bio-physical effects inherent to the complex interactions between vegetation dynamics and hydro-sedimentary processes (Xie et al., 2020). Both vegetation presence and bio-physical effects are ultimately controlled by the coastal conditions, including hydrodynamic forcing and sediment supply (Chapman, 1976; Woodroffe et al., 2016). Thus, investigating mangrove survival under a range of environmental factors becomes imperative.

Mangroves are found in intertidal areas with different coastal slopes and varying profile shapes (Figure 3.1), which have a governing effect on the response of mangroves to rising sea levels. Previous research has shown that the development of bare coastal profiles is significantly determined by the coastal conditions. Under dominant tidal forcing, coastal profiles develop a more convex equilibrium shape, whereas the addition of waves favors a more concave equilibrium shape (Waeles et al., 2004; Friedrichs, 2011). Furthermore, the balance between tidal range and sediment supply plays a

significant role in determining profile slopes. Previous numerical simulations indicate that the equilibrium bare slope becomes steeper/flatter with a higher/lower tidal range and lower/higher sediment supply (Roberts et al., 2000). Coastal profiles in nature do not typically remain bare, but rather often get colonized to become intertidal wetlands situated around the mean high water mark (Cahoon et al., 2020). Enhanced drag caused by the presence of mangrove forests contributes to the development of a more convex profile, compared with non-vegetated or sparse-vegetated flats, which may create a more linear profile (Bryan et al., 2017). Since the coastal profile controls water- and sediment transport and derived parameters such as flooding depth and duration, it consequently controls habitat suitability for mangroves under SLR (Krauss et al., 2014). Moreover, tidal range and the associated strength of tidal currents also determine the extent of sediment transport to higher intertidal areas, and thus sediment accumulation and development of the vegetated platform (Chen et al., 2018). Previous research also suggests that SLR will cause a greater relocation of mangroves in micro-tidal areas relative to macro-tidal areas assuming similar coastal slopes (Ellison, 2015). Thus, coastal slope and shape determined by tidal range potentially exert a major impact on mangrove drowning under SLR. For example, the drowning of a coastal plateau means a sudden set-back of mangrove vegetation, emphasizing the need to study the interaction between tidal dynamics, sediment transport, coastal slope and how this influences mangrove survival.

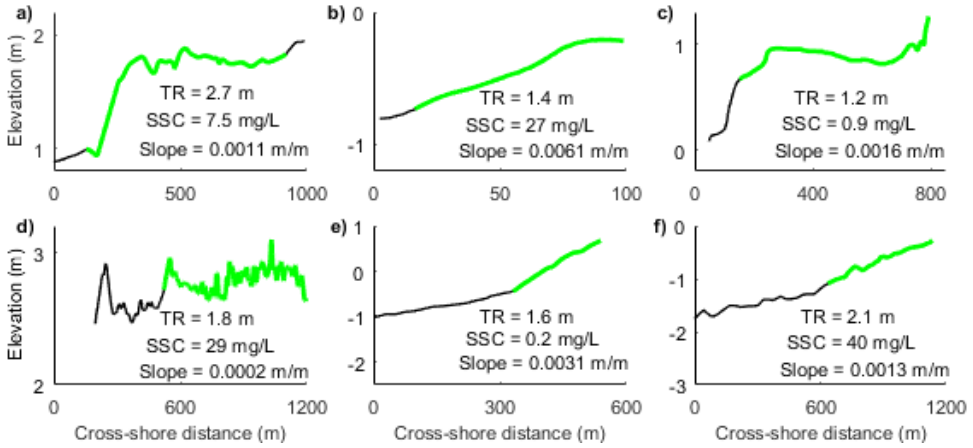

Figure 3.1 Cross-shore profiles of mangrove environments adapted from Bryan et al. (2017). (a) Firth of Thames, New Zealand (Swales et al., 2007); (b) Ba Lat Estuary, Red River Delta, Vietnam (Van Santen et al., 2007); (c) Glasshouse Mountains Creek, Queensland, Australia (tidal creek occurs further seaward) (Knight et al., 2009); (d) Macouria mud bank, French Guiana (Proisy et al., 2009); (e) Kantang Estuary in Thailand (Horstman et al., 2014) and (f) Cù Lao Dung in the Mekong River Delta, Vietnam (Bryan et al., 2017). Green dots indicate mangrove presence. TR is annual mean tidal range calculated from TPXO tide models (https://www.tpxo.net/home) and SSC is annual mean suspended sediment concentration derived from the satellite-borne GlobColor data (http://globcolor.info). Slope is based on the two endpoints of the profile. Note that these cross-shore profiles and vegetation distributions may not fully cover the landward portion of the forest, meaning the natural profile slopes could be different from slopes shown above.

In addition to tidal currents, wind waves exert additional bed shear stress enhancing sediment resuspension (Green and Coco, 2014) while mangroves protect the coast through dampening wave energy and facilitating net sediment deposition (Mazda et al., 1997a; Horstman et al., 2014). Recent research highlights the importance of small wind waves in determining the long-term stability of salt marsh systems (Schuerch et al., 2019). However, for mangrove sites, the majority of existing studies have focused on the dissipation of energetic waves by vegetation (Mazda et al., 1997a; Bao, 2011;

Horstman et al., 2014). The effects of small but frequently occurring wind waves on morphological evolution in mangrove ecosystems have received less attention (Van Santen et al., 2007; Green, 2011; Horstman et al., 2014). On the one hand, small waves (with significant wave height less than 20 cm) are capable of resuspending sediment over tidal flats (Green et al., 1997; Uncles and Stephens, 2000; Green, 2011) thereby potentially increasing sediment availability to adjacent wetlands and compensating the sediment deficit in sediment accumulation (Carling, 1982). On the other hand, shifting the limiting factors from sediment availability to sediment transport capacity may be altered by mangroves, causing spatial variations in accumulation rate (Swales et al., 2019). From an ecological point of view, strong tidal currents and waves limit the establishment of mangrove seedlings due to increased shear stresses so that the seaward edge of mangrove forests is not always at mid-tidal elevation (Balke et al., 2011; Friess et al., 2012). Such colonization restrictions not only control initial mangrove coverage, but potentially also affect mangrove responses under rising sea levels.

To understand and project future coastal development, we need to identify processes driving mangrove vulnerability under different coastal conditions. Global and regional assessments on mangrove vulnerability using first-order approximations show how increased vertical accretion can mitigate the effects of rising sea levels (Lovelock et al., 2015; Schuerch et al., 2018). Other field site-specific approaches predict morphological evolution and spatial mangrove development utilizing sophisticated interactions between mangroves and hydrodynamics but simplify non-linearities in sedimentary processes or exclude dynamic feedbacks between mangrove growth and coastal geomorphological change (Bryan et al., 2017; Rodriguez et al., 2017). Other more recent modelling studies have incorporated a broader range of dynamic feedbacks between mangrove growth and coastal geomorphological change (Breda et al., 2021), highlighting the potential and need to use such bio-morphodynamic models to assess mangrove resilience in various coastal conditions. Currently, different views exist on the fate of coastal wetlands, with some studies indicating that wetland area can increase as long as space for landward migration is available (Schuerch et al., 2018), while others suggest that longer-term wetland loss is inevitable (Törnqvist et al., 2021). Addressing this dispute requires new modelling approaches that account for dynamic vegetation growth (i.e. colonization, growth and mortality processes) and comprehensive treatment of hydro-sedimentary processes, including the development of newly generated accommodation space created by SLR which can potentially be filled in with sediment. Such modelling efforts have to be able to explore mangrove dynamics under varying boundary conditions to unravel the broad range of potential mangrove responses. In this study, we fill this knowledge gap and utilize a bio-morphodynamic numerical model to determine how non-linear bio-physical interactions control coastal profile evolution and mangrove coverage in the face of SLR in various coastal conditions. This will help to elucidate the key controlling factors governing mangrove vulnerability. To this end, we conducted 72 simulations to systematically explore the effects of tidal range, wave action, sediment supply and coastal slope under three different SLR scenarios.

3.2 Methods

Mangrove behaviors are simulated by considering different combinations of coastal conditions, including SLR, tidal range, wind waves (hereafter referred to as waves), sediment supply and coastal slope. Here we use a recently developed bio-morphodynamic model, which considers a two-way interaction between physical and biological processes (Xie et al., 2020). The model couples an open-source hydro-morphodynamic model (i.e. Delft3D, version 4.01.00) containing flow, wave and sediment transport modules (Lesser et al., 2004), and a dynamic vegetation model modified after van Maanen et al. (2015). The hydro-morphodynamic model provides information on local hydroperiod and bed shear stress to the vegetation model where this influences vegetation dynamics.

The vegetation model in turn feeds the hydro-morphodynamic model with updated vegetation information so that vegetation-induced flow resistance and bed roughness can be accounted for. Although mangroves have the capacity to elevate their soils through organic matter accretion, enhancing their ability to adapt to SLR (Krauss et al., 2014; Woodroffe et al., 2016), other sub-surface processes such as subsidence due to decomposition and sediment auto-compaction may decrease elevation, increasing the risk of mangroves being submerged (Rogers et al., 2005). We therefore decided to exclude these counteracting processes and focus on above-ground bio-morphodynamic feedbacks. Considering the number of scenarios that need to be tested, a one-dimensional cross-shore profile model is constructed, assuming alongshore uniformity in morphology and boundary conditions in order to reduce model complexity and computational time similar to previous studies (Roberts et al., 2000; Zhou et al., 2016; Xie et al., 2020). As the model does not incorporate the specific fluvial or estuarine characteristics affecting mangrove behaviours, our modelling study is set up to represent mangrove systems located in open coast systems, broad embayments or tidal dominated deltaic environments, such as the Suriname coast (de Jong et al., 2021), Firth of Thames (Swales et al., 2007) and the Mekong Delta (Nardin et al., 2016b). Still, the boundary and initial conditions are simplified in order to keep model output as transparent as possible and unravel the key feedbacks leading to system responses (van der Wegen et al., 2011; Murray, 2013).

3.2.1 Hydro-morphodynamic model

The Delft3D model suite, which has been widely used in both engineering applications and scientific research, is adopted to process hydro-morphodynamic calculations. Since the parameterization of the hydro-morphodynamic model is similar to the model in previous research (Xie et al., 2020), here it will only be briefly discussed. The Delft3D model computes flow fields, sediment transport and related profile changes. Water level and flow velocity are calculated by solving the shallow water equations and then are utilized to compute sediment transport. Mangroves are commonly found in muddy environments (Woodroffe et al., 2016), which can exhibit a range of cohesive behavior with varying critical erosion thresholds and erosion rate parameters determined by their sediment composition (van Ledden et al., 2004). In this research, we simplify the effects of different sediment fractions by only considering pure cohesive muddy sediment which can be eroded or deposited over the profile. The erosion and deposition fluxes of mud are calculated through the Partheniades-Krone formulations (Partheniades, 1965) and sediment is transported according to the advection-diffusion equation. The critical shear stress for erosion is set to 0.2 N/m2 and the threshold for sedimentation is set to 1000 N/m^2, following previous studies (Zhou et al., 2016; Xie et al., 2020). Other hydro-morphodynamic parameter settings can be found in Table 3.1. Bed level change will then be updated considering net changes in sediment fluxes following the principle of mass conservation and fed back instantly to update the flow field in order to start the next hydrodynamic calculation.

We applied the 'roller model' option to mimic wave action across the one-dimensional profile following van der Wegen et al. (2017). The roller model includes the effects of short waves on long waves. The application of the roller model is appropriate for short waves where the wave spectrum is narrow-banded for both frequency and direction. The roller energy is transformed from wave energy through wave breaking and is rapidly dissipated in shallow regions (Nairn et al., 1991; Reniers et al., 2004; Tajziehchi, 2006). Propagation of waves and roller energy associated with the dissipation of wave energy will cause spatio-temporal variations in wave characteristics and roller energy and thus a variation in radiation stress, which will influence bed shear stress resulting in extra sediment mobility (Reniers et al., 2002; Reniers et al., 2004). We applied an online coupling between the roller wave model and the flow model to account for wave-current interactions. In contrast to the strong interactions between large-wave energy and mangrove behaviors, we here focus on the effects of small waves that may control morphological change and related mangrove vulnerability over longer time scales, but which have so far received relatively little attention. As such, we apply a small wave height

(i.e. significant wave height = 5 cm) on the seaward boundary. Although the flow is affected by vegetation, the effects of mangroves on wave damping are not included in the current model framework. Therefore, our results may overestimate the role of waves in morphological evolution.

3.2.2 Dynamic vegetation model

The behaviors of mangrove forests are modelled in Matlab (R2017a), including the processes of colonization, growth and mortality, after van Maanen et al. (2015). For clarity, the key concepts of the vegetation model are described in detail. To realize the interaction between vegetation dynamics and hydro-morphodynamic processes, we couple the vegetation model with the hydro-morphodynamic model (Delft3D) described above, based on the framework introduced in previous studies van Oorschot et al. (2016) and Brückner et al. (2019). Here, the physical conditions determine vegetation colonization, growth and mortality, while the vegetation properties determine hydraulic resistance and bed roughness.

To account for vegetation effects in the hydro-morphodynamic model, we applied the trachytope approach with the Baptist formula (Baptist et al., 2007) that allows for multiple fractions of different vegetation characteristics existing within one numerical cell, including both stems and roots. A net roughness C_n ($m^{1/2}/s$) and additional resistance term M in both x and y directions (i.e. $M_x = -\lambda/2 \cdot u^2$ and $M_y = -\lambda/2 \cdot v^2$) are incorporated in the hydro-morphodynamic model in the presence of mangroves. u and v are the depth-averaged flow velocity in x and y directions, respectively. Both C_n and λ are calculated from vegetation characteristics and water depth (h; unit: m):

$$C_n = \begin{cases} C_b + \dfrac{\sqrt{g}}{\kappa} \ln\left(\dfrac{h}{h_v}\right) \sqrt{1 + \dfrac{C_D n h_v C_b^2}{2g}}, & \text{if } h \geq h_v \\ C_b, & \text{if } h < h_v \end{cases} \tag{3.1}$$

$$\lambda = \begin{cases} C_D n \dfrac{h_v}{h} \dfrac{C_b^2}{C_n^2}, & \text{if } h \geq h_v \\ C_D n, & \text{if } h < h_v \end{cases} \tag{3.2}$$

where C_b is the non-vegetated Chézy coefficient, set to 65 $m^{1/2}/s$; g = 9.81 m/s^2 is the gravity; $\kappa = 0.41$ is the Von Kármán constant; h_v (m) is the height of vegetation objects (stems or roots); C_D (-) is the drag coefficient accounting for roots and stems of mangroves, which can vary greatly between 0.7 and 3.5 (Nepf, 1999; Horstman et al., 2018a). Here we set C_D of tree stems to 1.5 and C_D of roots to 1 following previous studies (van Oorschot et al., 2017; Xie et al., 2020). The sensitivity analysis of C_D can be seen in Figure 3.12. $n = mD$ where m is the number of vegetation objects per square meter and D is the diameter of these objects. When different sizes of vegetation objects co-exist in one numerical cell, C_n and λ are calculated separately for each vegetation object and averaged with the specific fraction coverage of each vegetation object.

The ecological time step is set to 1 month so that the status of mangrove trees is updated 12 times per year. At the end of every ecological time step, the vegetation model requests result from the hydro-morphodynamic model, such as bed levels, water levels and bed shear stresses, to update vegetation characteristics, including tree diameter, height, density and their corresponding root elements, serving as new input for the next hydro-morphodynamic simulation. The seedlings colonize at the beginning of the year (i.e. 1st ecological time step), and at the end of the year (i.e. 12th ecological time step) the growth quality of each mangrove is evaluated as a basis for mangrove mortality.

Avicennia marina has been chosen as a representative mangrove species following a previous mangrove modelling study (van Maanen et al., 2015). Although mangrove growth patterns can be more complex (Kumbier et al., 2021), the habitat of *Avicennia marina* has been previously approximated as the area between mean sea level and mean high water level (Clarke and Myerscough,

1993). In the model, the hydrodynamic conditions for mangrove seedling establishment are 1) appropriate inundation regime and 2) limited hydrodynamic forces, both of which are evaluated at the first ecological time step. Relative hydroperiod, P, calculated as the proportion of time that one cell is inundated within one ecological time step, has been adopted to evaluate whether the inundation regime is appropriate for mangrove seedlings to settle. Here, for *Avicennia marina*, we assume grid cells inundated less than half of the time (i.e. $0 < P < 0.5$) are appropriate for mangrove colonization. Apart from this inundation requirement, limited hydrodynamic force is also required for successful seedling settlement, which has been regarded as windows of opportunity (Balke et al., 2011; Friess et al., 2012). Previous physical experiments show that wave- or current-induced hydrodynamic force determines seedling establishment, for example, bed shear stresses smaller than 0.2 N/m^2 will allow most seedlings to settle without being uprooted (Balke et al., 2011). Thus, for suitable seedling establishment areas, we calculate the 90th percentile bed shear stress at the end of every year and adopt 0.2 N/m^2 as a threshold under which mangrove colonization can occur. The initial number of seedlings is set to 30 per 100 m^2 which is also the maximum density that one grid cell can accommodate and the initial stem diameter is set to 1.37 cm (Berger and Hildenbrandt, 2000; van Maanen et al., 2015).

Mangrove growth in our model refers to the increase of stem diameter (D; cm), tree height (H; cm) and the number of corresponding root elements. The growth rates are assumed to relate to local flooding and available resources, described by the following relations (Chen and Twilley, 1998; Berger and Hildenbrandt, 2000; van Maanen et al., 2015):

$$\frac{dD}{dt} = \frac{GD\left(1-\left(DH\right)/\left(D_{max}H_{max}\right)\right)}{\left(274+3b_2D-4b_3D^2\right)} \cdot f \cdot C \tag{3.3}$$

$$H = 137 + b_2D - b_3D^2 \tag{3.4}$$

where t is time (month). D_{max} and H_{max} are maximum stem diameter and tree height, set to 40 and 1000 cm, respectively. G, b_2, and b_3 are growth constants which are set here to, respectively, 12.68 cm/month, 43 and 0.536 cm^{-1} such that a maximum increase in stem diameter is approximately 1 cm per year. f is a fitness function which is an inundation-based factor to define mangrove growth conditions (Figure 3.13a), calculated as follows van Maanen et al. (2015):

$$f = a \cdot P^2 + b \cdot P + c \tag{3.5}$$

where a, b and c are constants determining the appropriate growth area of mangroves, set to -8, 4 and 0.5, respectively. The fitness function is set up on the premise that there is an optimal relative hydroperiod (i.e. $f = 1$ when $P = 0.25$) for mangroves and the growth quality will decrease when the relative hydroperiod is either larger or smaller than this optimal value. Meanwhile, the tree growth rate is further reduced by limitations in resources, which is introduced as a competition stress factor (C) that captures the competition between one specific tree and surrounding mangrove vegetation. The competition stress factor is implemented as a sigmoid function linked to biomass (Figure 3.13b) with the following formula (van Maanen et al., 2015):

$$C = \frac{1}{1+exp\left[d\left(W_{0.5}-W\right)\right]} \tag{3.6}$$

where d is a constant controlling the decreasing rate of this function, set to -0.0003. W is the total biomass (kg) in one grid cell including both above-ground and below-ground biomass. $W_{0.5}$ is the biomass when $C = 0.5$ which is a critical value in the model as it defines when mangrove competition may result in tree mortality. To set $W_{0.5}$, the above-ground (W_a) and below-ground (W_b) biomass of a single *Avicennia marina* are first evaluated through allometric equations (Komiyama et al., 2008):

$$W_a = 0.308D^{2.11} \tag{3.7}$$

$$W_b = 1.28D^{1.17} \tag{3.8}$$

We then apply the 'zone of influence' approach by defining a circle around each tree to represent the area from where the tree obtains resources (Berger and Hildenbrandt, 2000):

$$R = 10\sqrt{D/2} \tag{3.9}$$

where R is the circle radius (m) and $D/2$ represents the stem radius (m). We define a critical status without competition as when one grid cell is full of mature mangroves but each mangrove obtains its resources within its own zone of influence, without interacting with other trees. Hence, $W_{0.5}$ can be estimated by:

$$W_{0.5} = \frac{A_{cell}}{(2 \cdot R)^2} \cdot W_{mature} \tag{3.10}$$

where A_{cell} is the grid cell surface area (m^2) and Wmature is the biomass of one mature mangrove (when D = 40 cm). As A_{cell} = 2500 m^2, the application of Equation 3.10 leads to $W_{0.5} = 2.61 \times 10^4$ kg for each grid cell (Figure 3.13b).

The mortality of mangrove trees is identified when consecutive depressional growth occurs (Berger and Hildenbrandt, 2000). In this study, we use the value of $f \cdot C$ to represent mangrove growth quality. At the end of every year, the vegetation model evaluates the growth quality of all mangrove trees by calculating $f \cdot C$ and a mangrove tree dies when the growth rate has been smaller than 50% of the optimal status (i.e. $f \cdot C < 0.5$) for 5 consecutive years (van Maanen et al., 2015). Dead trees are removed to reduce local competition stress until growth conditions ($f \cdot C$) exceed again 0.5, or when no vegetation is left. Mangroves with smaller diameters are assumed to be more vulnerable to negative growth condition so these trees are removed first when mangroves with multiple stem diameters coexist in one cell. Considering the potential morphological evolution resulting in a concave profile in the upper-intertidal area, water may stagnate as possibilities for lateral drainage (e.g. through channels) are absent, leading to a shallow but persistent layer of water causing relative hydroperiods to exceed critical inundation thresholds. In this case, mangroves in these areas are set to stay alive without further growth until the shallow water stagnation disappears. This protects vegetation growing in the upper tidal area against prolonged inundation under the current one-dimensional model settings and has no further physical consequences. This implementation does not significantly change morphological evolution based on our sensitivity tests and in nature, mangroves have been shown to persist in such situations (Bryan et al., 2017).

Mangrove root elements provide significant flow resistance and bed friction due to their dense number and pneumatophores (i.e. aerial roots) can grow to a few tens of centimeters high (Mazda et al., 2005; Liénard et al., 2016). To include the effects of these roots, we relate the number of root elements with stem diameter using a sigmoid function (van Maanen et al., 2015) and assume roots keep a fixed size over time. In this case, an increase of stem diameter will lead to a simultaneous increase of root number and thus increase resistance and friction for water movement. The density of root elements recorded in the literature show a broad range, some areas have only a few roots while others may have more than one thousand roots per square meter (Dahdouh-Guebas et al., 2007). In our model, we assume a mature *Avicennia marina* can have at most 1000 roots. The number of roots (N_{roots}) is evaluated with the following formula (van Maanen et al., 2015):

$$N_{roots} = \frac{1000}{1 + exp\left[k\left(\frac{D_{max}}{2} - D\right)\right]} \tag{3.11}$$

where k is a constant describing the growth rate of the root number with stem diameter (D; cm), here set to 0.3. An overview of the vegetation model settings can be found in Table 3.2.

3.2.3 Model set up

Mangroves exist in a variety of coastal conditions around the globe. They inhabit tropical/subtropical shorelines characterized by varying tidal ranges, waves, sediment supply and coastal slope. As previously highlighted by Friedrichs (2011), the slope of equilibrium profiles varies with environmental conditions, so based on earlier equilibrium tests (Figure 3.14), we create three computational domains with different initial slopes (i.e. gentle, medium and steep) of 0.00025 m/m, 0.0005 m/m and 0.001 m/m to represent different tidal systems (i.e. micro-, meso- and macro-tidal systems with tidal range of 1 m, 3 m and 5 m) (Figure 3.2). The domain is constructed by 360 grid cells, and each cell size is set to 50 m by 50 m which has shown to be accurate and efficient following previous research (Xie et al., 2020). In a subset, we also include the effects of small wind waves by adding waves with a 5-cm significant wave height (H_s) at the seaward boundary. Peak wave period (T_p) is set to 1 s following an approximate empirical relation between T_p and H_s as: $T_p \approx 5.3\sqrt{H_s}$) (Mangor et al., 2017). Three suspended sediment concentrations (10, 30 and 50 mg/L) at the seaward boundary are applied in our models. Lastly, projections of SLR are implemented by incrementally raising the water level at the seaward boundary following three different representative concentration pathway (RCP) scenarios, from the lowest (5%) quantile of RCP2.6 (29 cm by 2100) through the medium (50%) quantile of RCP4.6 (55 cm by 2100) to the highest (95%) quantile of RCP8.5 (110 cm by 2100) (Oppenheimer et al., 2019). A constant morphological acceleration factor (set to 30 based on sensitivity tests) is applied to enable long-term simulations (Roelvink, 2006; Coco et al., 2013). The hydrodynamic time step is set to 0.5 min so that the morphological timestep is 15 min. The total simulation period is 250 morphodynamic years including an initial period of 150 years without SLR, followed by 100 years with SLR. All combinations of the key environmental conditions, namely SLR rates, tidal ranges, waves, sediment supply and coastal slopes were simulated to study the responses of mangrove forests (Table 3.3; more detailed model parameter settings can be found in Tables 3.1 and 3.2).

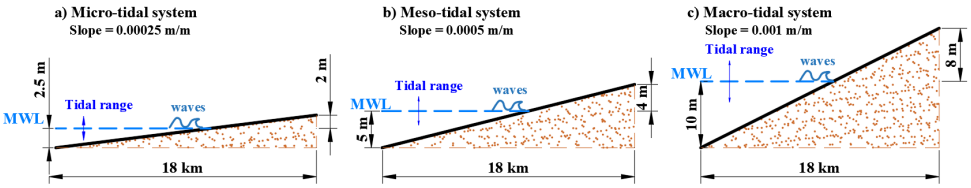

Figure 3.2 Initial bathymetries with the same cross-shore distance (18 km) but different bed elevations and slopes. a) Micro-tidal system. b) Meso-tidal system. c) Macro-tidal system. Tidal ranges in micro-, meso- and macro-tidal systems are set to 1, 3 and 5 m, respectively. The seaward edge bed elevation is -2.5 m in the micro-tidal system, -5 m in the meso-tidal system and -10 m in the macro-tidal system. These settings guarantee that the water depth at the seaward edge is deep enough to accommodate sediment accretion and bed level change even under high sediment supplies. By considering the highest possible elevation that tidal currents can reach under SLR effects, the landward edge elevation is set to 2 m in the micro-tidal system, 4 m in the meso-tidal system and 8 m in the macro-tidal system.

3.3 Results

We first (3.3.1) provide an overview of the coastal and mangrove development throughout the parameter space, i.e. varying tides, waves and sediment supply without SLR and then (3.3.2) show results of coastal and mangrove development with various rates of SLR. Subsequently (3.3.3), we compare sediment budget changes between the different scenarios introduced in Sections (3.3.1) and (3.3.2).

3.3.1 Mangrove behaviors under varying environmental conditions: *without* SLR

Accretion along the profile can be enhanced by increasing tidal range, sediment supply or adding wave effects, while changes in the mangrove seaward edge are modulated by the balance of tidal range and sediment supply, and waves will further limit mangrove seaward colonization around the mean water level (Figure 3.3).

Low sediment supply (10 mg/L) resulted in small changes in the cross-shore profile among different tidal systems (micro-, meso- and macro-tidal systems), where vegetation remained relatively stable covering nearly the complete upper-intertidal area, with vegetation occupying nearly 100%, 100% and 90% of upper-intertidal flats in micro-, meso- and macro-tidal systems, respectively (Figure 3.3a-c). Vegetation extent was mainly governed by the vertical and horizontal extent of the upper-intertidal area, which was determined by the tidal range and its corresponding coastal slope (Figure 3.4b-j; 10 mg/L without waves). Vertical vegetation extent under larger tidal range conditions ($\sim$ 1.5 m and 2.2 m in meso- and macro-tidal systems, respectively) was nearly three or four times the extent in micro-tidal systems ($\sim$ 0.5 m) (Figure 3.4e-g; 10 mg/L without waves), but their horizontal extent ($\sim$ 3.0 km and $\sim$ 2.8 km in meso- and macro-tidal systems, respectively) was only slightly larger than in micro-tidal systems ($\sim$ 2 km) (Figure 3.4h-j; 10 mg/L without waves).

Accretion along the profile was enhanced under intermediate sediment supply (30 mg/L), leading to both coastal propagation and the gradual development of a platform (Figure 3.3e-g). The size of the platform increased with increasing tidal range or sediment supply. Larger sediment supply elevated the platform closer to high water level compared to lower sediment supply conditions (e.g. Figure 3.3c,g&k). Thus, vegetated slopes with either larger tidal ranges or sediment supply developed gentler slopes significantly differing from the unvegetated seaward slope (Figure 3.4b-d; 30 or 50 mg/L without waves). Seaward mangrove colonization with larger tidal ranges is constrained to higher elevations above mean water level (Figure 3.3f-g), resulting in a comparable ($\sim$ 2.6 km in meso-tidal systems) or smaller horizontal vegetation extent ($\sim$ 2.0 km in macro-tidal systems) than in micro-tidal range system ($\sim$ 2.4 km) under intermediate sediment supply (Figure 3.4h-j; 30 mg/L without waves). Under high sediment supply, the formation of the platform elongated cross-shore mangrove presence, resulting in a larger horizontal vegetation extent (Figure 3.3j-k), especially for systems with a larger tidal range ($\sim$ 4.3 km and $\sim$ 3.9 km in meso- and macro-tidal systems, respectively) compared with systems with a micro-tidal range ($\sim$ 2.6 km) (Figure 3.4h-j; 50 mg/L without waves). Accompanied with increasing platform development for meso- and macro-tidal systems, the vertical proportion of the upper-intertidal area covered by mangroves drastically decreased, especially under high sediment supply (Figure 3.3j-k), making the vertical extent between the different tidal systems nearly equal (0.2-0.5 m) (Figure 3.4e-g; e.g. 50 mg/L without waves).

The presence of waves contributed to coastal platform development under intermediate and high sediment supply (30 and 50 mg/L) (Figure 3.3h&l), elevating the coastal platform closer to high water level (Figure 3.3m-n). Accretion along the profile was limited with less platform development under low sediment supply (10 mg/L) so vegetation remained relatively stable (Figure 3.3d). Apart from the high sediment supply simulations, the contribution of waves on platform formation and coastal propagation made the vegetated slope gentler, causing a larger slope difference compared with the offshore unvegetated area (Figure 3.4b-d; with waves). Vertical and horizontal vegetation extent

generally decreased when waves are included, especially in systems with larger tidal ranges and sediment supply (Figure 3.4e-g&h-j; with waves). This caused the vertical vegetation extent to remain nearly similar 0.2 ± 0.05 m) at high sediment supply (Figure 3.4e-g; 50 mg/L with waves), but horizontal vegetation extent in micro-tidal systems ($\sim$ 3 km) was nearly double or triple than in the larger tidal systems ($\sim$ 1.3 km and 1 km in meso- and macro-tidal systems, respectively) (Figure 3.4h-j; 50 mg/L with waves). Since the presence of waves exerted a more evident role in the reduction of the horizontal vegetation extent in the larger tidal range systems and profile evolution was small under low sediment supply, mangrove horizontal extent remained similar (1.4-1.7 km) among different tidal range systems (Figure 3.4h-j; 10 mg/L with waves).

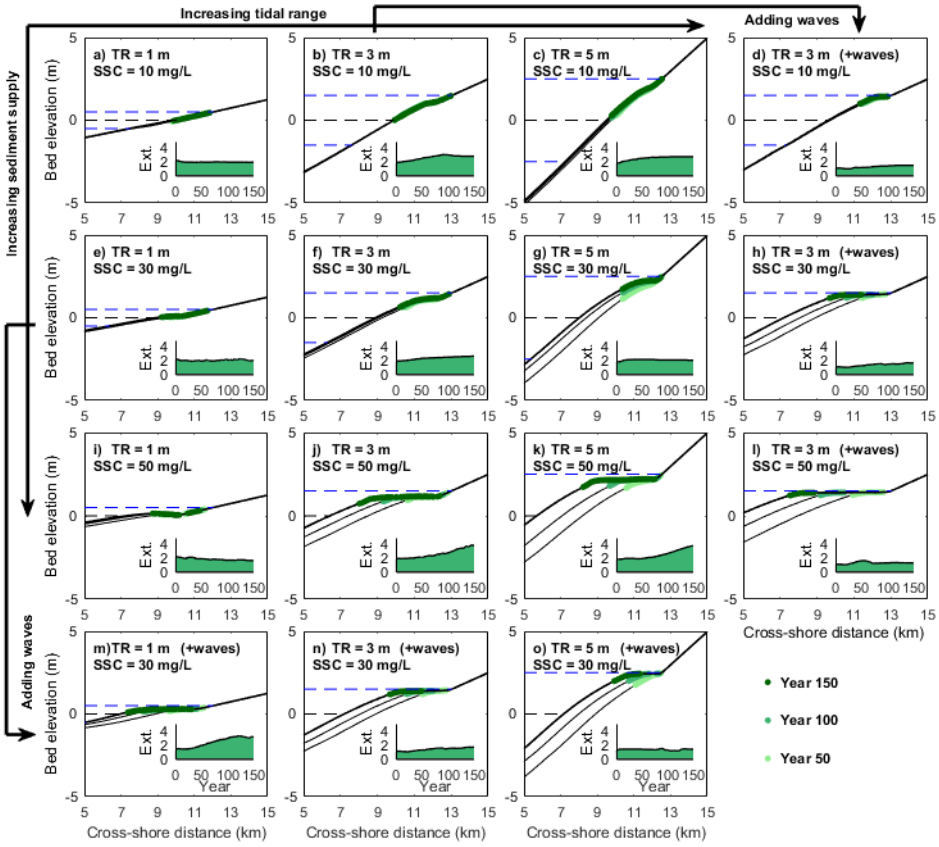

Figure 3.3 Mangrove development in response to different combinations of tidal range, sediment supply, wave action and coastal slope. Results from the first to the third column and the first to the third row indicate mangrove responses to increasing tidal range and sediment supply, respectively. Comparison results with wave effects are added with increasing tidal ranges in the fourth row (m-o) and with increasing sediment supply in the fourth column (d,h&l). The evolution of coastal profile and mangrove forest are shown after 50, 100 and 150 years. Green colors indicate mangrove presence, with increasingly darker shades representing temporal evolution. The black dashed line and its adjacent two blue dashed lines above and below represent mean water level, high water level and low water level, respectively. The inserts show temporal changes in the horizontal extent of mangrove forests (abbreviated as Ext., unit: km). TR and SSC represent the tidal range and external suspended sediment concentration applied at the seaward boundary, respectively.

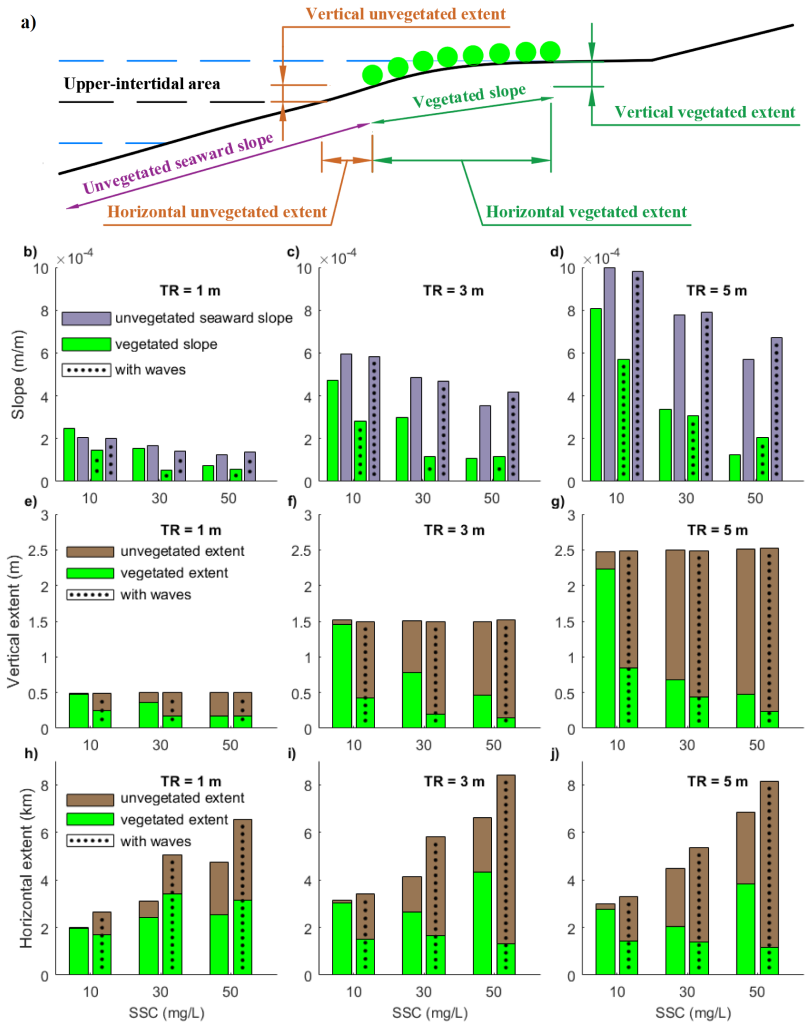

Figure 3.4 Comparison of slope and extent between unvegetated and vegetated areas. a) Schematic Figure indicating parameters for comparison in the following subplots. b-d) The comparison of coastal slope between seaward unvegetated area (purple bars, measured from seaward boundary to mangrove seaward edge) and vegetated area (green bars, measured from mangrove seaward edge to landward edge). e-g) The comparison of the vertical extent of unvegetated area within the upper-intertidal area (brown bars, measured from mean water level to mangrove seaward edge) and vegetated area (green bars, measured from mangrove seaward edge to landward edge). Thus, the vertical vegetation extent refers to the elevation range over which mangroves exist. h-j) The comparison of the horizontal extent of unvegetated area within the upper-intertidal area (brown bars, measured from mean water level to mangrove seaward edge) and vegetated area (green bars, measured from mangrove seaward edge to landward edge).

3.3.2 Mangrove behaviors under varying environmental conditions: *with* SLR

Our results illustrated mangroves in larger tidal range systems with higher sediment supply were able to survive or even expand seaward with slow or medium rates of SLR (Figure 3.5). Mangrove development in micro-tidal systems was greatly dependent on the rates of rising sea levels, which caused a persistent retreat of mangrove forests on a relatively stable profile with only minor changes in vegetation extent due to increased sediment supply (Figure 3.5a,e&i). In contrast, mangrove behaviors in larger tidal systems were more complex. Under low sediment supply (10 mg/L), the coastal profile experienced little accretion and mangroves kept a constant extent by landward transgression as sea level was rising (Figure 3.5b-c). In larger tidal systems (meso –macro tidal), although accretion across the profile was little under intermediate sediment supply (30 mg/L), the vegetation at the seaward edge remained stable with little landward transgression under slow/medium SLR rates (Figure 3.5f-g). Interestingly, during the fast SLR, the landward retreat of the seaward vegetation edge could be observed in meso-tidal systems (Figure 3.5f), however, the seaward edge remained stable in macro-tidal systems (Figure 3.5g). Under high sediment supply (50 mg/L), mangroves were able to propagate seaward under slow SLR rates, whereas high SLR rates led to a landward shift of the coastal profile (i.e. seaward erosion and landward accretion along the profile) and mangrove landward transgression (Figure 3.5j-k).

The effects of waves on mangrove responses were enhanced in larger tidal range or sediment supply conditions and adjusted by the rates of SLR (Figure 3.5). Under low sediment supply (10 mg/L), limited accretion along the profile occurred and waves had little effect so that the mangrove seaward edge retreated as sea level increased (Figure 3.5d). Under intermediate to high sediment supply (30 to 50 mg/L), waves contributed to sediment accretion under slow/medium SLR, enhancing coastal progradation and mangrove seaward expansion (Figure 3.5h&l). However, mangrove seaward edge retreated substantially when the SLR was fast. Meanwhile, among different tidal systems, waves helped to maintain a coastal platform under slow/medium SLR, and thus the vegetation extent increased, especially in larger tidal range systems (Figure 3.5m-o). Similar to the behaviors observed in the scenarios without wave effects (Figure 3.5e-g; 30 mg/L), fast SLR caused mangrove seaward edge to retreat landward in micro/meso-tidal systems but in macro-tidal systems this seaward edge remained stable (Figure 3.5m-o; 30 mg/L).

To identify the vulnerability of mangroves during various rates of SLR, we quantified and compared the movement of the seaward mangrove edge among different environmental conditions. Our results showed that mangroves in micro-tidal range systems were more sensitive to SLR and even slow SLR caused a substantial landward retreat, while in larger tidal range systems mangroves may even expand seaward despite a rising sea level (Figure 3.6). Also, mangrove seaward edge in the larger tidal range was more dependent on the balance between sediment supply and SLR rates. Low sediment supply and fast SLR rates would cause mangroves to retreat landward (blue-dashed lines in Figure 3.6b-c), while high sediment supply and slow SLR resulted in mangrove seaward expansion (red-dashed lines in Figure 3.6h-i). The role of waves on mangrove seaward movement differed with tidal range and SLR scenarios. In the absence of SLR effects, waves enhanced mangrove seaward expansion, especially when the tidal range was small (Figure 3.6). However, when sea level started to rise, waves caused mangroves to retreat faster in micro-tidal systems (solid lines with symbols in Figure 3.6a,d&g). In larger tidal range systems, the presence of waves could initially stabilize mangrove seaward edge even under fast SLR. Still, mangrove retreat may then be again faster when sea level was rising (e.g. blue-solid line in Figure 3.6h).

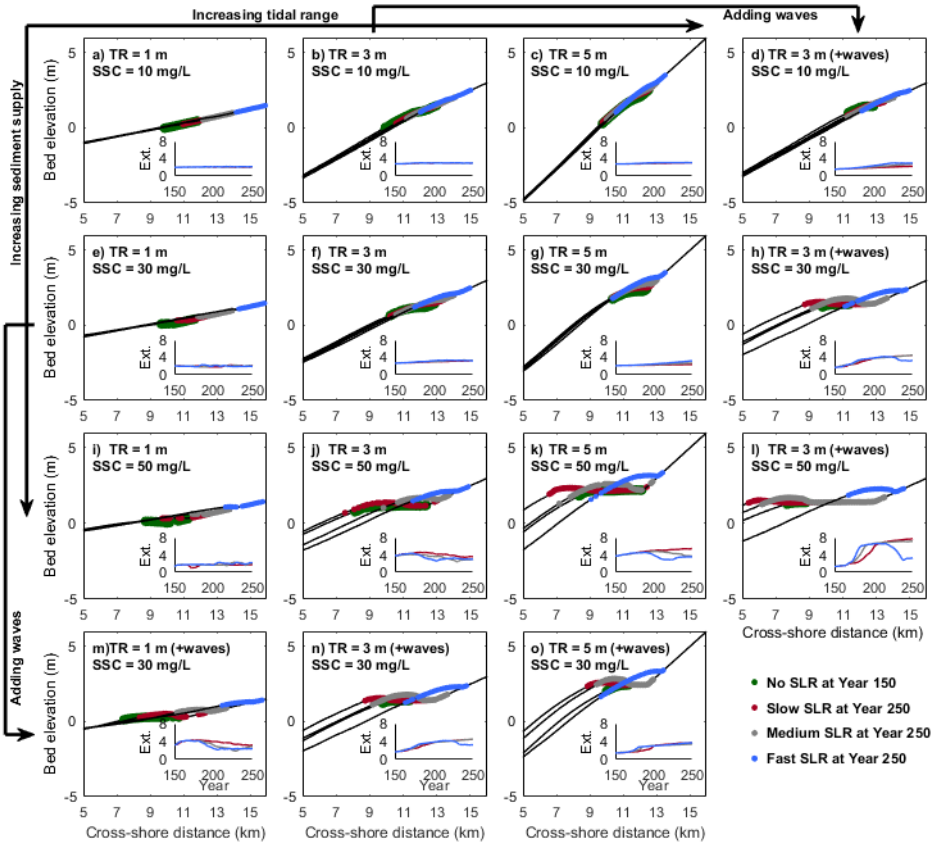

Figure 3.5 Mangrove behaviors in response to different rates of SLR. Results from the first to the third column and the first to the third row indicate mangrove responses to increasing tidal range and sediment supply, respectively. Comparison results with wave effects are added with increasing tidal range in the fourth row (m-o) and with increasing sediment supply in the fourth column (d,h&l). Green dots show vegetation distribution before SLR, which corresponds to the results from the vegetated profile in year 150 without SLR effects (Figure 3.3). Red, gray and blue dots indicate mangrove forests after 100-year slow, medium and fast SLR effects, respectively. The inserts of each Figure represent the temporal changes of mangrove horizontal extent over 100-year under different SLR effects (abbreviated as Ext., unit: km). A more detailed overview of mangrove behaviors can be seen in Figure 3.15.

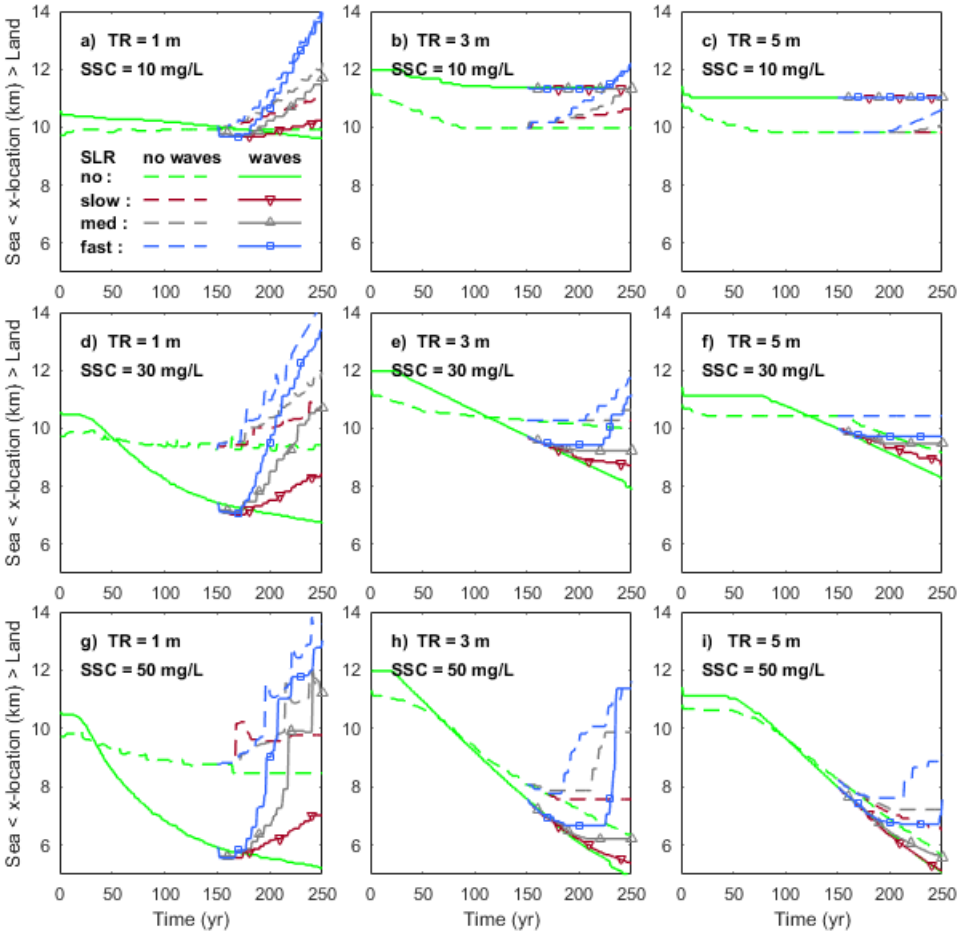

Figure 3.6 The movement of mangrove seaward edge without SLR effects (green lines) and with three different SLR scenarios. Y-axis includes two opposite directions, land and sea, showing the direction and distance over which the seaward mangrove edge moves. Increasing values represent landward retreat of the mangrove seaward boundary, while decreasing values represent seaward mangrove expansion. Red, gray and blue lines are used to represent the results of slow, medium (abbreviated as med in a)) and fast SLR. SLR was implemented after 150 years. Dashed and solid lines are used to indicate the simulations without waves and with waves, respectively.

3.3.3 Sediment budget changes under SLR

Finally, we analyzed how SLR altered sediment budgets and how this is dependent on coastal conditions. Since the amount of sediment accumulated and displaced along the profile and in intertidal zones during rising sea levels is important for mangroves to maintain their relative elevation in the tidal frame, we evaluated sediment budget changes over two distinct sections: 1) over the active profile up to the high-water level before SLR (HWL before SLR) (Zone 1 in Figure 3.7a-b) and 2) over the profile section that became flooded during SLR (between HWL after and HWL before SLR) (Zone 2 in Figure 3.7a-b) as the latter represented the potential new accommodation space available for mangroves. Under slow SLR rates and in the absence of waves, the sediment is mainly deposited in Zone 1 (Figure 3.7c). The amount of sediment accumulated in this zone in micro-tidal systems remained similar ($\sim$ 3 cm/m) despite changes in sediment supply (blue bars in Figure 3.7c), while in larger tidal range systems sediment accumulation in Zone 1 increased as sediment supply increased (brown or gray bars in Figure 3.7c). Under medium SLR rates, there was a slight increase in sediment deposition in Zone 1 for micro-tidal systems (blue bars in Figure 3.7d), while more sediment erosion occurred in meso-tidal systems (brown bars in Figure 3.7d) and sediment deposition became less in macro-tidal systems (gray bars in Figure 3.7d). Meanwhile, some sediment started to be deposited in Zone 2 in the systems with either a larger tidal range or sediment supply (green bars in Figure 3.7d). Under fast SLR rates, more sediment was deposited in Zone 1 in micro-tidal systems (blue bars in Figure 3.7e), while in larger tidal range systems this profile section (Zone 1) was further eroded, especially when sediment supply was large (brown or gray bars in Figure 3.7e). Sediment accumulation in Zone 2 increased for all tidal range systems under such high SLR rates (green bars in Figure 3.7e). The presence of waves generally enhanced sediment deposition in Zone 1 when the SLR was slow/medium (Figure 3.7f-g). Also, more sediment was deposited in Zone 2 when sediment supply was low (green bars in Figure 3.7f-g). Under fast SLR, with the exception of macro-tidal systems with high sediment supply, waves contributed to enhancing sediment deposition in Zone 2 (green bars in Figure 3.7h), but they also reduced sediment deposition or caused more sediment erosion in Zone 1 (e.g. blue or brown bars in Figure 3.7h).

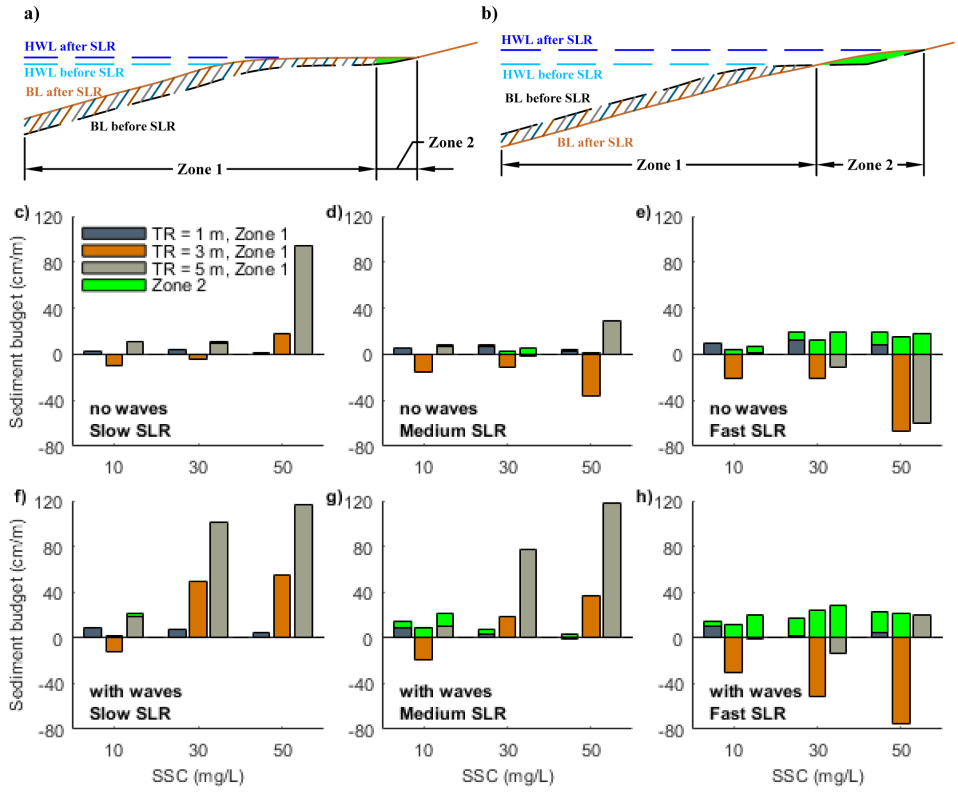

Figure 3.7 Sediment budget changes (converted to cm/m, representing vertical changes in profile elevation per meter in the cross-shore direction) during SLR under various coastal conditions. The sediment budget is calculated here as the sum of bed level differences in two respective zones (Zone 1 and Zone 2) within the 100-year SLR period and divided by their corresponding horizontal lengths. a-b) Schematic Figures indicating Zone 1 and Zone 2 in two different scenarios: a) coastal propagation where there is deposition in Zone 1 and limited deposition in Zone 2, and b) coastal retreat where there is erosion in Zone 1 and substantial deposition in Zone 2. HWL and BL here represent high water level and bed level, respectively. Sub-Figures c-e and f-h represent the results without wave effects and with wave effects, respectively. c&f, d&g and e&h are the results under slow, medium and fast SLR, respectively. Blue, brown and gray bars are used to indicate sediment budget changes in Zone 1 and green bars are used to indicate changes in Zone 2.

3.4 Discussion

Our numerical scenarios highlight that coastal conditions non-linearly influence mangrove behavior and determine their vulnerability to SLR. The analysis covers variations in tides, wave action, sediment supply and coastal slope, under different SLR scenarios, indicating distinct mangrove responses to SLR across various coastal systems. In this section, we discuss (3.4.1) how different coastal conditions control profile evolution and mangrove dynamics, (3.4.2) the key factors determining mangrove vulnerability to SLR, and (3.4.3) other relevant processes shaping vegetated coastal profiles.

3.4.1 Key controlling factors influencing the changes in coastal profile evolution and mangrove dynamics

Effects of coastal conditions on shaping vegetated coastal profiles

This study aims to unravel the controlling processes driving changes in mangrove forests and morphological evolution through idealized numerical simulations and, as such, modelling behaviours and trends become the main concern (Murray, 2013). Consistent with natural mangrove systems (Figure 3.1), the model predicts variations in profile shapes and vegetation distributions in response to different coastal environmental conditions. In our model as well as in field observations, linear intertidal profile shapes occur in systems with either small tidal range or low sediment supply, while increasing these two variables leads to the formation of a gently sloping vegetated platform occupied by mangroves (Figures 3.1,3.3&3.4b-d) (Bryan et al., 2017; Semeniuk, 2018; Nardin et al., 2021). The elevation of the vegetated platform tends to move closer to the high water level when sediment supply increases (e.g. Figure 3.3c,g&k), which is in agreement with previous field observations and numerical experiments (Kirwan et al., 2016a; Swales et al., 2019; Goodwin and Mudd, 2020). The comparison between different scenarios reveals that tidal range and sediment supply play a determining role on the overall coastal slope and mangrove extent with relatively gentle/steep profiles existing under small/large tidal range and high/low sediment supply, respectively (Figure 3.4b-d). These trends are consistent with modelling efforts of unvegetated tidal flats (Friedrichs, 2011). Additional small wind waves enhance accretion and coastal progradation in all our simulations (Figure 3.3) as a result of the enhanced onshore sediment fluxes (Figures 3.16 and 3.17), which has also been observed in the field (Swales et al., 2019). The role of small wind waves on sediment transport varies with the coastal condition (i.e. tidal range and associated coastal slope) (Figures 3.16 and 3.17). In micro-tidal systems, the presence of waves is able to shift a stable profile (e.g. Figure 3.3e) to a propagating profile (e.g. Figure 3.3m), promoting mangroves seaward expansion (Figure 3.6a,d&g) and increasing horizontal vegetation extent (Figure 3.4h) due to the shallower water depth and weaker currents (Carniello et al., 2011). In meso- and macro tidal systems, the presence of waves limits seaward vegetation colonization under low sediment supply due to the enhanced hydrodynamic forces and limited coastal propagation (Figure 3.3b&d); on the contrary, under intermediate and high sediment supply, waves further increase existing progradation (Figure 3.3f&h, j&l). This is in agreement with previous research that small waves (less than 20 cm) are capable of resuspending sediments over tidal flats (Green et al., 1997; Uncles and Stephens, 2000; Green, 2011; van der Wegen et al., 2017) and thereby potentially nourishing vegetated habitats (Carling, 1982). Thus, our simulations are able to highlight that tidal range, waves and sediment supply impact bio-physical feedbacks between vegetation extent (either in the horizontal or vertical dimension) and coastal slope. The complexity of these non-linear feedbacks further governs coastal landscape configuration and vegetation distribution, leading to different degrees of platform formation which have not been identified so far (Figure 3.4e-g&h-j).

Effects of hydrodynamic forcing and profile evolution on mangrove colonization

Tidal range and sediment supply have been identified as key factors determining mangrove distribution (Ellison, 2015). Mangrove extent has been linearly linked with tidal range (Ellison, 2015; Lovelock et al., 2015), however, our results show that vegetation extent (either in the horizontal or vertical dimension) varies non-linearly with changes in tidal range and sediment supply which results in unexpected responses compared to the first-order approximation (Figure 3.4e-g&h-j). This is linked to the conditions inhibiting mangrove colonization. Previous studies suggested that the establishment and survival of mangrove seedlings are constrained by high bed shear stress even under an appropriate inundation regime, and thus linked to so-called windows of opportunity (WoO) governed by variations in external forcings (Balke et al., 2011; Friess et al., 2012). Aligned with these studies, here we show, using constant hydrodynamic forcing (i.e. M2 tide, regular sediment supply and waves), that increased tidal range (i.e. stronger tidal currents) or additional wave action limits mangrove seaward colonization (e.g. Figure 3.3f,g&o), as is also observed at the Firth of Thames, New Zealand (Balke et al., 2015). Comparisons on the seaward edge elevation of mangrove forests between natural systems and our model simulations across a variety of tidal ranges confirm our model finding that mangrove elevations generally increase with tidal range (Figure 3.18 and Table 3.4). Moreover, our modelling results indicate that altered tidal currents in response to platform morphological adaptation further limit the colonization. More specifically, in macro-tidal systems, profile reconfiguration and platform formation enhance ebb tidal currents (Figure 3.8), increasing bed shear stresses and limiting vegetation colonization at the mid-intertidal moving mangroves towards higher bed elevations (Figure 3.3g&k). Our simulations thus indicate that mangrove colonization can be linked to profile reconfiguration through bio-morphodynamic feedbacks. As a consequence of these colonization constraints, the lower elevation limit for mangroves can be higher than mean sea level (e.g. Figure 3.3g&k), which has also been observed in the field (Balke et al., 2014; Bryan et al., 2017; Swales et al., 2021). In addition to capturing this behavior, we show that coastal environmental condition plays a key role in determining the lower limit mangroves can colonize in the intertidal.

3.4.2 Feedbacks between coastal conditions, mangrove vulnerability and SLR

On the role of tidal range, waves, sediment supply and coastal slope

Previous research illustrates that the balance between SLR rates and vertical accretion rates determines the resilience of mangroves against drowning (Woodroffe et al., 2016). As previously identified, external sediment supply plays a major role in driving vertical accretion rates (Lovelock et al., 2015). Simulations for meso- and macro-tidal systems with fast SLR rate and low sediment supply caused relatively stable coastal profiles over which mangroves transgressed landward (Figure 3.5b&c). However, an increase in sediment supply and reduction in SLR rate led to profile seaward propagation and thus mangrove expansion (Figure 3.5j&k). This reinforces the importance of the balance between SLR and sediment supply, at least under these tidal conditions. Yet, our simulations also show that sediment accretion rates are not necessarily enhanced by increased sediment supply, but may instead depend non-linearly on environmental conditions, such as tidal range, coastal slope and waves (Figure 3.7). Thus, changes in mangrove extent under SLR may vary for systems with varying tidal ranges despite similar sediment supplies (e.g. Figure 3.5i,j&k). More specifically, mangroves in micro-tidal systems are found to rapidly retreat landward even under slow SLR and high sediment supply (Figures 3.5i & 3.6g). The potential reasons are 1) the gentler coastal equilibrium slope in micro-tidal system (Figure 3.4b), where a small water level change will cause a large horizontal displacement of the inundation regime and thus strongly affect mangrove survival; and 2) the lower ability to capture sediment in micro-tidal systems where sediment deposition over the profile remains limited so that vertical accretion cannot allow mangroves to maintain their relative elevation within the tidal frame (Figure 3.7). In addition, since the presence of small wind waves enhances accretion and seaward profile propagation, mangrove seaward expansion is still possible under slow/medium SLR, compared to the results without wave effects (Figure 3.5h,l,n&o).

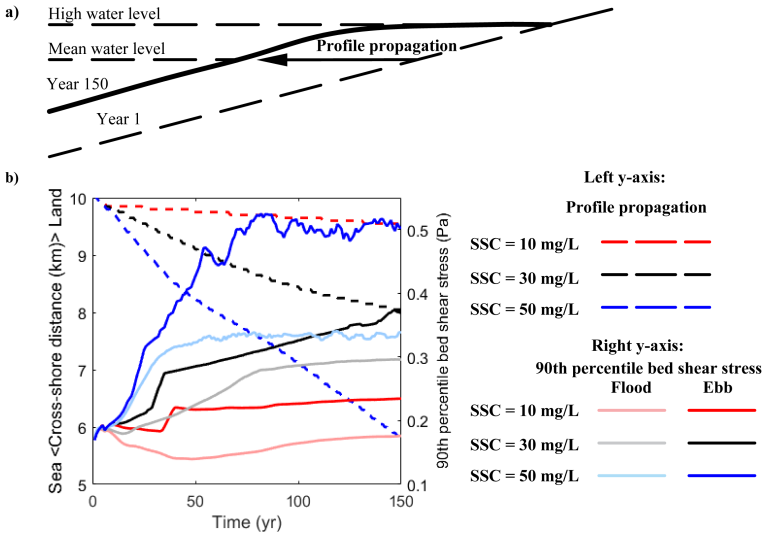

Figure 3.8 Relations between coastal profile propagation and bed shear stress changes. a) Schematic Figure illustrating profile propagation from year 1 to year 150. b) Relationships between coastal profile propagations (left y-axis) and bed shear stress (right y-axis) in the macro-tidal systems without waves before sea level rises (Figure 3.3c,g&k). The changes in cross-shore distance (dashed lines) and the corresponding flood/ebb bed shear stress (solid lines) in b) are based on the intersection between coastal profile and mean water level, as indicated by the arrow in a). Red, black and blue colors are used to show different scenarios with sediment supply of 10, 30 and 50 mg/L, respectively. Light color shades of solid lines indicate bed shear stress during the flood period and dark color shades indicate bed shear stress during the ebb period.

This implies that when small waves are present, the extra sediment stirring and resultant transport fluxes can play a role in enhancing the resilience of mangrove systems under SLR, which confirms earlier research showing the effects of waves on critical SLR rates in salt marsh systems (Schuerch et al., 2013; FitzGerald and Hughes, 2019).

Effects of inundation buffer

Our modelling results suggest that the mangrove seaward edge can remain stable even under fast SLR and no or limited sediment accretion (Figure 3.5g&o). This is because colonization restrictions can cause mangroves to establish at high elevations with an initially low hydroperiod, and thus potentially withstand increasing tidal inundation. This effectively creates an inundation buffer before SLR, such that the inundation threshold of mangrove trees is not immediately exceeded during rising sea levels (Figure 3.9). This can be exemplified by focusing on the changes in environmental parameters at the seaward edge of mangrove forests when SLR starts. Before SLR, the bed level is increasing which corresponds to a decreasing relative hydroperiod (Figure 3.9a,b,d&e). When waves are absent, mangroves are able to colonize as soon as both hydrodynamic forces and relative hydroperiod are below the thresholds (at year 10; Figure 3.9b&c). Excess bed shear stress induced by tides limits further seaward mangrove expansion despite ongoing coastal progradation (Figure 3.3g). Although the mangrove seaward edge thus remains stable, the inundation regime becomes more favorable (relative hydroperiod decreases from 0.4 to 0.3; Figure 3.9b). When waves are present, the excess bed shear stress is more profound and hinders mangrove colonization even though the inundation regime is highly suitable (Figure 3.9e-f). As such, when colonization eventually takes place (at year 150), mangrove presence is confined to higher elevations, where the relative hydroperiod is well below the

inundation threshold (relative hydroperiod is approximately 0.2; Figure 3.9e). Thus, the seaward mangrove forest edge prior to SLR (either with waves or without waves) is located at an elevation and inundation regime which constitutes an inundation buffer.

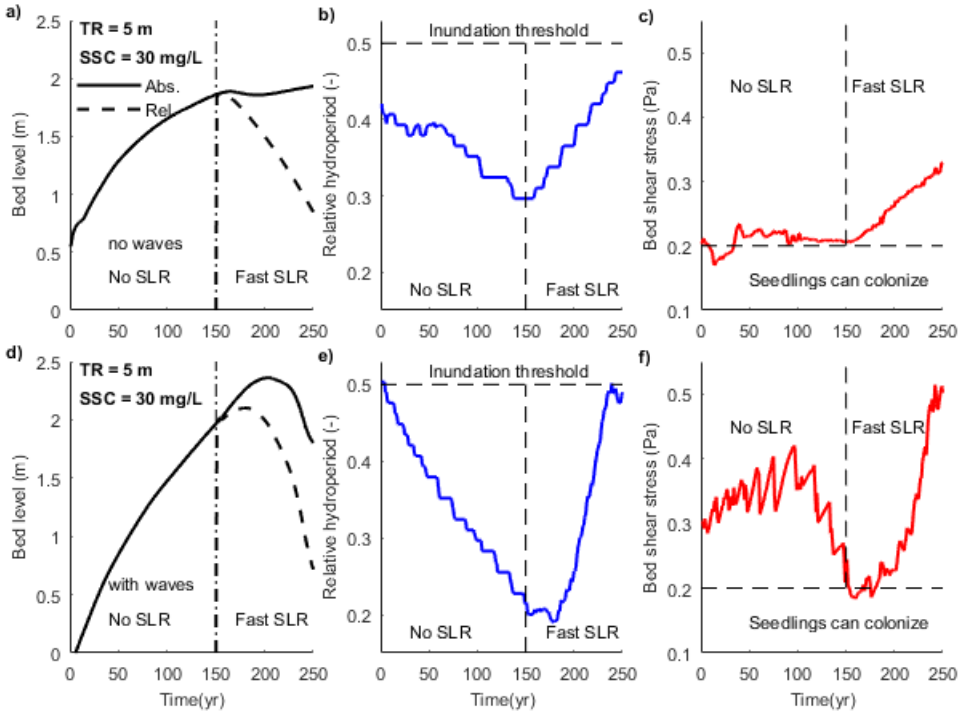

Figure 3.9 Temporal changes of key parameters over 250 years. The scenarios represent a stable seaward vegetation edge during fast SLR under intermediate sediment supply (30 mg/L) and large tidal range (5 m) (Figure 3.5g&o). SLR starts at year 150. The location for analysis is the seaward edge of mangrove forests at the beginning of SLR. These mangroves can subsequently survive fast SLR because of an inundation buffer. a-c) are results without waves and d-f) with waves. Temporal changes of a&d) absolute bed level (solid lines) and relative bed level (to mean water level; dashed lines), b&e) relative hydroperiod and c&f) 90th percentile of bed shear stress.

When SLR occurs, increasing bed shear stress limits accretion along the profile prohibiting bed levels to keep up with SLR, resulting in an increase in relative hydroperiod (Figure 3.9b&e). However, the inundation regime at the seaward mangrove edge still remains below the vegetation mortality threshold (Figure 3.9b&e) so that mangroves are able to persist under such fast SLR rates. This implies that the capacity of mangroves to survive SLR is not only based on the balance between SLR rates and vertical accretion rates which has been widely recognized (Woodroffe et al., 2016), but also based on the relative bed elevation occupied by mangroves, which in turn is controlled by vegetation colonization and morphology feedbacks. Although our model simplifies colonization thresholds, it clearly demonstrates that mangrove survival under SLR needs to account for complex growth dynamics. The set-up of our simulations is based on 150 years without SLR impacts followed by 100 years with SLR. This may overestimate the established inundation buffer in comparison to natural systems evolving under continuous SLR (Lovelock et al., 2015; Saintilan et al., 2020). However, our results nevertheless demonstrate that the acceleration of SLR predicted in the near future might severely reduce the resilience of mangrove systems, rendering them unable to maintain an inundation

buffer. The current study only uses a simplified M2 tide to drive tidal variations, however, in reality, differences in spring-neap cycles, barometric pressures and storm waves will potentially increase non-linearities of hydrodynamic conditions and thus complicate mangrove establishment (Balke et al., 2011). Including these factors goes beyond the scope of the current study, but is an important avenue for future research.

Effects of profile reconfiguration and infilling of accommodation space

Consistent with previous findings, the creation of landward habitats can compensate for the loss of seaward mangrove forests under rising sea levels, thus the total mangrove extent may remain stable or even increase (Figure 3.5) (Schuerch et al., 2018). Our model shows that mangrove landward expansion is possible without infilling of the newly generated accommodation space (e.g. Figure 3.5a-c). This is because mangroves can survive within a range of relative hydroperiods (Chapman, 1976) and the coastal conditions, determined by tidal range and coastal slope, create a gradient of inundation pattern across the profile. This finding seemingly contradicts other studies which note that increasing sediment mass is needed to completely infill newly created accommodation space in order to maintain wetland area (Törnqvist et al., 2019; Törnqvist et al., 2021). Yet, our centennial-scale simulations reveal that whether limited, partial or complete infilling occurs depends on coastal conditions and the bio-physical adaption of the coastal profile under SLR. For instance, if accretion along the profile is limited as a result of either low sediment supply or small tidal range, SLR may only shift the inundation zones landward with mangrove colonization occurring in newly created landward habitats (Figure 3.5). Alternatively, sediment infilling of new accommodation space may happen and in fact originate from erosion and reconfiguration of the lower coastal profile (Figure 3.7). This erosion is caused by the strengthening of tidal currents linked to increases in the tidal prism because of landward flooding (Figure 3.19). Meanwhile, the strengthening of tidal currents not only causes adjustments in the coastal profile, but also makes the mangroves in the seaward area particularly vulnerable (e.g. Figure 3.5j&k). This implies that profile reconfigurations, changes in mangrove coverage and infilling of accommodation space emerge from complex bio-morphodynamic interactions. Thus, infilling of the accommodation space may not be necessary for mangrove survival, however, it can be important for long-term sustainability and is highly dependent on bio-physical feedbacks (Rogers et al., 2019; Törnqvist et al., 2021).

These bio-physical feedbacks in turn strongly depend on the rates of SLR as also suggested by Fagherazzi et al. (2004). Offshore sediment erosion, onshore sedimentation and filling up of newly available accommodation space are enhanced under increasing rates of SLR (Figure 3.7). This is in agreement with field observations from salt marshes, showing moderate SLR causing coastal progradation, while increased SLR rates induced offshore sediment erosion and increased transport on the vegetated platform (Yang et al., 2020). Interestingly, apart from the influence of SLR rates, we find that offshore erosion (i.e. the decrease of bed level in seaward areas) and the landward shift of the coastal profile are most significant for the systems with high sediment supply (50 mg/L) in which a profound platform was formed (Figure 3.5k&l). This highlights that the established profile configuration, including the cross-shore extent of the platform, has a major impact on mangrove responses to SLR and filling up of the accommodation space.

Non-linear relations between SLR and sediment accretion rates

Previous research has investigated mangrove vulnerability by evaluating the relation between local SLR rate and surface accretion, as summarized by McKee et al. (2021) (black dots in Figure 3.10; Table 3.5). Consistent with these field observations, our model results not only capture the natural sediment accretion rates (Figure 3.20), but also show that sediment accretion rates may increase in response to increasing SLR rates (Figure 3.10b-d&e-g). This is because SLR enhances sediment deposition by increasing the relative hydroperiod and suspended sediment concentration over the

vegetated flats under fast-rising sea levels, in particular in larger tidal range systems (Figure 3.21). This is consistent with the current view that mangroves can keep up with SLR through bio-physical feedbacks involving enhanced deposition under prolonged inundation (Rodriguez et al., 2017; Schuerch et al., 2018), but also shows that SLR may increase sedimentation on vegetated flats by modifying sediment availability.

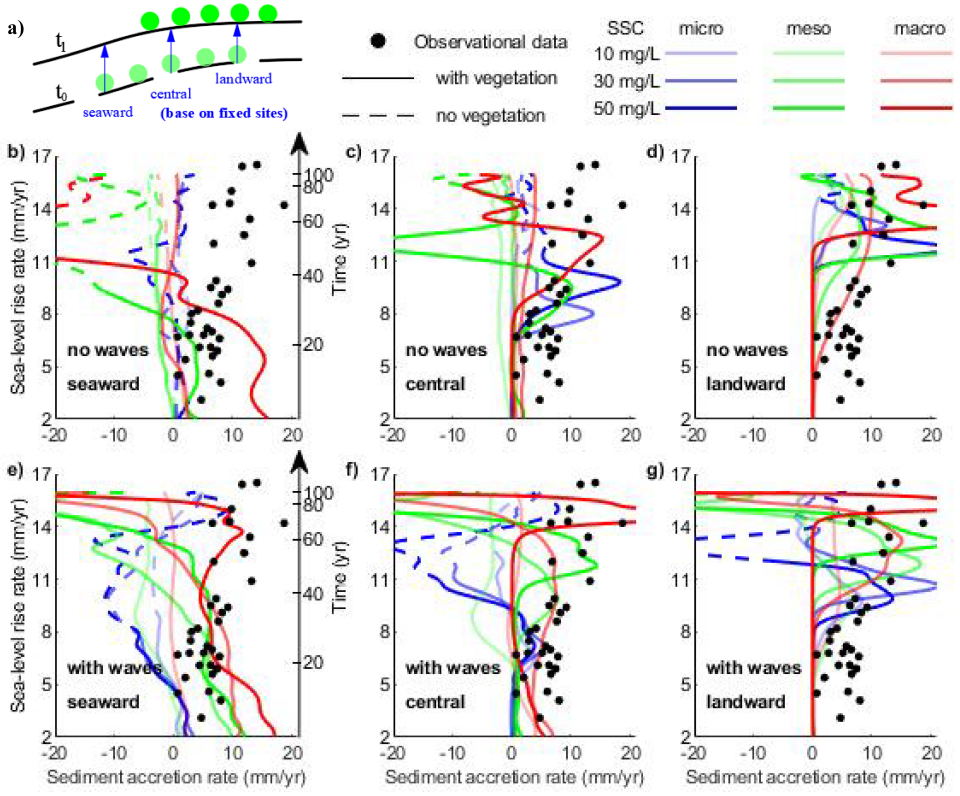

Figure 3.10 Comparison of SLR rates and sediment accretion rates between numerical simulations (lines) and field observations (black dots, summarized by McKee et al. (2021)), evaluated for the fast SLR scenarios. Schematic Figure a) illustrates how the relation is evaluated: in the seaward (b&e), central (c&f) and landward (d&g) region of the initial mangrove forest. Locations used to calculate seaward, central and landward accretion rates are based on fixed sites before the SLR. Blue, green and red color lines in subplots (b-g) are used to represent the micro-, meso- and macro-tidal systems, respectively. Light, medium and dark color shades are used to represent the low (10 mg/L), intermediate (30 mg/L) and high (50 mg/L) sediment supply, respectively. The switch from solid lines to dashed lines in b-g) represents the disappearance of vegetation at those specific locations due to SLR.

The timing and magnitude of accelerations in accretion depend non-linearly on the distance from the mangrove seaward edge (Figure 3.10). Strong spatial variations in accretion may initially occur across the forest, which has also been observed in the field (Swales and Lovelock, 2020; Swales et al., 2021). Our model results further suggest that such spatial variations in accretion rates are influenced by rising sea levels and vary with coastal conditions. In the absence of waves, accretion is initially low apart from in the most seaward region of the forest in the meso- and macro-tidal system (dark green and red in Figure 3.10b). However, when the SLR rate increases, accretion starts to accelerate in the central region (Figure 3.10c) and then also in the more landward region, especially when sediment supply is

high (Figure 3.10d). When waves are present, the initial accretion in the seaward region is enhanced across the majority of tidal range and sediment supply simulations (Figure 3.10e). Interestingly, in the central region of the forest, waves can either enhance (e.g. compare dark green lines in Figure 3.10c and f) or reduce (e.g. compare dark blue lines in Figure 3.10c and f) the acceleration in sediment accumulation. Also, SLR rates driving increasing accretion rates in the landward region are lower with waves (Figure 3.10d vs. Figure 3.10g).

The increase in accretion in the central and landward forests may coincide with reduced accretion and eventual erosion in the seaward region. This reflects the aforementioned profile reconfiguration which also results in mangrove mortality (see transitions from red and green solid lines to dashed lines in Figure 3.10b and from blue solid lines to dashed lines in Figure 3.10e). Recent paleorecord findings on mangrove vertical accretion preserved in the sedimentary archives show mangroves are very likely to be unable to initiate sustained accretion and be submerged when SLR rates exceed 6.1 mm/yr (Saintilan et al., 2020). Although the majority of our simulated scenarios show seaward mangrove mortality occurring for SLR rates below 10 mm/yr (see transitions to dashed lines in Figure 3.10b&e), our study highlights the spatial variation in the response of sediment accretion to SLR. This suggests the interpretation of paleoenvironmental records should encompass records derived along coastal gradients as critical SLR thresholds are inherently linked to the location within mangrove forest.

Synthesizing mangrove vulnerability and evaluating the effects of dynamic coastal profiles and complex vegetation behavior

The present study systematically explored mangrove vulnerability under various coastal conditions accounting for dynamic mangrove vegetation and profile evolution. Neglecting such dynamics will cause substantial differences in mangrove vulnerability projections (Figure 3.11). The application of a simplified approach with static coastal profile and 'bed level-based' vegetation characteristics is only appropriate in small tidal range systems under slow SLR and without wave effects, for which seaward vegetation behaviors are similar to our dynamic approaches (Figure 3.11a). The contrast between the static and dynamic approach becomes larger if tidal range or sediment supply is increased or additional wind waves are included, and the dynamic approach consistently suggests a lower mangrove vulnerability in comparison to the static approach (Figure 3.11). This finding not only supports conclusions from previous research that mangrove resilience is enhanced through bio-physical processes including sediment accretion (Krauss et al., 2014), but also shows that dynamic coastal profiles and vegetation exert distinct controls on mangrove behaviors in the context of SLR between different coastal environments.

3.4.3 Model limitations and perspectives

In this study we applied a comprehensive model incorporating detailed descriptions of bio-morphodynamic processes. While this allows for unravelling the effects of complex bio-physical interactions, it creates a trade-off in terms of the spatial scale of model simulations that can be considered. Even though similar types of models have been applied to entire estuarine systems (Brückner et al., 2021), the large number of model simulations carried out here necessitated a one-dimensional idealized modelling approach. Even though two-dimensional processes characteristic for estuaries are not incorporated, it is plausible that insights obtained from our idealized profile modelling (e.g. the increased vulnerability of mangroves in micro-tidal conditions) are applicable to mangroves in estuarine systems as well.

Although our research explores the effects of diverse coastal conditions and accounts for a range of bio-physical processes, model simulations struggle to capture certain profile characteristics, such as the abrupt slope difference between vegetated and unvegetated sections observed in some mangrove environments (e.g. Figure 3.1a&c). The causal factors can be related to different coastal processes and

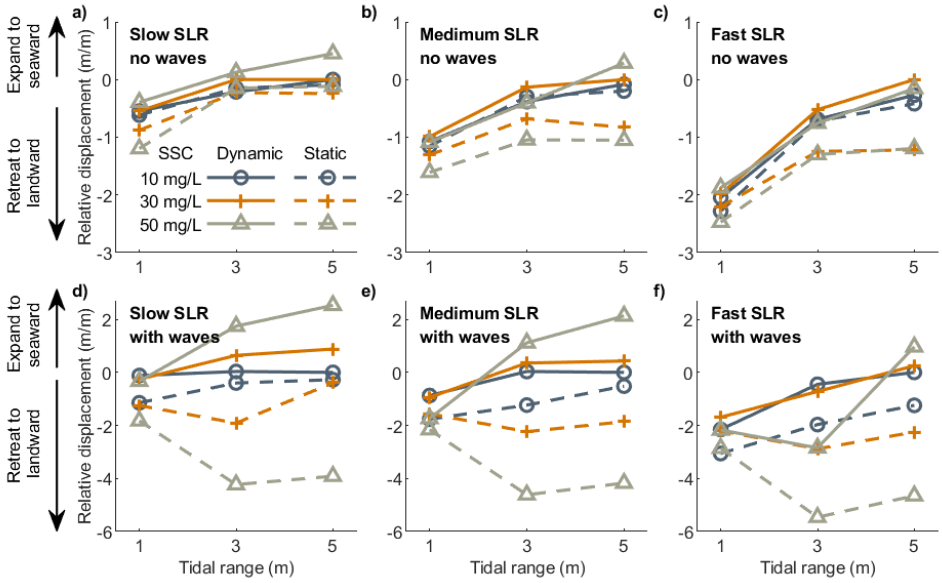

Figure 3.11 Relative displacement after 100-year SLR impacts. Here, relative displacement is defined as the retreat extent of mangrove seaward edge after SLR effects over the total horizontal vegetation extent before SLR. As an example, if the new mangrove seaward edge after 100-year SLR effects is exactly the landward edge before SLR, then this 'relative displacement' gets a value of -1. If it remains stable without retreat, it gets a value of 0. The top row and bottom row represent the relative displacement under no waves and waves, respectively. The dynamic approach accounts for profile evolution (marked with solid lines). The static approach assumes that vegetation retreats landward under rising sea levels without profile evolution (marked with dashed lines). The comparative analysis is based on the distinct profiles generated after 150 years under varying coastal conditions (Figure 3.3).

properties, including 1) variations in sediment composition, grain size and mangrove root density across the profile and through depth resulting in differences in sediment erodibility and potentially causing slope differences (Spenceley, 1977; Swales et al., 2007; Swales et al., 2021); 2) complex tidal forcing including overtides of the M2 tidal constituent, such as the M4 and M6 components which modify tidal asymmetry and influence landward sediment transport and thus profile shape (Wang et al., 1999); 3) energetic wave impacts reinforcing mud erosion at the mangrove forest edge (Winterwerp et al., 2013); 4) variations in mangrove distributions linked to species-specific colonization requirements such that some mangrove species can only colonize on the elevated, more gentle coastal platform (Chapman, 1976); 5) 2D effects in the horizontal plane such as tidal creeks and associated morphological features (e.g. Figure 3.1c) (Boechat Albernaz et al., 2020). Including some of these factors may improve comparisons with real vegetated profiles and potentially influence mangrove behaviors under SLR, but will also raise the difficulty of analyzing the complex bio-physical interactions controlling mangrove dynamics. The aim of accurately quantifying wetland changes for real mangrove sites can be achieved in the future with extra efforts in parameterizing our model.

Our wave scenarios, adding small waves at the open boundary, should mainly be interpreted as testing the sensitivity of the resulting coastal configuration to an increased resuspension flux potentially caused by wind. Small wind waves with heights between 0.03-0.27 m have been observed at various mangrove sites, but particularly develop in shallow water depth environments (Brinkman, 2006; Mazda et al., 2006; Quader et al., 2017; Bao, 2011; Horstman et al., 2014). The effects of wind

waves on morphology have been simulated by a relatively simple model (i.e. 'roller model'), with the benefit of high computation efficiency in comparison to more comprehensive wave models such as SWAN (Booij et al., 1999). However, limitations exist as wave attenuation by mangrove vegetation is not included, and thus, spatial variations in sediment deposition and erosion linked to such vegetation-induced wave attenuation is ignored. In reality, mangroves exert higher drag forces dissipating wave energy and reducing wave height across the flats thereby facilitating sediment settling and contributing to sediment accumulation (Mazda et al., 1997a; Quartel et al., 2007). Previous experimental and numerical studies have highlighted that the attenuation of waves by mangroves ranges between 20% - 60% (Phan et al., 2019). Although the omission of wave attenuation by mangroves in this study may overestimate sediment resuspension, wave attenuation depends on wave characteristics with wave attenuation efficiency being typically lower for smaller and shorter waves (Phan et al., 2019), such as in this study. Moreover, wave attenuation by mangroves observed in the field has been shown to vary between tidal systems (Horstman et al., 2014). A gentler coastal slope with shallower water depths is more sensitive to wave dampening by mangroves (Parvathy and Bhaskaran, 2017), implying that wave attenuation effects are more important in micro-tidal systems. So far, several models have been developed to simulate wave dampening within vegetation but still have some limitations in incorporating morphological changes, especially for long-term morphodynamic processes (Wu et al., 2016; Phan et al., 2019). Accurately capturing wave attenuation by vegetation and related effects on morphological development should account for the complex interactions between currents and waves over vegetated objects, sediment trapping and entrainment and canopy bending among other factors (Méndez et al., 1999; Carr et al., 2018), so that further research can assess more comprehensively the impacts of waves on mangrove ecosystem vulnerability.

In addition to more complex hydrodynamics, vegetation attributes such as mangrove stem density and the above-ground root system also affect sediment accretion over the vegetated flats (Quartel et al., 2007; Kumara et al., 2010; Xie et al., 2020), which eventually determines the overall functionality of mangrove forests and their capacity to provide coastal protection against the risk of flooding (Gijsman et al., 2021). Previous research has highlighted that dense mangrove vegetation contributes to sediment accretion in the seaward region of the forest, limiting landward sediment accretion and resulting in strong spatial variations in bed level changes, in turn controlling profile shape. However, more sediment can be transported landward under sparse mangrove vegetation, resulting in a more homogeneous accretion over vegetated flats (Xie et al., 2020). Although this study may underestimate the impacts of root density variations, it highlights the role of tidal range and sediment availability on shaping a gentle coastal platform, allowing mangrove colonization and extending mangrove coverage (Figure 3.3k). Therefore, our bio-morphodynamics modelling approach, as presented here, may be useful to study the persistence of mangroves for coastal flood protection in the face of SLR impacts.

Finally, the simulations conducted in this study only consider surface accretion, while organic accretion and other sub-surface processes can also play an important role in controlling surface elevation changes and thus mangrove vulnerability (Krauss et al., 2014; Cahoon et al., 2020; Breda et al., 2021). Organic matter accumulation by production of refractory roots and leaf litter contributes to vertical elevation gain of the soil surface (Middleton and McKee, 2001). Field observations have shown that these organic materials can play an important role in promoting mangrove persistence in the face of SLR, especially in areas with limited sediment inputs (McKee et al., 2007; McKee, 2011). However, other sub-surface processes, such as land subsidence, sediment compaction and organic decomposition can reduce the surface elevation, even leading to an elevation deficit (Figure 3.20). Clearly, the impact of sub-surface processes on mangrove vulnerability in different coastal conditions needs to be further explored, both through field measurements and modelling, also given the role that these processes play in the sequestration of carbon by mangrove ecosystems (Alongi, 2014).

3.5 Conclusions

Our numerical simulations show that the evolution and characteristics of the vegetated coastal profile, including platform development, is controlled by non-linear interactions between tidal range, small wind waves and sediment supply. This in turn influences the fate of mangroves under rising sea levels.

Mangrove expansion or retreat due to SLR is a function of tidal range with micro-tidal systems being the most vulnerable, already retreating under slow SLR rates even with ample sediment supply. In meso- and macro-tidal systems, dynamic profiles driven by sediment accretion across the vegetated flats can protect mangroves from submergence by SLR. For the time period simulated here, mangroves may survive SLR despite limited sediment accretion, as profile change and constraints during vegetation recruitment establish an inundation buffer, and as a consequence, the inundation threshold of mangrove trees is not immediately exceeded during rising sea levels. Still, rising sea levels reduce this inundation buffer such that mangroves are less resilient to ongoing SLR beyond the simulation period. The landward mangrove habitats (i.e. those areas that become suitable for mangrove growth as rising sea levels cause inundation of previously dry land) can be created with limited sediment supply. Nevertheless, infilling of new accommodation space may occur, potentially with sediment originating from erosion and reconfiguration of the lower coastal profile. Although sediment accretion rates across mangrove forests are generally enhanced by SLR rates, the timing and magnitude of accretion vary with coastal conditions and change non-linearly from the mangrove seaward edge. Overall, our results indicate that environmental conditions drive distinct mangrove responses to SLR and projections of mangrove vulnerability should account for coastal profile adjustments and complex mangrove growth dynamics that emerge from highly non-linear bio-morphodynamic feedbacks.

3.6 Supplementary material

This Supporting Information includes ten texts, ten supplementary figures (Figure 3.12 to Figure 3.21), five tables (Table 3.1 to Table 3.5). Texts (Section 3.6.1 to Section 3.6.10) will serve as further explanation of Figures (Figure 3.12 to Figure 3.21).

Figure 3.12 shows the sensitivity analysis of drag coefficients in influencing the model results. Figure 3.13 displays the shape of two key factors controlling mangrove growth rate based on Equations 3.5-3.6. Figure 3.14 shows the profile evolution with different combinations of tidal range and initial coastal slopes. Figure 3.15 is the zoomed in version of Figure 3.5 in the main text. Figure 3.16 to Figure 3.21 are model results supporting the main findings of this research. Figure 3.16 shows the spatio-temporal changes in the net sediment transport rate in the first 50 years. Figure 3.17 shows the sediment transport rate during flood and ebb at 3 particular years. Figure 3.18 displays the relations between mangrove seaward edge elevation and tidal ranges. Figure 3.19 exhibits the tidal prism throughout 250 years, including the first 150 years without sea-level rise followed by 100 years with sea-level rise. Figure 3.20 shows the vertical changes in numerical simulations and field observations. Figure 3.21 provides information on the changes in relative hydroperiod, suspended sediment concentration and bed shear stress at mangrove seaward edge over 250 years.

Table 3.1 and Table 3.2 show the parameter settings of the hydro-morphodynamic model and the vegetation model, respectively. Table 3.3 displays the overview of model simulations conducted with different coastal conditions, including tides, waves, sediment supply and sea-level rise scenarios. Table 3.4 provides data showing mangrove seaward edge elevation above MWL at different field sites. Table 3.5 presents the field observation data regarding sea-level rise rates and surface elevation change, surface accretions rates and shallow subsidence at several different mangrove sites, summarized by McKee et al. (2021).

3.6.1 Text S1

Figure 3.12 shows how the model results change with different drag coefficients (stems and roots), C_D. The panels display comparisons of bed level, 90th percentile depth-averaged velocity and suspended sediment concentration (SSC) across the coastal profiles in year 250. For lower drag coefficients (i.e. 0.5 for stems and 0.1 for roots) there will be a higher platform landward, with slightly larger velocities but lower suspended sediment concentrations in the intertidal area, causing the seaward vegetation edge to be positioned more landward. However, other combinations with larger drag coefficients show similar outcomes, with comparable velocity and sediment distributions. The seaward vegetation edge remains at the same cross-shore location; however, the seaward vegetation edge will occur at a slightly higher bed elevation with smaller drag (i.e. 1.5 for stems and 1 for roots). Thus, our chosen drag coefficients cover the characteristic behavior which is representative of a wide range of previously reported drag coefficients (i.e. 0.7-3.5; based on Nepf (1999) and Horstman et al. (2018a).

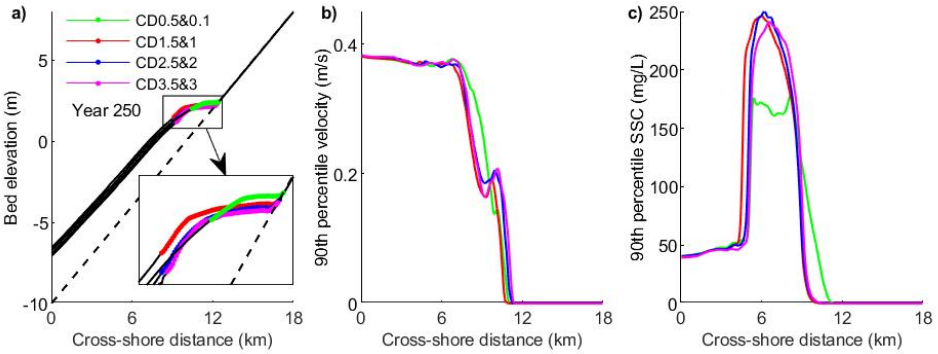

Figure 3.12 Comparisons of bed level, 90th percentile of depth-averaged velocity and suspended sediment concentration (SSC) across the coastal profiles with different C_D settings. The comparisons are developed under similar coastal conditions, that is, with large tidal range (5 m) and intermediate sediment supply (30 mg/L) without wave effects in the year 250. Green, red, blue and purple represent different C_D combinations and the drag coefficients for stems and roots are marked in the legend in subplot a). Green, red, blue and purple color dots in a) indicate mangrove presence along their corresponding profiles, which are shown as solid lines. The dashed lines indicate the initial bed profile. In this research, we use $C_D = 1.5$ for stems and $C_D = 1.0$ for roots.

3.6.2 Text S2

Figure 3.13 hows how the inundations stress factor changes with relative hydroperiod and how the competition stress factor changes with existing biomass within one grid cell. In the vegetation model, the product of these two factors determines the growth rates of mangrove trees and also serves as a key parameter evaluating 1) colonization conditions and 2) mortality conditions.

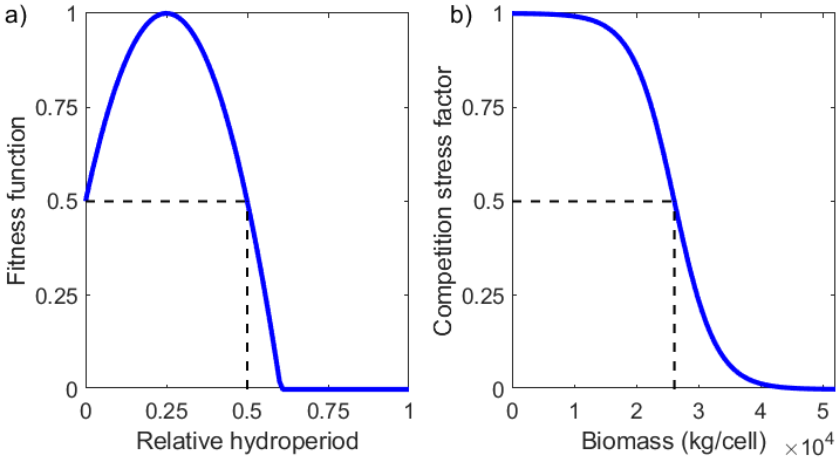

Figure 3.13 Growth control factors used in the vegetation model (van Maanen et al., 2015; Xie et al., 2020). (a) Fitness function, characterized by an optimal relative hydroperiod (P = 0.25). P > 0.6 implies over-inundation so mangroves stop growing completely. (b) Competition stress factor, representing the competition between trees as neighbouring trees have to share resources.

3.6.3 Text S3

Figure 3.14 shows how the profile shapes evolve under different initial coastal slopes forced by three tidal ranges. Profiles with a gentle slope in micro-tidal range systems, with a medium slope in meso-tidal range system and with a steep slope in macro-tidal range system, show relatively small adjustment before a stable configuration is reached. Other combinations will cause significant deposition or erosion along the profile before the stable profile is achieved.

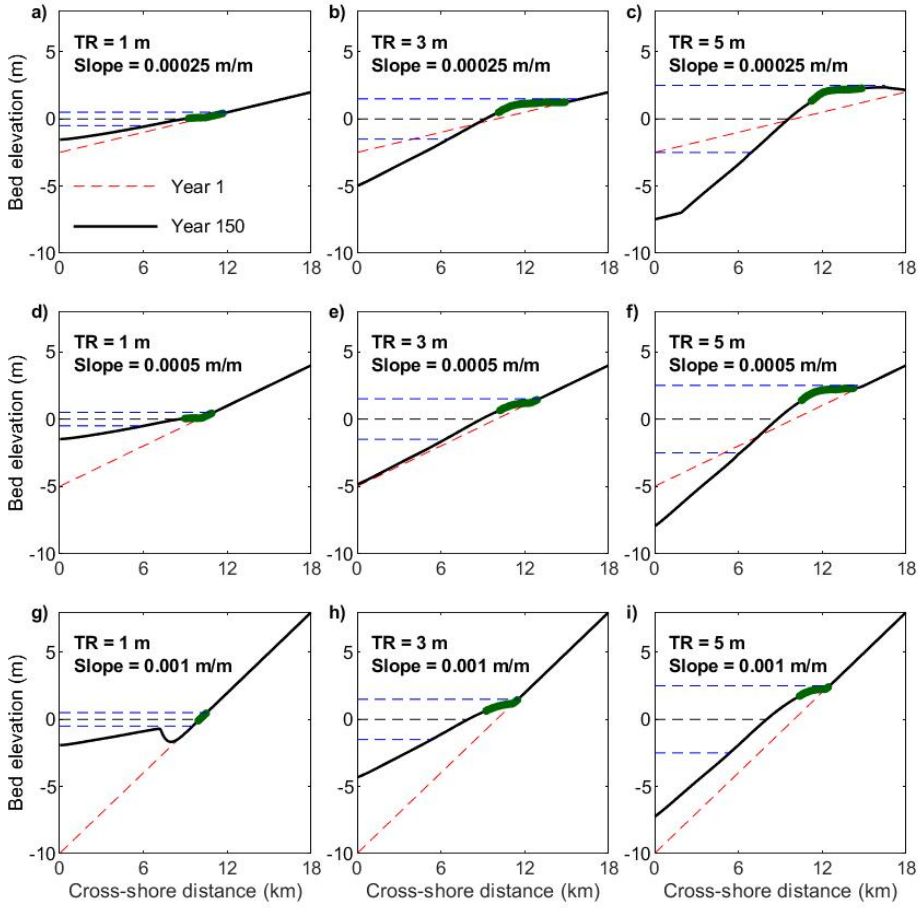

Figure 3.14 Bed level evolution under different combinations of tidal ranges and initial coastal slopes. The comparisons are based on intermediate sediment supply (30 mg/L) without wave effects. Bed level initialized with a-c) gentle coastal slope, d-f) medium coastal slope and g-i) steep coastal slope. a,d&g), b,e&h) and c,f&i) indicate the micro-, meso- and macro-tidal range systems, respectively. Red dashed lines show the initial bed level, while black solid lines with green dots show the bed level with the location of mangroves in year 150. TR and Slope represent the tidal range and initial coastal slope applied in the model.

3.6.4 Text S4

Figure 3.15 is a zoomed in version of Figure 3.5 to highlight differences between scenarios.

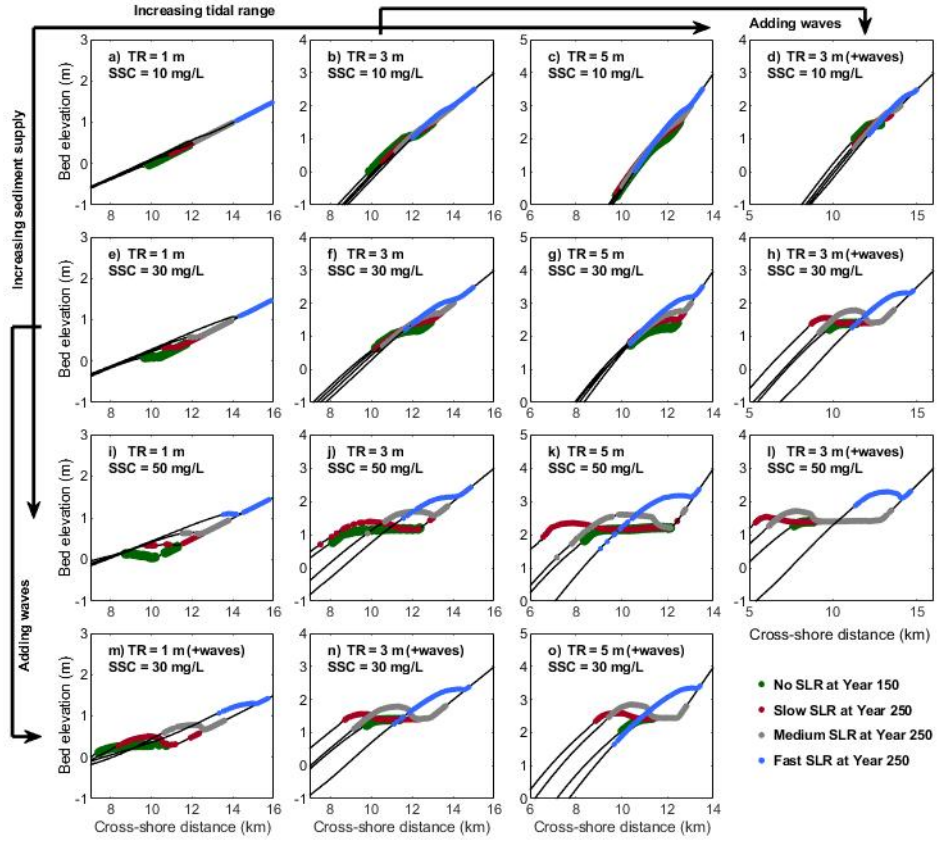

Figure 3.15 Zoomed in version of Figure 3.5) in the main text showing mangrove behaviors in response to different rates of SLR.

3.6.5 Text S5

Figure 3.16 shows how the sediment transport rate changes during the first 50 years in the absence and presence of waves. For similar tidal range systems, models with and without waves are initialized with the same bathymetry. Profile accumulation during the first 50 years is facilitated due to the net sediment flux in the flood direction (Figure 3.16). The onshore net sediment flux is further enhanced by wave effects, especially in the micro- and meso-tidal systems where water depths are shallower (Figure 3.16d-e).

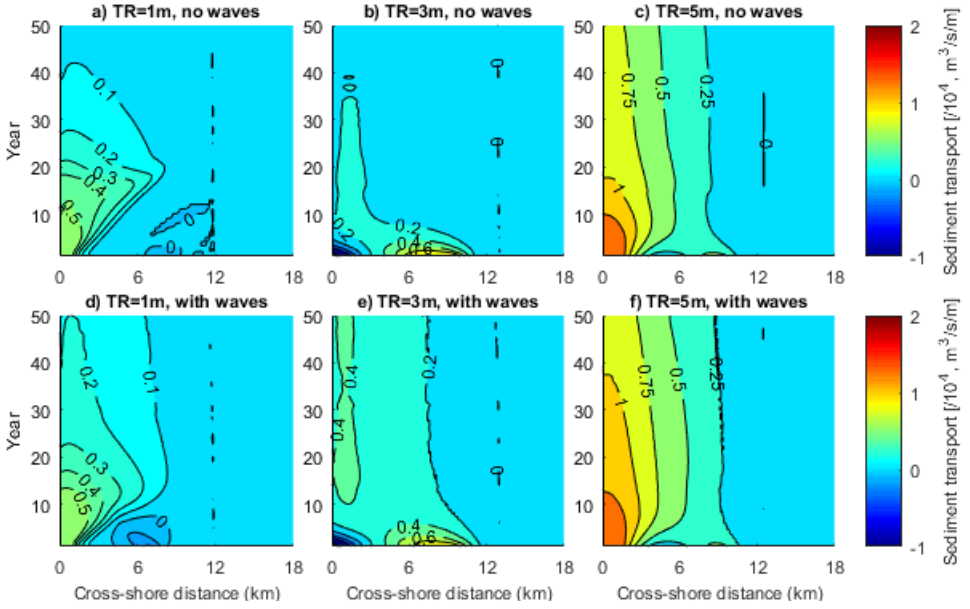

Figure 3.16 Spatio-temporal distribution of sediment transport rate under intermediate sediment supply (30 mg/L) over the first 50 years, without (a, b, c) and with (d, e, f) wave effects. Results are presented for micro-tidal (a, d), meso-tidal (b, e) and macro-tidal (c, f) conditions. The sediment transport rate is calculated over an entire tidal cycle.

3.6.6 Text S6

Figure 3.17 shows the difference in sediment flux during flood and ebb every 50 years. In general, small wind waves enhance sediment flux during the flood period more than during the ebb period, causing a larger net sediment input in the flood direction.

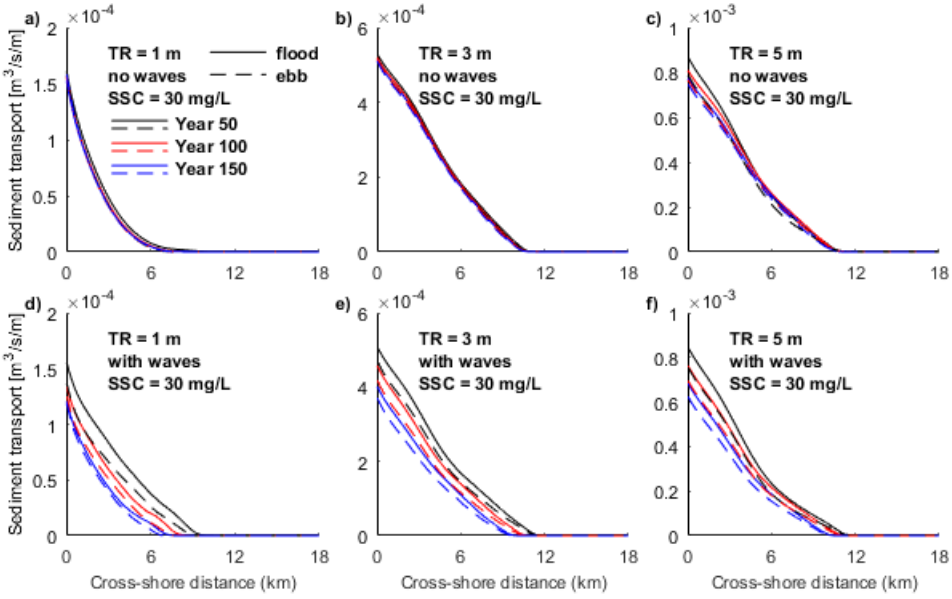

Figure 3.17 Sediment fluxes under intermediate sediment supply (30 mg/L) during the flood (solid line) and ebb periods (dashed line) evaluated over an entire tidal cycle in three particular years (50, 100 and 150), without and with wave effects. Results are presented for micro-tidal (a, d), meso-tidal (b, e) and macro-tidal (c, f) conditions. TR and SSC represent tidal range and suspended sediment concentration, respectively.

3.6.7 Text S7

Figure 3.18 compares the observed mangrove elevation with our model results for different tidal ranges. Both the model and field data show that an increased tidal range limits mangrove seaward colonization and constrains mangroves to higher bed elevations.

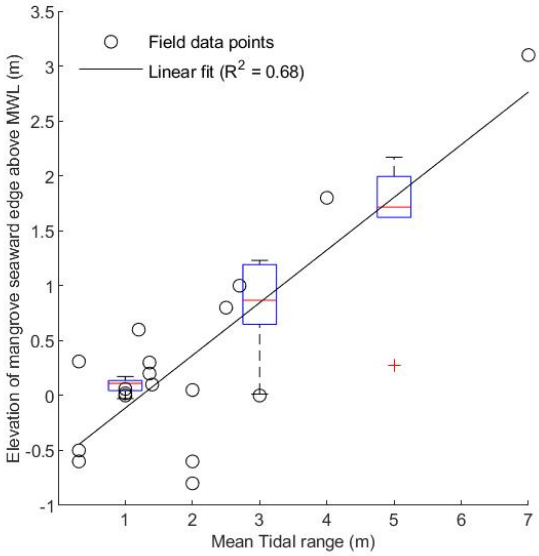

Figure 3.18 Comparing the location of the mangrove seaward edge relative to MWL between modelling results (box plots) and field observations (Table 3.4). Each box plot is based on 6 simulated mangrove seaward edge elevations at year 150, accounting for the combinations of 3 sediment supply settings (10, 30 and 50 mg/L) and 2 wave conditions (no waves and with waves).

3.6.8 Text S8

Figure 3.19 shows that the tidal prism first decreases as profile accumulates before sea-level rise, and then increases when sea-level rise occurs which creates new landward accommodation space.

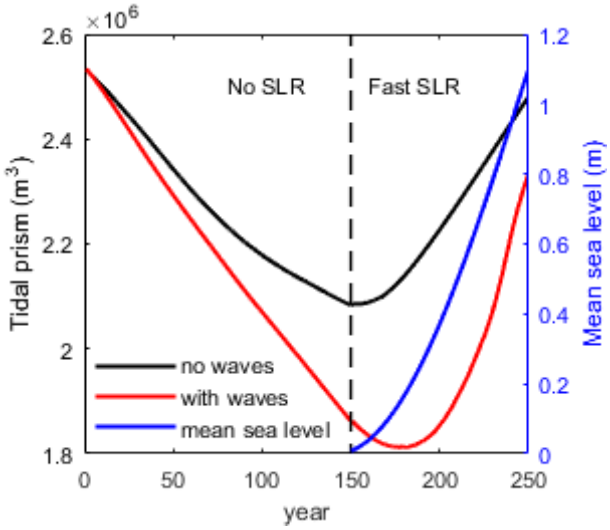

Figure 3.19 Temporal change of tidal prism under intermediate sediment supply (30 mg/L) and large tidal range (5m) throughout 250 years, with and without wave effects. The first 150 years were simulated without sea-level rise, followed by a 100-year fast-sea level rise. Black and red lines represent the changes of tidal prism without and with waves, respectively. The fast sea-level rise curve is shown in blue.

3.6.9 Text S9

Figure 3.20 shows sediment accretion calculated through our numerical modelling is comparable to field observations, which shows that our model is able to capture above-ground sedimentary processes throughout different coastal environmental conditions. In the meanwhile, that organic accretion can create an elevation gain that is of a similar magnitude as inorganic accretion, which however will be offset by other sub-surface processes potentially resulting in a net elevation deficit. Field data in Figure 3.20c is based on previous studies (McKee, 2011; McKee et al., 2021).

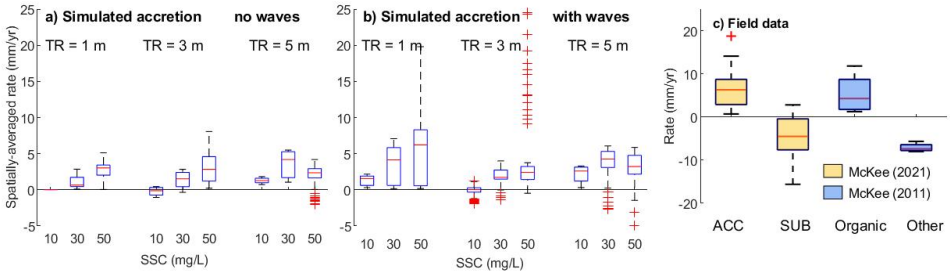

Figure 3.20 Box plots of vertical changes in numerical simulations and field observations. Spatially-averaged sediment accretion rates across different simulated scenarios without waves (a) and with waves (b); field observations on elevation change due to sediment accretion (ACC) and sub-surface processes (SUB) at different mangrove sites (yellow) (c). The sub-surface processes are further divided into organic matter accretion (Organic) and other sub-surface processes (Other), such as land subsidence, sediment compaction and organic decomposition (blue). The rates in a) and b) are averaged over the vegetated areas and computed for a 100-year time period.

3.6.10 Text S10

Figure 3.21 shows the temporal changes of relative hydroperiod, 90th percentile of suspended sediment concentration and bed shear stress at one fixed cross-shore location. In this analysis, the fixed location is based on mangrove seaward edge in year 150, which is the seaward green dots in each subplot of Figure 3.5 (without waves). Before sea-level rise, the relative hydroperiod generally decreases over years. Sediment concentration and bed shear stress remain stable in micro-tidal systems but drop over time in meso- and macro-tidal range systems. When sea level starts to increase, although the bed shear stress increases, the relative hydroperiod and sediment concentration at the front of mangrove forests also increase, leading to enhancing sediment accretion rates.

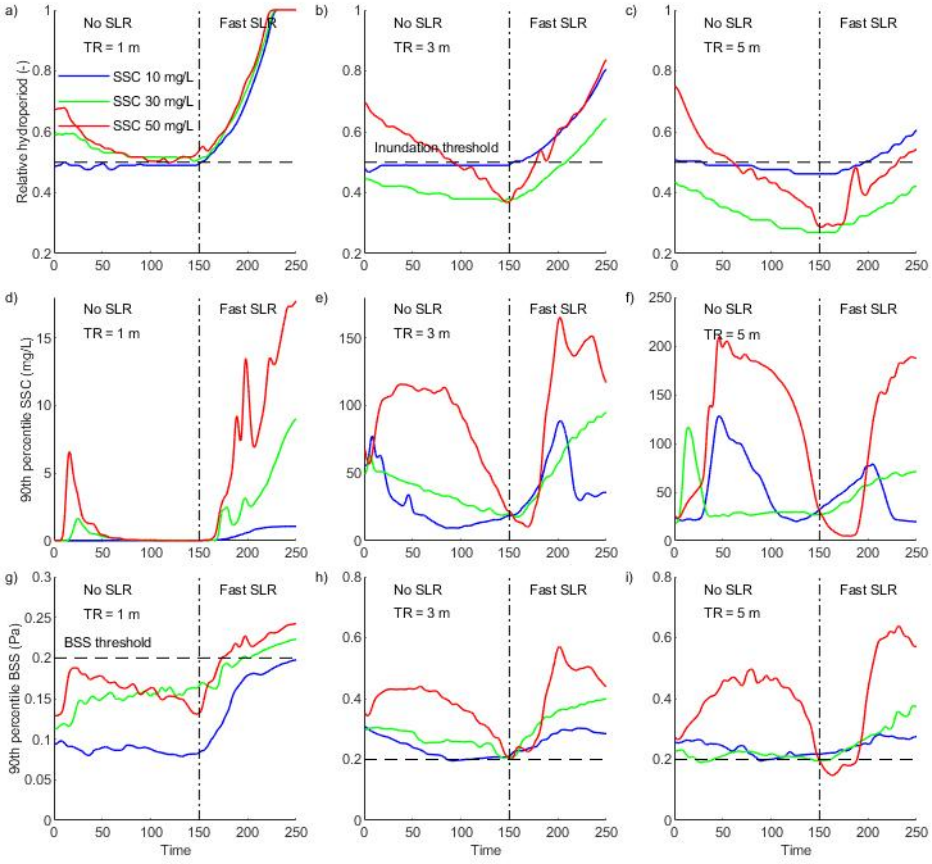

Figure 3.21 Temporal changes in relative hydroperiod, 90th percentile of suspended sediment concentration (SSC) and 90th percentile bed shear stress (BSS) at the mangrove seaward edge over 250 years (without waves). The first 150 years were simulated without sea-level rise, followed by a 100-year fast-sea level rise.

3.6.11 Supplementary tables

Table 3.1 Hydro-morphodynamic model parameter settings

Category	Applicable situation	Parameter	Value	Unit
Time reference	Not required	Hydrodynamic time step	0.5	min
	Not required	Morphological acceleration factor	30	-
	Not required	Ecological simulation period	250	years
Domain	Not required	Grid size	50×50	m
	Micro-tidal system slope	Slope	0.00025	m/m
		Domain size ($x \times y$)	18000×4.5 (-2.5 to 2)	m
	Meso-tidal system slope	Slope	0.0005	m/m
		Domain size ($x \times y$)	18000×9 (-5 to 4)	m
	Macro-tidal system slope	Slope	0.001	m/m
		Domain size ($x \times y$)	18000×18 (-10 to 8)	m
Boundary condition	Wave	Significant wave height	5	cm
		Peak wave period	1	s
	Micro-M2 tide	Tidal range	1	m
	Meso-M2 tide	Tidal range	3	m
	Macro-M2 tide	Tidal range	5	m
Sediment	Not required	Critical bed shear stress for erosion	0.2	N/m^2
	Not required	Critical bed shear stress for deposition	1000	N/m^2
	Not required	Settling velocity	5×10^{-4}	m/s
	Not required	Erosion parameter	5×10^{-5}	$kg/m^2/s$

Table 3.2 Dynamic vegetation model parameter settings

Category	Parameter	Value/Description	Unit
Vegetation parameters	Initial stem diameter, D0	1.37	cm
	Maximum root number, Nroots,max	1000	-
	Root diameter, Droots	1	cm
	Root height, Hroots	15	cm
	Drag coefficient of roots, CDr	1	-
	Drag coefficient of stems, CDs	1.5	-
Growth parameters	Maximum stem diameter	40	cm
	Maximum tree height	1000	cm
	Growth constant, G	12.68	cm/month
	Growth constant, b2	43	-
	Growth constant, b3	0.536	cm^{-1}
	Fitness function constant, a	-8	-
	Fitness function constant, b	4	-
	Fitness function constant, c	0.5	-
	Competition stress factor constant, d	-0.0003	-
	Roots formula constant, k	0.3	-

Table 3.3 Overview of coastal conditions explored in our study, amounting to 72 runs in total covering all combinations

Tidal systems	Tidal range (m)	Sediment supply (mg/L)	Wave height (cm)	Sea-level rise (SLR)
Micro	1			
Meso	3	10, 30 or 50	0 or 5	no SLR, RCP2.6, RCP4.6 or RCP8.5
Macro	5			

Table 3.4 Overview of field observations showing tidal ranges and mangrove seaward edge elevations relative to mean water level (MWL).

ID	Location	TR (m)	Elevation above MWL (m)	Source
1			2.00E-02	
2	Dongzhaigang Bay, China	1	0	Fu et al. (2019)
3			6.00E-02	
4	Futian, China	1.36	0.2	Chen et al. (2021)
5			0.3	
6	Macouria bank, French Guiana	2	5.00E-02	Anthony et al. (2008)
7			-0.5	
8	Sinú River Delta, Colombian Caribbean	0.31	0.31	Sánchez-Núñez et al. (2019)
9			-0.6	
10	The Firth of Thames, New Zealand	2.7	1	Swales et al. (2015)
11	Mekong delta, Vietnam	4	1.8	Phan et al. (2015)
12	CĚ Lao Dung, Vietnam	1.4	0.1	Bryan et al. (2017)
13	Queensland, Australia	1.2*	0.6	Knight et al. (2009)
14	Kantang, Thailand	2	-0.6	Horstman et al. (2014)
15	Palian, Thailand		-0.8	
16	Mahé Island, Seychelles	3	0	Sefton and Woodroffe (2021)
17	Sundarbans, Bangladesh	7	3.1	Ellison (2000)
18	Matapouri Estuary, New Zealand	2.5	0.8	Andrea (2006)

(*) Tidal range (TR) is calculated from TPXO tide models (https://www.tpxo.net/home).

Table 3.5 Summary of field data on vertical elevation dynamics across different mangrove hydrogeomorphic settings, including surface elevation change (mm/yr), surface accretion, relative sea-level rise (mm/yr) and shallow subsidence (mm/yr). The shallow subsidence (negative value) or expansion (positive value) is calculated from the differences between surface elevation change and surface accretion. Data was summarized by McKee et al. (2021).

ID	Location	Site	Surface elevation change (mm/yr)	Surface accretion (mm/yr)	RSLR (mm/yr)	Shallow subsidence /expansion (mm/yr)	Source
1	Rookery Bay, Florida, USA	Fringe	3.5	7.8	6.6	-4.3	1
2		Basin	3.7	6	4.6	-2.3	
3		Island shoreline	2.5	6.3	6.1	-3.8	
4		Island interior	0.6	4.4	6.1	-3.8	
5	Gulf of Fonseca, Honduras	Interior	4.6	2.9	-0.7	1.7	2
6		Shoreline	4.6	2.9	-0.7	1.7	
7	Roatan, Honduras	Interior	4.8	2	-0.8	2.8	3
8		Shoreline 1	4.8	2	-0.8	2.8	
9		Shoreline 2	4.8	2	-0.8	2.8	
10	New South Wales, Australia	Cararma Inlet	-0.8	3	8	-3.8	4
11		Currambene Creek	0.3	0.7	4.5	-0.4	
12		Homebush Bay	5.6	4.6	-0.2	1	
13		Kooragang Island	1.9	4.7	3.1	-2.8	
14		Ukerebagh Island	2.2	2.2	-0.4	0	
15		Minnamurra River	0.6	6.6	5.6	-6	
16	Victoria, Australia	French Island	-2.1	9.5	14.3	-11.6	
17		Kooweerup	0	7.2	9.9	-7.2	
18		Quail Island	-2.6	6.8	12	-9.4	
19		Rhyll/Phillip Island	0.9	5.1	6.8	-4.2	
20	Twin Cays, Belize	Transition	-1.1	2	5.4	-3.1	5
21		Dwarf	-3.7	0.7	6.7	-4.4	
22		Fringe	4.1	1.6	-0.2	2.5	

(*Continued*)

(*Continued*)

ID	Location	Site	Surface elevation change (mm/yr)	Surface accretion (mm/yr)	RSLR (mm/yr)	Shallow subsidence /expansion (mm/yr)	Source
23	Kosrae, Micronesia	Yela shoreline	-3	11.6	16.4	-14.6	6
24		Yela riverine	-2.7	12.9	17.4	-15.6	
25		Yela interior	1.3	12	12.5	-10.7	
26		Utwe shoreline	1.2	11.9	12.5	-10.7	
27		Utwe riverine	6.3	18.7	14.2	-12.4	
28		Utwe interior	1.3	12.9	13.4	-11.6	
29	Pohnpei, Micronesia	Sapwalap riverine	-0.6	14.1	16.5	-14.7	
30		Sapwalap shoreline	-2.3	4.1	8.2	-6.4	
31		Sapwalap interior	0.9	8.2	9.1	-7.3	
32		Enipoas shoreline	-5.8	6.6	14.2	-12.4	
33		Enipoas riverine	-1.4	6.3	9.5	-7.7	
34		Enipoas interior	-2.8	2.9	7.5	-5.7	
35	Everglades, Florida, USA	Shark River	1.4	6.5	7	-5.1	7
36	Rookery Bay, Florida, USA	Fringe	0.6	5.7	7.2	-5.1	8
37		Basin 1	3.9	2	0.2	1.9	
38		Basin 2	1.1	7.6	8.6	-6.5	
39	Queensland, Australia	Moreton Bay east	5.8	8	4.1	-2.2	9
40		Moreton Bay west	1.7	9.2	9.4	-7.5	
41	Louisiana, USA	Port Fourchon	3.8	9.8	15	-6	10
42	Hainan, China	Sanjiang	8.6	13.2	10.9	-4.6	11
43		Houpai	2.2	2.7	6.8	-0.5	
44		Houpai	7.8	7.4	5.9	0.4	

Source: *1*=Cahoon and Lynch (1997); *2*=Cahoon et al. (2002); *3*=Cahoon et al. (2003); *4*=Rogers et al. (2006); *5*=McKee et al. (2007); *6*=Krauss et al. (2010); *7*=Whelan et al. (2009); *8*=McKee (2011); *9*=Lovelock et al. (2015); *10*=McKee and Vervaeke (2018). *11*=Fu et al. (2018)

Conflict of Interest

The authors declare no conflicts of interest relevant to this study.

Acknowledgments

This study is financially supported by the China Scholarship Council (Grant No. 201706710005) and the Department of Physical Geography at Utrecht University. D. Xie acknowledges the supercomputer technological support from Edwin Sutanudjaja and Marcio Boechat Albernaz. B. van Maanen acknowledges funding from the NWO WOTRO Joint Sustainable Development Goal Research Program (W07.303.106). M. G. Kleinhans acknowledges funding from H2020 European Research Council (Grant No. ERC-CoG 647570). Z. Zhou acknowledges funding from the National Natural Science Foundation of China (Grant No. 41976156). The authors thank the reviewers for providing detailed and constructive feedback.

Data availability statement

The field data regarding mangrove seaward edge elevation relative to MWL is summarized from previous publications and is available as supplementary materials (Table 3.4).The field data regarding local SLR rates and vertical elevation dynamics is available as supplementary material (Table 3.5), summarized from the open-access publication by McKee et al. (2021). Delft3D is an open-source code available online (at https://oss.deltares.nl). The dynamic vegetation code with a representative model setting is available at https://github.com/xiedanghan/MangroveVulnerabilityModel.


4

Chapter 4 | Humans as Ecosystem Engineers: How upstream land-use change and mangrove removal cause deviating trajectories in estuarine landscape development

Abstract

Long-term upstream land-use activity has transformed downstream coastal ecosystems globally. Coastal management strategies aimed at restoring ecosystems often focus on local coastal processes. However, environmental stress operates over much larger scales involving complex interactions between environments. Activities inland/upstream can significantly change fluxes/processes at the coast. Here we use an idealized bio-morphodynamic model to isolate the effects of upstream land-use change on estuarine development over decades to centuries. More specifically, we hindcast the impact of the arrival of European settlers and accompanied deforestation on tidal lagoon morphodynamic change and mangrove expansion. We find that the common local practice of mangrove removal at the coast (sink) cannot achieve the desired outcome of returning low-functioning mud-dominated ecosystems to sand. Reducing mud import at the catchment (source) can slow mud accretion and mangrove expansion, but still cannot restore coastal systems to pre-settlement sand dominated mangrove-free areas. Our study highlights how diverse anthropogenic drivers along source-to-sink systems can cause irreversible impacts on coastal bio-geomorphic environments, and emphasizes that there is no substitute for sustainable catchment use.

Based on: Xie, D., Schwarz, C., Kleinhans, M. G., Bryan, K. R., Coco, G., Hunt, S., & van Maanen, B. (in prep.). Humans as Ecosystem Engineers: How upstream land-use change and mangrove removal cause deviating trajectories in estuarine landscape development. *journal t.b.d.*

4.1 Introduction

Over the last century, land-use changes and coastal development around the world have markedly increased sediment loads into estuarine and coastal habitats (Thrush et al., 2004; Syvitski et al., 2005; Erkens et al., 2009), leading to substantial physical transformations of coastal landscapes (Nienhuis et al., 2020) and ecosystems (Kirwan et al., 2011; Suyadi et al., 2019). Ecologically and economically important coastal ecosystems, such as mangrove forests, occupy the interface between land and sea, where they mediate effects of sea-level rise, dampen waves, trap fine sediments, and thus protect the coast from erosion (Woodroffe et al., 2016). The degree to which low lying coastal systems survive rising sea levels is highly dependent on external sediment supply, which is ultimately fed from continents by rivers and transported to marine environments by tides/waves (Coco et al., 2013; Mentaschi et al., 2018; Törnqvist et al., 2019). In many places in the world, following rapid European settlement, sedimentation in estuaries accelerated because of changes in land use upstream and increasing water turbidity, jeopardizing pristine ecosystems and threatening human living conditions (McCulloch et al., 2003; Jones, 2008; Kidane and Alemu, 2015; Restrepo et al., 2015). Previous paleorecords indicated that long-term fluvial sediment infilling would gradually silt up an estuary, causing coastal progradation and creating widespread coastal wetlands such as mangrove forests or salt marshes (Woodroffe, 1993; Kirwan et al., 2011), which are believed to further stabilize fine sediment components in the estuaries (Jones, 2008). Coastal restoration of these ecosystems is often focused on reducing the amount of fine sediment historically deposited in these estuaries and is often accompanied by vegetation clearance (Temmerman et al., 2012; Lundquist et al., 2014). Unfortunately, minimal information is available on the success of ecosystem restoration by vegetation clearance. Mangroves typically mature in decades and therefore differ from salt marshes which can mature within months (Chapman, 1976), which complicates any predictions on enduring ecosystem change. Thus, understanding the effects of hinterland change and mangrove removal on mangrove systems, especially from the long-term perspective, is crucial for future coastal management in these globally common habitats.

Here, we use European settlement in New Zealand as a setting to illustrate that poor understanding of large scale bio-geomorphic feedbacks could lead to failure in planning and implementation of coastal restoration. Following European settlement, most upstream regions of the North Island, New Zealand, experienced substantial conversions of forestland to agriculture or pasture, resulting in rapid and widespread hinterland soil erosion (Swales et al., 2021). These unsustainable land-use activities caused at least an order-of-magnitude increase of suspended sediment yields to the coast from pre-European stages (Hicks et al., 2019; Hicks et al., 2011). Sediment deposited in the estuaries was thus magnified from a relatively stable rate (0.1-1 mm/yr prior to European settlement) to continually increasing rates (ranging from as low as 1 mm/yr after European arrival to a maximum value around 100 mm/yr nowadays) (Figure 4.1f) (Hunt, 2019; Swales et al., 2021), creating widespread accumulations of intertidal mud, ideal for mangrove establishment (Figure 4.1e). Such excessive sediment deposition is believed to not only impact navigation, limit recreational activities and the amenity value of these areas (Lundquist et al., 2014), but also transforms coastal habitats at the expense of losing high-function ecosystems, such as those dominated by seagrass and filter-feeding shellfish (Jones, 2008). Coastal management can partially address the impacts of increased suspended sediment delivery to estuaries with varying levels of success. For example, although dredging can be used to remove deposited sediment and deepen a channel for navigation, other adverse impacts on the environment such as highly turbid water will still be apparent to the local community (Manap and Voulvoulis, 2016). Other coastal management approaches such as clearance nuisance vegetation in coastal areas may enhance coastal erosion as a result of wind/wind-wave impacts such that muddy sediment can be transported out of the system (Winterwerp et al., 2005), but hydrodynamic forces are often small in the New Zealand estuaries (even after clearance) (Hume and Herdendorf, 1993),

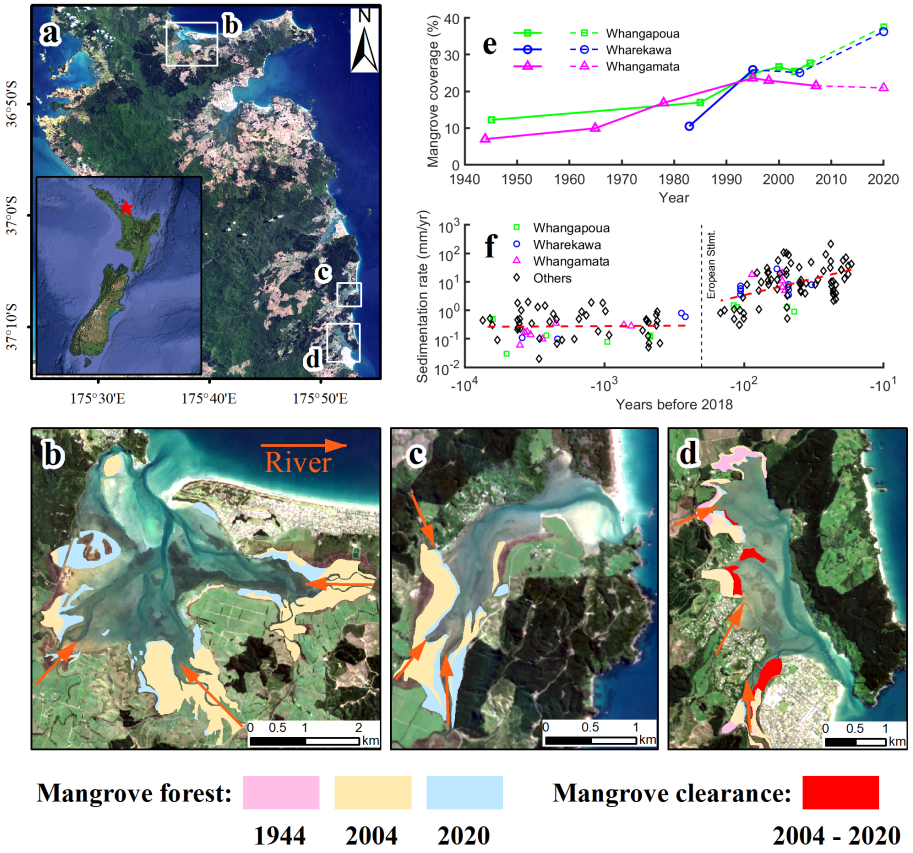

Figure 4.1 Temporal variation in mangrove distribution and sediment accumulation rates at three representative estuaries in the North Island, New Zealand. a) Location map for estuaries shown in b-d; b) Whangapoua estuary; c) Wharekawa estuary; d) Whangamata estuary; e) Observed changes in mangrove coverage at these three estuaries; f) Historical sediment accumulation rates (SAR). The blue arrows in b-d) indicate fluvial flow input. Mangrove coverage data in solid lines in e) comes from Jones (2008) and data in dashed lines are estimated from recent Landsat data. The reduction in mangrove cover in Whangamata estuary is due to the effect of mangrove clearance, also see panel f). Satellite images and mangrove distributions in year 2004 and 2020 are based on Landsat data from Giri et al. (2011) and datasets from LINZ (https://www.linz.govt.nz). Mangrove distributions in 1944 in panel d are based on historical archive data published in Lundquist et al. (2014). Mangrove clearance area is taken from datasets in Bulmer et al. (2017). Historical sediment accumulation rates (panel f) are based on datasets collected by Hunt (2019).

leading to only minor changes in sediment remobilisation following vegetation loss (Glover et al., 2022). These examples show distinct responses of coastal sedimentation changes driven by different ends, such as land-use activities from the catchments and vegetation clearance on the estuary. Coastal management therefore needs to be based on a clear understanding of bio-geomorphic interactions over large scales.

Mangroves mainly occupy the upper-intertidal flats between mean water level and mean high water level (Chapman, 1976). The import of terrestrial sediment associated with upstream land-use

activities contributes to the mud accumulation and mangrove forest establishment (Swales et al., 2007). In turn, the presence of mangrove forests enhances the trapping of sediment and stabilizes sediment from erosion, making it even more difficult to remobilize the mud (Furukawa et al., 1997; Roskoden et al., 2020). Because of this association between fine sediment deposition and mangroves, mangroves are perceived to be one of main constraints on sand flat restoration in New Zealand (Horstman et al., 2018b). Consequently, many permitted and unpermitted mangrove clearance projects have occurred over recent decades in the North Island, motivated by the desire to restore estuary sand flats that have been historically present prior to mangrove colonization (Harty, 2009). However, insights from current field observations or estimates are inconclusive. For example, some field observations found initial reductions in mud compositions at some mangrove clearance areas (Singleton, 2007; Lundquist et al., 2014), while others show transitions from mud to sand flats are unlikely (Bulmer et al., 2017; Glover et al., 2022). Discrepancies between these studies may arise from the relatively limited time/space scales studied post mangrove removal, and the failure to address appropriate long term trends and catchment-scale processes. Synthetic modelling approaches that account for both vegetation dynamics (i.e. colonization, growth and mortality processes) and comprehensive treatment of hydro-sedimentary processes, including the effects of vegetation on sediment transport and the responses of vegetation to coastal changes could address these discrepancies and improve understanding of the likely outcomes of mangrove removal.

The goal of this research is to understand whether common mangrove management options in a coastal tidal basin with a history of anthropogenically increased fine sediment supply can revert the system into a state before European settlement. To this end, we present results of a model that incorporates nonlinear interactions between vegetation dynamics, sediment transport and morphodynamics. The idealized setup represents a back-barrier lagoon typically with multiple river inputs as typically observed in estuarine systems in the North Island, New Zealand (Figure 4.1b-d and Figure 4.6). We first establish an equilibrium bathymetry (filled only with sand) representing an empty lagoon with an average platform elevation of -1.5 m relative to mean sea level. This is followed by a period with low mud supply (low mud scenarios) from three rivers discharging into the lagoon representing pre-disturbance conditions before European settlement. Subsequently, the mud sediment load of the rivers is increased (high mud scenario) representing the arrival of European settlers and transitioning the landscape into the post-disturbance period. To forecast potential future changes in the estuarine system, we simulate the impact of management actions upstream and in the estuary itself. More specifically, continued high mud supply or reduced mud supply from upstream and mangrove clearance in the estuary itself. A detailed model setup is described in the Method section. We find that excessive mud supply accelerates estuary infilling, facilitating mangrove expansion. Mangrove clearance will not help to reduce the mud content within the estuary, instead, it may distribute the mud more widely, increasing the mud cover and shallowing the channels.

4.2 Results

4.2.1 Estuary infilling and mangrove expansion accelerated by increasing fluvial sediment supply

An increasing fluvial sediment supply from pre-disturbance to post-disturbance led to significant differences in morphological development and mangrove distribution in the lagoon. At pre-disturbance stage (year 200- 400), mangroves first colonized levees (i.e. the edge of fluvial channels) close to the river mouths where sediment from catchments was first deposited (Figure 4.2b). The morphological evolution was characterized by coastal propagation, where fine sediment continued to deposit seaward, creating intertidal areas and contributing to channel formations carving through the basin (Figure 4.2b). Over these 200 years, vegetation propagated

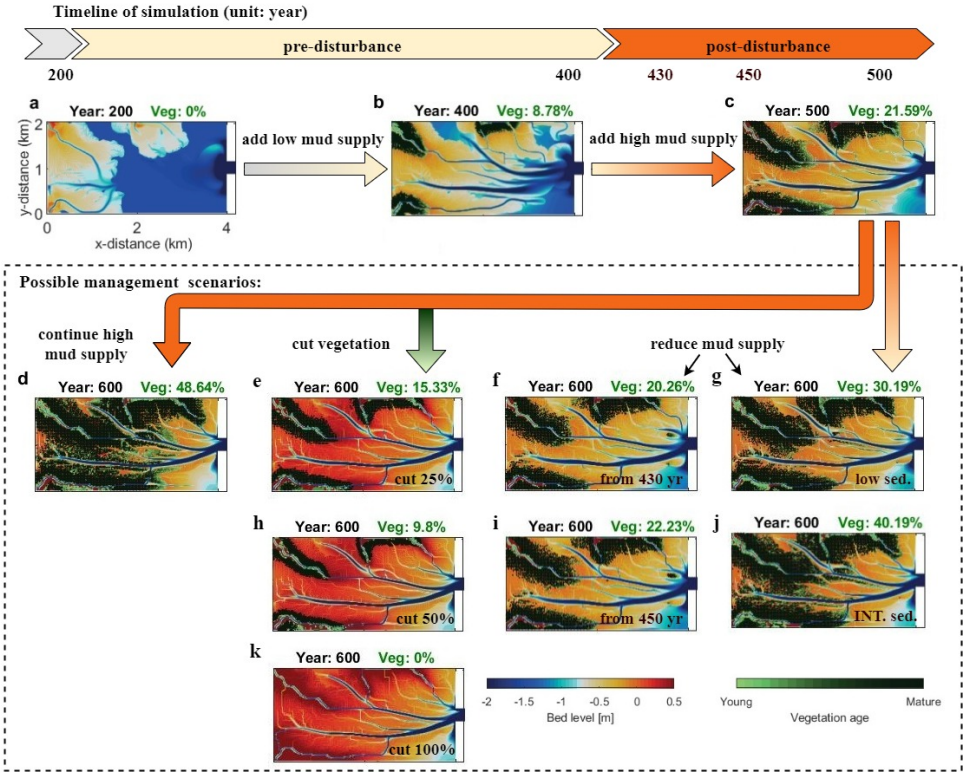

Figure 4.2 Mangrove distribution and morphological development phases. The vegetation cover as a fraction of lagoon is indicated in green number on top of each panel. Morphology after 200-year spinup (a), before European settlement with low mud input and mangrove colonization (b), after European settlement with high mud input and mangrove expansion (c). Possible management scenarios include: d) continued high mud input; e,h&k) removal of 25, 50% and 100% mangroves, respectively; and reduce mud supply from year 430 (f) and year 450 (i); and reduce mud supply to low level (g) and intermediate level (j) from year 500. yr = year; low sed. = low sediment supply; INT. sed. = intermediate sediment supply.

slowly seaward as inundation regimes became favourable, reaching a proportion of 8.78% over the basin area at the end of pre-disturbance period. At post-disturbance stage, with a high mud supply (year 400-500), morphological evolution was characterized by vertical mud accumulation. During this period, lagoon infilling was accelerated with further sedimentation on the intertidal areas, leading to a seaward expansion of mangrove forests along channels (Figure 4.2c). The proportion of vegetation covering over the basin therefore nearly tripled within 100 years under such high sediment loading (21.59%) (Figure 4.2c).

4.2.2 System-scale changes driven by enhanced mud supply and mangrove clearance

To understand the impact of management actions on the tidal lagoon, we investigated different mangrove removal scenarios: 25%, 50% and 100% mangrove coverage removal (Figure 4.2e,h&k). In addition to increasing mud supply from year 500 as is shown in Figure 4.2d, we also modeled mud reduction scenarios where mud supply was reduced earlier (i.e. from year 430 and 450) to explore the effects of disturbance duration (Figure 4.2f&i), and where mud supply was reduced to low and

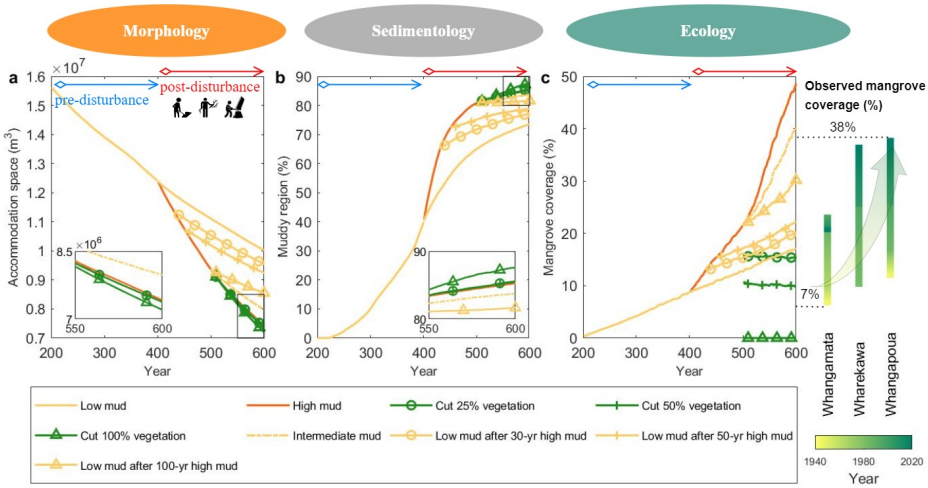

Figure 4.3 Temporal changes of the main effect variables in the basin for scenarios of mud supply and mangrove removal. a) accommodation space, b) muddy region fraction and c) vegetation coverage fraction. Muddy region is defined as the surface area for which the mud fraction in the top 1-m profile is larger than 30% (Van Ledden et al., 2006).

intermediate level from year 500 to explore the effects of different amounts of mud reduction actions (Figure 4.2g&j). A control run with continued low mud supply throughout the simulation was used for comparison.

Estuary infilling and vegetation expansion are highly dependent on the amount and the duration of high mud loading imposed on the systems. Increasing mud supply would accelerate accommodation space infilling and the expansion of the muddy regions over the estuary, concomitantly resulting in a faster mangrove expansion. Conversely, reducing mud supply decelerated the rate of infilling of accommodation space and expansion of mud areas, slowing mangrove expansion (Figure 4.3). Moreover, the timing when mud supply was reduced relative to the postulate human colonization and the magnitude of mud reduction determined the status of the ecosystem (Figure 4.9). Accommodation space, muddy region and mangrove coverage became comparable with situations under continued low mud supply when mud supply was reduced earlier, such as the LM30 scenario shown in Figure 4.9. A delayed reduction in mud supply (such as LM100 scenario) or a small mud supply reduction (such as INT scenario) reduced the accommodation space available (Figure 4.9a).

Mud supply overwhelmed any effect of mangrove expansion or clearance on estuary infilling (Figure 4.3). Mangrove clearance instead enhanced estuary infilling and resulted in more muddy regions. When mangroves were completely removed, the accommodation space became smaller, with an increased muddy area compared to scenarios of partial or no mangrove removal (see inserts in Figure 4.3a&b and also Figure 4.9a&b). Moreover, mangrove expansion was a function of mud supply and disturbance period that high mud was imposed. Mangrove coverage would continue to increase rapidly when high mud loading was imposed for longer (Figure 4.3c). However, when the high mud disturbance period was shortened, mangrove expansion could be constrained (Figure 4.3c; also see LM30 in Figure 4.9c).

4.2.3 Spatial variation in morphological changes driven by mud supply and mangrove clearance

The magnitude of morphological changes varied between channelized areas, platform areas close to channels (<100 m) and platform areas further away from channels (300-400 m) (shown as a 'violin' plot in Figure 4.4). In channelized areas, although high mud supply caused some deeper channels (yellow and orange violins in Figure 4.4a), the median mud thickness was increased due to the enhanced sedimentation rate (yellow and orange violins in Figure 4.4c&e). Continued high mud supply further elevated the median bed elevation but also allowed those deeper channel areas to become even deeper (purple violin in Figure 4.4a). In the meantime, the mud layer continued to accumulate with a slightly higher median mud thickness (purple violin in Figure 4.4c). Interestingly, mangrove clearance led to shallower channels with a larger mud thickness, compared to continued high mud supply scenario (purple and green violins in Figure 4.4a&c). This implied that more mud accumulated in channels after mangrove removal. Conversely, under the low mud supply, channels retained similar water depth, mud thickness and sedimentation rate to the pre-disturbance period (yellow and blue violins in Figure 4.4a,c&e).

In the platform areas, the distance to the nearest channels also influenced sediment distribution and thus bed level changes, with less sediment deposited in the area further away from the channels (Figure 4.4b,d&f). In the pre-disturbance period under low mud supply, the mud distribution on the platform areas was rather homogeneous (yellow violins in Figure 4.4b,d&f). However, during the post-disturbance period with high mud supply, more mud tended to deposit in areas close to the channels, resulting in a relatively high bed elevation, mud thickness and sedimentation rate on the platform close to channels (orange violins in Figure 4.4b,d&f). Continued high mud supply would further increase mud deposition on the platform, leading to an even higher bed elevation and mud thickness (orange and purple violins in Figure 4.4b&d). In the meantime, due to the unequal sediment distribution, the difference between bed elevation and mud thickness in different platform areas was further increased (purple violins in Figure 4.4b&d), although sedimentation rates in both regions remained high (purple violins in Figure 4.4f). When mangroves were removed, more mud was deposited in areas further away from channels, compared with the scenario of continued high mud supply (purple vs. green violins in Figure 4.4b,d&f). This pattern of deposition suggests that mud deposition after mangrove clearance was limited within the vegetated areas, but enhanced elsewhere. Similar to the results in channelized areas, under low mud supply, due to the lower sedimentation rate, both bed elevation and mud thickness remained low, compared to the scenario of continued high mud supply (orange and blue violins in Figure 4.4b,d&f).

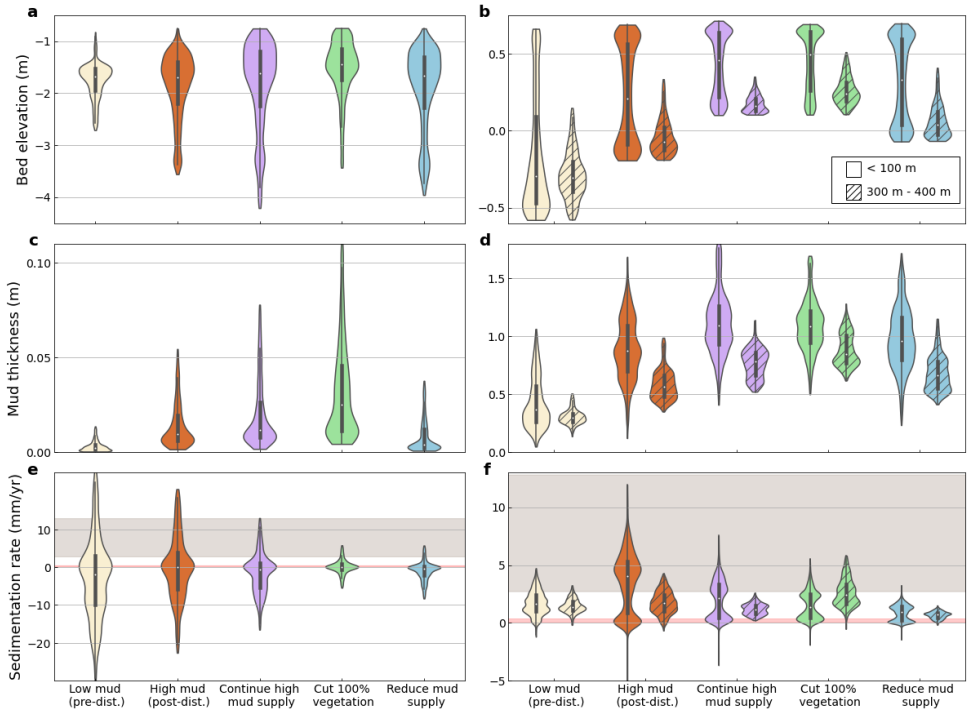

Figure 4.4 Comparison of the distribution of bed surface properties expressed as mean bed elevation, mud thickness and sedimentation rate for five representative scenarios in Figure 4.2. The comparisons are conducted in both channelized areas (a,c&e) and non-channelized areas (b,d&f), the latter of which have been further categorized into two classes based on the distance from the nearest channels (i.e. platform areas close (<100m) and further away from channels (300-400m)). Low mud scenario indicates the stage before European settlement accompanied by a limited amount of mud supply. High mud scenario represents the system disturbed by a large mud supply after European arrivals. Three possible management strategies following high mud supply scenario, with continued high mud supply, cut down of mangrove vegetation (100%), or reduce mud supply, are also listed in the plots. Yellow, orange, purple, green and blue colors are used to represent the scenarios in low mud (corresponding to Figure 4.2b), high mud (corresponding to Figure 4.2c), continue high mud (corresponding to Figure 4.2d), cut vegetation (corresponding to Figure 4.2k), and reduce mud supply (corresponding to Figure 4.2g). Violin thickness corresponds to probability density. Endpoints of violin depict minimum and maximum values. Box plot inside each violin covers the first to third quartiles, with a diamond representing the median value. Pink and grey shadings in e and f indicate the observed sedimentation rate range (99% confidence interval) at Whangapoua, Wharekawa and Whangamata estuaries before and after European settlement, respectively (Figure 4.1f).

4.2.4 Trajectories of coastal bio-geomorphic systems driven by human interventions

To understand the infilling processes at different disturbance periods, we plotted the dimensionless catchment sediment load (SY/TP) against the basin infilling fraction (AMH/AHT) following the previously described estuary infilling patterns found for mangroves in New Zealand (Figure 4.5) (Swales et al., 2021). The basin infilling fraction (AMH/AHT) was the area of intertidal flat above mean sea level as a proportion of the high tide area. The dimensionless catchment sediment loads are defined as the annual catchment sediment load divided by the tidal prism (SY/TP), as a proxy of how effective the processes causing sediment accumulation are relative to those removing sediment from the estuary through tides.

Our results show that the basin infilling fraction can be slowed down under human intervention, though may be irreversible, when upstream mud supply reduction is implemented (Figure 4.5). Continued high mud supply accelerated the creation of new tidal flat area (∗), while mangrove clearance may further enhance such estuary infilling process (◇). Less tidal flat area would be created when sediment yield was reduced (+ and △). The timing of reduction of the mud supply also played an important role in creating new tidal flat area. With continued low mud supply throughout these 600 years, the estuary infilling fraction was only approximately 0.2 (□). The fraction only increased by 0.1 when the mud reduction strategy was conducted immediately after a 50-year high mud supply (○). We concluded that mangrove removal has a minor effect on the estuary infilling; instead, the degree of mud reduction and the timing of that reduction played dominant roles in estuary infilling. Thus, we suggested a more efficient way to restore estuarine landscapes and mitigate mangrove expansion is not to remove mangroves, but to limit fluvial sediment supply by decreasing upstream land-use activities and stabilizing the sediment along riparian margins.

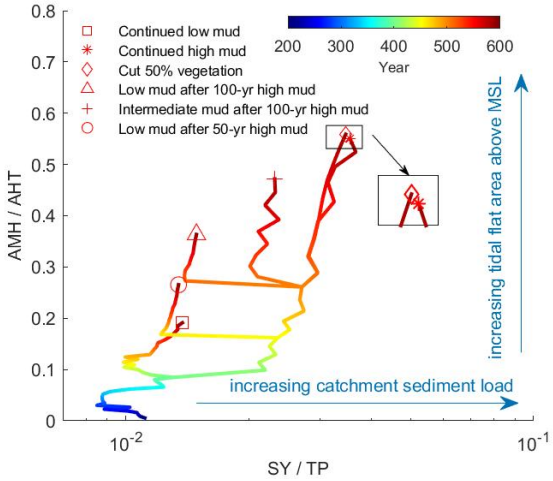

Figure 4.5 Relationships between the ratio of catchment annual sediment yield to estuary tidal prism volume (SY/TP) and the ratio of potential mangrove habitat to high-tide area (AMH/AHT). The annual catchment sediment load (SY) is the total sediment yield from three river inflows. The tidal prism (TP) was calculated as the water discharged through the inlet during one tidal cycle. The area of potential mangrove habitat (AMH) is estimated as the intertidal area above mean sea level. Estuary high tide area (AHT) refers to the basin area inundated during high tidal level. Six representative results are shown to indicate different infilling extent, including continued low mud supply, continued high mud supply, cutting 50% of the vegetation, low mud supply after a 100-yr high mud input, intermediate mud supply after 100-yr high mud input and low mud supply after 50-yr high mud.

4.3 Discussion

Our results suggest upstream land-use changes are the main driver of vegetation patterns observed in our tidal lagoon. Vegetation removal cannot restore pre-disturbed state, but rather accelerates estuary infilling. Differences in accommodation space, the extent of muddy regions and mangrove coverage suggest that a larger and earlier mud reduction would have led to less estuary infilling and mangrove expansion (Figure 4.3). The morphology remains similar between cases with continued high mud supply and partial vegetation removal (i.e. 25% and 50% mangrove removal); however, a complete mangrove removal resulted in less accommodation space and a wider muddy region within the basin (Figures 4.3&4.9). This is because complete mangrove removal reduces mud deposition on the pre-vegetated area, meaning more mud is available to be distributed in the channels and on the flats further away from the channels (Figure 4.4). We therefore conclude that a reduction in the extent of muddy areas and restoration of sandy flats are highly unlikely to be achieved by removing coastal mangroves. Instead, a more appropriate management focus is on catchments to conserve upstream soil and reduce mud loss to the rivers.

The main ramification of mangrove clearance on the estuary is increasingly evident sediment redistribution (Figures 4.3&4.4). The presence of vegetation near the channels can concentrate the flow in the channel (Nardin and Edmonds, 2014), leading to faster flow causing deeper channels. In coastal marsh or fluvial tree systems, such convergence effect has been observed to diminish as soon as vegetation loss occurred (also see our model results in Figures 4.10a-b&4.11a-b). This in turn causes less sedimentation on previously vegetated areas and more sedimentation in places further away from channels, and more channel infilling (Temmerman et al., 2012; van Oorschot et al., 2016; Kleinhans et al., 2018). These characteristics have been replicated by our models, with channels becoming shallower when mangroves are completely removed (Figure 4.4a). Meanwhile, changes in flow strength also increase sediment concentration in the channels (Figure 4.10c), and thus, channel shallowing is driven by the reduced flow strength as well as increased sediment availability (Figure 4.10e). Similarly, suspended sediment concentration is enhanced on the flat area due to the increasing flow strength, especially in areas further away from the channels (Figure 4.10d). As the strength of flow and the amount of sediment concentration both increase, the difference of bed level between the scenarios of continued high mud supply and mangrove removal remains minor (Figure 4.10f and Figure 4.11f). Thus, less sediment is able to settle in the areas previously occupied by mangroves due to the increased hydrodynamic forces, while more sediment can be eroded directly to the channels or be transported further away from channels, increasing mud accumulation and bed elevation at channels and tidal flats (Figure 4.4a&b); such behaviors have also been observed at the areas of mangrove clearance in the Whangamata estuary (Stokes and Harris, 2015).

Sediment supply, rather than vegetation loss, plays a much greater role in determining estuarine morphological changes. Previous research has suggested that the conversion of mangrove habitats to agriculture or aquaculture in coastal areas led to significant coastal erosion combined with ecological and economic function loss (Thampanya et al., 2006). However, here we show that sediment accumulation is nearly independent of mangrove removal but rather the mud supply rate determines the overall degree of morphological change. We interpret such differences with respect to the bio-morphodynamic feedbacks between hydrodynamics, sediment transport and vegetation impacts. The idealized estuarine basin we model here is typified by low energy hydrodynamics. Low energy estuarine systems can occur especially when the tidal range is small and the generation of wind waves are limited by short fetch due to the presence of islands or the orientation of the estuary relative to the prevailing wind direction (Hunt et al., 2016). Within low energy estuaries, the feedbacks between morphology and hydrodynamics are unable to produce substantial increases in sediment export to reduce mud fractions within the basin (Glover et al., 2022). In contrast, on open coasts or large fluvial systems where a suitable fetch allows the generation of wind waves (Hunt et al., 2016), after

mangroves have been removed, energetic waves or strong flows can cause sediment resuspension and coastline retreat (Winterwerp et al., 2013; Brunier et al., 2019). Removal eliminates the attenuation effects offered by mangrove forests, and the subsequent strong hydrodynamic forces such as tides, waves or river flows can easily erode the sediment (Montgomery et al., 2018; Montgomery et al., 2019).

Furthermore, the muddy region fraction and mangrove expansion rate are enhanced when upstream sediment supply is increased (Figure 4.3). Our long-term projections of mangrove expansion rate induced by high mud supply post-disturbance are almost double or triple when compared to the rate given by low mud supply during the pre-disturbance period. The vegetation coverage rate modelled here was similar to the historical mangrove coverage rate observed in the three representative estuaries prior to mangrove removal (around year 1990-2000 in Figure 4.1e). However, the vegetation coverage in the three estuaries observed with historical data in New Zealand increased at a much faster rate than in the modelled results. As an example, within the Whangapoua estuary, vegetation coverage increased from 10% to $\sim$ 40% within 60 years, implying the real sedimentation rate in the estuaries was greater than predicted in our model settings. The optimum time to set management limits on catchment sediment delivery in order to slow down mangrove expansion should be now instead of in the future (Figure 4.3c).

Compared with mangrove removal scenarios, our simulations on upstream mud supply reduction indicate that limiting the mud accumulation rate and mangrove expansion rate is possible, and the eventual estuary infilling state is highly linked to the level and timing of mud reductions (Figures 4.3&4.4). Sediment availability has been demonstrated as one of the key factors controlling bed level evolution and thus acting as a critical indicator when evaluating coastal wetland resilience to sea-level rise (Lovelock et al., 2015; Schuerch et al., 2018; Xie et al., 2020). The benefits of sediment availability need to be weighed against the negative effects of turbid water and reduced light availability to submarine systems (Jones, 2008). The connection to downstream ecosystems such as seagrass and coral reefs is two way, and for example, they may in turn potentially protect the landward mangrove or salt marsh systems from storms (Guannel et al., 2016). By comparing different levels and timing of mud reduction, we highlight the estuary infilling rate varies with mud reduction strategies conducted in the future. Reducing mud supply can significantly reduce water turbidity and decrease the extent of muddy areas (Figure 4.3 and Figures 4.10&4.11). More importantly, relatively small changes to the timing and level of mud reductions can have a disproportionately large impact on mitigating high estuary infilling rates and mangrove spreading (Figure 4.5).

Globally, the increase in sediment loading is reported in many studies over the last decade (Syvitski et al., 2005), albeit maybe not over such a compressed time frame as in New Zealand. Sediment production due to human activity (such as construction, mineral mining and deforestation) has increased globally by about 467% between 1950 and 2010 (Restrepo et al., 2015; Syvitski et al., 2022). Estuarine systems overfilled by sediment and accompanying vegetation expansion can be seen, not only in New Zealand studied here, but in other areas in the world, such as North America (Kirwan et al., 2011). A consequence of increasing the size of intertidal coastal ecosystems is a cost to other marine ecosystems, in particular the submarine ecosystems such as seagrass and coral reefs (Jones, 2008; Beck et al., 2018). These impacts have in turn jeopardized the living conditions of landward plant systems and humans due to the strong connections within coastal and marine ecosystems (Guannel et al., 2016). Locally-focused management approaches, such as mangrove removal, may not restore the pristine coastal environment, but rather even contribute to estuary infilling which further deteriorates condition. Conversely, upstream management to reduce soil input has been proved to be more effective at slowing down the estuary infilling and constrain vegetation expansion. We therefore suggest anthropogenic interventions leading to coastal system changes may be irreversible and

necessitate a comprehensive assessment considering both source and sink impacts before a coastal management solution is adopted.

4.4 Method

We extend the one-dimensional bio-morphodynamic model (Xie et al., 2020; Xie et al., 2022) to two-dimensions to capture spatial mangrove behaviors and sediment dynamics in an estuary, specifically a back-barrier fluvial-tidal basin. The two-dimensional bio-morphodynamic model is composed of a hydro-morphodynamic model (in Delft3D) and a dynamic vegetation model (in Matlab), which are connected seasonally. Delft3D models hydrodynamics and morphology by solving the momentum and continuity equations for unsteady, incompressible, turbulent flow. Our runs were conducted using the depth-averaged mode with the hydrostatic pressure approximation (Deltares, 2014). To link the vegetation model, Delft3D calculates local hydroperiod and bed shear stress, which control the mangrove life stages, such as colonization, growth and mortality, so that the effects of tidal flow and morphology on mangroves are accounted for. The vegetation model calculates the vegetation parameters, including the sizes and densities of vegetation objects (i.e. stems and roots), which are used to calculate hydraulic resistance in Delft3D so that the effects of mangroves on tidal flow and consequently sediment transport are accounted for (van Maanen et al., 2015; Brückner et al., 2019). A morphological acceleration factor (here set to 90) is applied to enable long-term simulations based on the sensitivity analysis (Roelvink, 2006; Coco et al., 2013). The ecological time scale is set to the same as the morphological time scale, such that within one morphological year the vegetation is updated four times (i.e. quarterly).

4.4.1 Idealized landscape settings

The estuarine systems usually vary with characteristics depending on various factors, including geomorphology, the evolutionary stage, hydrology and salinity or combinations of the above (Hume et al., 2007). New Zealand mangroves usually colonize barrier-enclosed or headland-enclosed estuaries with inlets restricted by rocky headlands, typically with multiple catchments that are small relative to estuary surface area (Swales et al., 2021). Here we simulate an idealized back-barrier fluvial-tidal basin geometry to represent these typical estuarine systems in the North Island, New Zealand, most of which are characterized by similar spatial scales, similar historical vegetation expansion trends and similar sedimentation accumulation processes (Figure 4.1). The model domain consists of a 4 km by 2 km flood-tidal basin enclosed by two non-erodible barriers, connected to the open coast with a 2 km by 2 km rectangle offshore area (Figure 4.6). The grid resolution is set to 15 m by 15 m to allow evolution of channel networks and changes of mangrove forests following previous research (Horstman et al., 2013; van Maanen et al., 2015; Brückner et al., 2019; de Ruiter et al., 2019). The initial bed elevation in the basin is set to 1.5 m below mean sea level, while the offshore area is set to a sharp slope from -1.5 in the inlet to -100 m on the most eastern seaward edge (Figure 4.6b). This large depth avoids shallowing by sedimentation outside the inlet, where wind and waves are not incorporated for computational efficiency. We include three fluvial inflows in our model from different directions, which is typical of estuarine systems on the North Island, New Zealand (Figure 4.1b-d). To avoid forcing symmetry, the rivers on the left and the bottom are put close to the land boundary (Figure 4.1a). Following a survey of the hydraulic geometry of 73 New Zealand river reaches, the average river width is around 28 m (see Table 4.1) (Jowett, 1998) and we set the river width equal to the cell size of 30 m (Figure 4.6). The chosen river width is consistent with the empirical relations between river discharge and river width described in the next section (Equation 4.9).

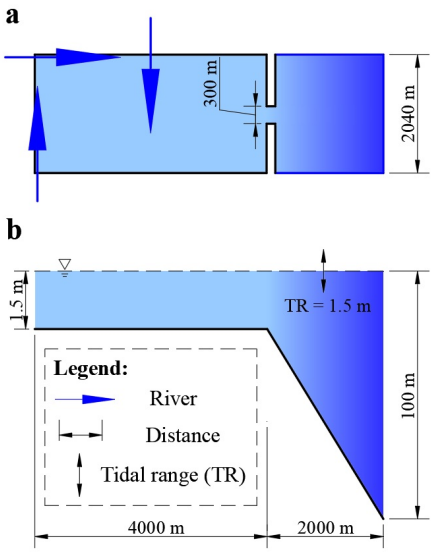

Figure 4.6 Model layout comprising size, initial bathymetry and boundaries. Plan view of model domain with a) three river inputs; b) cross-section view along the domain.

4.4.2 Hydro-morphodynamic processes

Delft3D (version 4.01.00), a process-based hydrodynamic modelling package, is adopted to simulate the flow fields and sediment transport since it has been widely used in both coastal engineering and scientific research (Lesser et al., 2004; Zhou et al., 2014). Water level and flow velocity are acquired by solving the depth-averaged shallow water equations as follows:

$$\frac{d\eta}{dt} + \frac{dhu}{dx} + \frac{dhv}{dy} = 0 \tag{4.1}$$

$$\frac{du}{dt} + u\frac{du}{dx} + v\frac{du}{dy} = -g\frac{d\eta}{dx} + \nu_c\left(\frac{d^2u}{dx^2} + \frac{d^2u}{dy^2}\right) - \frac{gu\sqrt{u^2+v^2}}{C^2h} + M_x \tag{4.2}$$

$$\frac{dv}{dt} + u\frac{dv}{dx} + v\frac{dv}{dy} = -g\frac{d\eta}{dy} + \nu_c\left(\frac{d^2v}{dx^2} + \frac{d^2v}{dy^2}\right) - \frac{gv\sqrt{u^2+v^2}}{C^2h} + M_y \tag{4.3}$$

where t is the time (s) and η is the water level (m) with respect to datum (e.g. mean sea level); h is the water depth (m); u is the depth-averaged flow velocity in the x direction (m/s) and v is the depth-averaged flow velocity in the y direction (m/s) ; g=9.81 m/s^2 is the gravitational acceleration; ν_c=1 m^2/s is the eddy viscosity coefficient; C is the Chézy friction coefficient (m$^{1/2}$/s); The presence of vegetation is incorporated by including additional hydraulic resistance, which is considered through calculation of the bed roughness and the additional resistance term ($M_x = -\frac{\lambda}{2}\cdot u^2$, $M_y = -\frac{\lambda}{2}\cdot v^2$). Both λ and C are derived from vegetation characteristics (diameter, height, density) and will be introduced in the next section.

Following previous observations in New Zealand estuaries, we specify both cohesive (mud) and non-cohesive (sand) sediments (Sheffieldt et al., 1995; Stokes et al., 2009). Large-scale upstream land-use changes, such as catchment deforestation, mining, forestry and agriculture has enhanced soil erosion, which is then washed into rivers and subsequently deposited in the estuary (Hunt, 2019;

Swales et al., 2021). To model sediment infilling levels due to different degrees of upstream land-use change and variations in catchment characteristics, low, intermediate and high sediment concentrations of cohesive sediment are supplied at the river boundaries in different simulation periods. We calculate the suspended sediment supply based on the measuring fluvial sediment yields from previous studies (Jones, 2008; Hicks et al., 2011). Sediment yields range from 5000 metric t/yr to 17000 metric t/yr depending on the estuary and period. According to the research on sediment cores, sedimentation rates in Whangamata Estuary remain minor (0.1 mm/yr to 0.3 mm/yr) as a result of the increasing agricultural activities before the 1880s, and then the rates increase from 2 mm/yr (1920s to 1970s) to 15 mm/yr (1970s to 1980s) due to widespread deforestation, which was followed by high mud content in coastal areas and previously sandy flats (Jones, 2008). Since the fluvial sediment supply in the dataset was collected in different periods, mainly until the late 1990s, we take a conservative value of supply before human interventions, i.e. 5 mg/L, and use 15 mg/L as the conditions when human interventions starts, consistent with the observations from Jones (2008) and Hicks et al. (2011). The deposition ($Q_{mud,d}; kg \cdot m^{-2}s^{-1}$) and erosion fluxes ($Q_{mud,e}; kg \cdot m^{-2}s^{-1}$) are computed through the Partheniades-Krone formulation (Partheniades, 1965) as follows:

$$Q_{mud,d} = \omega_s c \tag{4.4}$$

$$Q_{mud,e} = \begin{cases} M_e \left(\dfrac{\tau_c}{\tau_{cr,e}} - 1 \right), & \text{if } \tau_c > \tau_{cr,e} \\ 0, & \text{if } \tau_c \leq \tau_{cr,e} \end{cases} \tag{4.5}$$

where $\omega_s = 2 \times 10^{-4}$ m/s is the settling velocity, c is the depth-averaged sediment concentration (kg/m^3), $\tau_c = \rho g \cdot \left(u^2 + v^2\right)$ is the tide-induced bed shear stress (Pa), and $\tau_{cr,e}$=0.2 Pa are the critical shear stresses for mud deposition and erosion, respectively. $M_e = 5 \times 10^{-5}$ kg/m^2/s is the erosion parameter. These parameters are consistent with recent field research (Pritchard et al., 2016).

The transport of suspended sediment is calculated according to the advection-diffusion equation:

$$\frac{\partial (ch)}{\partial t} + \frac{\partial (uch)}{\partial x} + \frac{\partial (uch)}{\partial y} = Q_{mud,e} - Q_{mud,d} \tag{4.6}$$

where $Q_{mud,e} - Q_{mud,d}$ is the sink/source term of suspended sediment in the water column exchanging with the bed.

For non-cohesive sand, the Van Rijn transport predictor is used (van Rijn et al., 2004; van Rijn, 2007) because it is well-calibrated in a wide range of environments including tidal-fluvial conditions (Boechat Albernaz et al., 2020). The fluvial sediment boundary for non-cohesive sediment is set at equilibrium boundary conditions, such that the transport is at the capacity of the flow velocity at the boundary. The bed-load transport is computed as follows:

$$S_{sand} = 0.5 \rho_s d_{50} D_*^{-0.3} \left(\frac{\tau_c}{\rho} \right)^{0.5} T \tag{4.7}$$

where S_{sand} is the total sediment transport of sand particles (kg/m/s), ρ_s=2650 kg/m^3 and ρ=1000 kg/m^3 are the sediment density and the water density, respectively. d_{50}=250 μm is the median grain size consistent with previous observations (Stokes and Harris, 2015). D_* is the dimensionless particle size, calculated as $D_* = d_{50} \left[\left(\dfrac{\rho_s}{\rho} - 1 \right) \dfrac{g}{\nu_c^2} \right]^{1/3}$. τ_c is the effective current-related bed shear stress and τ is the excess bed shear stress, both of which are calculated as a function of bed roughness and the calculations can be referred to (van Rijn et al., 2004; van Rijn, 2007).

The transverse bed slope effect on bed-load transport is parameterized with Koch and Flokstra formulations (Koch et al., 1980), after Baar et al. (2019). The sediment transport vector in Koch and Flokstra formulations is rotated downslope as a function of transverse slope divided by $\alpha \cdot \theta^{\beta}$, where θ is the Shields mobility, and α and β are respectively set to 0.2 and 0.5 following recent findings (Baar et al., 2019).

Bed porosity is assumed to be constant at 0.4 (Zhou et al., 2016). At every hydrodynamic time step, the changes of bed level (Z; unit: m) is calculated based on the sediment mass balance as follows:

$$(1-\varepsilon_p)\frac{dZ}{dt}+\frac{1}{\rho_s}\left(\frac{dS_{sand,x}}{dx}+\frac{dS_{sand,y}}{dy}\right)=\frac{1}{\rho_s}\left(Q_{mud,d}-Q_{mud,e}\right) \tag{4.8}$$

where ε_p is a bed porosity (dimensionless), and $S_{sand,x}$ and $S_{sand,y}$ are the bed-load transport in x and y directions.

Boundary and initial conditions are constructed as follows. We use the NIWA tide model to calculate the annual mean tidal range at Whangapoua, Whangamata and Wharekawa estuaries (https://niwa.co.nz), the mean tidal range is around 1.5 m which is consistent with observations (Hume and Herdendorf, 1992; Healy, 2005). We apply an M2 tidal cycle with a 1.5-m range and 30-deg/hr frequency at the eastern-seaward boundary (Hunt, 2021). Both the northern- and southern-seaward boundaries are set as Neumann conditions. The river discharge is set to 18 m^3/s based on the average of the data from 73 New Zealand river reaches (Figure 4.13, also see Table 4.1) (Jowett, 1998). This value is similar to another dataset which contains both river discharge and the corresponding suspended sediment yields based on nearly 150 observational sites in North Island, New Zealand (Table 4.2) (Hicks et al., 2011). Furthermore, the selected river conditions are consistent with empirical relations between river width and flow discharge as (Moody and Troutman, 2002; Frasson et al., 2019):

$$W = 7.2Q^{0.5} \tag{4.9}$$

where W is the river width (m) and Q is the flow discharge (m^3/s). By applying the value of flow discharge Q to 18 m^3/s in Equation 4.9, the calculated empirical river width is about 30.5 m, which is nearly the same as our predefined value (i.e. 30 m) based on the measuring fluvial geometry data from Jowett (1998).

4.4.3 Dynamic vegetation processes

To account for the effects of vegetation on hydrodynamics, we quantify the vegetation-induced flow resistance through the Baptist predictor (Baptist et al., 2007), which was implemented to allow for multiple fractions of different vegetation types in one numerical grid cell (van Oorschot et al., 2016). Based on the relative relations between the height of vegetation objects (such as stems or roots) h_v (m) and local water depth h (m), the bed roughness C ($m^{1/2}/s$) is calculated as follows:

$$C=\begin{cases} C_b+\dfrac{\sqrt{g}}{\kappa}\ln\left(\dfrac{h}{h_v}\right)\sqrt{1+\dfrac{C_D n h_v C_b^2}{2g}}, & \text{if } h \geq h_v \\ C_b, & \text{if } h < h_v \end{cases} \tag{4.10}$$

where C_b is the Chézy coefficient for the unvegetated bed, set to 65 ($m^{1/2}/s$); κ=0.41 is the Von Kármán constant; C_D is the drag coefficient (dimensionless); n is the vegetation density (m/m^2) calculated as $n = mD$ where m is the number of vegetation objects per unit area($1/m^2$) and D is the diameter of this object (m).

Vegetation causes a higher hydraulic resistance which could then lead to a higher bed shear stress and larger sediment transport rates during morphological calculations. To correct this, Delft3D includes a

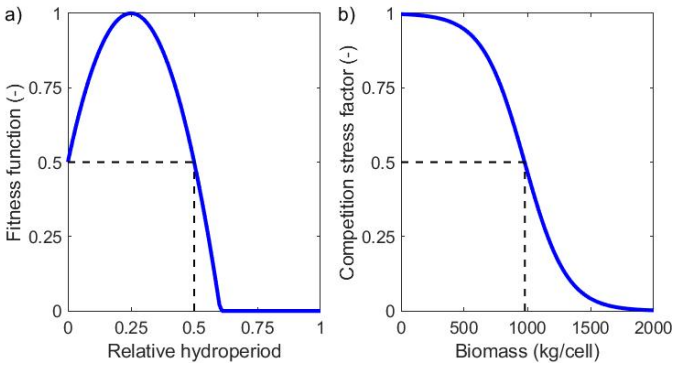

Figure 4.7 Growth control factors used in the vegetation model. (a) Fitness function, characterized by the optimal relative hydroperiod (Relative hydroperiod = 0 implies never inundated while Relative hydroperiod = 1 implies permanently inundated). (b) Competition stress factor represents the influence of vegetation population on growth conditions as neighbouring trees have to share resources.

term ($M_x = -\frac{\lambda}{2} \cdot u^2$, $M_y = -\frac{\lambda}{2} \cdot v^2$) in the momentum equations (Equations 4.2-4.3), where λ is calculated as:

$$\lambda = \begin{cases} C_D n \frac{h_v}{h} \frac{C_b^2}{C^2}, & \text{if } h \geq h_v \\ C_D n, & \text{if } h < h_v \end{cases} \tag{4.11}$$

If vegetation objects with different sizes co-exist in one grid cell, C and λ are accumulated weighted according to their relative surface area fraction (Deltares, 2014), which is analogous to parallel resistors. To consistently capture the effects of vegetation objects, vegetation information is updated quarterly to Delft3D, including stem and root height, diameter, surface area fraction and density. In turn, Delft3D provides hydrodynamic information to dynamic vegetation model (Matlab) including bed level, water depth, water level and velocity.

Avicennia marina is the main mangrove species in the North Island, New Zealand, we therefore set up vegetation properties based on *Avicennia marina* to represent local mangrove species (Bulmer et al., 2017). Since the dynamic mangrove model has been detailed described in our previous researches (Xie et al., 2020; Xie et al., 2022), below we briefly introduce the processes that control mangrove life stages: colonization, growth and mortality.

Mangrove colonization occurs at the first ecological season when both inundation regime and current strength are appropriate for the seedling settlement. As mangroves mainly occupy above mean water level (Chapman, 1976) and their seedlings are hard to grow above a bed shear stress threshold (i.e. 0.2 N/m^2) induced by currents/waves (Balke et al., 2011), we assign an initial vegetation number to the cells with relative hydroperiod ranging between 0 and 0.5 (Figure 4.7a), and bed shear stress below 0.2 N/m^2. The initial seedling density assigned on a bare cell is set to 3000 individuals/ ha following van Maanen et al. (2015).

After initial settling, the mangrove grows by each ecological season as an increase in stem diameter (D; cm) and height (H; cm) (Chen and Twilley, 1998; Berger and Hildenbrandt, 2000; van Maanen et al., 2015):

$$\frac{dD}{dt} = \frac{GD\left(1 - (DH)\,/\,(D_{max}H_{max})\right)}{(274 + 3b_2D - 4b_3D^2)} \cdot f \cdot C \tag{4.12}$$

$$H = 137 + b_2 D - b_3 D^2 \tag{4.13}$$

where t is the time (season), D_{max} and H_{max} are the maximum stem diameter and tree height, respectively. G, b_2 and b_3 are growth parameters (Table 4.3). Tree growth may be reduced by sub-optimal inundation conditions and because of limitations in available resources. This is incorporated through fitness function (f) and the competition stress factor (C). Both f and C range between 0 (no growth) and 1 (optimal growth) (van Maanen et al., 2015; D'Alpaos and Marani, 2016). f is dependent on hydroperiod (Figure 4.7) and implies that each mangrove has a specific hydroperiod for optimal growth while growth rate reduces when inundation is either longer or shorter. C is dependent on mangrove biomass (Figure 4.7b). In order to compute biomass (W), we consider the sum of both above-ground and below-ground biomass of every single tree by applying an allometric equation as (van Maanen et al., 2015):

$$W = \sum \left(\alpha_1 D^{\beta_1} + \alpha_2 D^{\beta_2} \right), \tag{4.14}$$

where α_1, β_1 and α_2, β_2 are constants controlling above-ground and below-ground, respectively. Following Komiyama et al. (2008), we set $\alpha_1 = 0.308$, $\beta_1 = 2.11$ and $\alpha_2 = 1.28$, $\beta_2 = 1.17$.

At the end of every ecological year, the mortality process is initialized. Mangrove mortality commences when growth suppression ($f \cdot C < 0.5$) of each mangrove age and size class continues for 5 consecutive years, following which a self-thinning process is initialized (van Maanen et al., 2015). The number of stems and roots will be reduced until their suppressed growth terminates or no vegetation left on the cell. After mortality and at the beginning of every new ecological year, colonization process restarts and the cells with suitable growth ($f \cdot C > 0.5$) are allowed to have new seedlings. The inclusion of new seedlings will increase vegetation biomass, leading to a low competition stress factor (Figure 4.7b). Thus, the number of new seedlings added to a cell is dependent on these two growth factors.

Finally, the model includes the mangrove root system as aerial roots provide additional flow resistance (Mazda et al., 1997b). The number of roots is evaluated with the following formula:

$$N_{roots} = \frac{1000}{1 + exp\left[k\left(\frac{D_{max}}{2} - D\right)\right]} \tag{4.15}$$

where k is a constant describing the growth rate of the root number with stem diameter (D; cm), which are supplied to the flow resistance calculation as a separate class in each grid cell.

4.4.4 Model scenario setup

The models were initiated by a 200-year spinup period to create initial morphology with a stable cross-sectional inlet depth (Figure 4.14). The following simulations span over pre-disturbance period and post-disturbance period (Figure 4.8). In the pre-disturbance period, low mud supply is added at the river boundary to simulate the natural conditions with minor human intervention, representing the situation before European settlement in New Zealand. In the post-disturbance period, mud supply at the river boundary instantaneously goes from low concentration to high concentration, representing the situation after European settlement (with deforestation and agricultural practices in the catchments). As the increased sediment caused muddy sediment accumulation in the estuaries (Jones, 2008), we also test the reverse: whether sand flats recover following a decrease of muddy sediment supply. Moreover, with the expectation that mangrove clearance will not immediately decrease the local mud fraction (Bulmer et al., 2017), we set up simulations to evaluate the role of

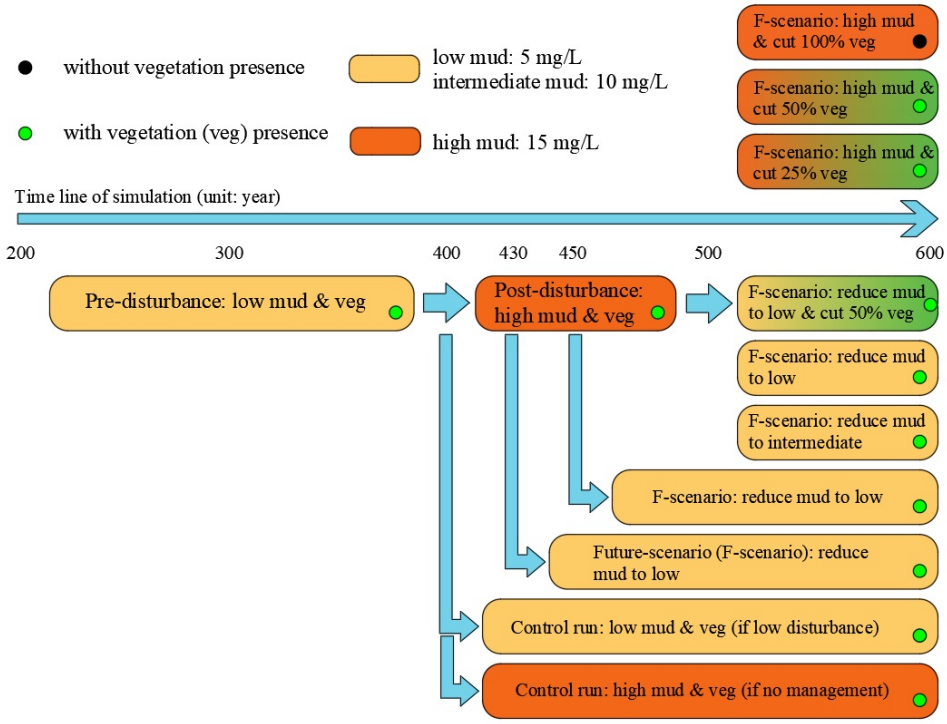

Figure 4.8 Flow chart of the design of model simulations. Light- and dark-brown color are used to highlight the sediment conditions of each river inflow: with low/intermediate mud and with high mud input. Vegetation presence is indicated by green dots on the bottom right of each box, while black dots indicate vegetation absence. Blue arrows show on which previous simulation result a scenario is started.

mangrove clearance on system changes. Eventually, a synthesis analysis is set up including the changes of muddy sediment supply and vegetation status.

4.5 Supplementary material

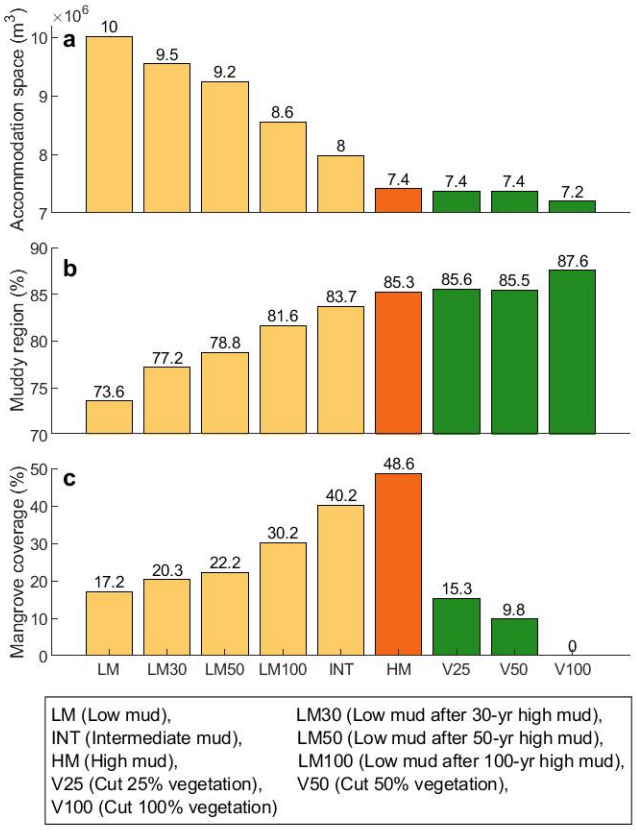

Figure 4.9 Values of main effect variables in scenarios of mud supply and mangrove removal at year 600. a) Accommodation space, b) muddy region fraction and c) vegetation coverage fraction. LM30 indicates that sediment supply was reduced to low mud levels after 30-years of high mud input during post-disturbance period.

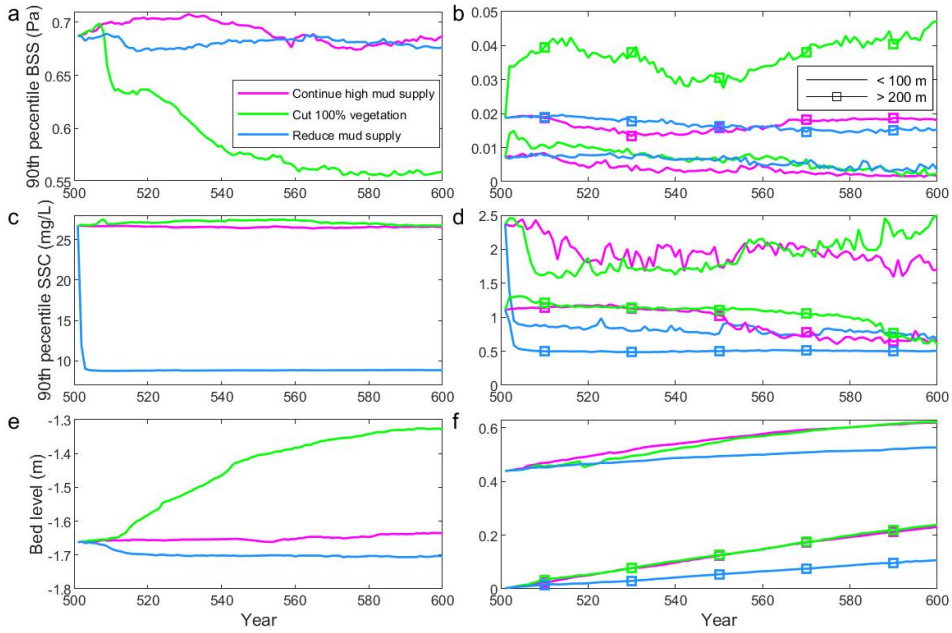

Figure 4.10 Temporal changes in 90th percentile bed shear stress (BSS), 90th percentile suspended sediment concentration (SSC) and bed level in future scenarios. The analysis is based on the southern reach of the system (see Figure 4.12) and further categorized as channel area (a,c&e) and tidal flat area (b,d&f). The tidal flat area is further divided into two regions, with one region close to the channel (< 100 m) and the other region further away from the channel (> 200 m). Comparisons of these three future scenarios are based on median values of each region (i.e. channel area, tidal flat area close to channels and tidal flat area further away from channels). In addition, integrate comparisons by considering all values of these regions are shown as box plots in Figure 4.11

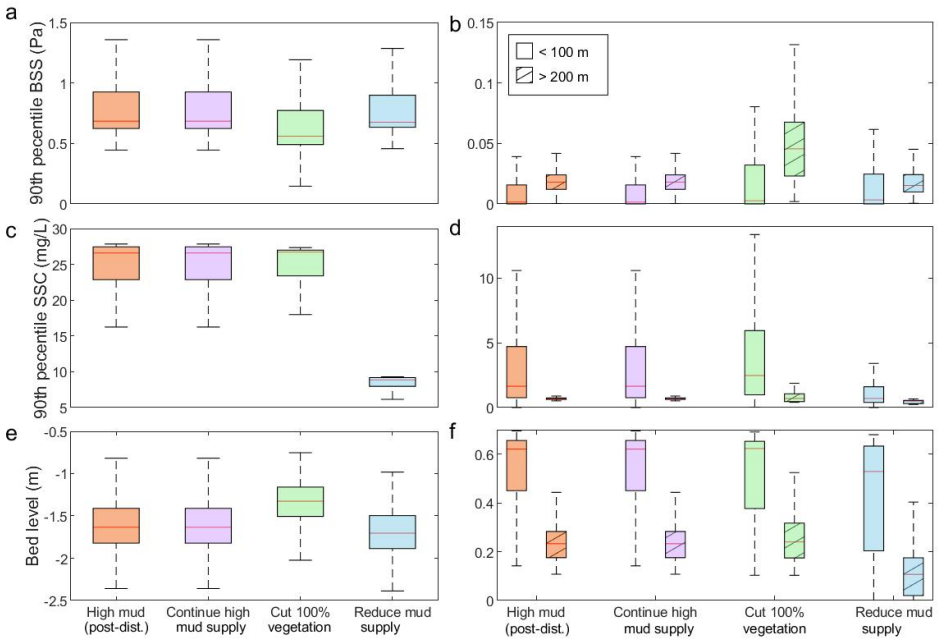

Figure 4.11 Comparisons of 90th percentile bed shear stress (BSS), 90th percentile suspended sediment concentration (SSC) and bed level in year 600. The comparisons are based on the region indicated in Figure 4.12

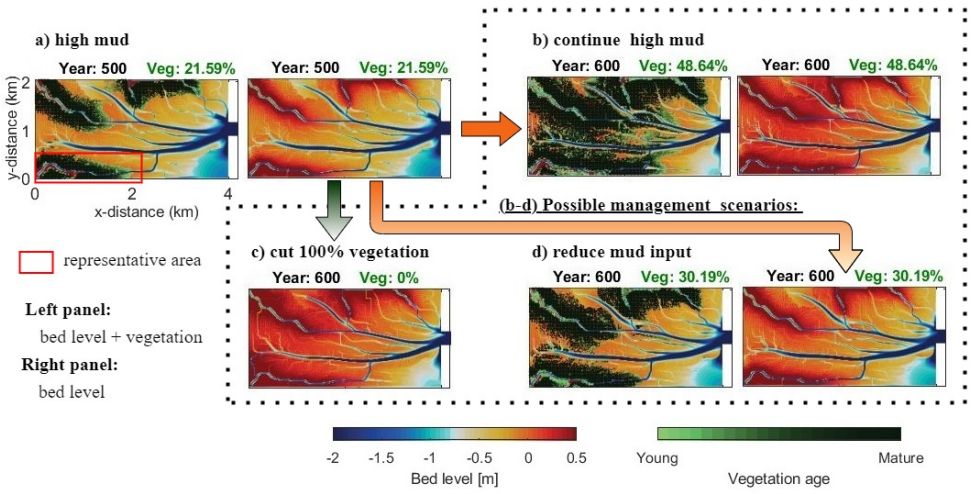

Figure 4.12 Representative area analyzing the changes of parameters in Figure 4.10 and Figure 4.11. Panel a, d&g contain two different panel, and the left panel shows the bed level and the presence of vegetation, while the right panel shows purely vegetation.

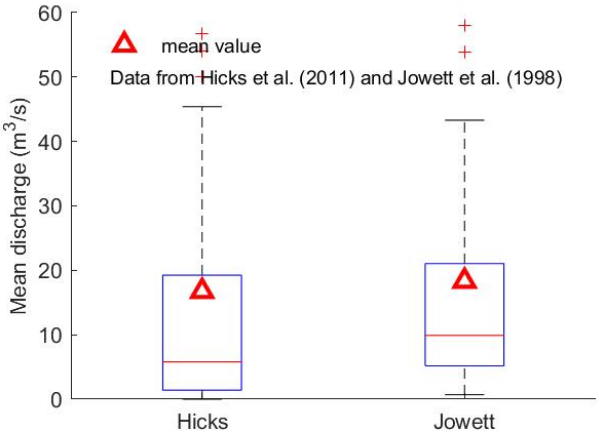

Figure 4.13 Statistics of river discharge from main rivers in North Island, New Zealand. Data source is based on Hicks et al. (2011) and Jowett (1998). Red triangles represent their mean value, which equal to 18 m^3/s. Data is summarized in Tables 4.1 & 4.2.

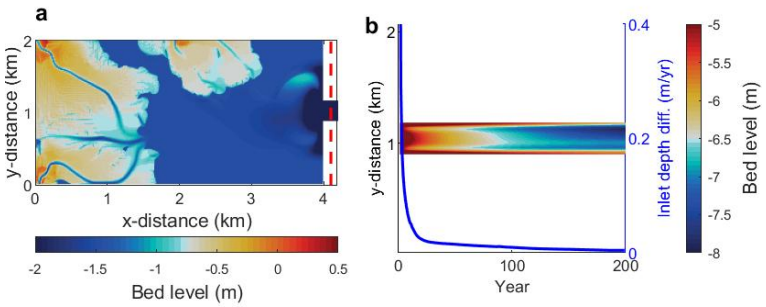

Figure 4.14 Basin morphology and inlet depth change during spinup period. a) Basin morphology at the end of the spinup period. The red dashed line indicates the transect across the basin in panel b). b) Bathymetry along the cross-sectional area at the inlet and annual difference of averaged inlet depth across the inlet section.

Table 4.1 Hydraulic characteristics of 73 New Zealand river reaches

No.	River	Q (m^3/s)	W (m)	No.	River	Q (m^3/s)	W (m)
1	Ahuriri	23.7	46.9	**38**	Oroua	11.2	20.8
2	Akatarawa	5.6	21	**39**	Otaki	28.1	34.6
3	Aorere	71.1	70.4	**40**	Otematata	7.6	27.2
4	Arnold	58	46.5	**41**	Patea	5.2	13.1
5	Baton	7.7	21.7	**42**	Pauatahanui	0.7	5.2
6	Buller	12.9	24.4	**43**	Pelorus	20.6	45.3
7	Clutha	203.6	88.4	**44**	Pohangina	17.3	27.9
8	Esk	5.5	16.4	**45**	Rai	17.5	29.5
9	Gowan	26.6	31	**46**	Rangitikei	20.1	43.2
10	Grey	53.8	77.4	**47**	Riwaka	2.5	15.4
11	Hakataramea	5.9	17.9	**48**	Ruabamanga	10.1	19.9
12	Hawea	80	37.6	**49**	Ruabamanga	22.5	39.9
13	Hurunui	25	40.4	**50**	Selwyn	3.4	18
14	Hutt	22.4	30.2	**51**	Shag	1.7	11.3
15	Inangahua	16.3	26.4	**52**	Stony	6.4	15.8
16	Kakanui	5.2	23.1	**53**	Taipo	43.3	42.2
17	Kapoaiaia	1.1	8.4	**54**	Takaka	14.9	33.7
18	Kapuni	1.8	12.4	**55**	Tauherenikau	9	23.2
19	Kauaeranga	6.5	33.6	**56**	Tauranga-Taupo	9.9	20.6
20	Kaupokonui	3.1	13.4	**57**	Tawhiti	0.7	4.8
21	Kopuaranga	2.6	8.4	**58**	Tongariro	11.6	34.3
22	Maerewhenua	3	14.9	**59**	Tutaekuri	16.1	35.8
23	Mangahao	15.3	37.2	**60**	Tongariro	32.2	42.6
24	Manganui	6.7	18.4	**61**	Waiari	4.2	9.8
25	Mangaoraka	2.1	13.7	**62**	Waihou	5.5	11.8
26	Mangatainoka	17.2	35.6	**63**	Waimana	7.6	28.4
27	Mangles	9.9	18.7	**64**	Waimakariri	5.1	11.9
28	Mararoa	34.2	36	**65**	Waingawa	10.4	22.2
29	Mataura	18.8	29.5	**66**	Waingongoro	2.7	11.9
30	Maowhango	4	16.4	**67**	Waiohine	31.2	47.6
31	Motueka	61	56.4	**68**	Waiongona	2.8	12.5
32	Ngaruroro	17.6	26.2	**69**	Wairoa (Auckland)	2.8	9.6
33	Ohau	6.4	27.8	**70**	Wairoa (Nelson)	16.5	30.7
34	Opihi	5.7	19.1	**71**	Waiwakaiho	7.8	20.8
35	Opihi	19	33.1	**72**	Wanganui	27.5	55
36	Orari	9.9	18.2	**73**	Whakatiki	1.7	13.4
37	Oreti	30.3	54.5	**Average:**		18.3	28.0

Note: Data is digitized from Jowett (1998). Q = Mean annual discharge. W = Width.

Table 4.2 River discharge records at Northisland Island sites

No.	River	Discharge (m^3/s)	No.	River	Discharge (m^3/s)
1	Awahou	1.7	**38**	Mokau	36.6
2	Awakino	12.7	**39**	Motu	91
3	Awanui	6.1	**40**	Motu	12.9
4	Awaroa	1	**41**	Ngarururoro	42.5
5	Esk	5.5	**42**	Ngarururoro	40.2
6	Hangaroa	16.5	**43**	Ngarururoro	16.9
7	Hautapu	4.5	**44**	Ngarururoro	39.3
8	Hinemaiaia	5.5	**45**	Ngongotaha	1.8
9	Hutt	7.6	**46**	Ohau	6.3
10	Kaiiwi	1.5	**47**	Ohinemuri	12.7
11	Kairuna	39	**48**	Omakere	0.9
12	Kaniwhaniwha	1.4	**49**	Ongarue	34.4
13	Kokopu	0.061	**50**	Orere	1
14	Kuratau	4.2	**51**	Oroua	11.3
15	Makohine	1.2	**52**	Otaka	2.8
16	Manawaru	103.4	**53**	Otaki	31.7
17	Manawatu	85.1	**54**	Otaki	29.3
18	Mangahao	6	**55**	Otane	0.162
19	Mangaheia	0.827	**56**	Otara	14.4
20	Mangakara	0.375	**57**	Oteke	0.304
21	Mangakino	11.4	**58**	Pahao	11.5
22	Mangakowhai	0.636	**59**	Pauatahanui	0.727
23	Manganui	1.5	**60**	Piako	1.7
24	Mangaokewa	5.3	**61**	Piako	7
25	Mangaonua	2.1	**62**	Pohangina	17.4
26	Mangatu	7.2	**63**	Pokaiwhenua	4.9
27	Mangawhai	0.069	**64**	Pomare	0.016
28	Mangawhero	13.7	**65**	Puarenga	1.7
29	Mangorewa	6.3	**66**	Punehu	1.1
30	Manukau	0.004	**67**	Puniu	15.8
31	Mara	15	**68**	Purukohokohu	0.006
32	Marokopa	4.3	**69**	Rangitaiki	54
33	Matahuru	1.92	**70**	Rangitaiki	21.6
34	Maungaparerua	0.446	**71**	Rangitikei	62.6
35	MillCreek	0.134	**72**	Rapurapu	0.889
36	Mohaka	38.4	**73**	Raukokore	30.6
37	Mohaka	80.7	**74**	Ruakokopatuna	0.694

(*Continued*)

(*Continued*)

No.	River	Discharge (m^3/s)
75	Ruarnahanga	81.1
76	Tahekenui	0.5
77	Tahunaatara	4.6
78	Tairua	5.9
79	Takaputahi	8.7
80	Tarawera	31.3
81	Taruarau	6.4
82	Taueru	6.6
83	Tauranga	0.086
84	Tauranga-Taupo	9.8
85	TeArai	2
86	TeTahi	0.155
87	Tongariro	27.9
88	Tongariro	41
89	Tongariro	11.9
90	Tukituki	45.4
91	Tukituki	11.6
92	Tutakina	9.4
93	Utuhina	0.199
94	Utuhina	2.1
95	Waiapu	86
96	Waiau	21.1
97	Waiaua	5
98	Waihaha	5.7
99	Waihi	1.9
100	Waihohonu	6.2
101	Waihou	26.4
102	Waihou	41.9
103	Waihou	41.8
104	Waihua	1.6
105	Waikohu	3.9
106	Waingaehe	0.239
107	Waingaromia	4.9
108	Waioeka	31.7
109	Waiohewa	0.344
110	Waiorongomai	0.435
111	Waiotahi	4
112	Waiotapu	1.4
113	Waiotapu	3.7
114	Waiowhiro	0.367
115	Waipa	13.5
116	Waipa	0.336
117	Waipa	86.6
118	Waipaoa	34.7
119	Waipaoa	33
120	Waipaoa	50.1
121	Waipaoa	3.2
122	Waipapa	1.55
123	Waipapa	5.63
124	Wairere	0.037
125	Wairnana	8.1
126	Wairoa	70.7
127	Waitangi	0.234
128	Waitangi	7.9
129	Waitara	33.7
130	Waiteti	1.3
131	Waitoa	5.3
132	Waitoa	3.5
133	Waitoa	1.6
134	Waitomo	1.9
135	Whakapapa	8.1
136	Whakapipi	0.918
137	Whakatane	56.7
138	Whangaehu	39.8
139	Whangaehu	0.529
140	Whangamarino	2.06
141	Whanganui	213.6
142	Whanganui	1.3
143	Whangapouri	0.05
144	Wharearna	6.6
145	Wharekahika	10.9
146	Wharekopae	3.9
147	Whenuakta	9.7
148	Whirinaki	14.8
Average		16.75

Note: Data is digitized from Hicks et al. (2011).

Table 4.3 Dynamic vegetation model parameter settings

Category	Parameter	Value	Unit	Reference
Vegetation parameters	Initial stem diameter, D_0	0.8	cm	Bulmer et al. (2017) and Suyadi et al. (2020)
	Maximum root number, $N_{roots,max}$	1000	-	Young and Harvey (1996) and Dahdouh-Guebas et al. (2007)
	Root diameter, D_{roots}	1	cm	van Maanen et al. (2015) and Xie et al. (2020)
	Root height, H_{roots}	15	cm	van Maanen et al. (2015) and Xie et al. (2020)
	Drag coefficient of roots, C_{Dr}	1	-	Xie et al. (2020) and Xie et al. (2022)
	Drag coefficient of stems, C_{Ds}	1.5	-	Xie et al. (2020) and Xie et al. (2022)
Growth parameters	Maximum stem diameter	18	cm	Bulmer et al. (2017) and Suyadi et al. (2020)
	Maximum tree height	320	cm	Bulmer et al. (2017) and Suyadi et al. (2020)
	Growth constant, G	36.88	cm/season	van Maanen et al. (2015) and Xie et al. (2020)
	Growth constant, b_2	31.94	-	van Maanen et al. (2015) and Xie et al. (2020)
	Growth constant, b_3	0.864	cm-1	van Maanen et al. (2015) and Xie et al. (2020)
	Roots formula constant, k	0.5	-	Xie et al. (2020)

Competing Interests

The authors declare no competing interests.

Data Availability Statement

The data regarding mean flow and width of New Zealand main rivers is available in Tables 4.1 & 4.2. Delft3D is an open-source code available online (at https://oss.deltares.nl). The dynamic vegetation code with a typical model setting is available at:
https://github.com/xiedanghan/MangroveVulnerabilityModel.

Chapter 5 | Synthesis

In this thesis, a novel bio-morphodynamic model has been presented that integrates the dynamics of mangrove forests with hydro-sedimentary processes involving so far neglected non-linear bio-physical interactions between vegetation with life-stage dependent traits (incl. colonization, growth and mortality process) and spatio-temporal variations in sediment transport and morphology. This model was used to achieve the following aims:
1) explore the role of non-linear bio-morphodynamic feedbacks in controlling mangrove system dynamics at different coastal environmental conditions, including tides, waves, sediment supply and coastal slope, and
2) create a better understanding of mangrove ecosystem response to changing boundary conditions due to sea-level rise and human interventions, with a particular emphasis on identifying the bio-geomorphic mechanisms that control system evolution over centuries.

In the following synthesis, present knowledge of mangrove ecosystems is reviewed and the novel contributions of this thesis are discussed. I will first discuss the role of bio-morphodynamic feedbacks on coastal wetlands, new insights on the impacts of sea-level rise and human activities, and set them into context to changes in accommodation space. Thereafter, I discuss challenges in model applicability by describing the type of systems that can be modelled, model robustness and how model simulations can inform coastal management. Additionally, I will explore limitations of this thesis and set the presented framework and modelling into a wider context. Finally, I answer the research questions posed in Chapter 1 and outline the conclusion of this thesis.

5.1 Physical and biological aspects of wetland response to sea-level rise

The rate of sea-level rise is projected to accelerate in the coming century while sediment supply to coasts and estuaries remain globally different (Syvitski et al., 2005; Hinkel et al., 2014). Although wetland vegetation, such as salt marshes and mangroves, may contribute to inorganic accretion and vertical organic expansion of the soil surface, there is increasing evidence that the sustainability of coastal wetlands is threatened by accelerating rates of sea-level rise (Lovelock et al., 2015; Woodroffe et al., 2016). Previously, various numerical models have been used to assess wetland vulnerability (Kirwan et al., 2016a; Spencer et al., 2016; Cahoon et al., 2020), but discrepancies emerged between predictions of different model approaches on whether coastal wetlands can maintain their relative elevation. For example, one side predicts that mangroves and salt marshes will be overwhelmed by accelerating sea-level rise (Crosby et al., 2016; Sasmito et al., 2016; Spencer et al., 2016), while others argue that future wetland vulnerability tends to be overestimated (Kirwan et al., 2016b; Schuerch et al., 2018). The uncertainties have been ascribed to key mechanisms controlling wetland persistence, in particular the failure to incorporate non-linear bio-physical interactions between vegetation, hydrodynamics and sediment transport (Woodroffe et al., 2016; FitzGerald and Hughes, 2019; Cahoon et al., 2020). Therefore, in this thesis, a numerical model incorporating detailed vegetation processes, comprehensive sediment transport processes, and morphological changes, has been developed to study the impacts of sea-level rise and human activity on mangrove survival.

Below, I discuss the main advancement on wetland understanding derived from model simulations carried out during this thesis.

5.1.1 Wetland resilience: from a physical perspective

Quantifying the amount of soil accretion at one specific location is important to assess the wetland resilience in the face of sea-level rise. Previous modelling studies on wetland vulnerability have quantified the vertical bed elevation changes proportional to water depth at high tide, a proxy for ground elevation or inundation duration and inundation frequency (Temmerman et al., 2003; D'Alpaos et al., 2007; Kirwan and Murray, 2007; Kirwan and Guntenspergen, 2010; Fu et al., 2019; Rietl et al., 2021). In such models, sedimentation rates are parameterized to increase with the rates of sea-level rise due to a prolonged inundation until the rates of sedimentation are identical to sea-level rise rates (Figure 5.1). The underlying assumption of these models are based on either a fully turbulent flow such that a prescribed sediment availability is assigned (D'Alpaos et al., 2007; Rodriguez et al., 2017), or a distance-based sediment availability such that sediment accretion reduces with the distance from sediment souces, such as adjacent channels or open waters (Furukawa and Wolanski, 1996; Fu et al., 2019). However, these assumptions simplify physical processes arising from the interactions between tidal current dynamics and sediment dynamics. As a result, not incorporating a more comprehensive treatment of hydro-sedimentary dynamics related to potential sediment erosion, deposition and transport during a tidal cycle may lead to either overestimation or underestimation of wetland surface elevation changes during sea-level rise. Recently, an increasing number of modelling studies simulate coastal landscapes by incorporating a broader range of dynamic feedbacks between wetland plants and coastal environmental changes (Mariotti and Canestrelli, 2017; Boechat Albernaz et al., 2020; Glover et al., 2022). This creates new opportunities and highlights the need to use such bio-morphodynamic models to explore mangrove dynamics.

The novel mangrove model coupled to the hydro-morphodynamic model Delft3D-Flow calculates the water level and velocity by solving the shallow water equations (conservation of mass and momentum) (Deltares, 2014). The presence of vegetation slows down tidal currents by adding an extra momentum resistance term and modifying the bed roughness (Baptist et al., 2007). Sediment transport is largely based on hydrodynamic conditions and treated according to sediment characteristics, i.e. cohesive or non-cohesive. For cohesive sediment particles (mud), erosion and deposition are estimated through the Partheniades-Krone formulations, and the transport of suspended sediment is calculated by the advection-diffusion equation. The sediment transport of non-cohesive sediment particles (sand) is estimated through the sediment transport predictor of van Rijn (van Rijn et al., 2004; van Rijn, 2007). Enhanced sedimentation may emerge as a response to extended inundation, which seems to be comparable with the results from previous wetland models assuming sedimentation is a function of the settling velocity, suspended sediment concentration and the time period of inundation (Figure 5.1) (D'Alpaos et al., 2007; Kirwan and Guntenspergen, 2010). However, the sedimentation is not specifically parameterized in relation to inundation periods. Rather, the results presented in this thesis show that sediment accretion may be decoupled from inundation time (Chapter 2), resulting in lower accretion rates even under a prolonged inundation period (Figure 2.4). This behaviour is therefore in contrast with established concepts on wetland resilience (Kirwan et al., 2010) and is initiated by the temporal changes in sediment delivery across the mangrove forest. Over time, advection of suspended material and erosion of bottom sediments diminish because tidal currents are being dissipated more strongly due to temporal changes in the forest extent (Figure 2.4). Thus, while inundation periods increase in the upper forest, accretion is hindered as sediment availability becomes limited (Figure 2.4p). This can in turn cause a shift in species occurrence because of temporal changes in inundation regimes (Figure 2.4d). The thesis results indicate that above-ground physical processes, in particular sediment dynamics, cause spatio-temporal variations in sediment accretion even under constant forcings, and these variations

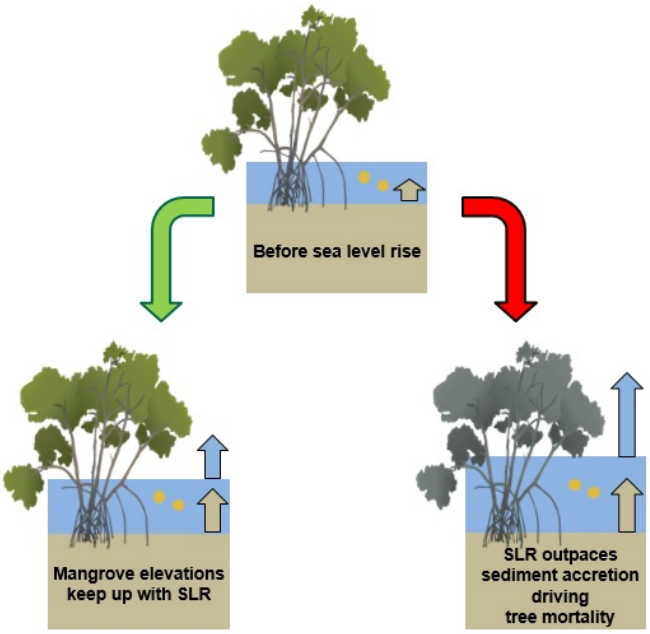

Figure 5.1 Vertical elevation change dynamics typically incorporated in wetland models. The sedimentation rates are parameterized as a function of inundation period, where extending inundation period may lead to increasing sediment accretion rates such that vegetation remains emerged, while vegetation may be submerged and die when sea-level rise (SLR) rates outpace sediment accretion rates.

are vital to assess mangrove vulnerability in the context of sea-level rise. The model simulations show such feedbacks can cause counterintuitive behaviours, where wetland accretion may fail to accelerate despite extended inundation driven by sea-level rise, and in the long term, changes in mangrove diversity can emerge. More importantly, such changes would not be captured by wetland models parameterizing sedimentation as a function of inundation period, therefore, a more comprehensive treatment of hydro-sedimentary processes as shown in this thesis should be considered when evaluating future coastal wetland evolution.

5.1.2 Wetland resilience: from a biological perspective

Impacts of vegetation on wetland morphology are mainly associated with soil structure and surface elevation change through organic matter accretion and inorganic sediment accumulation (Krauss et al., 2014; Cahoon et al., 2020). The modified wetland ecosystems in turn affect mangrove growth by creating a new habitat with changed surface elevation and inundation time (Woodroffe et al., 2016). In this thesis, mangrove establishment thresholds combined with growth trajectories are incorporated to investigate the responses of mangrove growth and geomorphic changes. Previous studies emphasize the contribution of organic matter accretion from mangroves to persist within the intertidal area (Krauss et al., 2014). Here in this thesis, Chapter 2 and Chapter 3 further illustrate that mangrove vulnerability to sea-level rise not only depends on the amount of external sediment supply, but is also determined by their own plant characteristics, such as the conditions of seedling establishment, the number of mangrove pneumatophores, and the optimal inundation period for vegetation growth.

In Chapter 2, different mangrove species with species-dependent optimal inundation regimes establish across the intertidal area, creating mangrove zonation with possibilities for different mangrove species to co-exist at the same area. If only the whole mangrove assemblage movement is tracked across the shore under the impacts of sea-level rise, mangrove behaviours are mainly determined by the balance between sediment supply and sea-level rise rates. For example, when landward habitat is available, increasing sea-level rise rate facilitates the landward migration of mangrove forests, resulting in a stable or even extended mangrove coverage. In contrast, enhanced sediment supply could stabilize the mangrove seaward edge and even lead to seaward propagation of mangrove forests, and eventually shaping an even extended mangrove coverage. These trends in terms of the whole mangrove forests movement under sea-level rise align with natural mangrove behaviours as reported in previous studies (Nardin et al., 2016b; Liu et al., 2018). However, the whole mangrove forest movement does not capture that there may be species-specific changes in cover within the system. That is, a reduction of one specific mangrove species may occur while the total mangrove coverage is extending (Figure 2.2). Since each mangrove species has their individual optimal inundation regime, they distribute across the tidal flats at different locations and potentially co-exist in some regions offering suitable inundation regimes for multiple species (Snedaker, 1982; Duke et al., 1998; Tomlinson, 2016; Fagherazzi et al., 2017). Chapter 2 illustrates that within mangrove assemblages, seaward mangrove species are the first to interact with hydrodynamics (e.g. tides and waves) and sediment transport, which would influence water movement and sediment reaching the upper land, and thus, the growth conditions of upper mangrove species. Due to the potential variations in the pneumatophore density across a mangrove forest, the resistance and friction generated by mangroves may vary with regions, exerting different effects on the hydro-sedimentary processes within the system. When seaward mangroves are characterized with dense roots limiting the hydrodynamic movement and sediment transport, less sediment from the sea can reach the upper land and more sediment would deposit on the seaward and middle regions of mangrove forests, reducing landward habitat accretion rates but extending the inundation regime as sea level rises. Such changes in the inundation regime allow those more water-tolerant mangrove species to colonize and dominate in this region, and eventually replace the original mangrove species in the upper intertidal area (Figure 2.4). As such, the thesis highlights that species interactions arising from the variations in soil accretion and inundation regime can be driven by vegetation's preference in inundation period and their pneumatophore density.

Successful mangrove seedling establishment requires suitable environmental conditions including 1) appropriate inundation regimes and 2) limited hydrodynamic forces (Balke et al., 2011). In addition to the restrictions by inundation regime (Chapter 2), an additional colonization threshold is included in the numerical model, i.e. hydrodynamic forces, below which mangrove seedlings can settle (Chapter 3). Such new model settings are applied to a broad range of environmental conditions, including different tidal ranges, waves, sediment supply and coastal slope. The results suggest that the elevation at which mangroves can colonize becomes higher as tidal range and sediment supply increase, elevating mangroves further above the mean water level (e.g. Figure 3.3k). In Chapter 3, I define this specific distance created during mangrove seedling colonization as an 'inundation buffer space', as mangroves colonize at a higher elevation with lower hydroperiod, and thus, they can remain emerged for a certain period of sea-level rise and even survive under fast sea-level rise with intermediate sediment supply for the simulation period explored in the study (e.g. Figure 3.5g&o). This finding implies that models without considering such processes could potentially overestimate mangrove vulnerability to sea-level rise, in particular in environments with strong hydrodynamic forces, such as macro-tidal systems or wave-active regions. Furthermore, it may also partly explain the reasons for the failure to restore mangrove ecosystems without considering the local hydrodynamic forces which could restrict the establishment of mangrove seedlings (Friess et al., 2012; Winterwerp et al., 2013).

In addition to mangrove seedling establishment, the model developed in the thesis also incorporated the self-thinning processes, implying a finite amount of resources available for mangrove growth, which further gets intensified under sustained stressful conditions. The self-thinning processes are incorporated through vegetation mortality to create space so that the impacts of vegetation on the hydro-sedimentary processes are eliminated. Tree mortality in the model occurs when 1) competition among trees is too large or 2) the inundation regime in the vegetated areas is no longer appropriate. As a result, the number of mangrove trees in seaward areas, where the inundation regime may be extended due to accelerating sea-level rise, can gradually reduce until the forest disappears. In the meanwhile, sea-level rise may create new landward habitats by flooding the upper land that was previously dry. The disappearance of seaward mangroves and appearance of landward seedlings due to sea-level rise provide an overall inland movement of mangrove forests (Figure 2.2). However, when seaward sedimentation is faster than rising sea levels, either due to the high sediment supply or dense vegetation densities, mangroves may expand in both seaward and landward directions (Figure 2.2). Thus, these distinct behaviours captured by the model developed in the thesis further highlight the necessity to incorporate interactions between vegetation and sediment transport so as to accurately predict wetland losses to sea-level rise (Cahoon et al., 2020).

5.1.3 Bio-morphodynamic feedbacks controlling wetland resilience disturbed by human activity

As discussed above, physical and biological processes are intrinsically linked resulting in bio-morphodynamic feedbacks that are crucial in driving system evolution. Physical processes relate to changes in hydrodynamic conditions, such as water level and velocity, which in turn affect geomorphological changes, including sediment erosion/deposition, sediment transport and profile evolution. The adjusted landscape subsequently modulates hydrodynamic processes, creating two-way interactions between hydrodynamic and morphodynamic changes, named as hydro-morphodynamic feedbacks (Coco and Murray, 2007; Coco et al., 2013). However, in coastal ecosystems vegetation (e.g. mangroves, salt marsh and seagrass), microphytobenthos (e.g. diatoms, flagellates and green algae) and macrobenthos (e.g. oyster, lobster and crabs) are common occurrences, which play a vital role in maintaining ecosystem functions including sediment mobility and eventually influence coastal morphology and thus ecosystem vulnerability to sea-level rise (Morris et al., 2002; Brückner et al., 2021). As such, this necessitates to consider effects of biological structures on physical processes and in wetland vulnerability assessments. Such interactions between physical processes and biological processes are referred to as bio-morphodynamic feedback (Murray et al., 2008; D'Alpaos, 2011; Kirwan et al., 2016b; Cahoon et al., 2020). For example, the model developed in this thesis accounting for such complex bio-morphodynamic feedbacks captures a spatio-temporal variation in sediment transport across mangrove forests driven by the expansion of mangrove vegetation, where sediment availability in upper intertidal areas gradually reduced, leading to a prolonged inundation and local mangrove mortality (Figure 2.4). This indicates the role of mangrove dynamics on sediment transport shaping the coastal profile, which in turn influences mangrove growth, highlighting the potential modulation on wetland vulnerability to sea-level rise arising from bio-morphodynamics.

Humans have a long history of influencing landscapes (Brierley, 2010). Over centuries humans not only adapt to the Earth's environment but at the same time modify the living conditions for food, water and other essential activities. Nearly half of the world's population lives close to the coastal area (Creel, 2003), physically transforming the coastal landscape through various activities (Goldberg et al., 2020), such as engineering constructions (Phan et al., 2015; Nienhuis et al., 2020), agriculture (Chong, 2006), deforestation (Restrepo et al., 2015; Hamilton and Friess, 2018) and other disturbances from related watershed areas (Syvitski et al., 2005; Kirwan et al., 2011). The importance of the two-way interactions between vegetation and morphodynamics has become widely recognized

over recent years, however, accounting for the role of humans in wetland modelling is arguable less well developed. To systematically evaluate future mangrove dynamics, the bio-morphodynamic feedbacks proposed in this thesis are not just limited in the scope of the mutual interactions between plants and hydro-morphodynamics, but also take into account the disturbance from human activity (Chapter 2 and Chapter 4). In Chapter 2, the responses of mangrove species to landward anthropogenic constructions (i.e. barriers) are investigated. The barriers are originally built to prevent sea water from flooding the hinterland due to sea-level rise or natural hazards, but they also constrain the potential landward habitats for the frontal vegetation, where rising sea levels may convert the previous supratidal area to intertidal area suitable for mangrove establishment. As a result, the prolonged inundation due to the increasing sea levels eventually drowns these mangroves and may cause extinction of some specific mangroves which can only grow under a certain hydroperiod (Figure 2.2b). The loss of mangrove species accompanying the mangrove diversity reduction not only reduces the ecological function, such as coastal protection, but also threaten the local ecological cycles and human livelihood as the provision of mangrove ecosystem services is highly species-dependent (Duke et al., 2007; Polidoro et al., 2010). For those coastal systems with limited sediment supply, especially in micro-tidal range systems, mangroves are more vulnerable to sea-level rise as landward migration occurs as soon as the water level increases (Chapter 3). Therefore, given the extreme vulnerability of mangroves in micro-tidal range systems, promoting sediment delivery to coastal systems and creating the possibility for mangroves to move upland by displacing human-made barriers are proved to be crucial to safeguard mangrove survival.

Apart from the coastal constructions limiting potential mangrove landward habitats, coastal landscapes have been observed to be transformed through human activities in upstream watersheds. Historically, colonial settlements (such as European settlement) were often based on sites close to rivers followed with natural resource exploitation, such as deforestation, pastel or agriculture (van der Werf et al., 2020). These disturbances from the upstream environment are often associated with increasing sediment loss, with more sediment transported through river flows and deposited in the affiliated estuary systems (Syvitski et al., 2005). Such a large sediment supply not only threatens the marine biology due to the increased water turbidity, but also physically transforms local ecosystems with changes in vegetation coverage, such as mangrove and salt marsh expansion in New Zealand (Swales et al., 2007; Horstman et al., 2018b) and North America (Kirwan et al., 2011). Although coastal restoration projects have been developed for several decades, the approach to efficiently recovering previous coastal environments varies with coastal systems. In New Zealand, mangrove removal is conducted with a desire to reduce muddy regions but the likelihood of a successful mud reduction through this management strategy remains unknown (Bulmer et al., 2017). The current muddy environment in the North Island estuaries, New Zealand, was modelled in an idealized setup for projections on several different management strategies that could be conducted in the future (Chapter 4). This study highlights that current management strategies, i.e. mangrove removal, may not contribute to addressing muddy situations in New Zealand (Figure 4.4). Instead, the systems may become even more infilled due to vegetation clearance. This has been ascribed to the impacts of bio-morphodynamic feedbacks, where limited sediment is able to reach the more distant tidal flats and currents are mainly concentrated in the channels when vegetation is present. However, the removal of vegetation diverges the flow and slows down the currents in the channels and allows mud to reach tidal flats further away from channels, leading to a shallower channel and elevating tidal flats. This finding aligns with previous studies where vegetation removal including salt marsh and riparian trees leads to higher sediment concentration in rivers, channels and the floodplains (Temmerman et al., 2012; van Oorschot et al., 2016; Kleinhans et al., 2018). In the end, the modelling shows that reducing fluvial mud supply is more effective to mitigate the mud accumulation in estuary than mangrove removal (Figure 4.4).

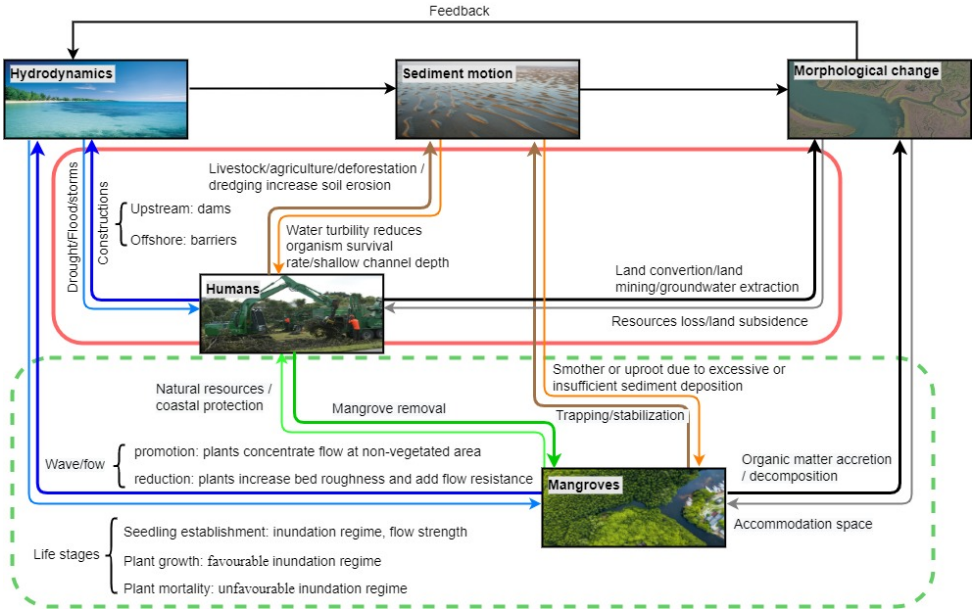

Figure 5.2 A framework of bio-morphodynamic models taking human interventions and biophysical processes into account.

Human impacts on bio-morphodynamic feedbacks govern coastal wetland evolution. In addition to typical two-way bio-physical interactions between hydro-morphodynamics and vegetation dynamics, humans are influencing the coastal wetland through both physical processes and biological processes (Figure 5.2). Coastal engineering structures are created to protect human life and assets from the threat of storms, waves and sea-level rise, but at the same time these structures set up an immovable boundary constraining the potential landward movement of vegetation in response to sea-level rise, and thus, reducing the ecosystem biodiversity (Chapter 2). Similarly, fluvial dams are increasingly constructed or to be constructed in the near future in order to reduce flooding risk and manage water resources (Zarfl et al., 2015), sediment supply from upstream sources is declining at both the continental scale (Weston, 2014) and global scale (Syvitski et al., 2005). In Chapter 2 and Chapter 3, sediment supply and available landward habitat spaces are emphasized to keep mangrove persistence with sea-level rise, which are also the main suggestions from recent studies on mangrove vulnerability assessment (Lovelock et al., 2015; Schuerch et al., 2018). Different from these constructions mentioned above, which tend to reduce flow and sediment availability to the coastal systems, humans may also enhance sediment concentration in the river flow as soil erosion is facilitated due to various activities such as deforestation, agriculture and livestock in the upstream or associated catchment area (Kirwan et al., 2011). Such high mud input from river systems enhances water turbidity and estuarine sedimentation rates, which shallows the channels and leads to a high mud cover with fast vegetation coverage changes. The presence of vegetation subsequently dampens hydrodynamic forces and stabilizes mud from erosion, making the system even muddier and constraining human recreations and livings (Jones, 2008). The underlying mechanisms of enhanced sediment infilling in estuarine systems are analyzed in Chapter 4, indicating that human activity in upstream catchments physically transforms landscapes further downstream, both in terms of morphology and ecology (Figure 5.2). At the same time, humans can also directly influence mangrove surface elevation through land mining or groundwater extraction, causing subsidence of

the soil surface and thus reducing the capability of mangroves to keep pace with sea-level rise (Cahoon and Lynch, 1997; Minderhoud et al., 2018; McKee et al., 2021). When the goal is to make room from coastal space for other activities, humans also conduct land conversion activities by removing existing vegetation, such as salt marsh (Temmerman et al., 2012). Similarly, in Chapter 4, the loss of mangroves removed by humans is investigated to inform society and policymakers that sediment redistribution is possible after vegetation disappearance, and the channel can become shallower due to the reduction in hydrodynamic forces (Figure 4.4).

Wetland models predicting vegetation vulnerability have been increasingly requested to include a detailed description of the bio-morphodynamic feedback loop to avoid inaccurate wetland behavior projections, based on which the policy and coastal management can be well developed (Friess et al., 2019; Cahoon et al., 2020). Given the continually increasing human interference in coastal ecosystems, in this thesis, I demonstrated the need to consider human activity within the bio-morphodynamic feedback loop to achieve a more complete perspective on interactions between components occurring within coastal ecosystems, and subsequently provide better predictions on future mangrove vulnerability in response to sea-level rise.

5.1.4 Changes of accommodation space controlled by bio-morphodynamic feedbacks

Accommodation space was first explicitly defined by Jervey (1988) as a space where sediment accumulates and is highly determined by subsidence, sedimentation and eustatic sea-level rise. It is originally a geologic concept but has been integrated with ecological processes such that mangrove dynamics in response to the future sea-level rise can be studied (Rogers, 2021). Accommodation space contains both vertical and lateral dimensions, and sea-level rise is able to increase both dimensions and subsequently influence mangrove distribution as mangroves are situated within a small component of accommodation space in the upper intertidal area (Schuerch et al., 2018). In this thesis, accommodation space determining mangrove resilience is demonstrated to be adjusted by bio-morphodynamic feedback.

Whether accommodation space needs to be infilled to allow mangrove establishment has been discussed in recent studies (Törnqvist et al., 2019; Schuerch et al., 2020). From a geologic view, the creation of accommodation space usually accompanies a retreating shoreline unless there is an increase in sediment supply, thus, it may not possible for mangroves to gain coverage without completely infilling the accommodation space driven by a large amount of sediment supply (Figure 5.3a) (Törnqvist et al., 2019). In other words, the increase of mangrove coverage through infilling accommodation space is highly dependent on sediment supply. However, this conclusion is based on the assumption that all vegetation is colonized at a single elevation above mean water level, without considering the fact that vegetation can exist within a range of elevation due to their biological characteristics. Actually, mangroves can grow within a range of hydroperiod, together with coastal slope and tidal range, which forms a gradual variation in inundation pattern along the tidal flats (Chapman, 1976; Kumbier et al., 2021). Especially for the upper intertidal areas, which are converted to wetlands as sea level rises, mangrove establishment can already occur before the available accommodation space is completely infilled by sediment (Figure 5.3b). This has been shown in both Chapter 2 and Chapter 3 in which mangrove coverage remains stable with a limited sediment supply. In addition, present model simulations suggest that mangrove landward expansion is possible with less or no sediment input as long as landward accommodation space is available (Figure 5.3c). Such mangrove inland migration is only driven by the conversion of terrestrial vegetation/land to a newly created mangrove habitat due to sea-level rise, particularly in micro-tidal range systems where mangrove retreat occurs directly when sea level rises without causing evident profile changes (Figure 3.5). This emphasizes again the importance of potential landward habitat resources on preserving total mangrove forests and further implies that dramatic mangrove coverage loss may

occur when inland migration is inhibited by natural or human barriers (Chapter 2). In the meanwhile, Chapter 3 further complements sediment infilling patterns of accommodation space, suggesting that erosion or reconfiguration of the lower coastal profile can compensate for the sediment needed to fill in the accommodation space such that mangrove inland migration may occur and even the whole mangrove coverage may extend (Figure 5.3d). This finding relevant for mangrove existence is ascribed to the non-linear approach that the thesis adopted, which accounts for complex bio-morphodynamic feedbacks allowing profile changes dynamically driven by sediment transport, and mangrove resilience is enhanced through bio-physical processes considering sediment transport and morphological changes (Figure 3.11) (Krauss et al., 2014). Thus, the thesis suggests that applying accommodation space as a framework for assessing mangrove vulnerability to sea-level rise necessitates a consideration of the complex bio-morphodynamic feedbacks (Rogers, 2021).

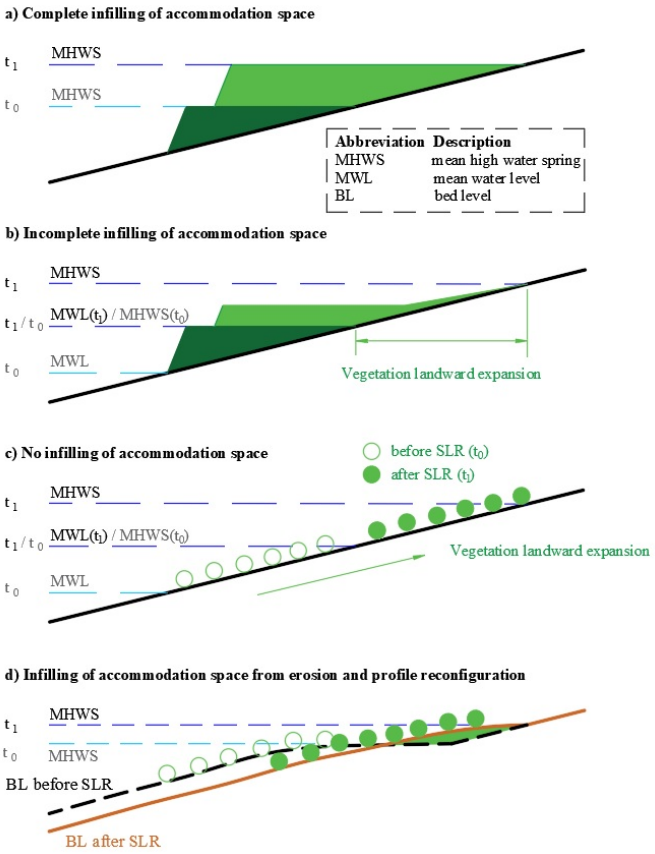

Figure 5.3 Different infilling patterns of accommodation space. a) Mangrove landward migration requires increasing sediment supply (Törnqvist et al., 2019); b) Mangrove landward migration based on less sediment import (Schuerch et al., 2020); c) No sediment infilling of accommodation space and d) infilling accommodation space from erosion and reconfiguration of the lower coastal profile. Here, completely infilling means the available accommodation space is completely filled by sediment, leading to wetland elevation reaching the Mean High Water Spring level (MHWS), while incomplete infilling means the elevation of wetland area does not need to reach MHWS such that less sediment is needed.

5.2 Model applicability for real systems

Wetland models with different levels of simplifications and processes of interest have been developed to investigate vegetation vulnerability in the face of sea-level rise, ranging from simple empirical models to complex process-based models that include highly non-linear interactions between hydrodynamics, morphological changes and vegetation dynamics (Fagherazzi et al., 2012; van Maanen et al., 2015; Cahoon et al., 2020; Gijsman et al., 2021). The type of model selected for one particular research is highly related to the purpose of the research (Murray, 2013). Previously, to unravel the underlying mechanisms, studies are often based on simple models with a minimum number of processes that lead to the observed behavior (Traill et al., 2010; Passeri et al., 2015; Menendez et al., 2018). Nowadays, more complex wetland models are developed that couple comprehensive hydro-sedimentary processes with vegetation dynamics (van Maanen et al., 2013; van Maanen et al., 2015; Mariotti and Canestrelli, 2017; Schwarz et al., 2018). These models are typically processed through idealized numerical simulations with simplified initial and boundary conditions. Although the use of such models has indeed become an integral part of bio-geomorphological research, interpreting the results and identifying the key processes that lead to the simulated behavior becomes increasingly difficult.

In this thesis, the results are based on a complex numerical model approach involving non-linear bio-morphodynamic feedbacks, but the modelling studies are based on conceptual domains. Both Chapter 2 and Chapter 3 investigate mangrove vulnerability under a broad range of coastal environmental conditions covering different tidal ranges, waves, sediment supply and coastal slopes. Considering the number of scenarios that needs to be tested, it is easier to conduct a systematic analysis under simplified model set-ups similar to previous research (Roberts et al., 2000). Such model settings are believed to have a better interpretation of model results by simplifying initial and boundary conditions (van der Wegen et al., 2011), while the application of current framework in real systems requests a more detailed model setup and calibration. Therefore, below I will discuss some trade-offs to contextualize my modelling approach and its implications for coastal management.

5.2.1 Model applicability in specific real systems

Idealized simulations are conducted in Chapter 2 and Chapter 3 based on a one-dimensional coastal profile, intrinsically excluding certain morphological features observed in nature such as channel networks, or estuarine environments and are therefore not strictly applicable to such systems. Since river discharge is not included in these two model studies, the results are more representative of mangrove systems located in open coast systems, broad embayments or tidal dominated deltaic environments, such as the Suriname coast (de Jong et al., 2021), Firth of Thames (Swales et al., 2007) and the Mekong Delta (Nardin et al., 2016b). In Chapter 4, although the research is representative of the North Island Estuaries in New Zealand, a two-dimensional idealized domain including the impacts of both tidal currents and river flow is applied to explore sediment distribution and morphological evolution driven by the changes in sediment supply and vegetation coverage. These models are all based on complex bio-morphodynamic feedbacks between vegetation dynamics and morphological changes, but at the same time, driven by simplified initial settings and boundary conditions, such as idealized initial bathymetry, constant sediment supply and periodic tidal cycle. Thus, whether it is possible to use such models to simulate real coastal systems remains a question.

Real coastal systems are shaped by both the internal processes (physical, chemical, biological, etc.) and the external drivers (primarily climatic and anthropogenic) from a broad range of spatial and temporal scales (Coco et al., 2013; Zhou et al., 2017). Variations in external forcing (e.g. tides, waves, sediment supply and extreme events), geologic controls and human perturbations complicate the system evolution. The highly non-linear and intertwined processes constrain the ability of numerical models to predict the same changes in the coastal system. Thus, it is not likely for one wetland model

to interpret the mechanisms behind the complex system behaviors considering all internal and external processes. Yet this does not mean numerical models contribute nothing to understanding feedbacks controlling coastal evolution. Instead, models are a useful tool to address hydrodynamic and morphodynamic behaviours of coastal systems over time (van der Wegen et al., 2011), which then are applied to inform the design of engineering and management actions (Zhou et al., 2017). Numerical models are often designed under different degrees of simplifications on processes that affect the behaviour of the system (Murray, 2013). Models aiming to gain a deeper insight into the role of individual process and interactions often rely on simplifications of the real processes so that the basic behaviour of a system can be captured. However, to reproduce the natural behaviour of a coastal system as accurately as possible, from the scope of this thesis study, some additional steps should be further improved to make the model outcome more representative to the real system behaviours. For example, including a detailed description of external forcing, a refinement of process formulation, or additional model variations may lead to a better model performance compared with the real situation (van der Wegen et al., 2011). In Chapter 3, comparisons between scenarios with only tides and scenarios with both tides and small wind waves highlight an addition of another external forcing (i.e. wind waves) can lead to significant differences in morphological changes and mangrove behaviours (Figure 3.3). The periodic tidal signal adopted on the seaward boundary (i.e. S2 tidal cycle) may fail to represent the real hydrodynamic condition, which then could lead to inaccurate estimations on sediment transport. In real coastal systems, the tidal signal can be more dynamic including both spring and neap tides, which show different capabilities on transporting sediment along intertidal areas (Goodwin and Mudd, 2019). Some other important factors such as the impacts of spatial and temporal scales should also be considered, which influence the credibility of the model outcome (Coco et al., 2013). For example, extreme events such as storms or El Niño climatic events disturb the system in a time scale of the order of months to years, while morphological evolution responses to the coastal environment conditions in centuries or even longer. A longer time scale or a larger research area often relies on a certain number of reduction/simplification of processes and factors so that the simulation can be feasibly modelled. Therefore, although the bio-morphodynamic model developed in this thesis presents a tool to quantify mangrove dynamics and coastal morphological changes, the model application in real estuary systems is highly dependent on the objective of the project and the scale of interest.

5.2.2 Implications for coastal management

Nowadays, protecting mangrove forests and restoring their ecosystems are considered as one of the primary tasks of a number of large international conservation initiatives, such as the International Blue Carbon Initiative and the Global Mangrove Alliance (Friess and Sidik, 2020; Spalding and Leal, 2021). Governments also realize the value of mangrove forests, with an increasing number of projects launched to restore mangroves in coastal areas, such as Indonesia, Vietnam and Malaysia, however, the conservation success is regionally variable (Ellison, 2000; Spalding and Leal, 2021). For example, although in east Asia mangrove extent remains relatively stable, some countries, such as Myanmar and Malaysia, they still suffer from an annual average loss rate of 0.41%-0.70% per year, which is substantially above the global average loss rate (0.16%) (Friess et al., 2019). Considering the projected 1-2 m sea-level rise by the end of this century and the increasing human interventions on land uses (Syvitski et al., 2005; Hinkel et al., 2014; Goldberg et al., 2020), mangrove conservation, restoration and management are suggested to be conducted through an interdisciplinary approach (Friess et al., 2019). The modelling in this thesis suggests implications for future coastal management.

First, removing unnecessary coastal barriers (i.e. landward flood protection constructions) to create available landward accommodation space for mangrove inland migration can mitigate the loss of mangrove coverage and mangrove diversity (Chapter 2). Coastal engineering structures have been globally constructed to protect the coasts since the twentieth century at the expense of wetland spaces

(Li et al., 2018). However, many structures have become abandoned due to the propagation of coastal lines and new constructions are consistently created seaward, leading to a further squeezed wetland space over time (Winterwerp et al., 2020). When the previous coastal structures already provide sufficient flood protection for the hinterland, creating new coastal barriers seaward could limit the potential inland migration of mangrove trees due to sea-level rise. Regarding the economic aspect, it costs even more to restore coastal wetlands than to conserve them, without considering the potential social and economic functions of the coastal wetland. Actually, wetland plants, such as mangroves, salt marsh and seagrass produce sufficient and efficient coastal protection to slow down tidal currents and dampen waves, mitigating the damage to coastal areas from natural disasters. Globally, mangroves protect around 15 million people from flooding and provide more than US 65 billion in flood protection benefits every year (Menéndez et al., 2020). Such nature-based solutions to protect people from climate change through ecosystems are globally recognized and increasingly prominent in the climate change policy, especially in developing countries (Seddon et al., 2020). The magnitude of the protection offered by the coastal ecosystem is highly related to the wetland coverage. For example, 100-m dense mangroves can reduce 90% tsunami pressure (Tanaka et al., 2007), and a 7-km wide strip of mangroves can reduce 70% of wave height during hurricanes (Zhang et al., 2012a). Increasing wetland coverage can further enhance the protection efficiency (Van Coppenolle et al., 2018), while in Chapter 2 and Chapter 3, both of landward accommodation space and sediment availability are critical to preserve existing mangrove coverage or to extend their distribution. Considering the significant role of mangroves on carbon storage and biodiversity conservation, it is efficient and economical to maintain current mangrove coverage, and remove the unnecessary landward structures which limit mangrove landward migration in the context of sea-level rise.

Second, creating calm hydrodynamic conditions for mangrove seedling establishment can facilitate mangrove expansion. Inundation regime has been identified as a key factor determining where mangroves can colonize (Kumbier et al., 2021), previous flume experiments further highlights the impacts of bed shear stress on the survival of mangrove seedlings (Balke et al., 2011), which then influence whether mangrove restoration would be successful or not (Friess et al., 2012). Such constrictions allow mangrove seedlings to only colonize at locations where both inundation regime and hydrodynamic forces are suitable for seedling establishment are called windows of opportunity (Balke et al., 2011). In micro-tidal range systems or systems under limited wave impacts, the location of pioneer mangroves is closer to mean water level (Figure 3.18). However, pioneer mangrove elevation increases with tidal range due to the strong hydrodynamic forces close to the mean water level, causing non-vegetated flats even though the inundation regime is appropriate (Figure 3.9). Currently, many structures have been installed seaward to dampen waves and strong tidal currents, such as bamboo fences and some dams, creating calm hydrodynamic conditions for mangrove seedling establishment, and at the same time, facilitating sediment settling (Winterwerp et al., 2020). Instead of completely isolating mangroves from water, these structures allow sediment to be transported toward the coast and mangroves and at the same time dampen waves and currents creating a relatively calm hydrodynamic environment. As a result, mangrove seedlings are able to colonize more seaward and further offer extra flow resistance when they become mature. Of course, there are limitations, for example, the bamboo fence can be decomposed into debris shortly after locating on sites, threatening the mangrove seedlings, fisherman activity and ship navigation (Pranchai et al., 2019). However, under some protection cover, the lifetime of a bamboo fence can be increased, and considering it is cheaper than other permanent constructions, for management with limited budget, this turns out to be a better approach for mangrove seedling protection (Winterwerp et al., 2020).

Third, increasing sediment availability in the coastal area to create extra seaward habitats for mangrove establishment is also a way to preserve or increase mangrove coverage (Chapter 2). However, the contribution of sediment supply to elevating surface elevation varies with mangrove

systems depending on local environmental conditions, including sea-level rise rates, tidal ranges and waves (Chapter 3). Mangroves in the micro-tidal range systems are found more vulnerable to sea-level rise as mangrove inland migration occurs as soon as sea level rises despite the amount of sediment supply. Similarly, when the sea-level rise rate is fast, mangrove landward migration becomes unstoppable in all coastal environment conditions except where a barrier is in place (Figure 3.5). Thus, when mangroves are in micro-tidal systems, keeping landward accommodation space unobstructed seems to be the only way to sustain local mangrove coverage. On the contrary, in the systems with larger tidal range or small wind waves, sufficient sediment supply under a slow or intermediate sea-level rise rate can even extend the whole mangrove forests by generating seaward mangrove habitats, and thus, removing landward structures seems not necessary if the goal is to maintain the present mangrove coverage (Figure 3.5). In a word, coastal conditions are playing a key role in determining how mangroves respond to sea-level rise.

Finally, preventing erosion of soils upstream of coastal wetlands to avoid sediment oversupply in the associated estuary system such that the physically transformation of coastal landscape can be prevented, for example, from sandy flats to muddy flats (Chapter 4). This seems to be a paradox from decreasing sediment supplies described above. As previously highlighted, sediment supply is important for mangrove surface elevation accumulation under sea-level rise. In some areas, however, the conservation of mangrove forests may only need a little sediment supply because their below-ground biomass accumulation can already compensate for the elevation deficit so as to keep pace with sea-level rise in the first several decades (Krauss et al., 2014). Oversupply of sediment from fluvial systems, especially the mud contents, would not only increase water turbidity at the coasts threatening the survival of underwater organisms, but also increase the mud content on the flats transforming the landscape ecosystem, thus, stimulating vegetation propagation which then further stabilize mud sediment in the system (Jones, 2008; Kirwan et al., 2011). In addition to natural triggers, such as landslides or rainstorms, human actions leading to sediment oversupply in estuaries are mainly driven by the conversion of upstream land resources (e.g. urbanization, agriculture, livestock and deforestation) (Kemp et al., 2020). These activities provide food, water, and other essential living products and activities for humans, but at the same time, the long-term unsustainable exploitation on land resources has ongoing negative impacts on the coastal ecosystems which will in turn influence human life (Figure 5.2). Considering the costs and efforts on the approaches to reduce local mud capture and restore sand flats can be high, which may end up with likely failure, therefore, it is better to take action as early as possible to mitigate sediment oversupply as a result of unsustainable human activities to avoid irreversible changes to coastal landscape development. Moreover, it remains controversial for upstream activities cause a great fluvial sediment import in the estuary. On one hand, such a larger mangrove expansion could enhance the function and services provided by mangrove forests, providing positive feedback to the society; on the other hand, the shrink or disappearance of other ecosystems due to the colonial of mangrove forests or the shifting of inappropriate environmental conditions exerts negative impacts to the society. For these reasons, how to evaluate mangrove expansion due to increasing fine sediment import depends on the demand of humans.

5.3 Future perspectives

In this thesis, I predominantly focused on the interactions between mangroves and their surrounding environment, including hydrodynamic forces, sediment transport and morphological changes, with a particular interest in the context of sea-level rise and human interventions. Non-linearly bio-physical interactions between mangroves are increasingly emphasized when estimating mangrove vulnerability (Cahoon et al., 2020). Here, a comprehensive wetland model involving non-linear

bio-morphodynamic feedbacks is applied to study mangrove vulnerability, compared to the natural mangrove systems, the simplifications of some key processes designed in this model may limit the model accuracy to present natural mangrove behaviors. Thus, these key processes clearly need further investigation and considered thoroughly in future research. Below I discuss five important processes that have not been included in the model yet but may influence future mangrove development, which are: (1) incorporating interactions between mangroves and waves, (2) testing the effects of boundary condition variations, (3) implementing organic matter contribution, (4) considering the impacts of mangrove and salt marsh ecotone and (5) improving theories controlling mangrove life stages.

5.3.1 Incorporating interactions between mangroves and waves

Although waves are taken into account in the model (Chapter 3), which exert extra bed sear stress enhancing sediment resuspension, only small wind waves were incorporated and the attenuation of waves due to the presence of vegetation is neglected. In this case, Chapter 3 may overestimate the role of waves on morphological changes and mangrove dynamics. Although such a small wave height, 5 cm, has been observed and studied in various mangrove sites (Horstman et al., 2014), it is also common to see mangroves grow in more energetic environments with a larger wave height, which means the thesis fails to cover a full picture of mangrove dynamics under wave environments. By applying different wave heights ranging from 0.3 m to 1.0 m using the same wave approach (roller model), the seaward propagation of the mangrove profile tends to reduce by increasing wave height, and a large wave height can even cause sediment erosion which eventually forms a steep coastal slope in the intertidal area (Belonje, 2019). This highlights the potential contrasting mangrove and morphology behaviors when wave height increases, such as storm waves. Previous numerical and experimental studies indicated that mangroves can attenuate waves by 20% to 60%, and the attenuation is more evident when wave heights are large (Phan et al., 2019) or when in micro-tidal systems where the water depth is shallow (Parvathy and Bhaskaran, 2017). Thus, to accurately capture the impacts of waves on mangrove dynamics and related effects on morphological changes, in particular in micro-tidal systems with large wave heights, the interactions between waves and vegetation should be taken into account.

The same approach can be adopted following previous studies considering the dissipation of waves by vegetation, such as salt marsh and alga (Suzuki et al., 2012; Zhou et al., 2016; Willemsen et al., 2022). Calibration is needed before these approaches are formally applied in mangrove systems as mangroves are commonly characterized by numerous pneumatophores or other types of root structures (Chapman, 1976). Compared to the Roller model conducted in Chapter 3, other complex wave models such as SWAN or MIKE-21 may significantly increase the time calculating the morphological changes and vegetation dynamics, especially when the goal is to investigate the long-term system behaviors with a large scale experimental domain (van der Wegen et al., 2017). Therefore, it would be worthwhile to systematically evaluate the calculation efficiency before the more comprehensive approach is adopted in the research.

5.3.2 Testing the effects of variations in boundary condition

Boundary conditions, such as river discharge, tidal range and sediment supply, applied in the models in this thesis as well as in many other wetland studies are kept constant overtime to reduce model complexity (Kirwan and Guntenspergen, 2010; Lovelock et al., 2015; Kirwan et al., 2016a; Zhou et al., 2016). However, adding a more detailed description of the hydrodynamic forcing (e.g. a full tidal signal or river discharge with multiple peak flows) or a calibrated sediment supply process would probably lead to an improvement in model results (van der Wegen et al., 2011). For example, constant river discharge is a suitable choice in morphological simulations when the river discharge is relatively small (compared to the tidal volume), as is the situation in Chapter 4, but the extension of the model to a larger river discharge system is suggested to consider the seasonality of river discharge such that a representative morphology can be reached (Guo et al., 2015). In addition, the spatial distribution of

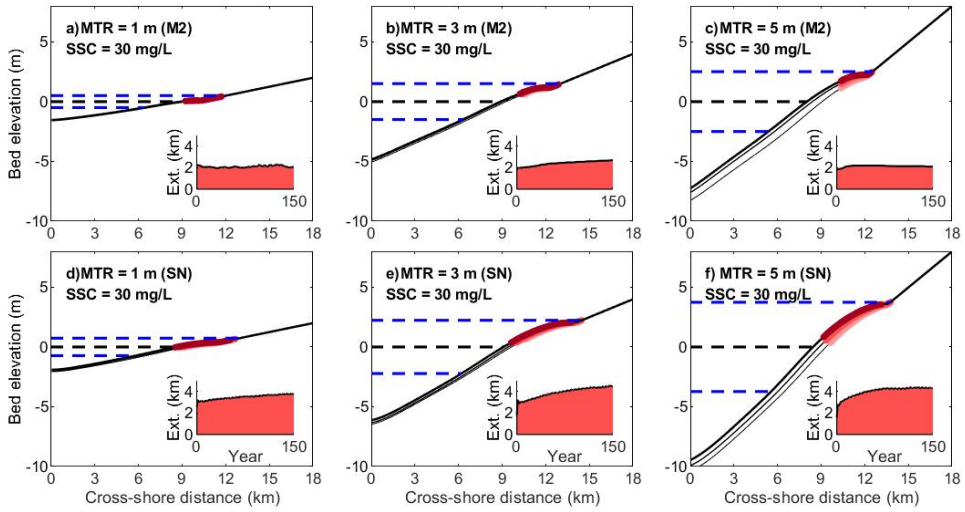

Figure 5.4 Comparisons of mangrove development in response to M2 and spring-neap tidal cycles (SN) at different tidal systems. The black dashed line represents mean water level, and its adjacent two blue dashed lines above and below in a-c) represent mean high water level and mean low water level, while the blue dashed lines in d-f) represent mean spring high water level and mean spring low water level. Mean tidal range is 1 m in a&d) micro-tidal systems, 3 m in b$e) meso-tidal systems, and 5 m in c&f) macro-tidal systems. Panels a-c) are the same as results from Figure 3.3e-g. The inserts show temporal changes in the horizontal extent of mangrove forests (abbreviated as Ext.). MTR and SSC represent mean tidal range and external suspended sediment concentration applied at the seaward boundary, respectively.

mangrove forests in this thesis is highly determined by coastal profile and tidal range, while M2 tidal cycle with a fixed tidal limit fails to represent a real tidal signal with variations in both time and range. In Chapter 3, a larger tidal range increases landward sediment supply and raises sediment concentration across the whole tidal area (Figure 3.10). Compared to a constant M2 tidal cycle, spring-neap tidal cycles create a larger mangrove zone and cause faster coastal progradation (Figure 5.4). This is likely due to an extensive flooding area during spring periods and a calm hydrodynamic environment during neap periods, creating more opportunities for mangroves to colonize. Moreover, landward sediment transport can be enhanced by tidal currents during the spring tidal cycle, which facilitates platform creation for coastal vegetation colonization (Fricke et al., 2017; Goodwin and Mudd, 2019). Similarly, a constant sediment supply from either seaward boundary or landward boundary may fail to illustrate mangrove dynamics due to great deposition caused by substantial changes in sediment environment, for example, the movement of mud banks in French Guiana creates new habitats for mangrove colonization (Proisy et al., 2009). These findings all point to one open question: how do variations in boundary conditions drive the changes in mangrove forests and coastal geomorphology?

The model presented in this thesis provides a first basis to answer this question. A more complex and realistic boundary condition can be further applied in the model settings, but to be able to use it for long-term morphological simulation, especially for the consideration of results interpretation, the patterns of the boundary signal can also be schematized as a certain level of periodic value such that the application of morphological acceleration factor and vegetation updates can be well processed (Lesser et al., 2004).

5.3.3 Implementing organic matter contribution

In this thesis, the main focus is above-ground bio-morphodynamic feedbacks between mangrove behaviors and morphological changes, the below-ground processes including organic matter accretion and sediment compaction are therefore excluded. Thus, the results in this thesis can only be interpreted as a general trend of mangrove movement due to above-ground inorganic sedimentary processes throughout different coastal environments. However, other processes may even dominate the system changing mangrove resilience to sea-level rise, such as organic accretion or subsurface processes (e.g. organic matter decomposition, re-mineralization, subsidence or sediment compaction). These processes may counteract each other, for example, organic matter decomposition counteracts organic build-up in a vertical direction. According to previous field observations, the balance between organic matter buildup and other sub-surface processes varies both between and within mangrove forests, making a process-based prediction very challenging (McKee, 2011), although the organic matter accretion can be more than twice the accretion due to inorganic sedimentation (Breda et al., 2021). Thus, it remains an open question how the organic matter contributes to mangrove survival in the face of sea-level rise and human interventions.

The approach developed in this thesis already incorporated non-linear bio-physical interactions between mangroves and landscapes accumulated with inorganic sediment, a further step towards answering this question should include extra processes dealing with organic matter changes. Recent wetland models including salt marsh and mangroves have captured plant resilience including processes of organic matter contribution (Kirwan and Mudd, 2012; Breda et al., 2021; Rietl et al., 2021), indicating the potential and need to include a broad range of dynamic feedbacks between mangrove growth and coastal morphological changes. Although salt marsh and mangroves are both common plants growing in the intertidal area, the components of organic accretion may be different. Salt marshes are more driven by below-ground biomass because their above-ground matter is decomposed faster than accumulated (Teal, 1962). Thus, the model to capture marsh organic accretion may mainly focus on below-ground biomass accumulation, while mangrove organic contribution should incorporate above-ground and below-ground biomass accumulation and decomposition processes as well as the transformation of residual biomass matter to the value of elevation change (Lovelock et al., 2022). The contribution of the organic matter will further adjust profile elevation and thus influence the whole bio-morphodynamic feedback loop including both above-ground and below-ground processes. Such models will further improve the accuracy to capture mangrove diversity under sea-level rise. Moreover, as recognized in coastal wetlands, carbon pool is also globally important (Kirwan and Mudd, 2012). Organic matter accumulation is inherently linked to the amount of carbon that wetland vegetation accumulates through time. The changes in coastal carbon is thus non-linearly related to bio-physical interactions between coastal landscape evolution and vegetation dynamics. Therefore, implementing such new models to investigate carbon pool changes is also possible (Rietl et al., 2021).

5.3.4 Considering the impacts of mangrove and salt marsh ecotone

Mangroves and salt marshes both occupy the interface between land and sea, which share similar mechanisms for stabilizing sediments and surface accretion. Mangroves typically colonize in tropical/subtropical areas comprising trees or shrub species, while salt marshes are made up of herbaceous plants distributed in the temperate zone (some reaching the Arctic). In recent years, due to the warming climate and changes in rainfall patterns, mangroves have been found to gradually encroach into salt marsh regions altering local species compositions (Cavanaugh et al., 2019). They may coexist as an ecotone and have been found in many geomorphic settings worldwide, such as North America and South China (Saintilan et al., 2014; Rodriguez et al., 2017; Chen, 2019). For example, the ecotone can be located within drowned river valleys, barrier coastal estuaries, or other low-energy environments (Roy et al., 2001). Along the east coast of Florida, mangrove and salt marsh

coexist in lagoon systems, in other places, they may coexist within the inactive deltaic environments or in coastal lagoons with low sediment loads (Saintilan and Hashimoto, 1999; Stevens et al., 2006). As described above, mangroves and salt marsh have different organic decomposition rates (Ouyang et al., 2017), so this vegetation species shift is believed to change the organic matter accumulation in the system. Such differences at the same time are expected to change local morphology by modulating flow conditions and sediment transport and thus enhancing the expansion of tidal creeks and the formation of new tidal creeks (Chen et al., 2018; Schwarz et al., 2022). Subsequently, wetland resilience is affected by the vegetation species replacement. But whether the wetland resilience is enhanced or reduced due to the poleward migration of mangrove forests and how the ecotone reshapes local geomorphology remain unknown.

The mangrove model presented in this thesis allows a modification on the vegetation characteristics and life stages so as to further incorporate the impacts of salt marsh, similar to previous research in salt marsh modelling research (Brückner et al., 2019). However, to be able to consider the interactions between mangroves and salt marshes, detailed competition rules for mangroves and salt marsh at the same location should be implemented (Guo et al., 2013). Only then it is possible to represent the shift of vegetation species due to the invasion of alien plants and study the impacts of such vegetation transitions on local hydrodynamics and geomorphology. A way to implement this would be to first identify the respective vegetation life stages (i.e. in seedlings or maturity stages), and subsequently determine the most competitive vegetation species based on current findings. For example, mature mangroves are assumed to out-compete salt marsh at different stages (seedlings and maturity) (Li et al., 2014; Saintilan et al., 2014) while mangrove seedlings are found to be less competitive compared to salt marsh due to the fast colonization traits of marsh plant (Zhang et al., 2012b; Peng et al., 2017). This implies that different vegetation life stages might have a strong effect on changing vegetation compositions and subsequently shaping local ecosystems.

5.3.5 Improving theories controlling mangrove life stages

The life stages in the mangrove model applied in this thesis are based on previous mangrove research (van Maanen et al., 2015), in which mangrove distributions are controlled by inundation regime, flow strength and competition between trees. This approach allows a long-term simulation to capture mangrove dynamics in the changing hydrodynamic environment due to sea-level rise. However, current mechanisms can still be further improved to understand mangrove changes driven by extreme events (such as storms and El Niño) and thus their associated impact on local ecosystems, in particular in terms of the long-term effects.

Temperature and rainfall are both key factors influencing mangrove diversity, biomass and presence because mangroves prefer to grow in inundated conditions with higher temperatures (Duke et al., 2021). Further, both factors influence water salinity, which determines mangrove occurrences along estuarine reaches upstream. A recent mangrove dieback event in Australia (Gulf of Carpentaria) has been ascribed to the severe El Niño of 2015-2016, during which sea level temporally dropped by 20 cm accompanying an increased temperature and reduced precipitation, resulting in a low water availability environment associated with potentially hypersaline conditions constraining mangrove growth. As a result, massive mangrove dieback occurred within a half year (Duke et al., 2017). Similarly, mangroves can resist storms but in turn can also be damaged by storm effects due to direct mechanical impacts such as branch broken or indirect effects like prolonged flooding or scouring of sediment within a short period (Ouyang et al., 2021; van Hespen et al., 2021). The modelling approach provided in this thesis may fail to illustrate such event-driven dieback phenomenon as the mortality processes of mangrove forests are only initialized under 5-year consecutively depressed growth (Dzimballa, 2022). Therefore, it is essential to comprehend the mechanisms of mangrove life stages and adopt necessary governing processes to simulate the changes of mangrove forests driven by external forcing.

5.4 Conclusions from this thesis

Mangroves grow in complex hydrodynamic conditions, interact with sediment transport and adjust habitats to adapt to sea-level rise. The failure to incorporate non-linear bio-physical interactions has led to discrepancies in mangrove vulnerability assessment under sea-level rise. To fill in this gap, this thesis creates and publicizes a bio-morphodynamic model involving complex interactions between mangrove dynamics, sediment transport and profile changes. The predominant goal of this thesis is to assess the long-term evolution of mangrove ecosystems under sea-level rise and human interventions. The findings from this work further improve the understanding of non-linear feedbacks arising from mangroves and their associated environment, and provide an approach to better capture the fate of mangrove forests and the evolution of mangrove ecosystems. Below, I answer the research questions posed in Chapter 1 based on the conclusions in Chapters 2-4.

1. How do spatial-temporal variations in sediment dynamics control coastal profile evolution and species distribution?

The modelling shows that bio-morphodynamic feedbacks can cause spatio-temporal variations in sediment dynamics. Thus, sediment accretion at one specific location is not simply determined by the duration of tidal inundation, but also related to the amount of sediment availability and flow strength, both of which are affected by mangrove objects (i.e. stems and pneumatophores). A sparse mangrove cover allows more sediment to be delivered landward, increasing upper intertidal surface elevation. As a result, such mangroves are more likely to keep up with sea-level rise, or even expand seaward. In contrast, a dense pioneer mangrove forest slows down tidal currents and reduces the landward sediment delivery such that the upper intertidal accretion is suppressed. When the sea level starts to rise, the upper intertidal inundation will then be prolonged increasingly due to the lower sediment accretion rate, leading to an unsuitable habitat for the mangrove species present there. As a result, the upland mangrove species may disappear from the location and migrate upslope. The space where upper mangrove species previously occupied will be replaced by the mangrove species which can endure longer inundation. Thus, from a systemic perspective, mangrove species gradually shift landward without evident sediment accretion on upper land (Chapter 2).

2. How does the role of bio-morphodynamic feedbacks in determining system dynamics vary under different levels of environmental pressure, such as sea level, sediment availability and coastal accommodation space?

The amount of sediment supply and the rates of sea-level rise are the main environment variables controlling mangrove growth. Low environment pressure is defined when the sea-level rise rate is low and sediment supply is high, so that mangrove coverage can extend both seaward and landward. In this situation, the species richness and evenness are strongly controlled by bio-morphodynamic feedbacks. On the other hand, dense forests cause an unequal sediment accretion across the mangrove forests, leading to different coverage changes between mangrove species, although the whole forest coverage may be increasing. Inversely, high environment pressure is defined when sea-level rise rates are high and sediment supply is low. In this case, the role of bio-morphodynamic feedbacks on mangrove movement is low, while abiotic factors such as increasing hydroperiod dominate mangrove dynamics. As a result, mangroves shift landward with increasing sea level, and may maintain a stable forest coverage and equal vegetation coverage between species. However, both forest coverage and species distribution will be reduced when landward accommodation space is not available, for example, the inland migration of upper mangrove species is obstructed by anthropogenic barriers (Chapter 2).

3. How does the presence of human constructions (such as dikes and seawalls) dictate hydro-sedimentary processes and mangrove survival (i.e. coastal squeeze) under sea-level rise?

Human constructions obstruct the inland migration of mangrove forests during sea-level rise. On the other hand, these constructions enhance vertical accretion when there is a low or intermediate sediment supply. While this allows mangroves to survive under a higher sea-level rise rate with less inland migration of the seaward mangrove forest edge, both mangrove coverage and vegetation diversity would decrease with the reduction or loss of the upper mangrove species. It is only when sea-level rise rates are low and sediment supply is high that the loss of upper mangrove forests is mitigated, showing a similar evolution pattern compared to the mangrove system without human constructions (Chapter 2).

4. How do multiple colonization restrictions control initial mangrove colonization and potentially the subsequent mangrove response to sea-level rise?

Mangrove seedling establishment depends on suitable hydroperiod and limited flow strength, both of which are determined by coastal conditions, such as tidal range, wave climate, sediment supply and coastal slope. Sediment supply contributes to the profile reconfiguration and platform formation, leading to extended horizontal coverage. Meanwhile, increasing bed level enhances ebb tidal currents, increasing bed shear stress and limiting vegetation to colonize at the mid-intertidal area. Mangroves are then moved toward higher bed elevation, causing a reduced vertical vegetation extent. The impact of such feedbacks is evident in meso-tidal and macro-tidal systems with platform formation and seaward vegetation edge colonizing at a distance higher than mean water level, creating a gentler vegetated slope, whereas in micro-tidal systems profile remains relatively stable with a gentler slope. Waves generally increase bed shear stresses around mid-tide and facilitate sediment and mangroves to the upper intertidal, limiting mangrove vertical extent. In the thesis, mangroves establish at high elevations with an initially low hydroperiod are found to withstand increasing tidal inundation under fast sea-level rise and no or limited sediment accretion. Wetland estimation without taking into account these feedbacks may overestimate mangrove vulnerability and cause inappropriate coastal management strategies. Thus, it is important to consider complex vegetation growth dynamics when assessing mangrove vulnerability (Chapter 3).

5. How do coastal profile evolution and seaward mangroves respond to combinations of sea-level rise and sediment availability among different coastal conditions?

Profile evolution and mangrove responses due to sea-level rise are different between tidal range systems. In micro-tidal systems, profile shape remains stable and mangroves retreat landward rapidly even under slow sea-level rise rate and high sediment supply. Similar behaviours are also observed in meso-tidal and macro-tidal systems in fast sea-level rise and low sediment supply, where mangroves transgress landward on the stable coastal profile as sea level increases. However, profile seaward expansion is possible when the sea-level rise rate is low and sediment supply is high in meso-tidal and macro-tidal systems, allowing mangroves to expand seaward simultaneously. In addition, wind waves would enhance sediment accretion and seaward profile propagation, such that mangrove seaward propagation is still possible (Chapter 3).

6. How does profile reconfiguration affect coastal accommodation space and mangrove vulnerability?

Sediment erosion from offshore as a result of a strengthening of tidal currents can act as sediment supply filling in new accommodation space during sea-level rise. Such sediment composition from the reconfiguration of lower coastal profile contributes to the formation of mangrove habitats in upper

land and increases mangrove resilience to sea-level rise. More interestingly, sediment erosion from the offshore area and the landward shift of coastal profile is more significant in the systems with high sediment supply or wind waves, in which a profound platform was formed (Chapter 3).

7. How do changes in the hinterland due to land use change of humans influence mangrove expansion, morphology evolution and sediment composition?

Increasing fine sediment import through river systems is one of the main outcomes caused by human interventions on hinterland. The thesis indicates sediment accretion and mangrove expansion are a function of sediment supply. Increasing sediment supply leads to a fast profile propagation and mangrove colonization associated with larger muddy regions. Accommodation space is reduced as mud input increases, and the reduction rate could be accelerated by increasing mud supply. Mangrove coverage increases linearly under low sediment supply, but could also be accelerated by high mud supply. Differently, the muddy region initially increases faster as mud sediment starts to infill, however, the increasing rate of the muddy region decreases when the proportion of the muddy region within the basin exceeds 50% despite sediment supply (Chapter 4).

8. How does mangrove clearance affect morphological evolution and sediment distribution?

The presence of mangroves firstly captures sediment transported through channels and stabilizes local sediment near channels by reducing flow strength. However, when mangroves are removed, more sediment would deposit along either channels or tidal flats further away from channels, increasing the mud thickness and elevating the bed level in both channels and those tidal areas. Thus, mangrove clearance may not contribute to mitigating the mud deposition in the back-barrier estuary (Chapter 4).

9. How will the back-barrier estuary system evolve in the future under different human actions, such as continued high mud supply, vegetation clearance and reduced mud supply?

The thesis is based on the specific estuary systems in North Island, New Zealand, simulating the long-term morphological evolution in different scenarios. It is shown that continuing high mud supply would further increase mud thickness and elevation of the estuary systems, including channel areas and tidal flats. Vegetation clearance would not help reduce mud accumulation. Instead, more areas could become muddier because more mud is able to deposit in channels and tidal flats further away from channels after mangroves are removed. The effective way is to reduce mud supply from the upstream systems, thus, less mud will remain along the channels leading to a deeper channel. Moreover, it is also an effective way to reduce mud thickness and reduce bed elevation on the tidal flats, compared to the approach by removing vegetation (Chapter 4).

Finally, the advances made in this thesis are summarized as follows. A new non-linear bio-physical wetland model was developed. The approach accounts for complex interactions between hydrodynamics, sediment transport and morphological changes under the impacts of sea-level rise and human interventions in a long-term scale. This model was used to study mangrove vulnerability in a broad range of coastal conditions. This confirmed earlier findings that sediment availability is important for mangrove survival during sea-level rise, but more importantly, the spatio-temporal pattern in sediment availability arising from complex bio-morphodynamic feedbacks turns out to be important factors controlling morphological changes and mangrove behaviours. Such feedbacks have been shown to vary with vegetation characteristics (such as the density of vegetation objects) and coastal environment conditions, including tidal range, waves, sediment supply and coastal slope. Furthermore, human interventions also modulate coastal systems and mangrove dynamics. Human constructions such as sea walls can limit inland mangrove migration, reducing their extent and

diversity. Human activity in the catchment changes sediment import, which eventually transforms the downstream estuary morphology and vegetation dynamics. These findings have implications for coastal management: not only local interference needs to be considered, but also the management of land at or beyond the coastal system boundary is needed. The model system developed in this thesis can serve as a basis to study other important processes within the wetland systems, such as the interactions between mangroves and waves, the variations in boundary conditions, the role of organic matter accretion and carbon storage, the formations of mangrove and salt marsh ecotones and their impacts on future morphology, and other important processes influencing mangrove life stages, such as the control from salt, nutrient and temperature (Chapter 5). Overall, the thesis sheds new light on the evolution of mangrove systems under sea-level rise pressure and human interventions.

References

Aburto-Oropeza, O., Ezcurra, E., Danemann, G., Valdez, V., Murray, J. & Sala, E. (2008). Mangroves in the Gulf of California increase fishery yields. *Proceedings of the National Academy of Sciences of the United States*, 105 (10456-10459).

Akumu, C.E., Pathirana, S., Baban, S. & Bucher, D. (2011). Examining the potential impacts of sea level rise on coastal wetlands in north-eastern NSW, Australia. *Journal of Coastal Conservation*, 15 (1), pp. 15–22.

Alongi, D.M. (2002). Present state and future of the world's mangrove forests. *Environmental Conservation*, 29 (03), pp. 331–349.

Alongi, D.M. (2012). Carbon sequestration in mangrove forests. *Carbon Management*, 3 (3), pp. 313–322.

Alongi, D.M. (2014). Carbon cycling and storage in mangrove forests. *The Annual Review of Marine Science*, 6, pp. 195–219.

Alongi, D.M. (2008). Mangrove forests: Resilience, protection from tsunamis, and responses to global climate change. *Estuarine, Coastal and Shelf Science*, 76 (1), pp. 1–13.

Alongi, D.M. & Mukhopadhyay, S.K. (2015). Contribution of mangroves to coastal carbon cycling in low latitude seas. *Agricultural and Forest Meteorology*, 213, pp. 266–272.

Analuddin, K., Suwa, R. & Hagihara, A. (2009). The self-thinning process in mangrove Kandelia obovata stands. *Journal of Plant Research*, 122 (1), pp. 53–59.

Andrea, C.A. (2006). Tidal Migration Influences the Zonation of Grazing Snails (Turbo smaragdus) in a Mangrove-Seagrass Estuary, Northern New Zealand. *Estuaries and Coasts*, 29 (5), pp. 731–736.

Anthony, E.J., Gardel, A., Gratiot, N., Proisy, C., Allison, M.A., Dolique, F. & Fromard, F. (2010). The Amazon-influenced muddy coast of South America: A review of mud-bank–shoreline interactions. *Earth-Science Reviews*, 103 (3-4), pp. 99–121.

Anthony Edward, J., Dolique, F., Gardel, A., Gratiot, N., Proisy, C. & Polidori, L. (2008). Nearshore intertidal topography and topographic-forcing mechanisms of an Amazon-derived mud bank in French Guiana. *Continental Shelf Research*, 28 (6), pp. 813–822.

Asbridge, E., Lucas, R., Ticehurst, C. & Bunting, P. (2016). Mangrove response to environmental change in Australia's Gulf of Carpentaria. *Ecol Evol*, 6 (11), pp. 3523–3539.

Asbridge, E., Bartolo, R., Finlayson, C.M., Lucas, R.M., Rogers, K. & Woodroffe, C.D. (2019). Assessing the distribution and drivers of mangrove dieback in Kakadu National Park, northern Australia. *Estuarine, Coastal and Shelf Science*, 228, p. 106353.

Baar, A.W., Boechat Albernaz, M., van Dijk, W.M. & Kleinhans, M.G. (2019). Critical dependence of morphodynamic models of fluvial and tidal systems on empirical downslope sediment transport. *Nature Communications*, 10 (1), p. 4903.

Balke, T., Bouma, T.J., Horstman, E.M., Webb, E.L., Erftemeijer, P.L.A. & Herman, P.M.J. (2011). Windows of opportunity: thresholds to mangrove seedling establishment on tidal flats. *Marine Ecology Progress Series*, 440, pp. 1–9.

Balke, T. & Friess, D.A. (2016). Geomorphic knowledge for mangrove restoration: a pan-tropical categorization. *Earth Surface Processes and Landforms*, 41 (2), pp. 231–239.

Balke, T., Herman, P.M.J., Bouma, T.J. & Nilsson, C. (2014). Critical transitions in disturbance-driven ecosystems: identifying Windows of Opportunity for recovery. *Journal of Ecology*, 102 (3), pp. 700–708.

Balke, T., Swales, A., Lovelock, C.E., Herman, P.M.J. & Bouma, T.J. (2015). Limits to seaward expansion of mangroves: Translating physical disturbance mechanisms into seedling survival gradients. *Journal of Experimental Marine Biology and Ecology*, 467, pp. 16–25.

Bao, T.Q. (2011). Effect of mangrove forest structures on wave attenuation in coastal Vietnam. *Oceanologia*, 53 (3), pp. 807–818.

Baptist, M., Babovic, V., Rodriguez Uthurburu, J., Keijzer, M., Uittenbogaard, R., Mynett, A. & Verwey, A. (2007). On inducing equations for vegetation resistance. *Journal of Hydraulic Research*, 45 (4), pp. 435–450.

Barbier, E.B., Hacker, S.D., Kennedy, C., Koch, E.W., Stier, A.C. & Silliman, B.R. (2011). The value of estuarine and coastal ecosystem services. *Ecological Monographs*, 81 (2), pp. 169–193.

Barbier, E.B., Koch, E.W., Silliman, B.R., Hacker, S.D., Wolanski, E., Primavera, J., Granek, E.F., Polasky, S., Aswani, S., Cramer, L.A., Stoms, D.M., Kennedy, C.J., Bael, D., Kappel, C.V., Perillo, G.M.E. & Reed, D.J. (2008). Coastal Ecosystem-Based Management with Nonlinear Ecological Functions and Values. *Science*, 319 (5861), pp. 321–323.

Beck, M.W., Losada, I.J., Menéndez, P., Reguero, B.G., Díaz-Simal, P. & Fernández, F. (2018). The global flood protection savings provided by coral reefs. *Nature Communications*, 9 (1), p. 2186.
Belonje, R. (2019). *Modelling the effect of wave action on sediment transport, morphological evolution and vegetation dynamics in coastal mangrove systems*. PhD dissertation.
Berger, U. & Hildenbrandt, H. (2000). A new approach to spatially explicit modelling of forest dynamics: spacing, ageing and neighbourhood competition of mangrove trees. *Ecological Modelling*, 132, pp. 287–302.
Best, U.S.N., Van der Wegen, M., Dijkstra, J., Willemsen, P.W.J.M., Borsje, B.W. & Roelvink, D.J.A. (2018). Do salt marshes survive sea level rise? Modelling wave action, morphodynamics and vegetation dynamics. *Environmental Modelling and Software*, 109, pp. 152–166.
Bij de Vaate, I., Brückner, M.Z.M., Kleinhans, M.G. & Schwarz, C. (2020). On the Impact of Salt Marsh Pioneer Species-Assemblages on the Emergence of Intertidal Channel Networks. *Water Resources Research*, 56 (3), e2019WR025942.
Blasco, F., Saenger, P. & Janodet, E. (1996). Mangroves as indicators of coastal change. *CATENA*, 27 (3), pp. 167–178.
Boechat Albernaz, M., Roelofs, L., Pierik, H.J. & Kleinhans, M.G. (2020). Natural levee evolution in vegetated fluvial-tidal environments. *Earth Surface Processes and Landforms*, 45 (15), pp. 3824–3841.
Booij, N., Ris, R.C. & Holthuijsen, L.H. (1999). A third-generation wave model for coastal regions: 1. Model description and validation. *Journal of Geophysical Research: Oceans*, 104 (C4), pp. 7649–7666.
Boon, P.I., Allen, T., Brook, J., Carr, G., Frood, D., Hoye, J., Harty, C., McMahon, A., Mathews, S., Rosengren, N., et al. (2011). Mangroves and coastal saltmarsh of Victoria: distribution, condition, threats and management.
Branch, G., Branch, M. & Bannister, A. (1981). *The Living Shores of Southern Africa*. C. Struik.
Brander, L.M., Wagtendonk, A.J., Hussain, S.S., McVittie, A., Verburg, P.H., de Groot, R.S. & van der Ploeg, S. (2012). Ecosystem service values for mangroves in Southeast Asia: A meta-analysis and value transfer application. *Ecosystem Services*, 1 (1), pp. 62–69.
Breda, A., Saco, P.M., Sandi, S.G., Saintilan, N., Riccardi, G. & Rodríguez, J.F. (2021). Accretion, retreat and transgression of coastal wetlands experiencing sea-level rise. *Hydrol. Earth Syst. Sci.*, 25 (2), pp. 769–786.
Brierley, G.J. (2010). Landscape memory: the imprint of the past on contemporary landscape forms and processes. *Area*, 42 (1), pp. 76–85.
Brinkman, R.M. (2006). *Wave attenuation in mangrove forests: an investigation through field and theoretical studies*. PhD dissertation. James Cook University.
Brunier, G., Anthony, E.J., Gratiot, N. & Gardel, A. (2019). Exceptional rates and mechanisms of muddy shoreline retreat following mangrove removal. *Earth Surface Processes and Landforms*, 44 (8), pp. 1559–1571.
Bryan, K.R., Nardin, W., Mullarney, J.C. & Fagherazzi, S. (2017). The role of cross-shore tidal dynamics in controlling intertidal sediment exchange in mangroves in Cù Lao Dung, Vietnam. *Continental Shelf Research*, 147, pp. 128–143.
Brückner, M.Z.M., Schwarz, C., van Dijk, W.M., van Oorschot, M., Douma, H. & Kleinhans, M.G. (2019). Salt Marsh Establishment and Eco-Engineering Effects in Dynamic Estuaries Determined by Species Growth and Mortality. *Journal of Geophysical Research: Earth Surface*, 124 (12), pp. 2962–2986.
Brückner, M.Z., Schwarz, C., Coco, G., Baar, A., Boechat Albernaz, M. & Kleinhans, M.G. (2021). Benthic species as mud patrol-modelled effects of bioturbators and biofilms on large-scale estuarine mud and morphology. *Earth Surface Processes and Landforms*, 46 (6), pp. 1128–1144.
Bullock, E.L., Fagherazzi, S., Nardin, W., Vo-Luong, P., Nguyen, P. & Woodcock, C.E. (2017). Temporal patterns in species zonation in a mangrove forest in the Mekong Delta, Vietnam, using a time series of Landsat imagery. *Continental Shelf Research*, 147, pp. 144–154.
Bulmer, R.H., Lewis, M., O' Donnell, E. & Lundquist, C.J. (2017). Assessing mangrove clearance methods to minimise adverse impacts and maximise the potential to achieve restoration objectives. *New Zealand Journal of Marine and Freshwater Research*, 51 (1), pp. 110–126.
Cahoon, D.R., Hensel, P., Rybczyk, J., McKee, K.L., Proffitt, E. & C., P.B. (2003). Mass tree mortality leads to mangrove peat collapse at Bay Islands, Honduras after Hurricane Mitch. *Journal of Ecology*, 91, pp. 1093–1105.
Cahoon, D.R. & Lynch, J.C. (1997). Vertical accretion and shallow subsidence in a mangrove forest of southwestern Florida, U.S.A. *Mangroves and Salt Marshes*, 1 (3), pp. 173–186.
Cahoon, D.R., Lynch, J.C., Hensel, P., Boumans, R., Perez, B.C., Segura, B. & Day John W., J. (2002). High-Precision Measurements of Wetland Sediment Elevation: I. Recent Improvements to the Sedimentation-Erosion Table. *Journal of Sedimentary Research*, 72 (5), pp. 730–733.
Cahoon, D.R., McKee, K.L. & Morris, J.T. (2020). How Plants Influence Resilience of Salt Marsh and Mangrove Wetlands to Sea-Level Rise. *Estuaries and Coasts*, pp. 1–16.
Carling, P.A. (1982). Temporal and spatial variation in intertidal sedimentation rates. *Sedimentology*, 29 (1), pp. 17–23.
Carlton, J.M. (1974). Land-building and stabilization by mangroves. *Environmental conservation*, 1 (4), pp. 285–294.

Carniello, L., D ' Alpaos, A. & Defina, A. (2011). Modeling wind waves and tidal flows in shallow micro-tidal basins. *Estuarine, Coastal and Shelf Science*, 92 (2), pp. 263–276.
Carr, J., Mariotti, G., Fahgerazzi, S., McGlathery, K. & Wiberg, P. (2018). Exploring the Impacts of Seagrass on Coupled Marsh-Tidal Flat Morphodynamics. *Frontiers in Environmental Science*, 6 (92).
Cavanaugh, K.C., Dangremond, E.M., Doughty, C.L., Williams, A.P., Parker, J.D., Hayes, M.A., Rodriguez, W. & Feller, I.C. (2019). Climate-driven regime shifts in a mangrove–salt marsh ecotone over the past 250 years. *Proceedings of the National Academy of Sciences*, 116 (43), pp. 21602–21608.
Chakraborty, S., Saha, S.K. & Ahmed Selim, S. (2020). Recreational services in tourism dominated coastal ecosystems: Bringing the non-economic values into focus. *Journal of Outdoor Recreation and Tourism*, 30, p. 100279.
Chapman, V.J. (1976). *Mangrove vegetation*. Vol. 447. J. Cramer: Vaduz.
Chen, L. (2019). Invasive Plants in Coastal Wetlands: Patterns and Mechanisms. In: *Wetlands: Ecosystem Services, Restoration and Wise Use*. Ed. by S. An & J.T.A. Verhoeven. Springer International Publishing: Cham, pp. 97–128.
Chen, L., Lin, Q., Krauss, K.W., Zhang, Y., Cormier, N. & Yang, Q. (2021). Forest thinning in the seaward fringe speeds up surface elevation increment and carbon accumulation in managed mangrove forests. *Journal of Applied Ecology*, 58 (9), pp. 1899–1909.
Chen, L., Tam, N.F.Y., Wang, W., Zhang, Y. & Lin, G. (2013). Significant niche overlap between native and exotic Sonneratia mangrove species along a continuum of varying inundation periods. *Estuarine, Coastal and Shelf Science*, 117, pp. 22–28.
Chen, R. & Twilley, R.R. (1998). A gap dynamic model of mangrove forest development along gradients of soil salinity and nutrient resources. *Journal of Ecology*, 86, pp. 37–51.
Chen, Y., Li, Y., Thompson, C., Wang, X., Cai, T. & Chang, Y. (2018). Differential sediment trapping abilities of mangrove and saltmarsh vegetation in a subtropical estuary. *Geomorphology*, 318, pp. 270–282.
Chong, V. (2006). Sustainable utilization and management of mangrove ecosystems of Malaysia. *Aquatic Ecosystem Health and Management*, 9 (2), pp. 249–260.
Clarke, P.J. (1992). Predispersal mortality and fecundity in the grey mangrove (Avicennia marina) in southeastern Australia. *Australian Journal of Ecology*, 17 (2), pp. 161–168.
Clarke, P.J. & Myerscough, P.J. (1993). The intertidal distribution of the grey mangrove (Avicennia marina) in southeastern Australia: The effects of physical conditions, interspecific competition, and predation on propagule establishment and survival. *Australian Journal of Ecology*, 18 (3), pp. 307–315.
Coco, G. & Murray, A.B. (2007). Patterns in the sand: From forcing templates to self-organization. *Geomorphology*, 91 (3-4), pp. 271–290.
Coco, G., Zhou, Z., van Maanen, B., Olabarrieta, M., Tinoco, R. & Townend, I. (2013). Morphodynamics of tidal networks: Advances and challenges. *Marine Geology*, 346, pp. 1–16.
Cohen, M.C.L., Filho, P.W.M.S., Lara, R.J., Behling, H. & Angulo, R.J. (2005). A Model of Holocene Mangrove Development and Relative Sea-level Changes on the Bragança Peninsula (Northern Brazil). *Wetlands Ecology and Management*, 13 (4), pp. 433–443.
Crosby, S.C., Sax, D.F., Palmer, M.E., Booth, H.S., Deegan, L.A., Bertness, M.D. & Leslie, H.M. (2016). Salt marsh persistence is threatened by predicted sea-level rise. *Estuarine, Coastal and Shelf Science*, 181, pp. 93–99.
Dahdouh-Guebas, F., Kairo, J., De Bondt, R. & Koedam, N. (2007). Pneumatophore height and density in relation to microtopography in the grey mangrove Avicennia marina. *Belgian Journal of Botany*, 140, pp. 213–221.
D'Alpaos, A. (2011). The mutual influence of biotic and abiotic components on the long-term ecomorphodynamic evolution of salt-marsh ecosystems. *Geomorphology*, 126 (3), pp. 269–278.
D'Alpaos, A., Lanzoni, S., Marani, M. & Rinaldo, A. (2007). Landscape evolution in tidal embayments: Modeling the interplay of erosion, sedimentation, and vegetation dynamics. *Journal of Geophysical Research*, 112 (F1).
D'Alpaos, A. & Marani, M. (2016). Reading the signatures of biologic–geomorphic feedbacks in salt-marsh landscapes. *Advances in Water Resources*, 93, pp. 265–275.
De Jong, S.M., Shen, Y., de Vries, J., Bijnaar, G., van Maanen, B., Augustinus, P. & Verweij, P. (2021). Mapping mangrove dynamics and colonization patterns at the Suriname coast using historic satellite data and the LandTrendr algorithm. *International Journal of Applied Earth Observation and Geoinformation*, 97, p. 102293.
De Ruiter, P.J., Mullarney, J.C., Bryan, K.R. & Winter, C. (2019). The links between entrance geometry, hypsometry and hydrodynamics in shallow tidally dominated basins. *Earth Surface Processes and Landforms*, 44 (10), pp. 1957–1972.
Deltares (2014). *Simulation of multi-dimensional hydrodynamic flows and transport phenomena, including sediments - User Manual (Version: 3.15.34158)*. Deltares: Delft, the Netherlands.
Duke, N., Mackenzie, J., Hutley, L., Staben, G. & Brouke, A (2021). Assessing the Gulf of Carpentaria mangrove dieback 2017–2019. *Field studies*, p. 150.

Duke, N., Meynecke, J.-O., Dittmann, S., Ellison, A., Anger, K., Berger, U., Cannicci, S., Diele, K., Ewel, K., Field, C., Koedam, N., Lee, S., Marchand, C., Nordhaus, I. & Dahdouh-Guebas, F. (2007). A world without mangroves? *Science*, 317 (5834), pp. 41–42.

Duke, N.C., Ball, M. & Ellison, J. (1998). Factors influencing biodiversity and distributional gradients in mangroves. *Global Ecology and Biogeography Letters*, 7, pp. 27–47.

Duke, N.C., Kovacs, J.M., Griffiths, A.D., Preece, L., Hill, D.J.E., van Oosterzee, P., Mackenzie, J., Morning, H.S. & Burrows, D. (2017). Large-scale dieback of mangroves in Australia ' s Gulf of Carpentaria: a severe ecosystem response, coincidental with an unusually extreme weather event. *Marine and Freshwater Research*, 68 (10), pp. 1816–1829.

Duncan, C., Owen, H.J.F., Thompson, J.R., Koldewey, H.J., Primavera, J.H., Pettorelli, N. & Wegmann, M. (2018). Satellite remote sensing to monitor mangrove forest resilience and resistance to sea level rise. *Methods in Ecology and Evolution*, 9 (8), pp. 1837–1852.

Dzimballa, S. (2022). *Impacts of Mangrove Dieback and Recovery on Coastal Wetland: A Case Study in the Gulf of Carpentaria, Australia*. MSc thesis.

Ellison, A.M. (2000). Mangrove Restoration: Do We Know Enough? *Restoration Ecology*, 8 (3), pp. 219–229.

Ellison, J.C. (2014). Vulnerability of Mangroves to Climate Change. In: *Mangrove Ecosystems of Asia*. Ed. by I. Faridah-Hanum, A. Latiff, K.R. Hakeem & M. Ozturk. Springer: New York, pp. 213–231.

Ellison, J.C. (2015). Vulnerability assessment of mangroves to climate change and sea-level rise impacts. *Wetlands Ecology and Management*, 23 (2), pp. 115–137.

Erkens, G., Cohen, K., Gouw, M., Middelkoop, H. & Hoek, W.Z. (2009). Holocene sediment budgets of the Rhine Delta (The Netherlands): A record of changing sediment delivery. *Nederlandse Geografische Studies*, 306.

Fagherazzi, S., Palermo, C., Rulli, M.C., Carniello, L. & Defina, A. (2007). Wind waves in shallow microtidal basins and the dynamic equilibrium of tidal flats. *Journal of Geophysical Research*, 112 (F2).

Fagherazzi, S., Bryan, K. & Nardin, W. (2017). Buried alive or washed away: The challenging life of mangroves in the Mekong Delta. *Oceanography*, 30 (3), pp. 48–59.

Fagherazzi, S., Howard, A.D. & Wiberg, P.L. (2004). Modeling fluvial erosion and deposition on continental shelves during sea level cycles. *Journal of Geophysical Research: Earth Surface*, 109, F03010.

Fagherazzi, S., Kirwan, M.L., Mudd, S.M., Guntenspergen, G.R., Temmerman, S., D'Alpaos, A., van de Koppel, J., Rybczyk, J.M., Reyes, E., Craft, C. & Clough, J. (2012). Numerical models of salt marsh evolution: Ecological, geomorphic, and climatic factors. *Reviews of Geophysics*, 50 (1), RG1002.

FitzGerald, D.M., Fenster, M.S., Argow, B.A. & Buynevich, I.V. (2008). Coastal Impacts Due to Sea-Level Rise. *Annual Review of Earth and Planetary Sciences*, 36 (1), pp. 601–647.

FitzGerald, D.M. & Hughes, Z. (2019). Marsh Processes and Their Response to Climate Change and Sea-Level Rise. *Annual Review of Earth and Planetary Sciences*, 47 (1), pp. 481–517.

Frasson, R.P.d.M., Pavelsky, T.M., Fonstad, M.A., Durand, M.T., Allen, G.H., Schumann, G., Lion, C., Beighley, R.E. & Yang, X. (2019). Global Relationships Between River Width, Slope, Catchment Area, Meander Wavelength, Sinuosity, and Discharge. *Geophysical Research Letters*, 46 (6), pp. 3252–3262.

French, J. (2006). Tidal marsh sedimentation and resilience to environmental change: Exploratory modelling of tidal, sea-level and sediment supply forcing in predominantly allochthonous systems. *Marine Geology*, 235 (1), pp. 119–136.

Fricke, A.T., Nittrouer, C.A., Ogston, A.S. & Vo-Luong, H.P. (2017). Asymmetric progradation of a coastal mangrove forest controlled by combined fluvial and marine influence, Cù Lao Dung, Vietnam. *Continental Shelf Research*, 147, pp. 78–90.

Friedrichs, C.T. (2011). Tidal flat morphodynamics: a synthesis. In: *Treatise on estuarine and coastal science: Sedimentology and geology*. Ed. by B. Flemming & J. Hansom. Elsevier, pp. 137–170.

Friess, D. & Sidik, F. (2020). *Dynamic Sedimentary Environments of Mangrove Coasts*. Elsevier Science.

Friess, D.A., Krauss, K.W., Horstman, E.M., Balke, T., Bouma, T.J., Galli, D. & Webb, E.L. (2012). Are all intertidal wetlands naturally created equal? Bottlenecks, thresholds and knowledge gaps to mangrove and saltmarsh ecosystems. *Biol Rev Camb Philos Soc*, 87 (2), pp. 346–66.

Friess, D.A., Rogers, K., Lovelock, C.E., Krauss, K.W., Hamilton, S.E., Lee, S.Y., Lucas, R., Primavera, J., Rajkaran, A. & Shi, S. (2019). The State of the World's Mangrove Forests: Past, Present, and Future. *Annual Review of Environment and Resources*, 44 (1), pp. 89–115.

Friess, D.A., Yando, E.S., Abuchahla, G.M., Adams, J.B., Cannicci, S., Canty, S.W., Cavanaugh, K.C., Connolly, R.M., Cormier, N. & Dahdouh-Guebas, F. (2020). Mangroves give cause for conservation optimism, for now. *Current Biology*, 30 (4), R153–R154.

Fu, H., Wang, W., Ma, W. & Wang, M. (2018). Differential in surface elevation change across mangrove forests in the intertidal zone. *Estuarine, Coastal and Shelf Science*, 207, pp. 203–208.

Fu, H., Zhang, Y., Ao, X., Wang, W. & Wang, M. (2019). High surface elevation gains and prediction of mangrove responses to sea-level rise based on dynamic surface elevation changes at Dongzhaigang Bay, China. *Geomorphology*, 334, pp. 194–202.
Furukawa, K., Wolanski, E. & Mueller, H. (1997). Currents and sediment transport in mangrove forests. *Estuarine, Coastal and Shelf Science*, 44, pp. 301–310.
Furukawa, K. & Wolanski, E. (1996). Sedimentation in mangrove forests. *Mangroves and Salt Marshes*, 1 (1), pp. 3–10.
Gijsman, R., Horstman, E.M., van der Wal, D., Friess, D.A., Swales, A. & Wijnberg, K.M. (2021). Nature-Based Engineering: A Review on Reducing Coastal Flood Risk With Mangroves. *Frontiers in Marine Science*, 8.
Gilman, E., Ellison, J. & Coleman, R. (2007). Assessment of Mangrove Response to Projected Relative Sea-Level Rise And Recent Historical Reconstruction of Shoreline Position. *Environmental Monitoring and Assessment*, 124 (1), pp. 105–130.
Gilman, E.L., Ellison, J., Duke, N.C. & Field, C. (2008). Threats to mangroves from climate change and adaptation options: A review. *Aquatic Botany*, 89 (2), pp. 237–250.
Giri, C., Ochieng, E., Tieszen, L.L., Zhu, Z., Singh, A., Loveland, T., Masek, J. & Duke, N. (2011). Status and distribution of mangrove forests of the world using earth observation satellite data. *Global Ecology and Biogeography*, 20 (1), pp. 154–159.
Glover, H., Stokes, D., Ogston, A., Bryan, K. & Pilditch, C. (2022). Decadal-scale impacts of changing mangrove extent on hydrodynamics and sediment transport in a quiescent, mesotidal estuary. *Earth Surface Processes and Landforms*.
Goldberg, L., Lagomasino, D., Thomas, N. & Fatoyinbo, T. (2020). Global declines in human-driven mangrove loss. *Global Change Biology*, 26 (10), pp. 5844–5855.
Goodwin, G.C.H. & Mudd, S.M. (2019). High Platform Elevations Highlight the Role of Storms and Spring Tides in Salt Marsh Evolution. *Frontiers in Environmental Science*, 7.
Goodwin, G.C.H. & Mudd, S.M. (2020). Detecting the Morphology of Prograding and Retreating Marsh Margins —Example of a Mega-Tidal Bay. *Remote Sensing*, 12 (1), p. 13.
Green, M.O. (2011). Very small waves and associated sediment resuspension on an estuarine intertidal flat. *Estuarine, Coastal and Shelf Science*, 93 (4), pp. 449–459.
Green, M.O., Black, K.P. & Amos, C.L. (1997). Control of estuarine sediment dynamics by interactions between currents and waves at several scales. *Marine Geology*, 144 (1), pp. 97–116.
Green, M.O. & Coco, G. (2014). Review of wave-driven sediment resuspension and transport in estuaries. *Reviews of Geophysics*, 52 (1), pp. 77–117.
Guannel, G., Arkema, K., Ruggiero, P. & Verutes, G. (2016). The Power of Three: Coral Reefs, Seagrasses and Mangroves Protect Coastal Regions and Increase Their Resilience. *PLOS ONE*, 11 (7), e0158094.
Guo, H., Zhang, Y., Lan, Z. & Pennings, S.C. (2013). Biotic interactions mediate the expansion of black mangrove (A vicennia germinans) into salt marshes under climate change. *Global change biology*, 19 (9), pp. 2765–2774.
Guo, L., van der Wegen, M., Roelvink, D. & He, Q. (2015). Exploration of the impact of seasonal river discharge variations on long-term estuarine morphodynamic behavior. *Coastal Engineering*, 95, pp. 105–116.
Hamilton, S.E. & Casey, D. (2016). Creation of a high spatio-temporal resolution global database of continuous mangrove forest cover for the 21st century (CGMFC-21). *Global Ecology and Biogeography*, 25 (6), pp. 729–738.
Hamilton, S.E. & Friess, D.A. (2018). Global carbon stocks and potential emissions due to mangrove deforestation from 2000 to 2012. *Nature Climate Change*, 8 (3), pp. 240–244.
Hanebuth, T., Stattegger, K. & Grootes, P.M. (2000). Rapid Flooding of the Sunda Shelf: A Late-Glacial Sea-Level Record. *Science*, 288 (5468), pp. 1033–1035.
Harty, C. (2009). Mangrove planning and management in New Zealand and South East Australia –A reflection on approaches. *Ocean and Coastal Management*, 52 (5), pp. 278–286.
Healy, T.R. (2005). New Zealand, Coastal Geomorphology and Oceanography. In: *Encyclopedia of Coastal Science*. Ed. by M.L. Schwartz. Springer Netherlands: Dordrecht, pp. 709–714.
Hicks, D.M., Shankar, U., McKerchar, A.I., Basher, L., Lynn, I., Page, M. & Jessen, M. (2011). Suspended sediment yields from New Zealand rivers. *Journal of Hydrology (New Zealand)*, 50 (1), pp. 81–142.
Hicks, M., Semadeni-Davies, A., Haddadchi, A., Shankar, U. & Plew, D. (2019). *Updated sediment load estimator for New Zealand*. Tech. rep. NIWA.
Hill, M.O. (1973). Diversity and evenness: A unifying notation and its consequences. *Ecology*, 54 (2), pp. 427–432.
Hinkel, J., Lincke, D., Vafeidis, A.T., Perrette, M., Nicholls, R.J., Tol, R.S.J., Marzeion, B., Fettweis, X., Ionescu, C. & Levermann, A. (2014). Coastal flood damage and adaptation costs under 21st century sea-level rise. *Proceedings of the National Academy of Sciences*, 111 (9), pp. 3292–3297.
Hoppe-Speer, S.C.L., Adams, J.B., Rajkaran, A. & Bailey, D. (2011). The response of the red mangrove Rhizophora mucronata Lam. to salinity and inundation in South Africa. *Aquatic Botany*, 95 (2), pp. 71–76.

Horstman, E.M., Bryan, K.R., Mullarney, J.C., Pilditch, C.A. & Eager, C.A. (2018a). Are flow-vegetation interactions well represented by mimics? A case study of mangrove pneumatophores. *Advances in Water Resources*, 111, pp. 360–371.
Horstman, E.M., Dohmen-Janssen, C.M., Bouma, T.J. & Hulscher, S.J.M.H. (2015). Tidal-scale flow routing and sedimentation in mangrove forests: Combining field data and numerical modelling. *Geomorphology*, 228, pp. 244–262.
Horstman, E.M., Dohmen-Janssen, C.M., Narra, P.M.F., van den Berg, N.J.F., Siemerink, M. & Hulscher, S.J.M.H. (2014). Wave attenuation in mangroves: A quantitative approach to field observations. *Coastal Engineering*, 94, pp. 47–62.
Horstman, E., Dohmen-Janssen, M. & Hulscher, S. (2013). Modeling tidal dynamics in a mangrove creek catchment in Delft3D. In: *Coastal dynamics*. Vol. 2013, pp. 833–844.
Horstman, E.M., Lundquist, C.J., Bryan, K.R., Bulmer, R.H., Mullarney, J.C. & Stokes, D.J. (2018b). The dynamics of expanding mangroves in New Zealand. In: *Threats to Mangrove Forests: Hazards, Vulnerability, and Management*. Ed. by C. Makowski & C.W. Finkl. Springer, pp. 23–52.
Hume, T.M. & Herdendorf, C.E. (1992). Factors controlling tidal inlet characteristics on low drift coasts. *Journal of Coastal Research*, pp. 355–375.
Hume, T.M. & Herdendorf, C.E. (1993). On the use of empirical stability relationships for characterising estuaries. *Journal of Coastal Research*, pp. 413–422.
Hume, T.M., Snelder, T., Weatherhead, M. & Liefting, R. (2007). A controlling factor approach to estuary classification. *Ocean and Coastal Management*, 50 (11), pp. 905–929.
Hunt, S. (2019). *Summary of historic estuarine sedimentation measurements in the Waikato region and formulation of a historic baseline sedimentation rate*. Tech. rep. Waikato Regional Council Technical Report 2019/08.
Hunt, S. (2021). *Optimisation of the Waikato Regional Council tide gauge network*. Tech. rep. Waikato Regional Council Technical Report 2021/25.
Hunt, S., Bryan, K.R., Mullarney, J.C. & Pritchard, M. (2016). Observations of asymmetry in contrasting wave-and tidally-dominated environments within a mesotidal basin: implications for estuarine morphological evolution. *Earth Surface Processes and Landforms*, 41 (15), pp. 2207–2222.
Jennerjahn, T.C., Gilman, E., Krauss, K.W., Lacerda, L.D., Nordhaus, I. & Wolanski, E. (2017). Mangrove ecosystems under climate change. In: *Mangrove Ecosystems: A Global Biogeographic Perspective*. Ed. by V. Rivera-Monroy, S. Lee, E. Kristensen & T. R. Springer, pp. 211–244.
Jervey, M. (1988). Quantitative Geological Modeling of Siliciclastic Rock Sequences and Their Seismic Expression. In: *Sea-Level Changes: An Integrated Approach*. Ed. by C.K. Wilgus, B.S. Hastings, H. Posamentier, J.V. Wagoner, C.A. Ross & C.G.S.C. Kendall. Vol. 42. SEPM Society for Sedimentary Geology, p. 23.
Jones, C.G., Lawton, J.H. & Shachak, M. (1994). Organisms as ecosystem engineers. In: *Ecosystem management*. Springer, pp. 130–147.
Jones, G.W. (2014). The population of Southeast Asia. In: *Routledge Handbook of Southeast Asian Economics*. Routledge, pp. 223–251.
Jones, H.F.E. (2008). *Coastal sedimentation: what we know and the information gaps*. Tech. rep. Waikato Regional Council (Environment Waikato).
Jowett, I.G. (1998). Hydraulic geometry of New Zealand rivers and its use as a preliminary method of habitat assessment. *Regulated Rivers: Research and Management*, 14 (5), pp. 451–466.
Kathiresan, K. & Bingham, B.L. (2001). Biology of mangroves and mangrove Ecosystems. In: *Advances in Marine Biology*. Vol. 40. Academic Press, pp. 81–251.
Kathiresan, K. & Rajendran, N. (2005). Mangrove ecosystems of the Indian Ocean region. *Indian Journal of Marine Sciences*, 34 (1).
Kemp, D.B., Sadler, P.M. & Vanacker, V. (2020). The human impact on North American erosion, sediment transfer, and storage in a geologic context. *Nature Communications*, 11 (1), p. 6012.
Kidane, D. & Alemu, B. (2015). The effect of upstream land use practices on soil erosion and sedimentation in the Upper Blue Nile Basin, Ethiopia. *Research Journal of Agriculture and Environmental Management*, 4 (2), pp. 55–68.
Kirwan, M.L. & Megonigal, J.P. (2013). Tidal wetland stability in the face of human impacts and sea-level rise. *Nature*, 504 (7478), pp. 53–60.
Kirwan, M.L., Walters, W.G., Reay, W.G. & Carr, J.A. (2016a). Sea level driven marsh expansion in a coupled model of marsh erosion and migration. *Geophysical Research Letters*, 43, pp. 4366–4373.
Kirwan, M.L. & Guntenspergen, G.R. (2010). Influence of tidal range on the stability of coastal marshland. *Journal of Geophysical Research: Earth Surface*, 115 (F2).
Kirwan, M.L., Guntenspergen, G.R., D'Alpaos, A., Morris, J.T., Mudd, S.M. & Temmerman, S. (2010). Limits on the adaptability of coastal marshes to rising sea level. *Geophysical Research Letters*, 37 (23), p. L23401.

Kirwan, M.L. & Mudd, S.M. (2012). Response of salt-marsh carbon accumulation to climate change. *Nature*, 489 (7417), pp. 550–553.
Kirwan, M.L. & Murray, A.B. (2007). A coupled geomorphic and ecological model of tidal marsh evolution. *Proceedings of the National Academy of Sciences*, 104, pp. 6118–6122.
Kirwan, M.L., Murray, A.B., Donnelly, J.P. & Corbett, D.R. (2011). Rapid wetland expansion during European settlement and its implication for marsh survival under modern sediment delivery rates. *Geology*, 39 (5), pp. 507–510.
Kirwan, M.L., Temmerman, S., Skeehan, E.E., Guntenspergen, G.R. & Fagherazzi, S. (2016b). Overestimation of marsh vulnerability to sea level rise. *Nature Climate Change*, 6 (3), pp. 253–260.
Kitaya, Y., Yabuki, K., Kiyota, M., Tani, A., Hirano, T. & Aiga, I. (2002). Gas exchange and oxygen concentration in pneumatophores and prop roots of four mangrove species. *Trees*, 16 (2), pp. 155–158.
Kleinhans, M.G., de Vries, B., Braat, L. & van Oorschot, M. (2018). Living landscapes: Muddy and vegetated floodplain effects on fluvial pattern in an incised river. *Earth Surf Process Landf*, 43 (14), pp. 2948–2963.
Knight, J.M., Dale, P.E.R., Spencer, J. & Griffin, L. (2009). Exploring LiDAR data for mapping the micro-topography and tidal hydro-dynamics of mangrove systems: An example from southeast Queensland, Australia. *Estuarine, Coastal and Shelf Science*, 85 (4), pp. 593–600.
Koch, F.G., Flokstra, C., Waterloopkundig, L., International Association for Hydraulic, R. & Congress (1980). *Bed level computations for curved alluvial channels*. Delft Hydraulics Laboratory: Delft [Netherlands].
Komiyama, A., Ong, J.E. & Poungparn, S. (2008). Allometry, biomass, and productivity of mangrove forests: A review. *Aquatic Botany*, 89 (2), pp. 128–137.
Kozhikkodan Veettil, B. & Quang, N.X. (2019). Mangrove forests of Cambodia: Recent changes and future threats. *Ocean and Coastal Management*, 181, p. 104895.
Krauss, K.W., Allen, J.A. & Cahoon, D.R. (2003). Differential rates of vertical accretion and elevation change among aerial root types in Micronesian mangrove forests. *Estuarine, Coastal and Shelf Science*, 56 (2), pp. 251–259.
Krauss, K.W., McKee, K.L., Lovelock, C.E., Cahoon, D.R., Saintilan, N., Reef, R. & Chen, L. (2014). How mangrove forests adjust to rising sea level. *New Phytol*, 202 (1), pp. 19–34.
Krauss, K.W., Cahoon, D.R., Allen, J.A., Ewel, K.C., Lynch, J.C. & Cormier, N. (2010). Surface Elevation Change and Susceptibility of Different Mangrove Zones to Sea-Level Rise on Pacific High Islands of Micronesia. *Ecosystems*, 13 (1), pp. 129–143.
Kumara, M.P., Jayatissa, L.P., Krauss, K.W., Phillips, D.H. & Huxham, M. (2010). High mangrove density enhances surface accretion, surface elevation change, and tree survival in coastal areas susceptible to sea-level rise. *Oecologia*, 164 (2), pp. 545–53.
Kumbier, K., Hughes, M.G., Rogers, K. & Woodroffe, C.D. (2021). Inundation characteristics of mangrove and saltmarsh in micro-tidal estuaries. *Estuarine, Coastal and Shelf Science*, 261, p. 107553.
Lambeck, K., Rouby, H., Purcell, A., Sun, Y. & Sambridge, M. (2014). Sea level and global ice volumes from the Last Glacial Maximum to the Holocene. *Proceedings of the National Academy of Sciences*, 111 (43), pp. 15296–15303.
Lesser, G.R., Roelvink, J.A., van Kester, J.A.T.M. & Stelling, G.S. (2004). Development and validation of a three-dimensional morphological model. *Coastal Engineering*, 51 (8-9), pp. 883–915.
Li, X., Bellerby, R., Craft, C. & Widney, S.E. (2018). Coastal wetland loss, consequences, and challenges for restoration. *Anthropocene Coasts*, 1 (1), pp. 1–15.
Li, Z., Wang, W. & Zhang, Y. (2014). Recruitment and herbivory affect spread of invasive Spartina alterniflora in China. *Ecology*, 95 (7), pp. 1972–1980.
Liu, M., Zhang, H., Lin, G., Lin, H. & Tang, D. (2018). Zonation and directional dynamics of mangrove forests derived from time-series satellite imagery in Mai Po, Hong Kong. *Sustainability*, 10 (6), p. 1913.
Liénard, J., Lynn, K., Strigul, N., Norris, B.K., Gatziolis, D., Mullarney, J.C., Bryan, K.R. & Henderson, S.M. (2016). Efficient three-dimensional reconstruction of aquatic vegetation geometry: Estimating morphological parameters influencing hydrodynamic drag. *Estuarine, Coastal and Shelf Science*, 178, pp. 77–85.
Lovelock, C.E., Cahoon, D.R., Friess, D.A., Guntenspergen, G.R., Krauss, K.W., Reef, R., Rogers, K., Saunders, M.L., Sidik, F., Swales, A., Saintilan, N., Thuyen le, X. & Triet, T. (2015). The vulnerability of Indo-Pacific mangrove forests to sea-level rise. *Nature*, 526 (7574), pp. 559–63.
Lovelock, C.E., Adame, M.F., Butler, D.W., Kelleway, J.J., Dittmann, S., Fest, B., King, K.J., Macreadie, P.I., Mitchell, K., Newnham, M., Ola, A., Owers, C.J. & Welti, N. (2022). Modeled approaches to estimating blue carbon accumulation with mangrove restoration to support a blue carbon accounting method for Australia. *Limnology and Oceanography*, p. 11.
Lovelock, C.E., Krauss, K.W., Osland, M.J., Reef, R. & Ball, M.C. (2016). The Physiology of Mangrove Trees with Changing Climate. In: *Tropical Tree Physiology: Adaptations and Responses in a Changing Environment*. Ed. by G. Goldstein & L.S. Santiago. Springer International Publishing: Cham, pp. 149–179.
Lovelock, C.E., Sorrell, B.K., Hancock, N., Hua, Q. & Swales, A. (2010). Mangrove forest and soil development on a rapidly accreting shore in New Zealand. *Ecosystems*, 13 (3), pp. 437–451.

Lugo, A.E. (1980). Mangrove ecosystems: successional or steady state? *Biotropica*, pp. 65–72.
Lugo, A.E. & Snedaker, S.C. (1974). The ecology of mangroves. *Annual Review of Ecology and Systematics*, 5, pp. 39–64.
Lundquist, C., Morrisey, D., Gladstone-Gallagher, R. & Swales, A. (2014). Managing Mangrove Habitat Expansion in New Zealand. In: *Mangrove Ecosystems of Asia*. Ed. by I. Faridah-Hanum, A. Latiff, K.R. Hakeem & M. Ozturk. Springer: New York, pp. 415–438.
Malini, B.H. & Rao, K.N. (2004). Coastal erosion and habitat loss along the Godavari delta front- a fallout of dam construction (?) *Current Science*, 87 (9), pp. 1232–1236.
Manap, N. & Voulvoulis, N. (2016). Data analysis for environmental impact of dredging. *Journal of cleaner production*, 137, pp. 394–404.
Mangor, K., Drønen, N., Kaergaard, K. & Kristensen, N. (2017). *Shoreline Management Guidelines*. DHI: Hirschholm: Denmark.
Mariotti, G. & Canestrelli, A. (2017). Long-term morphodynamics of muddy backbarrier basins: Fill in or empty out? *Water Resources Research*, 53 (8), pp. 7029–7054.
Mazda, Y., Kobashi, D. & Okada, S. (2005). Tidal-scale hydrodynamics within mangrove swamps. *Wetlands Ecology and Management*, 13 (6), pp. 647–655.
Mazda, Y., Magi, M., Ikeda, Y., Kurokawa, T. & Asano, T. (2006). Wave reduction in a mangrove forest dominated by Sonneratia sp. *Wetlands Ecology and Management*, 14 (4), pp. 365–378.
Mazda, Y., Magi, M., Kogo, M. & Hong, P.N. (1997a). Mangroves as a coastal protection from waves in the Tong King delta, Vietnam. *Mangroves and Salt Marshes*, 1 (2), pp. 127–135.
Mazda, Y., Wolanski, E., King, B., Sase, A., Ohtsuka, D. & Magi, M. (1997b). Drag force due to vegetation in mangrove swamps. *Mangroves and Salt Marshes*, 1 (3), pp. 193–199.
McCulloch, M., Fallon, S., Wyndham, T., Hendy, E., Lough, J. & Barnes, D. (2003). Coral record of increased sediment flux to the inner Great Barrier Reef since European settlement. *Nature*, 421 (6924), pp. 727–730.
McKee, K.L. (2011). Biophysical controls on accretion and elevation change in Caribbean mangrove ecosystems. *Estuarine, Coastal and Shelf Science*, 91 (4), pp. 475–483.
McKee, K.L., Cahoon, D.R. & Feller, I.C. (2007). Caribbean mangroves adjust to rising sea level through biotic controls on change in soil elevation. *Global Ecology and Biogeography*, 16 (5), pp. 545–556.
McKee, K.L., Krauss, K.W. & Cahoon, D.R. (2021). Chapter 11 - Does geomorphology determine vulnerability of mangrove coasts to sea-level rise? In: *Dynamic Sedimentary Environments of Mangrove Coasts*. Ed. by F. Sidik & D.A. Friess. Elsevier, pp. 255–272.
McKee, K.L. & Vervaeke, W.C. (2018). Will fluctuations in salt marsh–mangrove dominance alter vulnerability of a subtropical wetland to sea-level rise? *Global Change Biology*, 24 (3), pp. 1224–1238.
Menendez, P., Losada, I.J., Beck, M.W., Torres-Ortega, S., Espejo, A., Narayan, S., Díaz-Simal, P. & Lange, G.-M. (2018). Valuing the protection services of mangroves at national scale: The Philippines. *Ecosystem services*, 34, pp. 24–36.
Mentaschi, L., Vousdoukas, M.I., Pekel, J.-F., Voukouvalas, E. & Feyen, L. (2018). Global long-term observations of coastal erosion and accretion. *Scientific reports*, 8 (1), pp. 1–11.
Menéndez, P., Losada, I.J., Torres-Ortega, S., Narayan, S. & Beck, M.W. (2020). The Global Flood Protection Benefits of Mangroves. *Scientific Reports*, 10 (1), p. 4404.
Middleton, B.A. & McKee, K.L. (2001). Degradation of mangrove tissues and implications for peat formation in Belizean island forests. *Journal of Ecology*, 89 (5), pp. 818–828.
Minderhoud, P., Coumou, L, Erban, L., Middelkoop, H, Stouthamer, E & Addink, E. (2018). The relation between land use and subsidence in the Vietnamese Mekong delta. *Science of The Total Environment*, 634, pp. 715–726.
Mogensen, L.A. & Rogers, K. (2018). Validation and comparison of a model of the effect of sea-level rise on coastal wetlands. *Sci Rep*, 8 (1), p. 1369.
Montgomery, J.M., Bryan, K.R., Mullarney, J.C. & Horstman, E.M. (2019). Attenuation of Storm Surges by Coastal Mangroves. *Geophysical Research Letters*, 46 (5), pp. 2680–2689.
Montgomery, J.M., Bryan, K.R., Horstman, E.M. & Mullarney, J.C. (2018). Attenuation of Tides and Surges by Mangroves: Contrasting Case Studies from New Zealand. *Water*, 10 (9), p. 1119.
Moody, J.A. & Troutman, B.M. (2002). Characterization of the spatial variability of channel morphology. *Earth Surface Processes and Landforms*, 27 (12), pp. 1251–1266.
Morris, J.T., Sundareshwar, P.V., Nietch, C.T., Kjerfve, B. & Cahoon, D.R. (2002). Responses of coastal wetlands to rising sea level. *Ecology*, 83 (10), pp. 2869–2877.
Morrisey, D., Beard, C., Morrison, M. & Lowe, M.L. (2007). *The New Zealand mangrove: review of the current state of knowledge*. Auckland Regional Council Technical Publication Number 325.
Murray, A.B., Knaapen, M.A.F., Tal, M. & Kirwan, M.L. (2008). Biomorphodynamics: Physical-biological feedbacks that shape landscapes. *Water Resources Research*, 44 (11), W11301.

Murray, A. (2013). Contrasting the Goals, Strategies, and Predictions Associated with Simplified Numerical Models and Detailed Simulations. In: *Prediction in Geomorphology*. Ed. by P.W. Iverson & R.M., pp. 151–165.
Méndez, F.J., Losada, I.J. & Losada, M.A. (1999). Hydrodynamics induced by wind waves in a vegetation field. *Journal of Geophysical Research: Oceans*, 104 (C8), pp. 18383–18396.
Nairn, R.B., Roelvink, J.A. & Southgate, H.N. (1991). Transition Zone Width and Implications for Modelling Surfzone Hydrodynamics. In: *Coastal Engineering 1990*, pp. 68–81.
Nardin, W., Edmonds, D.A. & Fagherazzi, S. (2016a). Influence of vegetation on spatial patterns of sediment deposition in deltaic islands during flood. *Advances in Water Resources*, 93, pp. 236–248.
Nardin, W. & Edmonds, D.A. (2014). Optimum vegetation height and density for inorganic sedimentation in deltaic marshes. *Nature Geoscience*, 7 (10), pp. 722–726.
Nardin, W., Locatelli, S., Pasquarella, V., Rulli, M.C., Woodcock, C.E. & Fagherazzi, S. (2016b). Dynamics of a fringe mangrove forest detected by Landsat images in the Mekong River Delta, Vietnam. *Earth Surface Processes and Landforms*, 41 (14), pp. 2024–2037.
Nardin, W., Vona, I. & Fagherazzi, S. (2021). Sediment deposition affects mangrove forests in the Mekong delta, Vietnam. *Continental Shelf Research*, 213, p. 104319.
Nepf, H.M. (1999). Drag, turbulence, and diffusion in flow through emergent vegetation. *Water Resources Research*, 35 (2), pp. 479–489.
Nienhuis, J.H., Ashton, A.D., Edmonds, D.A., Hoitink, A.J.F., Kettner, A.J., Rowland, J.C. & Törnqvist, T.E. (2020). Global-scale human impact on delta morphology has led to net land area gain. *Nature*, 577 (7791), pp. 514–518.
Odum, W.E., McIvor, C.C. & Smith III, T.J. (1982). *The ecology of the mangroves of south Florida: a community profile*. Bureau of Land Management, Fish and Wildlife Service, Dept. of the Interior.
Oppenheimer, M., B.C., G., J., H., van de Wal R., A.K., M., A., A.-E., R., C., M., C.-J., R.M., D., T., G., J., H., F., I., B., M., B., M. & Z., S. (2019). Sea Level Rise and Implications for Low-Lying Islands, Coasts and Communities. In: *IPCC Special Report on the Ocean and Cryosphere in a Changing Climate*. Ed. by P. H.-O., R. D.C., M.-D. V., Z. P., T. M., P. E., M. K., A. A., N. M., O. A., P. J., R. B. & W. N.M. Cambridge University Press: Cambridge, UK.
Orson, R.A., Warren, R.S. & Niering, W.A. (1998). Interpreting Sea Level Rise and Rates of Vertical Marsh Accretion in a Southern New England Tidal Salt Marsh. *Estuarine, Coastal and Shelf Science*, 47 (4), pp. 419–429.
Ouyang, X., Guo, F. & Lee, S.Y. (2021). The impact of super-typhoon Mangkhut on sediment nutrient density and fluxes in a mangrove forest in Hong Kong. *Science of The Total Environment*, 766, p. 142637.
Ouyang, X., Lee, S.Y. & Connolly, R.M. (2017). The role of root decomposition in global mangrove and saltmarsh carbon budgets. *Earth-Science Reviews*, 166, pp. 53–63.
Partheniades, E. (1965). Erosion and deposition of cohesive soils. *Journal of the Hydraulics Division*, 91 (1), pp. 105–139.
Parvathy, K. & Bhaskaran, P.K. (2017). Wave attenuation in presence of mangroves: A sensitivity study for varying bottom slopes. *The International Journal of Ocean and Climate Systems*, 8 (3), pp. 126–134.
Passeri, D.L., Hagen, S.C., Medeiros, S.C., Bilskie, M.V., Alizad, K. & Wang, D. (2015). The dynamic effects of sea level rise on low-gradient coastal landscapes: A review. *Earth's Future*, 3 (6), pp. 159–181.
Peet, R. (1974). The measurement of species diversity. *Annual Review of Ecological and Systematics*, 5, pp. 285–307.
Peng, Y., Zhang, M. & Lee, S.Y. (2017). Food availability and predation risk drive the distributional patterns of two pulmonate gastropods in a mangrove-saltmarsh transitional habitat. *Marine Environmental Research*, 130, pp. 21–29.
Phan, K.L., Stive, M.J.F., Zijlema, M., Truong, H.S. & Aarninkhof, S.G.J. (2019). The effects of wave non-linearity on wave attenuation by vegetation. *Coastal Engineering*, 147, pp. 63–74.
Phan, L.K., van Thiel de Vries, J.S.M. & Stive, M.J.F. (2015). Coastal mangrove squeeze in the Mekong Delta. *Journal of Coastal Research*, 300, pp. 233–243.
Polidoro, B.A. et al. (2010). The loss of species: mangrove extinction risk and geographic areas of global concern. *PLoS One*, 5 (4), e10095.
Pranchai, A., Jenke, M. & Berger, U. (2019). Well-intentioned, but poorly implemented: Debris from coastal bamboo fences triggered mangrove decline in Thailand. *Marine Pollution Bulletin*, 146, pp. 900–907.
Pritchard, M., Reeve, G., Gorman, R. & Robinson, B. (2016). *Modelling the effects of coastal reclamation on tidal currents and sedimentation within Mangere Inlet*. Tech. rep. NIWA Client Report.
Proisy, C., Gratiot, N., Anthony, E.J., Gardel, A., Fromard, F. & Heuret, P. (2009). Mud bank colonization by opportunistic mangroves: A case study from French Guiana using lidar data. *Continental Shelf Research*, 29 (3), pp. 632–641.
Punwong, P., Marchant, R. & Selby, K. (2013). Holocene mangrove dynamics in Makoba Bay, Zanzibar. *Palaeogeography, Palaeoclimatology, Palaeoecology*, 379-380, pp. 54–67.
Quader, M.A., Agrawal, S. & Kervyn, M. (2017). Multi-decadal land cover evolution in the Sundarban, the largest mangrove forest in the world. *Ocean and Coastal Management*, 139, pp. 113–124.

Quartel, S., Kroon, A., Augustinus, P.G.E.F., Van Santen, P. & Tri, N.H. (2007). Wave attenuation in coastal mangroves in the Red River Delta, Vietnam. *Journal of Asian Earth Sciences*, 29 (4), pp. 576–584.
Reniers, A.J.H.M., Roelvink, J.A. & Thornton, E.B. (2004). Morphodynamic modeling of an embayed beach under wave group forcing. *Journal of Geophysical Research: Oceans*, 109 (C1), p. C01030.
Reniers, A.J.H.M., van Dongeren, A.R., Battjes, J.A. & Thornton, E.B. (2002). Linear modeling of infragravity waves during Delilah. *Journal of Geophysical Research: Oceans*, 107 (C10), pp. 1–1–1–18.
Restrepo, J.D., Kettner, A.J. & Syvitski, J.P. (2015). Recent deforestation causes rapid increase in river sediment load in the Colombian Andes. *Anthropocene*, 10, pp. 13–28.
Rietl, A.J., Megonigal, J.P., Herbert, E.R. & Kirwan, M.L. (2021). Vegetation Type and Decomposition Priming Mediate Brackish Marsh Carbon Accumulation Under Interacting Facets of Global Change. *Geophysical Research Letters*, 48 (8), e2020GL092051.
Roberts, W., Le Hir, P. & Whitehouse, R. (2000). Investigation using simple mathematical models of the effect of tidal currents and waves on the profile shape of intertidal mudflats. *Continental Shelf Research*, 20 (10), pp. 1079–1097.
Rodriguez, J.F., Saco, P.M., Sandi, S., Saintilan, N. & Riccardi, G. (2017). Potential increase in coastal wetland vulnerability to sea-level rise suggested by considering hydrodynamic attenuation effects. *Nat Commun*, 8, p. 16094.
Roelvink, J.A. (2006). Coastal morphodynamic evolution techniques. *Coastal Engineering*, 53 (2), pp. 277–287.
Rogers, K., Saintilan, N. & Heijnis, H (2005). Mangrove encroachment of salt marsh in Western Port Bay, Victoria: The role of sedimentation, subsidence, and sea level rise. *Estuaries*, 28, pp. 551–559.
Rogers, K., Wilton, K.M. & Saintilan, N. (2006). Vegetation change and surface elevation dynamics in estuarine wetlands of southeast Australia. *Estuarine, Coastal and Shelf Science*, 66 (3), pp. 559–569.
Rogers, K. (2021). Accommodation space as a framework for assessing the response of mangroves to relative sea-level rise. *Singapore Journal of Tropical Geography*, 42 (2), pp. 163–183.
Rogers, K., Kelleway, J.J., Saintilan, N., Megonigal, J.P., Adams, J.B., Holmquist, J.R., Lu, M., Schile-Beers, L., Zawadzki, A., Mazumder, D. & Woodroffe, C.D. (2019). Wetland carbon storage controlled by millennial-scale variation in relative sea-level rise. *Nature*, 567 (7746), pp. 91–95.
Rogers, K., Saintilan, N. & Copeland, C. (2012). Modelling wetland surface elevation dynamics and its application to forecasting the effects of sea-level rise on estuarine wetlands. *Ecological Modelling*, 244, pp. 148–157.
Roskoden, R.R., Bryan, K.R., Schreiber, I. & Kopf, A. (2020). Rapid transition of sediment consolidation across an expanding mangrove fringe in the Firth of Thames New Zealand. *Geo-Marine Letters*, 40 (2), pp. 295–308.
Roy, P., Williams, R., Jones, A., Yassini, I, Gibbs, P., Coates, B, West, R., Scanes, P., Hudson, J. & Nichol, S (2001). Structure and function of south-east Australian estuaries. *Estuarine, coastal and shelf science*, 53 (3), pp. 351–384.
Saintilan, N & Hashimoto, T. (1999). Mangrove-saltmarsh dynamics on a bay-head delta in the Hawkesbury River estuary, New South Wales, Australia. In: *Diversity and Function in Mangrove Ecosystems*. Springer, pp. 95–102.
Saintilan, N., Khan, N.S., Ashe, E., Kelleway, J.J., Rogers, K., Woodroffe, C.D. & Horton, B.P. (2020). Thresholds of mangrove survival under rapid sea level rise. *Science*, 368 (6495), pp. 1118–1121.
Saintilan, N., Wilson, N.C., Rogers, K., Rajkaran, A. & Krauss, K.W. (2014). Mangrove expansion and salt marsh decline at mangrove poleward limits. *Global Change Biology*, 20 (1), pp. 147–157.
Sasmito, S.D., Murdiyarso, D., Friess, D.A. & Kurnianto, S. (2016). Can mangroves keep pace with contemporary sea level rise? A global data review. *Wetlands Ecology and Management*, 24 (2), pp. 263–278.
Schaffelke, B., Mellors, J. & Duke, N.C. (2005). Water quality in the Great Barrier Reef region: responses of mangrove, seagrass and macroalgal communities. *Marine Pollution Bulletin*, 51 (1), pp. 279–296.
Schuerch, M., Spencer, T., Temmerman, S., Kirwan, M.L., Wolff, C., Lincke, D., McOwen, C.J., Pickering, M.D., Reef, R., Vafeidis, A.T., Hinkel, J., Nicholls, R.J. & Brown, S. (2018). Future response of global coastal wetlands to sea-level rise. *Nature*, 561 (7722), pp. 231–234.
Schuerch, M., Vafeidis, A., Slawig, T. & Temmerman, S. (2013). Modeling the influence of changing storm patterns on the ability of a salt marsh to keep pace with sea level rise. *Journal of Geophysical Research: Earth Surface*, 118 (1), pp. 84–96.
Schuerch, M., Spencer, T. & Evans, B. (2019). Coupling between tidal mudflats and salt marshes affects marsh morphology. *Marine Geology*, 412, pp. 95–106.
Schuerch, M., Spencer, T., Temmerman, S., Kirwan, M., Wolff, C., Lincke, D., McOwen, C., Pickering, M., Reef, R., Vafeidis, A., Hinkel, J., Nicholls, R. & Brown, S. (2020). Reply to "Global coastal wetland expansion under accelerated sea-level rise is unlikely". *EarthArXiv*, pp. 1–5.
Schwarz, C., Gourgue, O., van Belzen, J., Zhu, Z., Bouma, T.J., van de Koppel, J., Ruessink, G., Claude, N. & Temmerman, S. (2018). Self-organization of a biogeomorphic landscape controlled by plant life-history traits. *Nature Geoscience*, 11 (9), pp. 672–677.
Schwarz, C., van Rees, F., Xie, D., Kleinhans, M.G. & van Maanen, B. (2022). Salt marshes create more extensive channel networks than mangroves. *Nature Communications*, 13 (1), p. 2017.

Secretariat, R. (2001). Wetland values and functions: climate change mitigation. *Gland, Switzerland*.
Seddon, N., Daniels, E., Davis, R., Chausson, A., Harris, R., Hou-Jones, X., Huq, S., Kapos, V., Mace, G.M. & Rizvi, A.R. (2020). Global recognition of the importance of nature-based solutions to the impacts of climate change. *Global Sustainability*, 3, p. 12.
Sefton, J.P. & Woodroffe, S.A. (2021). Assessing the use of mangrove pollen as a quantitative sea-level indicator on Mahé, Seychelles. *Journal of Quaternary Science*, 36 (2), pp. 311–323.
Semeniuk, V. (2018). Tidal Flats. In: *Encyclopedia of Coastal Science*. Ed. by C.W. Finkl & C. Makowski. Springer International Publishing: Cham, pp. 1–20.
Sheffieldt, A., Healy, T. & McGlone, M. (1995). Infilling rates of a steepland catchment estuary, Whangamata, New Zealand. *Journal of Coastal Research*, pp. 1294–1308.
Singleton, P. (2007). *Whangamata Harbour Plan Looking forward to a healthier harbour*. Tech. rep. Environment Waikato Internal Report 2007/14.
Sippo, J.Z., Lovelock, C.E., Santos, I.R., Sanders, C.J. & Maher, D.T. (2018). Mangrove mortality in a changing climate: An overview. *Estuarine, Coastal and Shelf Science*, 215, pp. 241–249.
Sippo, J.Z., Sanders, C.J., Santos, I.R., Jeffrey, L.C., Call, M., Harada, Y., Maguire, K., Brown, D., Conrad, S.R. & Maher, D.T. (2020). Coastal carbon cycle changes following mangrove loss. *Limnology and Oceanography*, 65 (11), pp. 2642–2656.
Snedaker, S.C. (1982). Mangrove species zonation: why? In: *Contributions to the Ecology of Halophytes*. Springer, pp. 111–125.
Spalding, M., Kainuma, M. & Collins, L. (2010). *World Atlas of Mangroves*. Vol. 39. Earthscan, London, Washington DC: Washington, DC.
Spalding, M., Blasco, F. & Field, C. (1997). World mangrove atlas.
Spalding, M.D. & Leal, M. (2021). *The State of the World's Mangroves 2021*. Tech. rep. Global Mangrove Alliance.
Spellerberg, I.F. & Fedor, P.J. (2003). A tribute to Claude Shannon (1916–2001) and a plea for more rigorous use of species richness, species diversity and the 'Shannon–Wiener' Index. *Global Ecology and Biogeography*, 12 (3), pp. 177–179.
Spenceley, A.P. (1977). The role of pneumatophores in sedimentary processes. *Marine Geology*, 24 (2), pp. M31–M37.
Spencer, T., Schuerch, M., Nicholls, R.J., Hinkel, J., Lincke, D., Vafeidis, A.T., Reef, R., McFadden, L. & Brown, S. (2016). Global coastal wetland change under sea-level rise and related stresses: The DIVA Wetland Change Model. *Global and Planetary Change*, 139, pp. 15–30.
Stevens, P.W., Montague, C.L. & Sulak, K.J. (2006). Patterns of fish use and piscivore abundance within a reconnected saltmarsh impoundment in the northern Indian River Lagoon, Florida. *Wetlands Ecology and Management*, 14 (2), pp. 147–166.
Stokes, D., Healy, T. & Cooke, P. (2009). Surface elevation changes and sediment characteristics of intertidal surfaces undergoing mangrove expansion and mangrove removal, Waikaraka Estuary, Tauranga Harbour, New Zealand. *International Journal of Ecology and Development*, 12.
Stokes, D.J. & Harris, R.J. (2015). Sediment properties and surface erodibility following a large-scale mangrove (Avicennia marina) removal. *Continental Shelf Research*, 107, pp. 1–10.
Suyadi, Gao, J., Lundquist, C.J. & Schwendenmann, L. (2019). Land-based and climatic stressors of mangrove cover change in the Auckland Region, New Zealand. *Aquatic Conservation: Marine and Freshwater Ecosystems*, 29 (9), pp. 1466–1483.
Suyadi, Gao, J., Lundquist, C.J. & Schwendenmann, L. (2020). Aboveground Carbon Stocks in Rapidly Expanding Mangroves in New Zealand: Regional Assessment and Economic Valuation of Blue Carbon. *Estuaries and Coasts*, 43 (6), pp. 1456–1469.
Suzuki, T., Zijlema, M., Burger, B., Meijer, M.C. & Narayan, S. (2012). Wave dissipation by vegetation with layer schematization in SWAN. *Coastal Engineering*, 59 (1), pp. 64–71.
Swales, A., Reeve, G., Cahoon, D.R. & Lovelock, C.E. (2019). Landscape Evolution of a Fluvial Sediment-Rich Avicennia marina Mangrove Forest: Insights from Seasonal and Inter-annual Surface-Elevation Dynamics. *Ecosystems*, 22 (6), pp. 1232–1255.
Swales, A., Bentley, S.J., Lovelock, C. & Bell, R.G. (2007). Sediment Processes and Mangrove-Habitat Expansion on a Rapidly-Prograding Muddy Coast, New Zealand, pp. 1441–1454.
Swales, A., Bentley Sr, S.J. & Lovelock, C.E. (2015). Mangrove-forest evolution in a sediment-rich estuarine system: opportunists or agents of geomorphic change? *Earth Surface Processes and Landforms*, 40 (12), pp. 1672–1687.
Swales, A. & Lovelock, C.E. (2020). Comparison of sediment-plate methods to measure accretion rates in an estuarine mangrove forest (New Zealand). *Estuarine, Coastal and Shelf Science*, 236, p. 106642.
Swales, A., Pritchard, M. & McBride, G.B. (2021). Chapter 1 - Biogeomorphic evolution and expansion of mangrove forests in New Zealand's sediment-rich estuarine systems. In: *Dynamic Sedimentary Environments of Mangrove Coasts*. Ed. by F. Sidik & D.A. Friess. Elsevier, pp. 3–45.

Swanson, K.M., Drexler, J.Z., Schoellhamer, D.H., Thorne, K.M., Casazza, M.L., Overton, C.T., Callaway, J.C. & Takekawa, J.Y. (2014). Wetland accretion rate model of ecosystem resilience (WARMER) and its application to habitat sustainability for endangered species in the San Francisco Estuary. *Estuaries and Coasts*, 37 (2), pp. 476–492.

Syvitski, J., Ángel, J.R., Saito, Y., Overeem, I., Vörösmarty, C.J., Wang, H. & Olago, D. (2022). Earth's sediment cycle during the Anthropocene. *Nature Reviews Earth and Environment*.

Syvitski, J.P.M., Vörösmarty, C.J., Kettner, A.J. & Green, P. (2005). Impact of Humans on the Flux of Terrestrial Sediment to the Global Coastal Ocean. *Science*, 308 (5720), pp. 376–380.

Sánchez-Núñez, D.A., Bernal, G. & Mancera Pineda, J.E. (2019). The Relative Role of Mangroves on Wave Erosion Mitigation and Sediment Properties. *Estuaries and Coasts*, 42 (8), pp. 2124–2138.

Tajziehchi, M. (2006). *Experimental and numerical modelling of wave-induced current and wave transformation in presence of submerged breakwaters*. PhD dissertation. The University of New South Wales.

Tanaka, N., Sasaki, Y., Mowjood, M., Jinadasa, K. & Homchuen, S. (2007). Coastal vegetation structures and their functions in tsunami protection: experience of the recent Indian Ocean tsunami. *Landscape and ecological engineering*, 3 (1), pp. 33–45.

Teal, J.M. (1962). Energy flow in the salt marsh ecosystem of Georgia. *Ecology*, 43 (4), pp. 614–624.

Temmerman, S., Govers, G., Wartel, S. & Meire, P. (2003). Spatial and temporal factors controlling short-term sedimentation in a salt and freshwater tidal marsh, Scheldt estuary, Belgium, SW Netherlands. *Earth Surface Processes and Landforms*, 28 (7), pp. 739–755.

Temmerman, S., Meire, P., Bouma, T.J., Herman, P.M., Ysebaert, T. & De Vriend, H.J. (2013). Ecosystem-based coastal defence in the face of global change. *Nature*, 504 (7478), pp. 79–83.

Temmerman, S., Moonen, P., Schoelynck, J., Govers, G. & Bouma, T.J. (2012). Impact of vegetation die-off on spatial flow patterns over a tidal marsh. *Geophysical Research Letters*, 39 (3).

Thampanya, U., Vermaat, J.E., Sinsakul, S. & Panapitukkul, N. (2006). Coastal erosion and mangrove progradation of Southern Thailand. *Estuarine, Coastal and Shelf Science*, 68 (1), pp. 75–85.

Thorne, K., MacDonald, G., Guntenspergen, G., Ambrose, R., Buffington, K., Dugger, B., Freeman, C., Janousek, C., Brown, L., Rosencranz, J., Holmquist, J., Smol, J., Hargan, K. & Takekawa, J. (2018). U.S. Pacific coastal wetland resilience and vulnerability to sea-level rise. *Science Advances*, 4 (2), eaao3270.

Thrush, S., Hewitt, J., Cummings, V., Ellis, J., Hatton, C., Lohrer, A. & Norkko, A. (2004). Muddy waters: elevating sediment input to coastal and estuarine habitats. *Frontiers in Ecology and the Environment*, 2 (6), pp. 299–306.

Tomlinson, P.B. (2016). *The Botany of Mangroves*. 2nd ed. Cambridge University Press: Cambridge.

Traill, L.W., Bradshaw, C.J., Delean, S. & Brook, B.W. (2010). Wetland conservation and sustainable use under global change: a tropical Australian case study using magpie geese. *Ecography*, 33 (5), pp. 818–825.

Törnqvist, T.E., Cahoon, D.R., Day, J.W. & Morris, J.T. (2019). Global coastal wetland expansion under accelerated sea-level rise is unlikely. *EarthArXiv*, pp. 1–7.

Törnqvist, T.E., Cahoon, D.R., Morris, J.T. & Day, J.W. (2021). Coastal Wetland Resilience, Accelerated Sea-Level Rise, and the Importance of Timescale. *AGU Advances*, 2 (1), e2020AV000334.

Uncles, R.J. & Stephens, J.A. (2000). Observations of currents, salinity, turbidity and intertidal mudflat characteristics and properties in the Tavy Estuary, UK. *Continental Shelf Research*, 20 (12), pp. 1531–1549.

Van Hespen, R., Hu, Z., Peng, Y., Borsje, B.W., Kleinhans, M., Ysebaert, T. & Bouma, T.J. (2021). Analysis of coastal storm damage resistance in successional mangrove species. *Limnology and Oceanography*, 66 (8), pp. 3221–3236.

Van Ledden, M., van Kesteren, W.G.M. & Winterwerp, J.C. (2004). A conceptual framework for the erosion behaviour of sand–mud mixtures. *Continental Shelf Research*, 24 (1), pp. 1–11.

Van Maanen, B., Coco, G. & Bryan, K.R. (2015). On the ecogeomorphological feedbacks that control tidal channel network evolution in a sandy mangrove setting. *Proc Math Phys Eng Sci*, 471 (2180), p. 20150115.

Van Maanen, B., Coco, G. & Bryan, K.R. (2013). Modelling the effects of tidal range and initial bathymetry on the morphological evolution of tidal embayments. *Geomorphology*, 191, pp. 23–34.

Van Oorschot, M., Kleinhans, M.G., Geerling, G.W., Egger, G., Leuven, R.S.E.W. & Middelkoop, H. (2017). Modeling invasive alien plant species in river systems: Interaction with native ecosystem engineers and effects on hydro-morphodynamic processes. *Water Resources Research*, 53 (8), pp. 6945–6969.

Van Oorschot, M., Kleinhans, M., Geerling, G. & Middelkoop, H. (2016). Distinct patterns of interaction between vegetation and morphodynamics. *Earth Surface Processes and Landforms*, 41 (6), pp. 791–808.

Van Rijn, L.C., Walstra, D.J.R. & Ormondt, M. (2004). Description of TRANSPOR2004 and implementation in Delft3D-online, Z3748.

Van Rijn, L.C. (2007). Unified View of Sediment Transport by Currents and Waves. I: Initiation of Motion, Bed Roughness, and Bed-Load Transport. *Journal of Hydraulic Engineering*, 133 (6), pp. 649–667.

Van Coppenolle, R., Schwarz, C. & Temmerman, S. (2018). Contribution of Mangroves and Salt Marshes to Nature-Based Mitigation of Coastal Flood Risks in Major Deltas of the World. *Estuaries and Coasts*, 41 (6), pp. 1699–1711.

Van der Stocken, T., Wee, A.K.S., De Ryck, D.J.R., Vanschoenwinkel, B., Friess, D.A., Dahdouh-Guebas, F., Simard, M., Koedam, N. & Webb, E.L. (2019). A general framework for propagule dispersal in mangroves. *Biological Reviews*, 94 (4), pp. 1547–1575.
Van der Wegen, M, Jaffe, B. & Roelvink, J. (2011). Process-based, morphodynamic hindcast of decadal deposition patterns in San Pablo Bay, California, 1856–1887. *Journal of Geophysical Research: Earth Surface*, 116 (F2).
Van der Wegen, M., Jaffe, B., Foxgrover, A. & Roelvink, D. (2017). Mudflat morphodynamics and the impact of sea level rise in South San Francisco Bay. *Estuaries and Coasts*, 40 (1), pp. 37–49.
Van der Werf, K., Gilissen, H.K., Kleinhans, M. & van Rijswick, M. (2020). On dynamic naturalness, static regulation and human influence in the Ems-Dollard estuary. *International Journal of Water Resources Development*, pp. 1–20.
Van Ledden, M., Wang, Z.-B., Winterwerp, H. & De Vriend, H. (2006). Modelling sand–mud morphodynamics in the Friesche Zeegat. *Ocean Dynamics*, 56 (3), pp. 248–265.
Van Santen, P., Augustinus, P.G.E.F., Janssen-Stelder, B.M., Quartel, S. & Tri, N.H. (2007). Sedimentation in an estuarine mangrove system. *Journal of Asian Earth Sciences*, 29 (4), pp. 566–575.
Waeles, B., Le Hir, P. & Silva Jacinto, R. (2004). Modélisation morphodynamique cross-shore d'un estran vaseux. *Comptes Rendus Geoscience*, 336 (11), pp. 1025–1033.
Wang, Z., Jeuken, C. & De Vriend, H. (1999). *Tidal asymmetry and residual sediment transport in estuaries*. Tech. rep.
Watson, J.G. (1928). *Mangrove forests of the Malay Peninsula*. Vol. 6. Malasian Forest Records.
Wells, S. (2006). *In the front line. Shoreline protection and other ecosystem services from mangroves and coral reefs. UNEP-WCMC Biodiversity Series 24*. Vol. 2006. Cambridge, UK.
Whelan, K.R.T., Smith Iii, T.J., Anderson, G.H. & Ouellette, M.L. (2009). Hurricane Wilma's impact on overall soil elevation and zones within the soil profile in a mangrove forest. *Wetlands*, 29 (1), pp. 16–23.
Willemsen, P.W.J.M., Smits, B.P., Borsje, B.W., Herman, P.M.J., Dijkstra, J.T., Bouma, T.J. & Hulscher, S.J.M.H. (2022). Modeling Decadal Salt Marsh Development: Variability of the Salt Marsh Edge Under Influence of Waves and Sediment Availability. *Water Resources Research*, 58 (1), e2020WR028962.
Winterwerp, J.C., Erftemeijer, P.L.A., Suryadiputra, N., van Eijk, P. & Zhang, L. (2013). Defining Eco-Morphodynamic Requirements for Rehabilitating Eroding Mangrove-Mud Coasts. *Wetlands*, 33 (3), pp. 515–526.
Winterwerp, J.C., Albers, T., Anthony, E.J., Friess, D.A., Mancheño, A.G., Moseley, K., Muhari, A., Naipal, S., Noordermeer, J., Oost, A., Saengsupavanich, C., Tas, S.A.J., Tonneijck, F.H., Wilms, T., Van Bijsterveldt, C., Van Eijk, P., Van Lavieren, E. & Van Wesenbeeck, B.K. (2020). Managing erosion of mangrove-mud coasts with permeable dams –lessons learned. *Ecological Engineering*, 158, p. 106078.
Winterwerp, J.C., Borst, W.G. & De Vries, M.B. (2005). Pilot study on the erosion and rehabilitation of a mangrove mud coast. *Journal of Coastal Research*, 21 (2), pp. 223–230.
Woodroffe, C.D. (2018). Mangrove response to sea level rise: Palaeoecological insights from macrotidal systems in northern Australia. *Marine and Freshwater Research*, 69 (6), pp. 917–932.
Woodroffe, C.D., Rogers, K., McKee, K.L., Lovelock, C.E., Mendelssohn, I.A. & Saintilan, N. (2016). Mangrove Sedimentation and Response to Relative Sea-Level Rise. *Ann Rev Mar Sci*, 8, pp. 243–66.
Woodroffe, C. (1993). Mangrove sediments and geomorphology. *Coastal and estuarine studies*, pp. 7–7.
Woodroffe, C.D., Thom, B.G. & Chappell, J. (1985). Development of widespread mangrove swamps in mid-Holocene times in northern Australia. *Nature*, 317 (6039), pp. 711–713.
Wu, W.-C., Ma, G. & Cox, D.T. (2016). Modeling wave attenuation induced by the vertical density variations of vegetation. *Coastal Engineering*, 112, pp. 17–27.
Xie, D., Schwarz, C., Brückner, M.Z.M., Kleinhans, M.G., Urrego, D.H., Zhou, Z. & van Maanen, B. (2020). Mangrove diversity loss under sea-level rise triggered by bio-morphodynamic feedbacks and anthropogenic pressures. *Environmental Research Letters*, 15 (11), p. 114033.
Xie, D., Schwarz, C., Kleinhans, M.G., Zhou, Z. & van Maanen, B. (2022). Implications of Coastal Conditions and Sea-Level Rise on Mangrove Vulnerability: A Bio-Morphodynamic Modeling Study. *Journal of Geophysical Research: Earth Surface*, 127 (3), e2021JF006301.
Yang, S.L., Luo, X., Temmerman, S., Kirwan, M., Bouma, T., Xu, K., Zhang, S., Fan, J., Shi, B., Yang, H., Wang, Y.P., Shi, X. & Gao, S. (2020). Role of delta-front erosion in sustaining salt marshes under sea-level rise and fluvial sediment decline. *Limnology and Oceanography*, 65 (9), pp. 1990–2009.
Young, B.M. & Harvey, E.L. (1996). A Spatial Analysis of the Relationship Between Mangrove (Avicennia marinavar.australasica) Physiognomy and Sediment Accretion in the Hauraki Plains, New Zealand. *Estuarine, Coastal and Shelf Science*, 42 (2), pp. 231–246.
Zarfl, C., Lumsdon, A.E., Berlekamp, J., Tydecks, L. & Tockner, K. (2015). A global boom in hydropower dam construction. *Aquatic Sciences*, 77 (1), pp. 161–170.
Zhang, K., Liu, H., Li, Y., Xu, H., Shen, J., Rhome, J. & Smith III, T.J. (2012a). The role of mangroves in attenuating storm surges. *Estuarine, Coastal and Shelf Science*, 102, pp. 11–23.

Zhang, X., Leonardi, N., Donatelli, C. & Fagherazzi, S. (2019). Fate of cohesive sediments in a marsh-dominated estuary. *Advances in Water Resources*, 125, pp. 32–40.
Zhang, Y., Huang, G., Wang, W., Chen, L. & Lin, G. (2012b). Interactions between mangroves and exotic Spartina in an anthropogenically disturbed estuary in southern China. *Ecology*, 93 (3), pp. 588–597.
Zhou, Z., Coco, G., Jiménez, M., Olabarrieta, M., van der Wegen, M. & Townend, I. (2014). Morphodynamics of river-influenced back-barrier tidal basins: The role of landscape and hydrodynamic settings. *Water Resources Research*, 50 (12), pp. 9514–9535.
Zhou, Z., Coco, G., Townend, I., Olabarrieta, M., Van Der Wegen, M., Gong, Z., D'alpaos, A., Gao, S., Jaffe, B.E., Gelfenbaum, G., et al. (2017). Is "morphodynamic equilibrium" an oxymoron? *Earth-Science Reviews*, 165, pp. 257–267.
Zhou, Z., Ye, Q. & Coco, G. (2016). A one-dimensional biomorphodynamic model of tidal flats: Sediment sorting, marsh distribution, and carbon accumulation under sea level rise. *Advances in Water Resources*, 93, pp. 288–302.
Zhu, X., Hou, Y., Weng, Q. & Chen, L. (2019). Integrating UAV optical imagery and LiDAR data for assessing the spatial relationship between mangrove and inundation across a subtropical estuarine wetland. *ISPRS Journal of Photogrammetry and Remote Sensing*, 149, pp. 146–156.

Acknowledgements

Before I started my PhD research, I thought of many different images that my PhD would look like. That it should be an enviable profession full of flowers and applause, and I would be a glowing young man wearing a neat suit talking confidently about my profound research. However, looking back at the beginning of my PhD track, I realized that I was like a small child who knew nothing but was eager to know everything. Numerical modelling, what is that? Where should I start? How am I supposed to convince myself before narrating my story and selling it to others? After this step-by-step process, I am presenting to you my dissertation which I have worked on for the last four years. Personally, it is a great milestone in my life, and I shall never forget the people who helped me and encouraged me along the way. I truly appreciate that, and taking this opportunity, I would like to thank some of you in particular.

Barend. I would like to express my deepest gratitude to you. I am so lucky to have you as my daily supervisor. Thank you so much for guiding me during my PhD track and always listening to me to see what problems I am stuck on. Your patience and encouragement made me more confident to implement different ideas and solve questions independently. You guided me to a new horizon of mangrove science. I still remember we had an exciting discussion on what scientific questions could be addressed when we were on a train back from the NCK conference, and we were so deep in our discussion that we completely forgot we were in a silent carriage until another passenger came up to stop us. This was awkward but it was the first time I felt so excited about my science because it is so much more important to society than I ever imagined. In addition to academics, you also treated me as a friend helping me deal with my housing problems, inviting me to your King's day party and introducing me to your other friends. All of these warmed and enriched my life in Utrecht. The only unfortunate thing should be that the covid19 constraints hindered me from working together with you at the end of my PhD period, but your detailed responses to my emails kept on pointing me in the right direction. Thanks for everything you have done for me, Barend van Maanen.

Christian and Maarten. I am also grateful for your dedicated supervision and sincere care during my PhD research. Christian, you taught me a lot about the model principles, data analysis and other research skills. I am not sure if my writing or speaking really improved as you said, but your kind words always acted as a reward for my small progress, encouraging me to do a better job next time. These four years you have actively responded to my meeting or email requests, and your valuable suggestions have significantly reduced a lot of unnecessary work. Thanks for lighting a lamp to the destination when I am sailing through the mist, Christian Schwarz. Maarten, I would also like to express my sincere gratitude to you for being an enthusiastic, positive and supportive mentor, especially during the final stage of my PhD study. It is not only the brilliant ideas you suggested for my research, but also your efforts to make me feel at home in our department that I can always be proud of. Every time I come to you for any help, you will immediately find a solution for me or reach out to someone who could solve my problems. I cannot work during covid19, you helped me get a spot in our VM office. I need more computer power, you came to me with the cluster. My flight got cancelled, you recommended me with a new job. We always joke that Maarten never has holidays, but I know, Maarten puts the requests of his students as a priority and therefore everyone thinks he works day and night. Many thanks, Maarten Kleinhans, for being a person I could always rely on in my PhD study.

I am also grateful to be a part of a lovely and close research group. The weekly group meeting allowed me to know and learn from all other people's work, life and funny stories. I gained considerable support from the group over these years. Anne and Lisanne, thanks for coming to me and showing many other enthusiastic colleagues when it was my first PhD working day. Muriel, thanks for teaching me step by step how to set up the vegetation model and answering my questions whenever my model crashed.

Marcio, I really appreciated your time for helping me install a new model in the cluster, that really facilitated my research progress and thus I could foresee when I could finish my projects. Arya, thanks for having coffee/tea and sharing your stories with me during our break, you always showed your smiles to me even when you were also under pressure. Steven, thanks for not only guiding me through the thesis Overleaf so that I could eventually have a nice thesis format, but also showing many important steps from thesis writing to printing, as I believe you must have spent a lot of time collecting these tips. Jana, driving to visit the dredging museum with Maarten and Steven was my first "scientific excursion" during my PhD. It was so fun that we had jokes all the way and we got to know each other further. Débora, and also my master students Sarah and Remco, I really enjoy the moments where we shared the modelling skills together. Honestly, I learn more from you than you have learned from me, and I am so proud and happy to see your great achievements so far.

Moreover, I would like to extend my appreciation to my colleagues who shared cakes, coffees and cookies and offered great help whenever I passed by. Steven, Friederike, Laura, Ruth and Marina, thanks for processing/explaining my repetitive requests about either traveling to the UK during covid19 or extending my residence permit after my flight got cancelled. I was especially touched by your greeting card where you collected our colleague's signatures and told me "stay strong, we are all together with you" during my quarantine. Meng, thanks for teaching me to pursue science calmly, and even in my last year you would also calm me down by saying "you still have six months". Maybe this is the truth of life but I still cannot control myself to reach inner peace when the deadline is approaching. Sheng, thanks for your company to walk around the Botanic Garden almost every afternoon. It is more useful than coffee to refresh my brain and keep my mind clear. Job, we have the same supervisor so we always have a lot of common topics to share. I want to thank you for showing me your results, and especially for your kind support of those attractive mangrove images you took. Some of these images have now been used to decorate my chapter pages and I am very happy I can also make my documents vivid. Jakob, Daniël, Sepehr, Jannis and Joeri, I would remember our drinks on Friday afternoon and it helped so much to reduce my stress by listening to your 'happy' life, and thanks for always inviting me, though I may "sometimes" have excuses for not showing up. Math, Jorge, Edward, Sandra, Sanita, Steye, Fabian, Tim, Lonneke, Willem-Jan, Bas and Bas, I am very happy to have you as my colleagues with whom I can share stories and life. Thanks for your lots of valuable suggestions, tips and experience on the life and study, which are never possible to learn from any books.

Special thanks to the members of the Assessment Committee (Karin Bryan, Kerrylee Rogers, Zheng Bing Wang, Luzhen Chen and Tjeerd Bouma), for your valuable time to evaluate my PhD dissertation and formulate the questions. Thanks should also go to the Chair (Marc Bierkens) and the quorum (Derek Karssenberg and Katja Philippart) for your time and involvement in my PhD promotion. I also appreciate many of my collaborators who kindly shared their knowledge without hesitation. Zeng, thanks for introducing me to Barend and also showing me your settings of numerical models. Dunia, thanks for proposing to use a special index so that we can handle two variables at the same time, before that I was stuck on that for a while. Karin, Giovanni and Steve, it is so nice of you to show me your knowledge of New Zealand estuaries, and let me know that what seems necessary to the world may turn out to have unexpected negative impacts. Floris and Xuejiao, I learned a lot about processing the satellite images from you, and you definitely inspired me to do more than only modelling. Jaap, I appreciated your patience when we had meetings where you explained your ideas over and over again.

I would be remiss in not mentioning my Chinese friends who cared about me so much during my PhD daily life. Wanxiang and Xing, it is so warm to have you as my roommates spending nearly 4 years together, and thanks for never leaving me alone even during your Valentine's (which sounds a bit weird now). Dongsheng, Puqiao and Shuyang, we can always come up with a reason to gather together to have a big meal, and thanks for always letting me wash the dishes in the end so that I can stay away from the stove. Yurui, I still remember you kept on waiting for me at the airport when your flight was several

hours earlier than mine, and before that, we never saw each other physically, and I am so happy that I have such a close friend like you that I can talk with about everything. Haoming and Yan, thanks for your special care during covid19 and the year after. Wish one day we would have our restaurant opened in the Netherlands. Haorui and Linyu, I am still confused about who is the most handsome boy from our group that you first met. Anyway, this is a funny topic that we will never have a winner, but thanks for offering me so many different cuisines. Peikai, you know I like selfies and you have taken tons of beautiful photos for me at the beginning, I appreciate your work and will keep your photos for long. Jingyu, Yanyan, Mei and Shuang, even now we kept in touch with each other and thanks for your meals and other living support. Jiannan, Qingwu, Xuefeng, Boning, Mingxi, Lei, Yanyi and Chujun, we play sports or games, learn skills and help each other here and there, great to meet you in Utrecht. Yixin, I cannot believe I met a friend from the same home city and study at the same university, thanks for touring me around the places where I had never been.

To my family, I could not have undertaken this journey without your support and greetings. Mom and Dad, you work so hard for our family without requiring any reward. I am extremely grateful that you always show me the positive side of your life so I can completely focus on my PhD study. Even though I have stayed in the Netherlands for several years without seeing you physically, I never felt lonely and strange in our family. We communicate so frequently that I even think you are a metre away from me. Dad, I found it was amazing that whenever I was stuck on some issues, I could always get some hints from your perspective. When I was a kid, I thought my dad knew everything. Even today, I would have the same feeling that you are a man with a broad knowledge knowing quite a lot including my PhD research. We have a wide range of topics, covering sciences, life, and the future. I know you keep on learning from what I did so that we would never see a gap between us. Dad, thanks for expressing your love in this way remotely. Mom, you are not as good at speaking as my dad, so every time you just smiled at me listening to what I and my dad discussed. Thanks for supporting me in everything that I want to do and for completely believing in me since I was a child. You never asked me to learn anything, but I was gradually affected by your personality on how to be a righteous, honest and brave person. Words cannot express my gratitude to you, mom. My sister and my brother, I also want to thank you for being thoughtful, for your sweet laughter you bring to our family. I love you so much.

Last but not least, I would like to express my sincere gratitude to you, my faithful readers for spending time reading my dissertation and getting to know me a bit more. We may never have met before but I believe you are also a person loving life, nature and our planet. I am deeply indebted to the actions you have taken so far! I understand you may be suspicious of my model results as *the model never tells the full truth*, however, if by any chance you found my work can be useful to society, then it would be worthy of my four-year efforts during my PhD.

About the author

Danghan Xie grew up in Putian, China. In 2010, he moved to Nanjing and started his bachelor in Harbor, Waterway and Coastal Engineering, Hohai University, and graduated in 2014. He continued his master research at the same year focusing on the analysis and prediction of storm surges along the Jiangsu shoreline. In 2017, he received his master degree, and in the next year, he received a Young Scientist Award in the 15th International Coastal Symposium (Busan, Republic of Korea). After he obtained his MSc degree, he worked as a research assistant for 4 months writing a research proposal on Coastal Biomorphodynamics. In October 2017, he started as a PhD researcher at the Department of Physical Geography at Utrecht University, working on the project entitled *Bio-morphodynamics of coastal wetlands with mangrove vegetation* through numerical modelling.

During his PhD, Danghan gained experience in working with international collaborators from the Netherlands, Belgium, UK, New Zealand and China. In addition to his expertise in numerical modelling, he is also experienced working with and processing existing datasets, and he also has ample experience in analyzing spatial datasets using remote sensing products. Apart from his own research, he also engaged in student supervision and attended several conferences. He is currently appointed as a Researcher at Utrecht University to process three-dimensional animations based on flume experiments. From June 2022, Danghan will continue his research as a postdoc fellow at Boston University, focusing on the coastline evolution in Massachusetts, USA. Danghan loves to do fitness and play basketball after work. He enjoys reading and hiking and spends most of his weekends in the library and nature.

List of Publications

Refereed journal papers as first author

Xie, D., Schwarz, C., Kleinhans, M. G., Bryan, K. R., Coco, G., Hunt, S., & van Maanen, B. (in prep.). Humans as Ecosystem Engineers: How upstream land-use change and mangrove removal cause deviating trajectories in estuarine landscape development. *journal t.b.d.*

Xie, D., Schwarz, C., Kleinhans, M. G., Zhou, Z., & van Maanen, B. (2022), Implications of coastal conditions and sea-level rise on mangrove vulnerability: A bio-morphodynamic modeling study. *Journal of Geophysical Research: Earth Surface, 127, e2021JF006301*. DOI: https://doi.org/10.1029/2021JF006301.

Xie, D., Schwarz, C., Brückner, M. Z. M., Kleinhans, M. G., Urrego, D. H., Zhou, Z., & van Maanen, B. (2020). Mangrove diversity loss under sea-level rise triggered by bio-morphodynamic feedbacks and anthropogenic pressures. *Environmental Research Letters, 15(11), 114033*. DOI: https://doi.org/10.1088/1748-9326/abc122.

Xie, D., Tan, Y., Chu, A., Zhou, T., and van Maanen, B. (2018). Distribution characteristics of the extreme storm tides in the radial sand ridges area of the south Yellow Sea in China. *Journal of Coastal Research, 85(10085), 856-860*. DOI: https://doi.org/10.2112/SI85-172.1.

Refereed journal articles as co-author

Hou, X., Nienhuis, J., & **Xie, D.** (in prep). Increase in coastal sediment concentrations near river deltas despite river sediment supply decline. *journal t.b.d.*

van Hespen, R., Hu, Z., Borsje, B., Dominicis, M. D., Friess, D. A., Jevrejeva, S., Kleinhans, M. G., Maza, M., van Bijsterveldt, C. E., Van der Stocken, T., van Wesenbeeck, B., **Xie, D.**, & Bouma, T. J. (in prep). Mangrove forests as a nature-based solution for coastal flood protection: biophysical and ecological considerations. *journal t.b.d.*

Schwarz, C., van Rees, F., **Xie, D.**, Kleinhans, M. G., & van Maanen, B. (2022), Salt marshes create more extensive channel networks than mangroves. *Nature communications, 13(1), 2017*, DOI: 10.1038/s41467-022-29654-1.

Conference abstracts

Kleinhans, M. G., Weisscher, S. A. H., **Xie, D.**, & Boechat-Albernaz, M. (2022). What determines estuary planform shape, size and channel-bar patterns? *EGU 2022, Vienna, Austria*.

Dzimballa, S., **Xie, D.**, van Maanen, B., & Kleinhans, M. G. (2022). Feedbacks between estuarine morphology and mangrove dieback and recovery in the Gulf of Carpentaria, Australia. *NCK 2022, Enschede, Netherlands.*

Hou, X., Nienhuis, J., & **Xie, D.** (2021). Global coastal sediment near river mouths: controls and its impacts on delta geomorphology? *AGU 2021, New Orleans, USA*.

Xie, D., Schwarz, C., Kleinhans, M. G., Zhou, Z., and van Maanen, B. (2021). Responses of mangrove forests to sea-level rise and human interventions: a bio-morphodynamic modelling study. *CORE 2021, Nanjing, China*.

Xie, D., Schwarz, C., Kleinhans, M. G., Zhou, Z., and van Maanen, B. (2021). A bio-morphodynamic modelling study to determine how environmental conditions control mangrove vulnerability to sea-level rise. *INTERCOH 2021, Delft, Netherlands*.

Xie, D., Schwarz, C., Kleinhans, M. G., Zhou, Z., and van Maanen, B. (2021). Mangrove vulnerability to sea-level rise under varying environmental conditions: A bio-morphodynamic modelling study involving vegetation dynamics and coastal profile change. *ECSA 2021, Hull, UK*.

Xie, D., Schwarz, C., Brückner, M. Z. M., Zhou, Z., and van Maanen, B. (2019). The fate of mangrove assemblages in the face of changing coastal systems. *EGU 2019, Vienna, Austria*.

Outreach

Awards

Young Scientist Award in the 15th International Coastal Symposium, Busan, Republic of Korea, 2018.

Media coverage

Press in 2020, based on the press release at:
https://www.uu.nl/en/news/triple-trouble-for-mangrove-coasts.

Utrecht University
Faculty of Geosciences
Department of Physical Geography

ISSN 2211-4335